Regioselective Synthesis of Hydrazines and Heterocycles by Catalytic and Electrochemical N–N Bond Formation

by

Subrata Patra

A thesis submitted in partial fulfillment of the requirements for the degree of

Master of Science

Department of Chemistry
University of Alberta

Abstract

Two new synthetic methods for preparing N–N bond-containing heterocycles have been presented: one, by copper-catalyzed oxidative N–N bond formation and two, by electrochemical reduction of N-nitroso compounds and subsequent ring-closing. The first method is copper(I)- and copper(II)-mediated pyrazole synthesis through a catalytic oxidative N–N bond formation between an imidate and amine under air. Arylimidate esters prepared from β-amino acrylonitrile undergo intramolecular oxidative N–N bond formation in the presence of a 1 : 1 combination of copper acetate and copper iodide in DMSO at 60 °C, with concomitant aromatization in the presence of molecular oxygen, providing 3-ethoxy-1-arylpyrazoles.

The second method is a novel and general electroreductive synthesis, producing substituted hydrazines, pyrazoles, and pyrazolines regioselectively from N-nitroso compounds. Nitrosylation of corresponding aniline derivatives affords the desired N-nitrosamines in high yields using standard methodology. Electrochemical reduction of N-nitrosamines in an undivided cell leads to the respective hydrazines, followed by intramolecular ring closure to give either pyrazolidinones of pyrazolines in one-pot. Inexpensive and non-toxic stainless steel and zinc electrodes were used as the cathode and anode, respectively. Different combinations of other standard electrode systems do not improve the results, producing the N-nitroso bond cleavage product, sometimes exclusively. Furthermore, the use of lithium bromide as the electrolyte and mildly basic pyridine improves the selectivity of the reaction. Various aryl functional groups with different electronic effects, as well as heteroaryl and alkyl groups, are well tolerated under the reaction conditions. Moreover, electrochemical oxidation of pyrazolidinones to the corresponding pyrazoles was also investigated. Electrochemical reduction of N-nitroso compounds is under-reported in the literature and mostly require a divided cell and/or toxic electrodes. This work fills this void and provides a valuable new strategy for the synthesis of hydrazines and heterocycles

– structurally vital building blocks for agricultural and pharmaceutical intermediates under very mild reaction conditions using a simple, scalable set-up.

Earlier work, on the installation of sulfur at *meta*-position of phenols to make *meta*-arylsulfanyl- and *meta*-(alkylsulfanyl)phenols starting from cyclohexane-1,3-dione, was done under the direction of Prof. Derrick Clive and is included as an appendix.

“Sometimes you just have to die a little inside in order to be ***Reborn*** and ***Rise*** again as a ***Stronger*** and ***Wiser*** version of you.”

Acknowledgements

First and foremost, I would like to express my gratitude to my supervisor and mentor Prof. Jeffrey M. Stryker, who helped me a lot with his supervision, ample of precious suggestions and inspiration during the vicissitudes throughout my master's degree.

I am highly intended to extend my deep sense of gratitude to the chair of the Department of Chemistry Prof. Rik Tykwinski and my committee members Prof. Steven H. Bergens and Prof. John C. Vederas.

I would also like to thank my previous supervisor Prof. Derrick L. J. Clive and all the group members Dr. Ashok Kumar Pazhznivel, Dr. Heshmatollah Samimishalamzari, Dr. Nayeem Ahmed, and Nhan Do.

I express gratitude to all the past and current members of the Stryker Group for sharing ideas, limitless assistance in lab and presentation preparation: Dr. Robin Hamilton, Dr. Shaohui Yu, Dr. Orain Brown, Dr. Asama Vorapattanapong, Dr. David Scott, Dr. Sanjay Jadhav, Kseniya Revunova, Yaowei Guo, Mark Aloisio, Nathanael King, Munashe Chizema, Noah Depner. In particular, I am thankful to Mark for extending his helping hand whenever I needed. Words fail to express my gratitude to Robin whose unique ideas, inspiring guidance and constant help made this journey a successful one. Without his support, I would have been at a loss.

Many thanks to my friends Dr. Jaya Pal, Abhoy Karmakar, Amit Bhattachatya, Shrwan Kumar for making my life in Canada interesting.

I am grateful to the technical stuff at the University of Alberta for providing me all the facilities to carry out my thesis work successfully.

Finally, my deepest gratitude goes to my parents and family for support in all my academic endeavors. I feel intensely beholden to them for whatever I have achieved so far.

Table of Contents

List of Figures

List of Equations

List of Schemes

List of Tables

List of Abbreviations

Å	Ångström
ACAC	acetylacetonate
ACN	acetonitrile
Aq	aqueous
Ar	aryl moiety
Bu	butyl
°C	degrees Celsius
Ca	circa
C_{gr}	glassy carbon electrode
Cp	cyclopentadienyl
Cp*	pentamethylcyclopentadienyl
CyPF-*t*Bu	(1-dicyclohexylphosphino2-di-*tert*-butylphosphinoethylferrocene
δ	chemical shift
DCB	1,2-dichlorobenzene
DCM	dichloromethane
DMA	dimethylacetamide
DMAP	4-dimethylaminopyridine
DME	1,2-dimethoxyethane
DMF	*N*,*N*-dimethylformamide
DMSO	dimethyl sulfoxide
DMU	dimethylurea
EI	electron ionization
ESI	electrospray ionisation
Et	ethyl
FTIR	fourier transform infrared

HRMS	high-resolution mass spectrometry
Hz	hertz
i-PrOH	isopropanol
Me	methyl
MeCN	acetonitrile
MeOH	methanol
MHz	megahertz
NBS	N-bromosuccinimide
NEt_3	triethylamine
NMP	N-methylpyrrolidinone
NMR	nuclear magnetic resonance
PIFA	phenyliodine(III)bis-(trifluoroacetate)
Ph	phenyl
R	alkyl
SS	stainless steel
TBAB	*tetra*-*N*-butylammonium bromide
TBACl	*tetra*-*N*-butylammonium chloride
TBN	*tert*-butyl nitrite
TCCA	trichloroisocyanuric acid
TEA	triethylamine
TFA	trifluroacetate
THF	tetrahydrofuran
TLC	thin-layer chromatography
TMEDA	tetramethylethylenediamine
TPPA	tris(pyrrolidino)phosphoramide
TsCl	4-toluenesulfonyl chloride

Chapter 1: Importance of Hydrazines and Pyrazoles and Issues in their Synthesis

1.1 Introduction

Nitrogen (N) is one of the most important heteroatoms found in biologically active drugs.[1-3] Biological, chemical, and physical properties change drastically in presence of a nitrogen atom in drugs and bioactive compounds. Approximately 84% of small molecule drugs approved by the FDA contain at least one nitrogen atom. Further, approximately 59% contain nitrogen heterocycles.[4] Heterocycles with two adjacent nitrogen are also a common motif in biologically active molecules. However, preparing these compounds without using dangerous hydrazine starting materials remains largely an unsolved problem.

1.2 Hydrazines

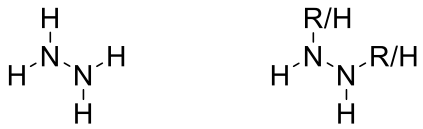

1 **2**

Figure 1-1 Hydrazine and hydrazines

Hydrazines **2**, are central building blocks in synthetic organic chemistry, derived from hydrazine **1** by replacing hydrogen atom(s) by an organic group (Figure 1-1). Hydrazine is highly toxic whereas hydrazines are promising drug candidates (Figure 1-2). Antiparkinsonic agent carbidopa, vasodilator hydralazine, and antidepressant phenelzineor are examples of drugs possessing a hydrazine moiety. Diuretic clopamide, insecticidal active dibenzoylhydrazine, and antidepressant isocarboxazid contain acyl derivatives of hydrazine.

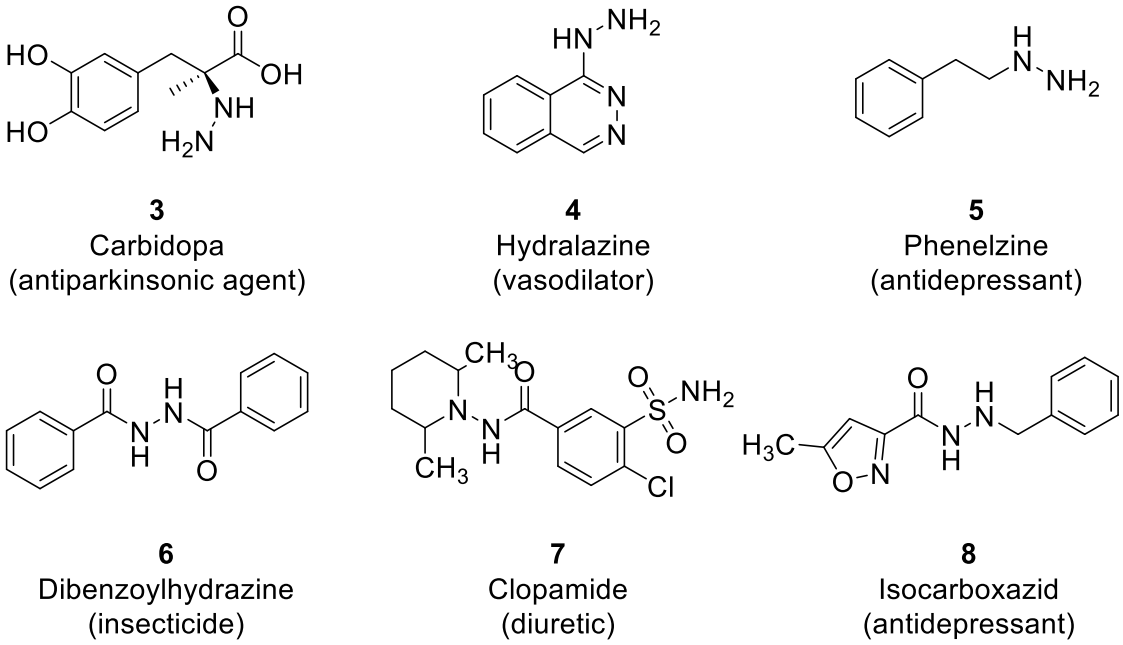

3
Carbidopa
(antiparkinsonic agent)

4
Hydralazine
(vasodilator)

5
Phenelzine
(antidepressant)

6
Dibenzoylhydrazine
(insecticide)

7
Clopamide
(diuretic)

8
Isocarboxazid
(antidepressant)

Figure 1-2 Bioactive hydrazines

1.2.1 Hydrazine scaffolds

Hydrazines are commonly used to synthesize pharmaceuticals and dyes, and in synthetic chemistry laboratories as a precursor. Condensation reactions of hydrazines with dicarbonyl compounds form heterocyclic compounds such as pyrazoles, diazenes, and 1,2,4-triazoles.[5-7] Substituted hydrazines are also used to make other crucial heterocyclic molecules such as thiosemicarbazides, pyridazines, and 1,3,4-thiadiazoles (Scheme 1-1).[8-10]

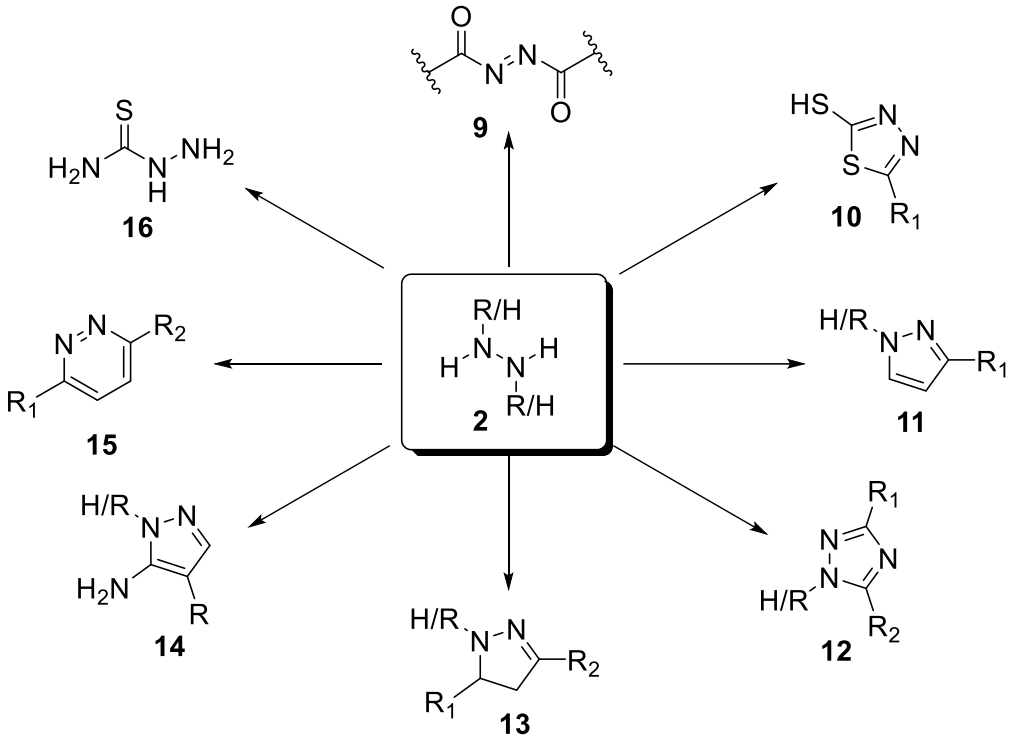

Scheme 1-1 Hydrazine building blocks

1.2.2 Preparation of hydrazines

Substituted hydrazine synthesis has been well studied, and their scope and limitations were established (Scheme 1-2).[11-13] Hydrazines are commonly prepared by reducing already established N–N bonds (**A**, **B**, and **C**).[14-15] Reducing two equivalents of a nitro compound is another approach to form N–N bond (**D**).[16] Reducing both azo and nitro compounds require excess, or at least stoichiometric, reducing agent such as zinc powder. Both procedures generate large quantities of reagent waste. Intermolecular nucleophilic substitution reaction by amines forms N–N bond and affords hydrazines (**E**).[17] Direct installation of hydrazines by transition metal catalyzed cross-coupling reactions between amines and aryl halides offer access to *N*,*N*′-substituted hydrazines (**F**).[18-22] However, in these reactions highly toxic and carcinogenic hydrazine is needed, and atom efficiency is low.

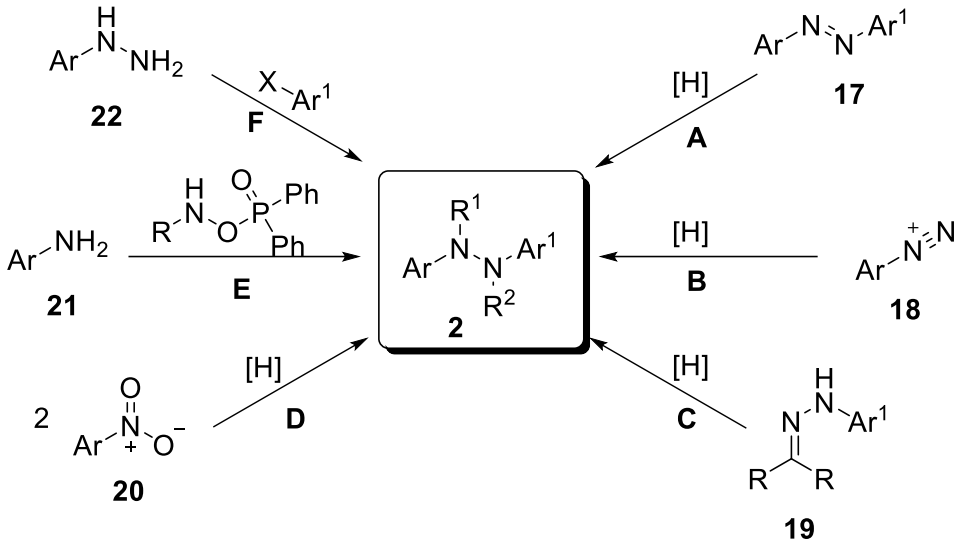

Scheme 1-2 Synthetic routs for the synthesis of hydrazine derivatives

1.3 Pyrazoles

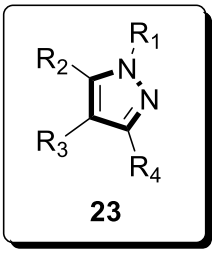

More than 300 pharmaceuticals and natural products contain N–N bonds.[23] The agrichemical and pharmaceutical industries use substituted pyrazoles **23** (five-membered cyclic aromatic organic molecules that contain two adjacent nitrogen atoms) extensively.[24-33] In particular, 1,3,5- and 1,3,4,5-substituted pyrazoles make up the core of several commercialized drugs (e.g. Viagra **24**, Acomplia **25**, Celebrex **26**) and agricultural chemicals (e.g. Pyraclostrobin **27**, Tebufenpyrad **28**, Fipronil **29** (Figure 1-3). The ubiquity of biologically active pyrazole containing compounds inspired researchers to focus on novel methods of forming N–N bonds.

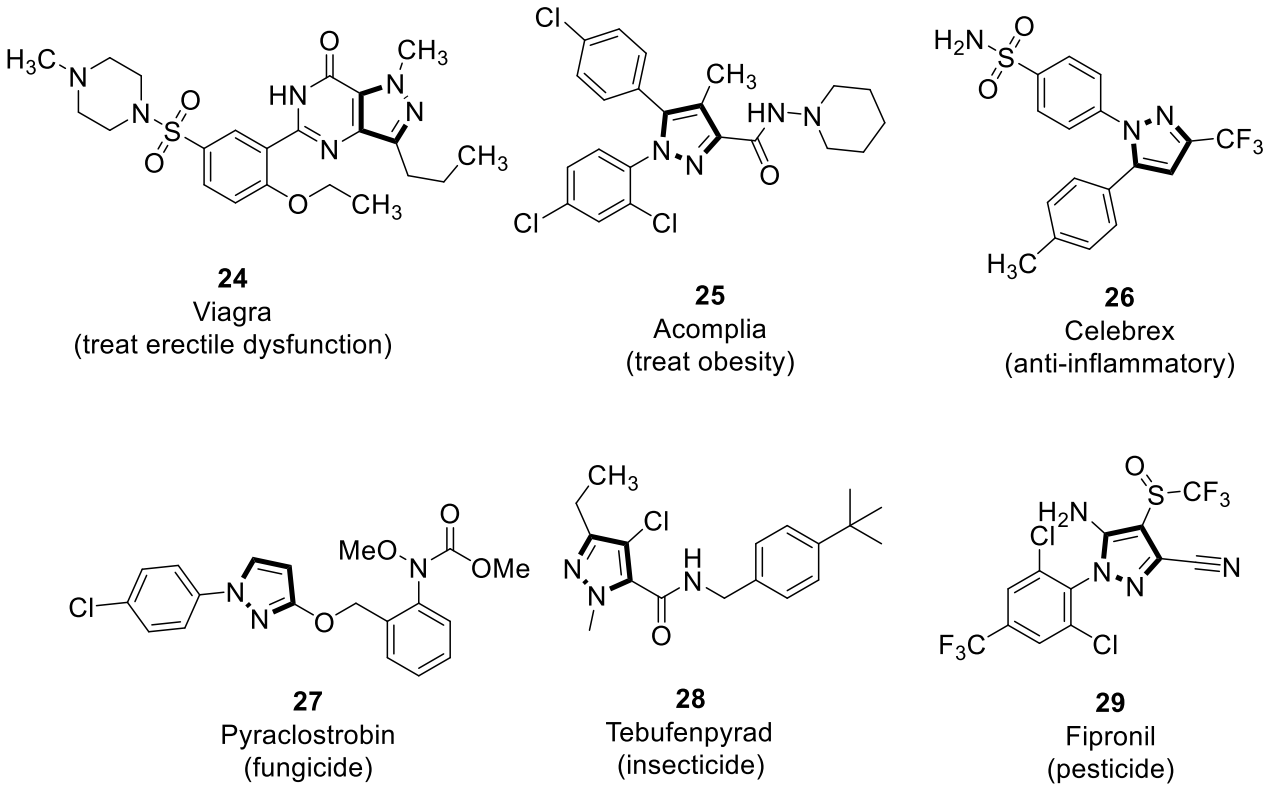

Figure 1-3 Bioactive pyrazoles

1.3.1 Overview of common methods to prepare pyrazoles

Cyclocondensation of an appropriate hydrazine with difunctional three-carbon building blocks, such as 1,3-dicarbonyl compounds or *α,β*-unsaturated carbonyl compounds (**30** and **34-39**), is the classical synthetic method for preparing substituted pyrazoles and remains the standard method used today (Figures 1-4 and 1-5).[30,32-51]

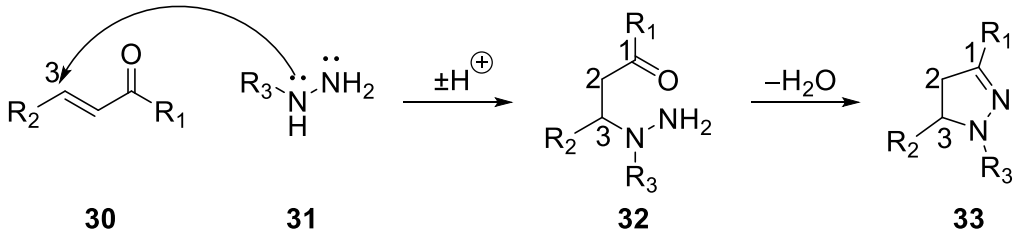

Figure 1-4 Cyclocondensation of α,β-unsaturated carbonyl compounds

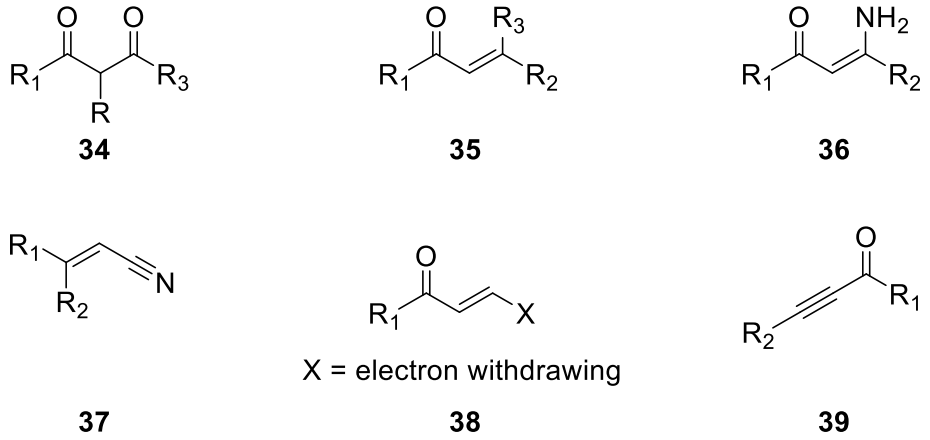

Figure 1-5 3-Carbon building blocks for pyrazole synthesis

German chemist Ludwig Knorr first synthesized a pyrazole compound in1884. Knorr found that ethyl acetoacetate **41** reacts with phenylhydrazine **40** in the presence of an acid catalyst to afford 1-phenyl-3-methyl-5-pyrazolone **42** (Equation 1-1).[52]

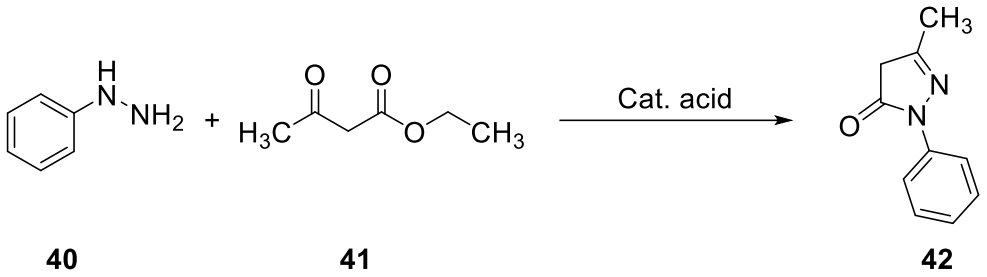

Equation 1-1 Knorr synthesis

Knorr named this class of compounds pyrazoles to indicate that the core was derived from pyrrole, replacing a carbon atom with nitrogen. The main limitation for Knorr-type pyrazole synthesis is the absence of regioselectivity; unsymmetrically substituted 1,3-diketones ($R_1 \neq R_3$) **34** have two electrophilic centers, which results in two regioisomers (Scheme 1-3).

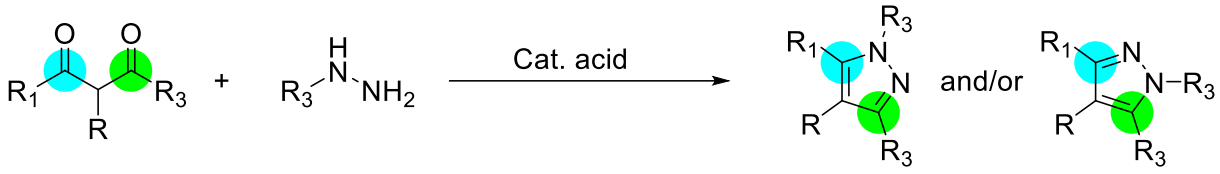

34 **31** **43** **44**

Scheme 1-3 Regioisomers in Knorr synthesis

Pyrazole synthesis using hydrazones **45**, semicarbazides **46**, and diazonium salts **47** as starting material are common in literature (Figure 1-6).[53-72] Hydrazine or diazo derivatives are known explosives and environmental neurotoxins.[73-76] Use of these starting materials limits application to large-scale commercial synthesis of pyrazoles.[77-78] Many classical pyrazole syntheses suffer from further disadvantages, including unsatisfactory yields, low selectivity, harsh reaction conditions, expensive starting materials, hazardous solvents, high catalyst loading, and/or limited substrate scope. Efficient, regioselective synthesis of substituted pyrazoles using less hazardous materials remains an unsolved problem.

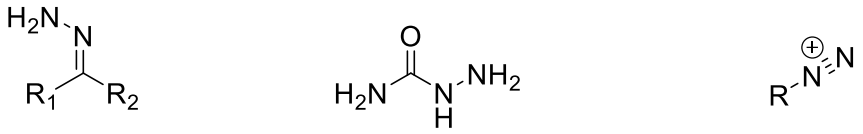

45 **46** **47**

Figure 1-6 Pre-formed N–N bond starting materials

1.3.2 Pyrazole synthesis: without relying on pre-formed N–N bond

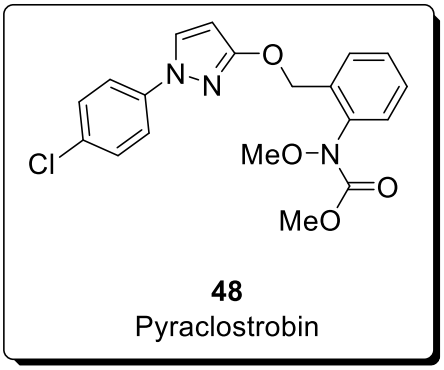

48
Pyraclostrobin

Our interest in pyrazole synthesis was to solve the limitations in large-scale pyraclostrobin **48** synthesis. Pyraclostrobin is an agricultural pesticide, used to preserve valuable crops. A general synthetic route is outlined in Scheme 1-4. The first two steps of this procedure are the main limitations. Both 4-chlorobenzenediazonium salt **50** and 4-chlorophenylhydrazine **51** are known explosives and requires extra precautions in large-scale synthesis. These reactions also require dilute aqueous solution, which generates huge amounts of wastewater every year. An ideal synthetic route would make pyraclostrobin without forming explosive intermediates.

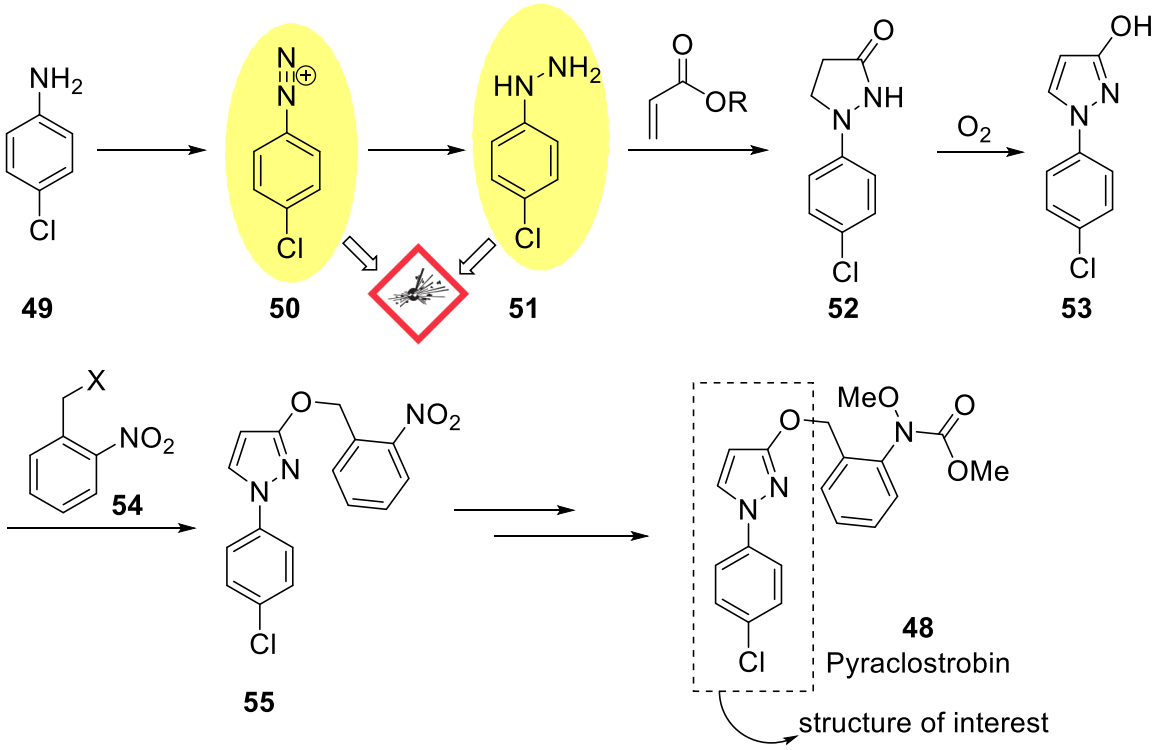

Scheme 1-4 Synthetic route of Pyraclostrobin

Our goals for hydrazine-free pyrazoles synthesis are outlined in Scheme 1-5. We envisioned three ways to synthesize pyrazoles: (1) by intramolecular nucleophilic displacement (route I), (2) by transition metal catalyzed oxidative coupling N–N bond formation (route II), and (3) electrochemical N–N bond formation (route III).

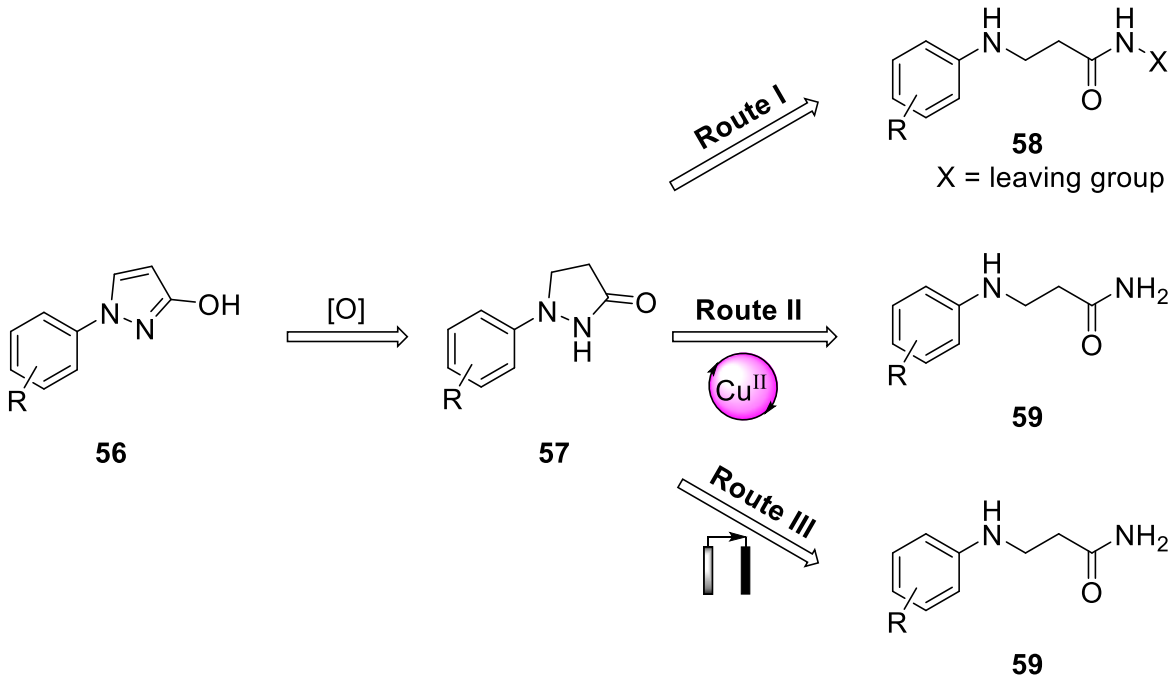

Scheme 1-5 Three possible pathways to make N–N bond

All three possible pathways shown above will be evaluated within this thesis. It was our wish to not only modify the pyraclostrobin synthesis, but also to develop a robust, general methodology for the synthesis of hydrazines, pyrazoles, and other similar heterocycles. Our efforts to synthesize pyrazoles by intramolecular nucleophilic displacement are discussed in this chapter.

1.4. Route I: N–N bond formation by nucleophilic displacement

1.4.1 Nucleophilic displacement of N-haloamides

There are several reports showing that N–N bonds are formed by intermolecular nucleophilic displacement of *N*-haloamides.[79-82] Selective oxidation of amides to *N*-chloroamide or *N*-bromoamide using halogenating reagents is well documented.[83-86] The nitrogen of *N*-haloamides are electrophilic since the halides are good leaving groups (Scheme 1-6). In 1968, Marcus and Neal prepared **62** by nucleophilic displacement of *N*-chloroamine (Figure 1-7). Later,

Baum and Grakauskas reported a similar reaction where **64** is formed as a side product during direct fluorination of urea (Figure 1-7). Bergman used nucleophilic displacement to synthesize 6-(dimethylamino)-6*H*-indolo[2,3-b]-quinoxaline **66** from indophenazine and dimethylchloroamine (Figure 1-7).

Scheme 1-6 Formation of N-haloamides

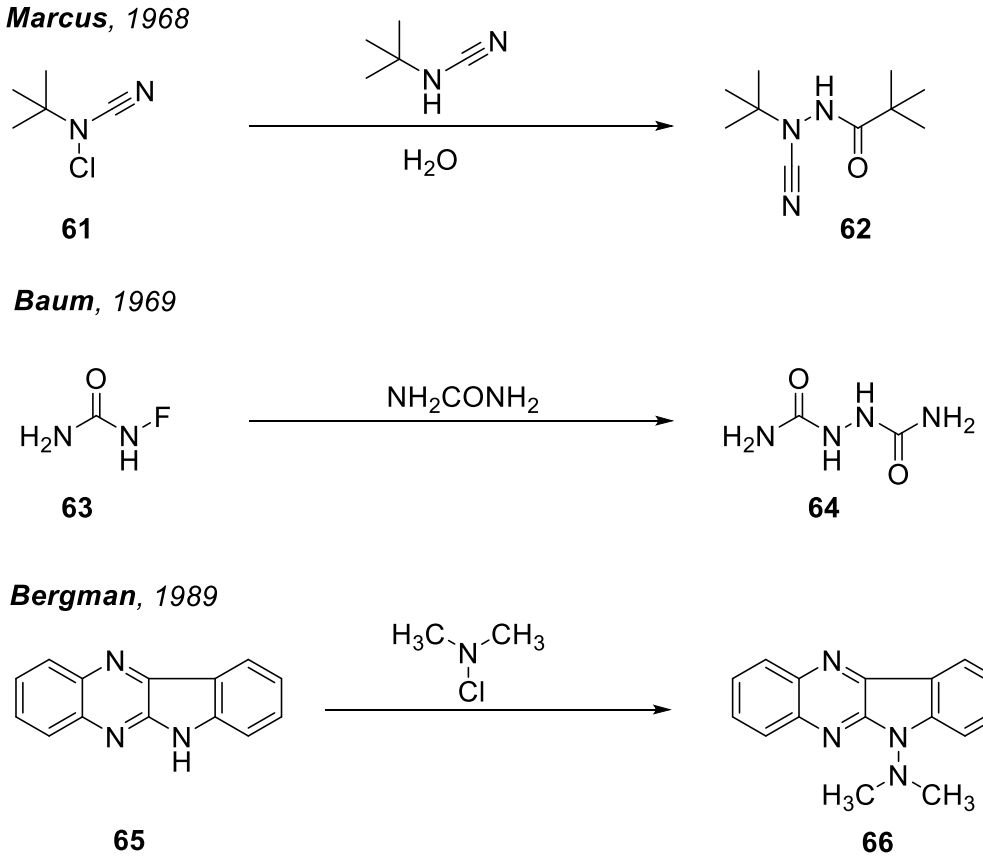

Figure 1-7 N–N Bond formation by nucleophilic displacement

We expected selective oxidation of the amide nitrogen in 3-(phenylamino)propanamide **67** to a N-haloamide intermediate **68**. Subsequent intramolecular cyclization by nucleophilic displacement would form an N–N bond, affording 1-phenylpyrazolidin-3-one **69** (Scheme 1-7).

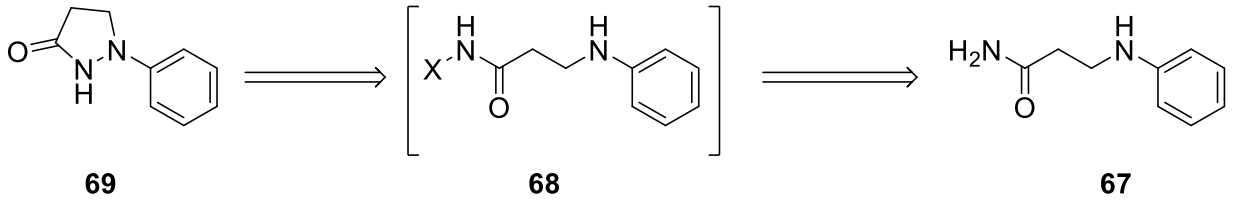

69 **68** **67**

Scheme 1-7 Reaction hypothesis for nucleophilic displacement of N-haloamides

However, reactions between 3-(phenylamino)propanamide **67** and N-bromosuccinimide (NBS) or N-chloroosuccinimide (NCS) or trichloroisocyanuric acid (TCCA) did not afford 1-phenylpyrazolidin-3-one **69**. Instead, the phenyl ring was halogenated since the *ortho*/*para* directing amine activates the phenyl group, and a complex mixture was obtained (Equation 1-2).

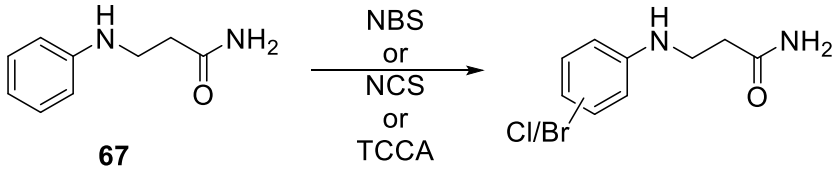

67 complex mixture

Equation 1-2 Reaction with halogenated reagents

1.4.2 Nucleophilic displacement of hydroxamic acid derivatives

Okawara et al. reported a procedure for N–N bond formation by nucleophilic displacement to give 1-acyl-2alkylhydrazine **73** (Figure 1-8). In this reaction, hydroxamic acid **70** reacts with activating groups, such as 2-chloro-1-methylpyridiniumiodide **74** and *p*-toluenesulfonyl chloride **75**, to convert the hydroxyl group into a good leaving group (**71**, **72**). An intermolecular

nucleophilic substitution reaction occurs with benzylamine in the presence of a base to give 1-acyl-2-alkyl hydrazines **73**.[87]

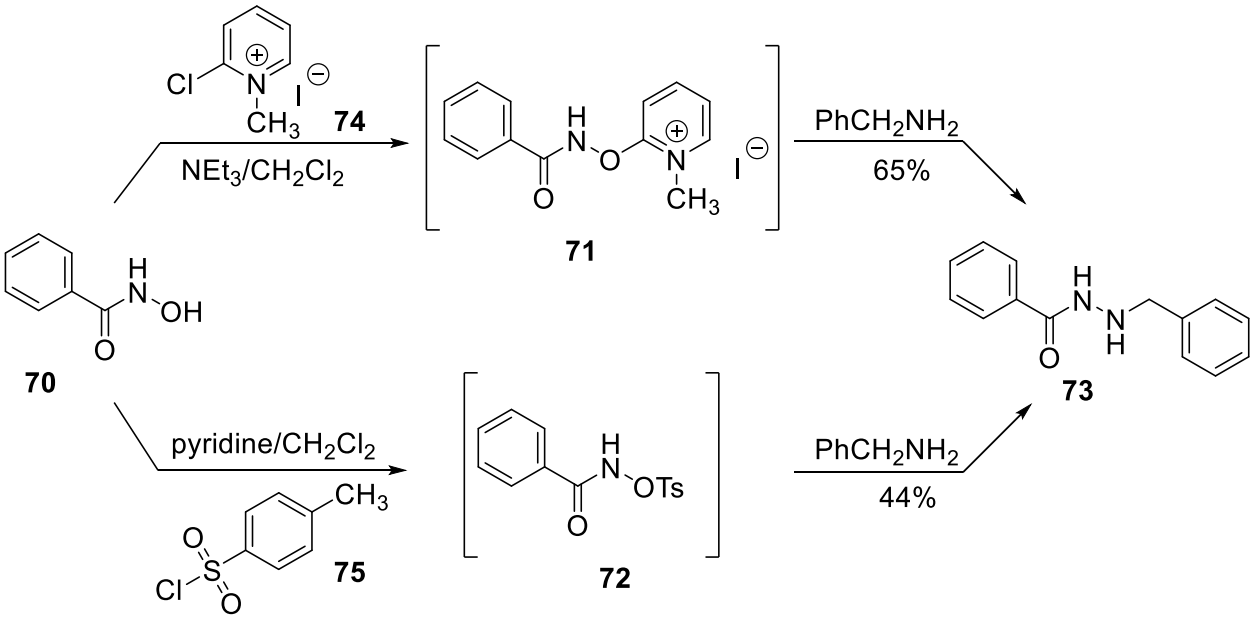

Figure 1-8 Okawara's N–N formation reaction

Stambuli and coworkers reported a similar metal-free N–N bond formation to prepare 1*H*-indazoles **78** by an intramolecular nucleophilic substitution reaction starting from *ortho*-aminobenzoximes **76** under mild reaction conditions (Equation 1-3).[88-89]

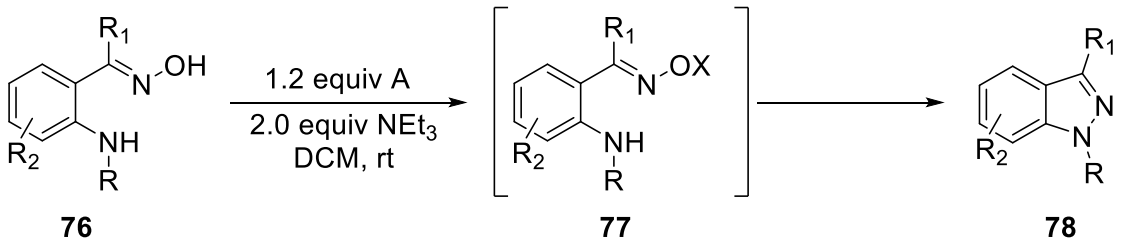

activating agent
A = acetyl chloride, Boc_2O, methyl chloroformate, MsCl, TsCl
X = OAc, Boc, CH_3OCO, Ms, Ts

Equation 1-3 Stambuli's reaction

The Okawara and Stambuli syntheses are very robust with broad substrate scope. The results were promising enough for us to try a pyrazole synthesis by intramolecular substitution reaction. In particular, Okawara's results show that the intermolecular substitution reaction by an amine is the major reaction pathway, despite the possibility of Lossen rearrangement. We believed an intramolecular displacement reaction could afford our desired pyrazole as shown in Scheme 1-8.

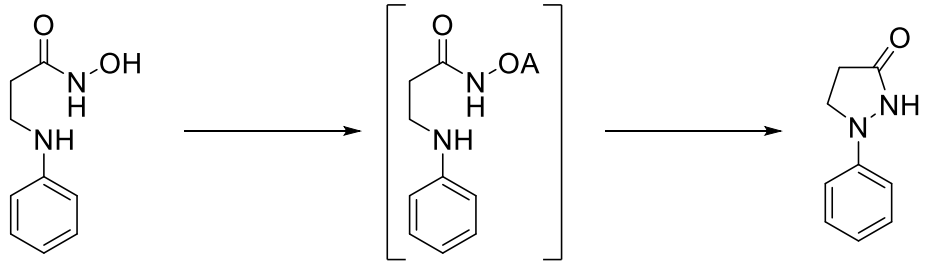

79 **80** **69**

Scheme 1-8 Reaction hypothesis for nucleophilic displacement of hydroxamic acids

To test this, N-hydroxy-3-(phenylamino)propanamide **79** was prepared via a Michael addition reaction between commercially available stable starting materials aniline **81** and methyl acrylate **82**. Subsequent conversion to N-hydroxy-3-(phenylamino)propanamide **79** with hydroxylamine hydrochloride should give us a pathway to N–N bonds by replacing the N-hydroxyl functionality with a good leaving group (Equation 1-4).

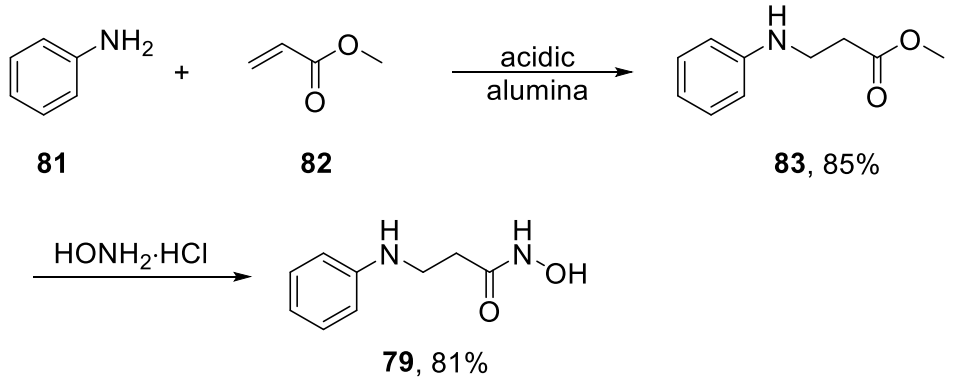

Equation 1-4 Preparation of N-hydroxy-3-(phenylamino)propanamide

Unfortunately, similar reaction conditions to Okawara's work with N-hydroxy-3-(phenylamino)propanamide **79** did not form an N–N bond. Rather, I found that arylimidazolidone **84** was formed *via* Lossen Rearrangement instead of 1-phenylpyrazolidin-3-one **69** (Equation 1-5).

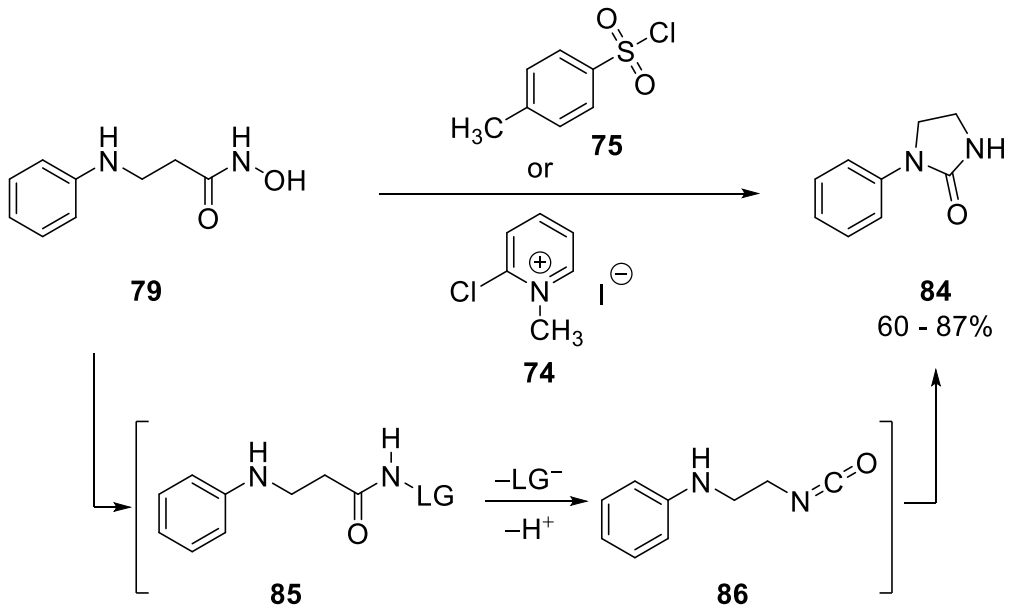

Equation 1-5 Lossen rearrangement product formation

1.5 Summary

Intramolecular nucleophilic displacement of both N-haloamides and hydroxamic acid derivatives were tested. However, both the reactions were equally unsuccessful. A complex mixture was observed with halogenated reagents whereas Lossen rearrangement product was formed using Okawara's reaction conditions.

Chapter 2: Copper-catalyzed Hydrazine-free Synthesis of Substituted Pyrazoles by Oxidative N–N Bond Formation

2.1 Goal of the project

Undoubtedly transition metal catalysis is a powerful tool in modern chemistry, used to cleave/form carbon–hydrogen, carbon–carbon, and carbon–heteroatom bonds and, importantly, to form nitrogen–nitrogen bonds. Transition metals such as both Cu(I) and Cu(II), Ni^{II}/Ni^{III}, Rh^{III}/Cu^{II}, and palladium complexes are commonly used for N–N bond-forming reactions (Figure 2-1).[90-92,99-101] General strategies also involve oxidizing agents such as hypervalent iodine reagents, e.g., phenyliodine(III)bis-(trifluoroacetate) (PIFA), potassium permanganate ($KMnO_4$), silver(I) oxide (Ag_2O), or sodium dichromate ($Na_2Cr_2O_7$).[93-97]

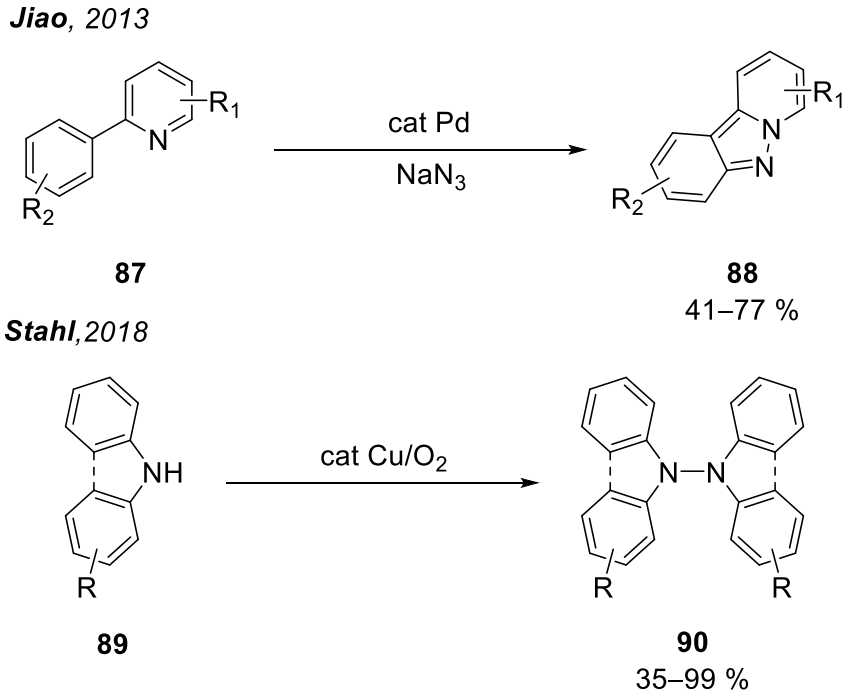

Figure 2-1 Selective examples of N–N bond formation reactions

There are primarily three classes of coupling partners used to form N–N bonds: (i) amide–amine coupling, (ii) imine/imidate–amine coupling, and (iii) amine–amine coupling. However, only first two types are related to pyrazole synthesis (Figure 2-2).

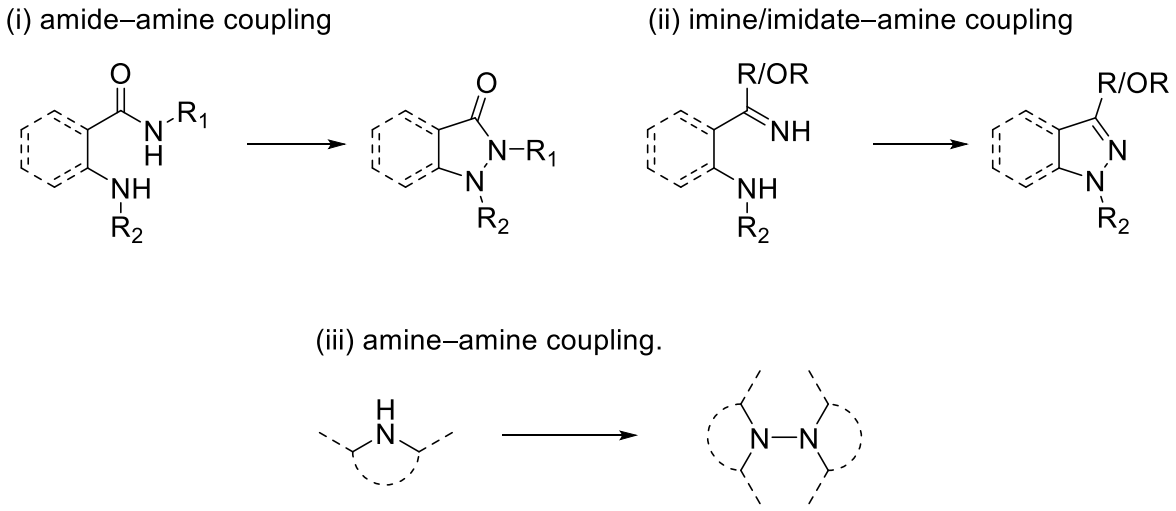

Figure 2-2 Possible N–N coupling routes

2.2 Route II: Oxidative N–N bond formation

2.2.1 Representative examples of amide-amine coupling

In 2006 the Tellitu and Domínguez group reported a hypervalent iodide phenyliodine(III)bis-(trifluoroacetate) (PIFA) catalyzed synthesis of indazol-3-ones **92** through intramolecular N–N bond formation from N-phenyl-2-(phenylamino)benzamide **91** in the presence of trifluoroacetate (TFA) (Equation 2-1).[96-97] The authors proposed that the reaction proceeds *via* an N-acylnitrenium intermediate **93**. The reaction was unsuccessful when R_1 = H or an electron-withdrawing group, suggesting that the cyclization step requires highly nucleophilic amines. On the other hand, neither alkyl nor alkoxyamides rendered the desired indazolones. An aryl group is necessary to stabilize the corresponding N-acylnitrenium intermediate.

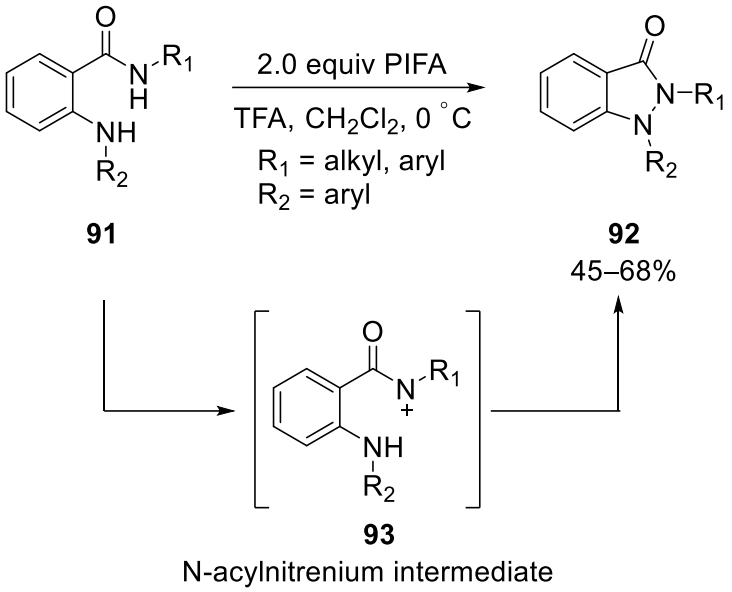

Equation 2-1 PIFA mediated indazol-3-ones synthesis

The Zhou group reported a similar reaction using a copper bromide catalyst in air at 120 °C.[98] The reaction proceeds via a single electron transfer process as shown in Equation 2-2. However, the reaction became sluggish when R_1 group is alkyl, and the reaction failed when one or both of the R_1 and R_2 groups were hydrogen.

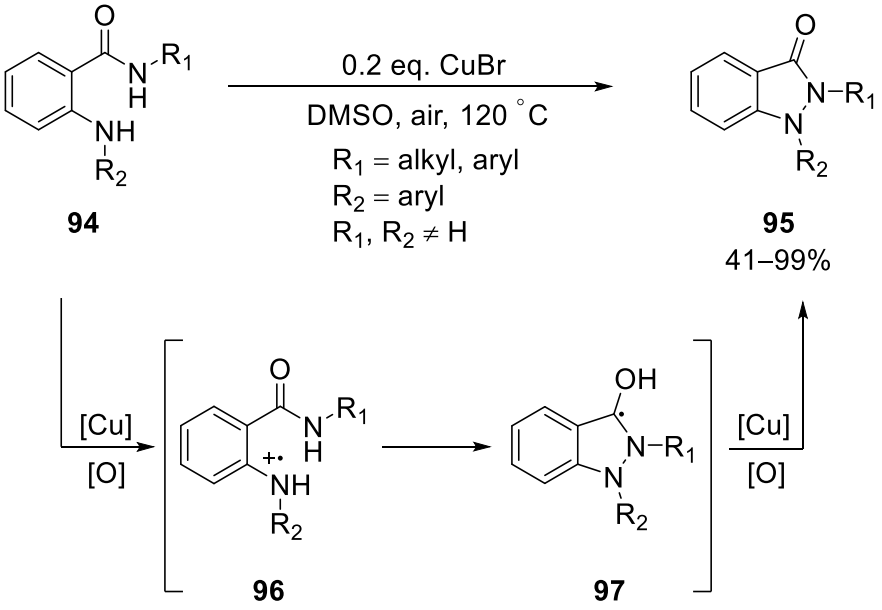

Equation 2-2 Zhou's copper-catalysed indazole synthesis

2.2.2 Attempts towards amide– amine coupling

Our attempts to oxidize 3-(phenylamino)propanamides either **67** or **98** directly with different oxidants such as $KMnO_4$, Cu(II)/O_2, [bis(trifluoroacetoxy)iodo]benzene, with subsequent cyclization did not provide the desire products (Equation 2-3). This shows the unreactive nature of the primary amide.

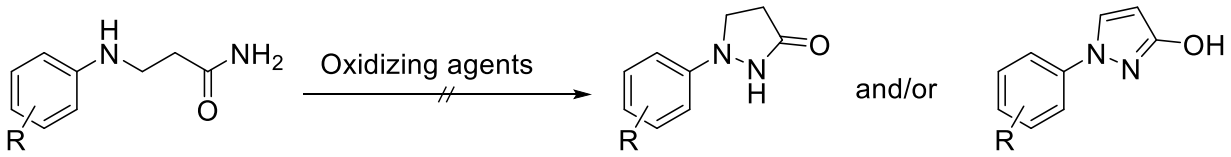

R = H, **67**
R = Cl, **98**

R = H, **69**
R = Cl, **52**

R = H, **99**
R = Cl, **53**

Equation 2-3 Initial attempts to oxidize 3-(phenylamino)propanamides

To test the reactivity of secondary amides, I prepared 3-(4-chlorophenylamino)-N-phenylpropanamide **101** and N-benzyl-3-(4-chloroanilino)propanamide **105** (Equations 2-4 and 2-5). However, under similar conditions, the reactions were equally unsuccessful.

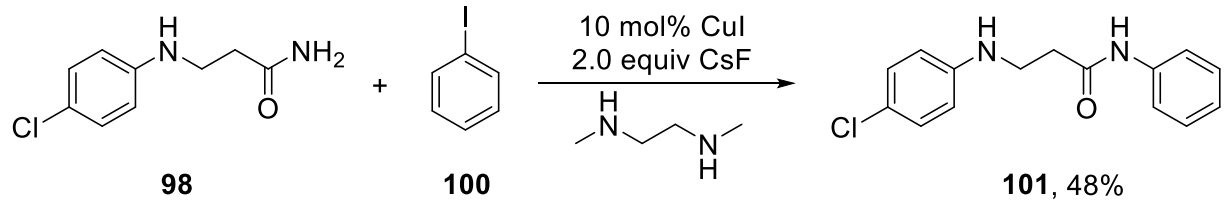

98 **100** **101**, 48%

Equation 2-4 Preparation of **101**

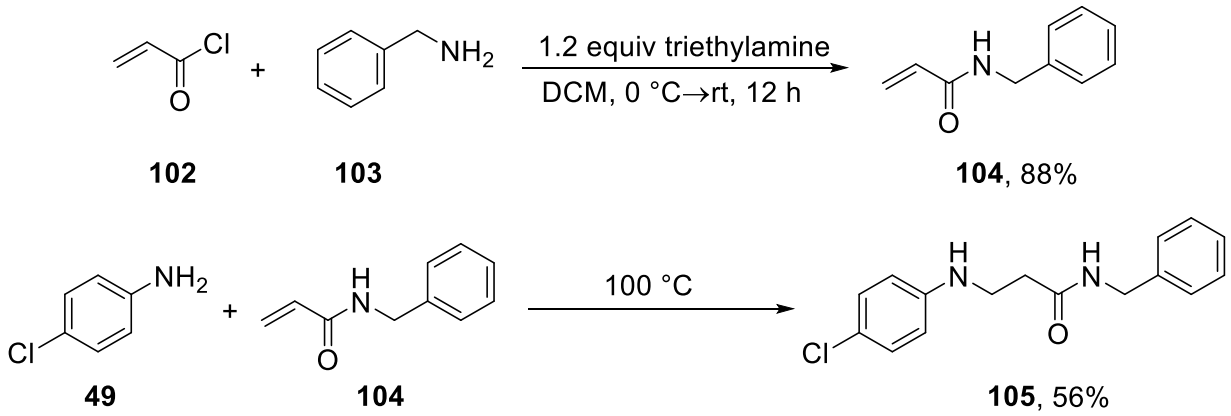

Equation 2-5 Preparation of **105**

2.2.3 Representative examples of imine/imidate-amine coupling

Nagasawa and Ueda reported the copper-catalyzed synthesis of 1,2,4-triazoles **107** *via* oxidative N–N bond formation (Equation 2-6).[99] The reaction performed equally well under several reaction conditions. They found that 2-phenyl-1,2,4-triazolopyridine formed in 89% of yield in presence of 5 mol% CuBr, 5 mol% 1,10-phenanthroline (1,10-Phen) and 10 mol% of ZnI_2 in 1,2-dichlorobenzene (DCB) in air. Similar results were obtain when stoichiometric $Cu(OAc)_2$ was used under an argon atmosphere at 130 °C. The presence of a copper catalyst was essential for the reaction, but the role of zinc iodide is unknown in first reaction conditions. Transmetallation can be the possible reason in presence zinc: zinc coordinates to the substrate first then the intermediate **108**, which forms by transmetallation and goes on to the product. However, the authors only proposed that reaction proceeds through an amidine intermediate **108**. Cyclization occurs via intramolecular oxidative N–N bond formation. The copper is oxidized by molecular oxygen present in air and completes the catalytic cycle.

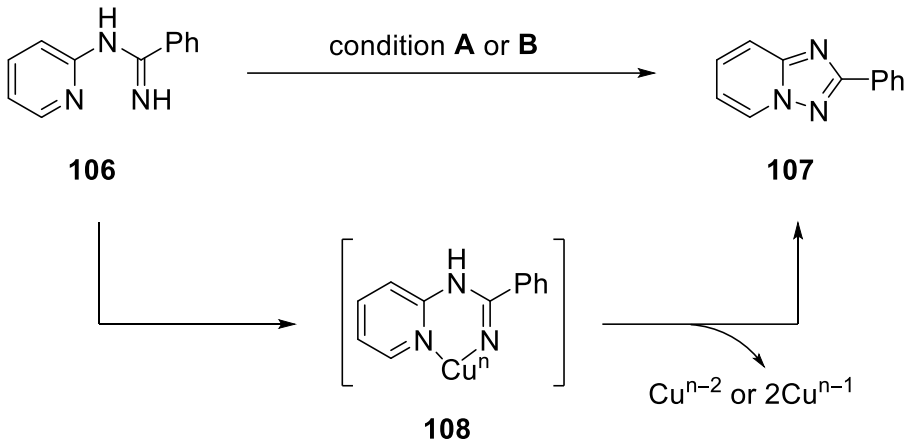

A: CuBr (5 mol%), 1,10-phen (5 mol%),
ZnI_2 (10 mol%), DCB, 130 °C, air, 24 h, 89% yield
B: $Cu(OAC)_2$ (100 mol%), DCB, Ar, 130 °C, 12 h, 79% yield

Equation 2-6 Nagasawa's 1,2,4-triazoles synthesis

In 2010, the Glorius group reported a copper mediated tetrasubstituted pyrazole **112** synthesis from enamines **109** and nitriles **110** (Equation 2-7).[100] They propose that the reaction proceeds through a six-membered Cu^{II} chelate **111** and subsequent reductive elimination provides pyrazoles (Figure 2-3).

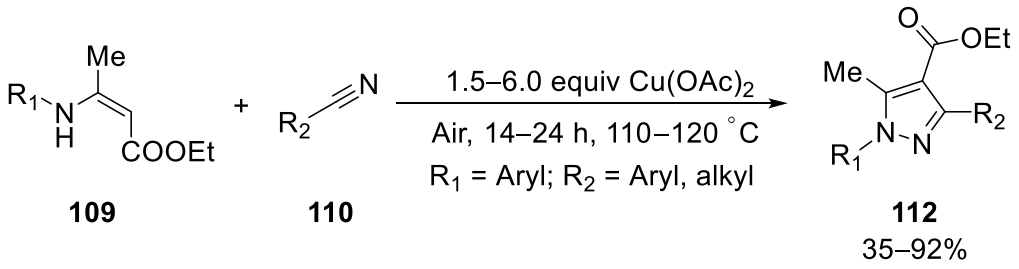

Equation 2-7 Glorius's copper-catalyzed pyrazole synthesis

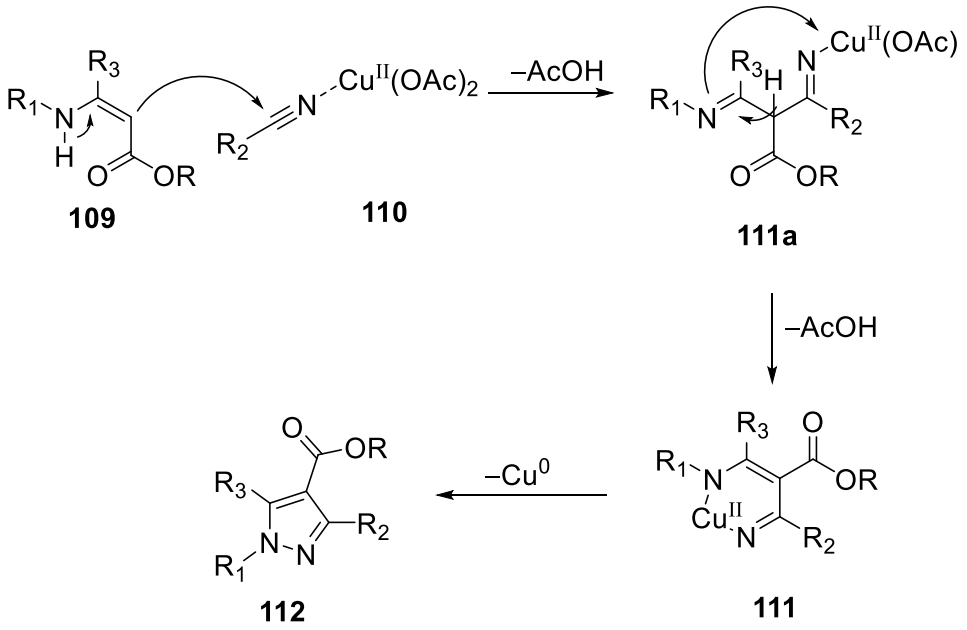

Figure 2-3 Proposed mechanism of Glorius's pyrazole synthesis

The Glorius group also showed a Rh^{III}/Cu^{II} co-catalyzed 1*H*-indazoles **116** synthesis from ethyl phenylimidate **113** and tosyl azide **114** *via* C–H amidation and subsequent N–N bond formation (Equation 2-8).[101] The authors proposed that $[Cp^*Rh_2]_2$ is oxidized to cationic $[Cp^*Rh^{III}]$ in situ in the presence of $AgSbF_6$. The imidate then coordinates to $[Cp^*Rh^{III}]$, enabling *ortho*- C–H bond activation. The tosyl azide then coordinates to the rhodium and C–N bond formation provides the imidate intermediate **115**. Imidate **115** coordinates with copper acetate, and transmetallation followed by N–N bond formation by reductive provides desired compound **116**.

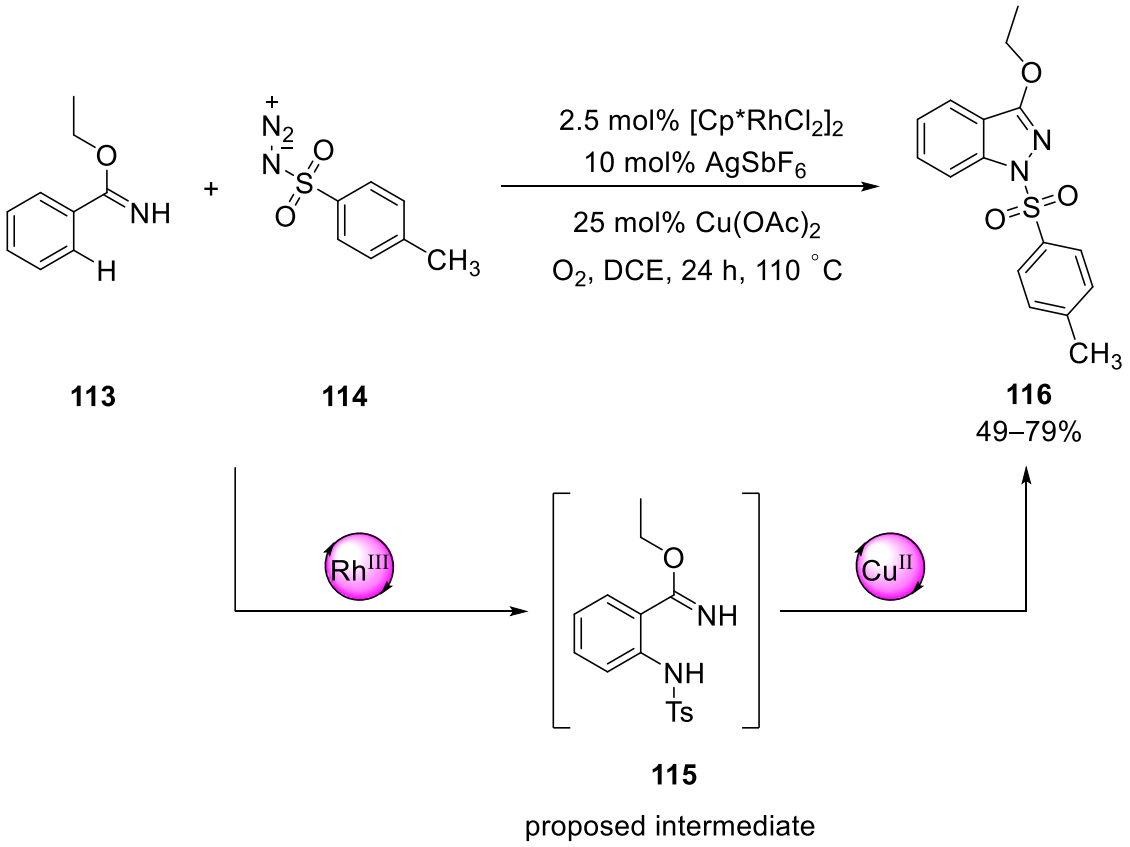

Equation 2-8 Glorius's 1*H*-indazoles synthesis

Recently, the Chen group reported a similar copper-catalyzed reaction. They found that 1-(ortho-hydroxyaryl)-1*H*-indazoles **120** are formed from *ortho*-aminoaryl N–H ketimines. Further, they showed that indazoles **118** are favoured when using copper salts like Cu(OAc), CuCl, CuBr, $CuBr_2$ and CuI, whereas copper salts such as $Cu(OTf)_2$, $Cu(NO_3)_2$, $CuSO_4$, CuO, and $Cu(acac)_2$ favoured 1-(*ortho*-hydroxyaryl)-1*H*-indazoles **120** by tandem C–H *ortho*-hydroxylation and N–N bond-formation (Figure 2-4).[102-103]

Chen, 2016

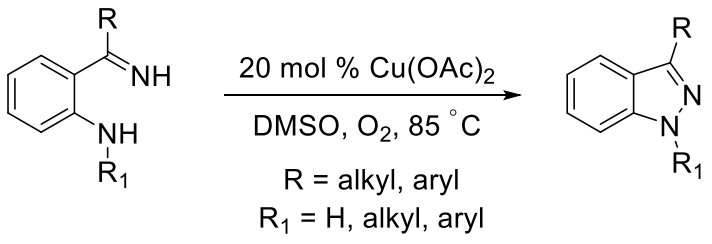

117 **118**
51–90%

Chen, 2017

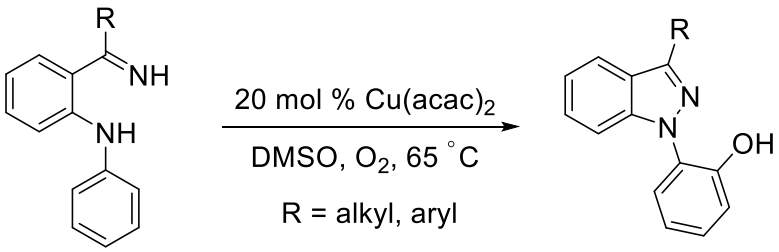

119 **120**
51–86%

Proposed mechanism:

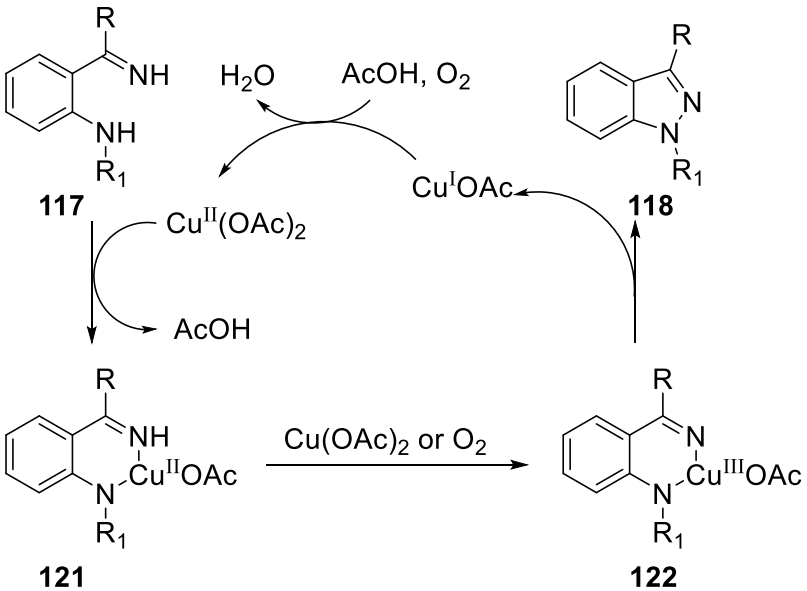

Figure 2-4 Chen's N–N bond formation

2.2.4 Attempts towards amide-amine coupling

We envisioned that imidate ester **125** would be more reactive than the amides **67**, **98**, **101**, **105** and might form the desired intramolecular N–N bond. We hypothesized that nitrile **126** would react with alcohols to afford imidate ester **125**, which could provide 4,5-dihydro-1*H*-pyrazole **124** *via* PIFA or copper-catalyzed oxidative N–N bond formation. Oxidation of 4,5-dihydro-1*H*-pyrazole **124** would afford pyrazole **123** (Scheme 2-1).

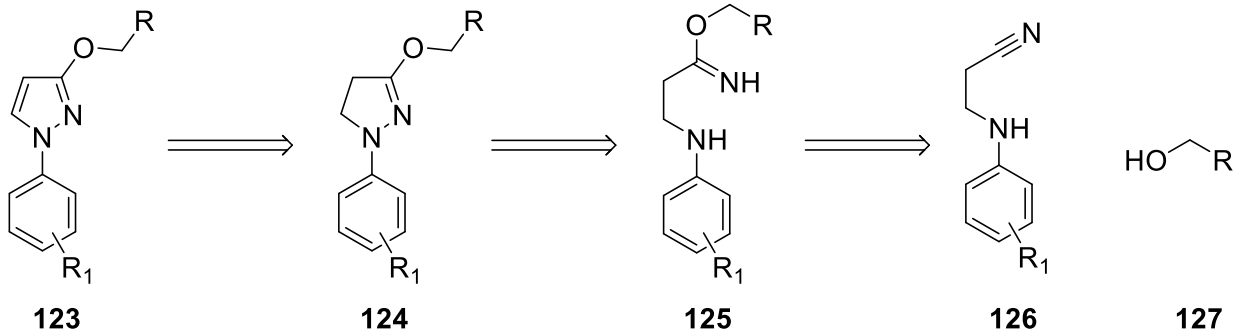

Scheme 2-1 Reaction hypothesis for amide-amine coupling

2.2.4.1 Preparation of amino acrylonitriles

β-Amino acrylonitriles **130** were prepared from anilines and acrylonitrile by a Micheal addition reaction in the presence of catalytic lithium tetrafluoroborate (Figure 2-5).

Pyridazines, a six-membered aromatic ring with two adjacent nitrogen atoms, are important structural motifs often found in bioactive natural products. 4-Aminobutanenitriles **139** and **140** were prepared to test if we can prepare 1,4,5,6-tetrahydropyridazines by oxidative N–N bond formation (Figure 2-6).

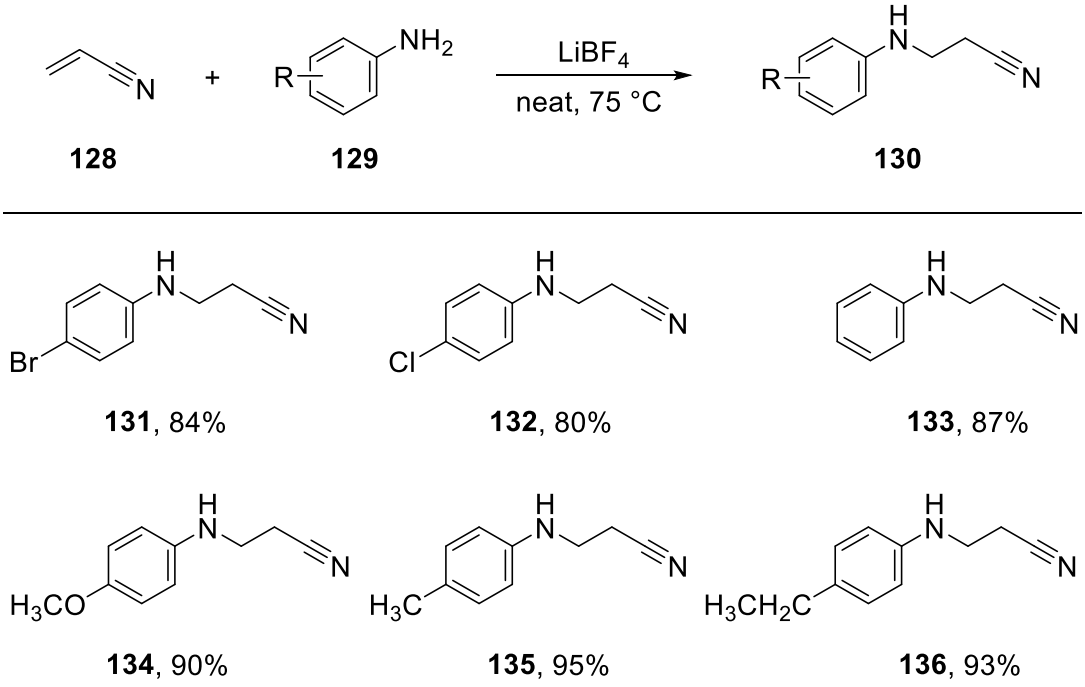

Figure 2-5 Preparation of β-amino acrylonitrile

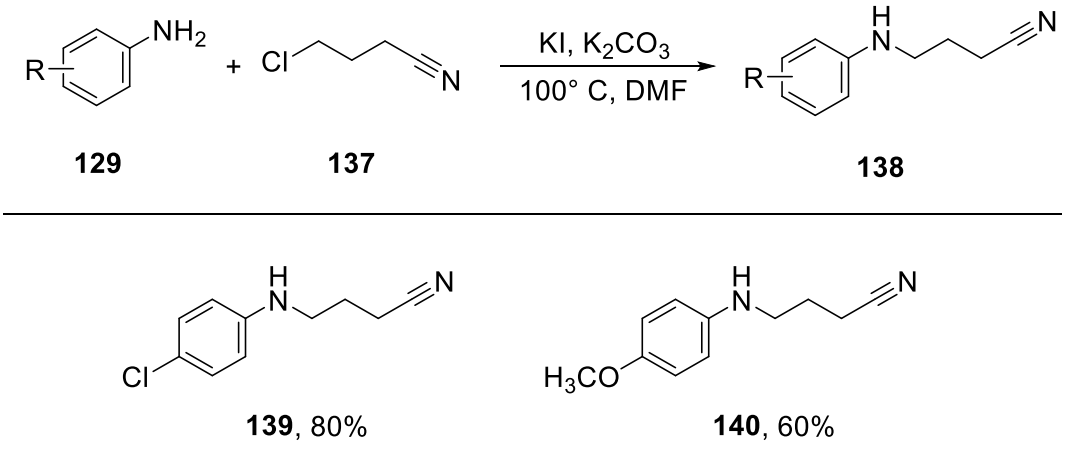

Figure 2-6 Preparation of 4-aminobutanenitrile

2.2.4.2 Optimization study

To test the hypothesis, we used 3-(4-chloro-anilino)-propionimidic acid ethyl ester **142** as a model compound. Compound **142** was prepared from β-amino acrylonitrile **132** and ethanol with hydrochloric acid present (Equation 2-9).

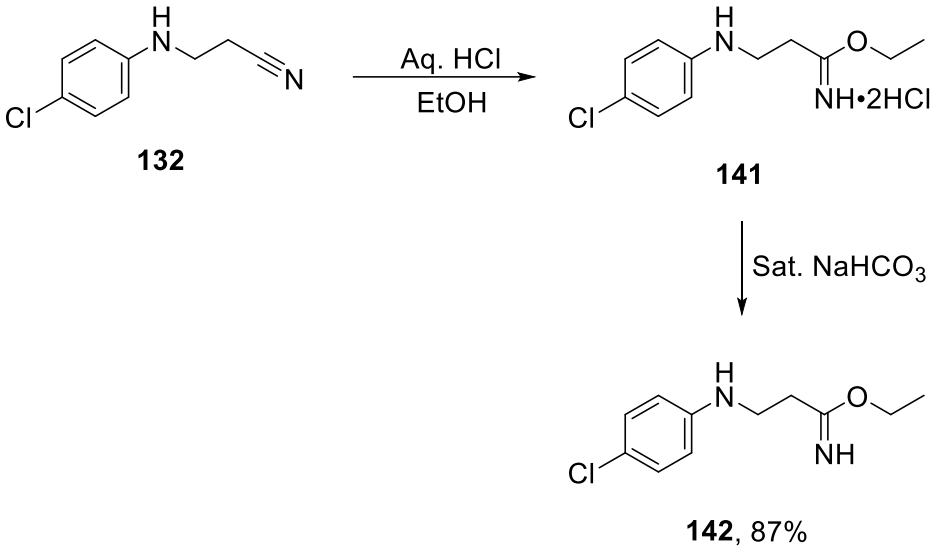

132 **141** **142**, 87%

Equation 2-9 Preparation of 3-(4-chloro-anilino)-propionimidic acid ethyl ester

We first tried Tellitu's PIFA mediated conditions on 3-(4-chloro-anilino)-propionimidic acid ethyl ester **142** to make an N–N bond. Treatment with two equivalents of phenyliodine(III)bis-(trifluoroacetate) gave 3-ethoxy-1-(4-chlorophenyl)pyrazole **143**, but the yield was poor with a complex reaction mixture (Equation 2-10).

142 **143**
very low yield

Equation 2-10 PIFA mediated N–N bond formation

Copper-catalyzed oxidative N–N bond formation is a more attractive option than using stoichiometric hypervalent iodine reagents. We found that using 20 mol% copper(II) 2-ethylhexanoate as a catalyst in DMSO at 80 °C yielded only 17% of **143**. Copper(II) acetate monohydrate improved the reaction to some extent, but we observed that the starting material hydrolyzed and formed ethyl 3-(4-chlorophenylamino)propanoate **147** (ca. 38%) (entry 2, Table 2-1). Using copper acetate $Cu(OAc)_2$ reduced the amount of side product **147** and improved the yield of 3-ethoxy-1-(4-chlorophenyl)pyrazole **143** to 43% (entry 3, Table 2-1). The yield of **143** decreased to 14% with lowering the catalyst loading (entry 4, Table 2-1). We observed that the amount of ethanol elimination side product 3-(4-chlorophenylamino)propanenitrile **132** increased with an increase in temperature. The ratio of **143**:**132** was the highest at 60 °C, and this was selected as the optimal temperature for further studies (entry 7, Table 2-1). With increased loading of copper acetate the yield of pyrazole **143** decreased. When one equivalent copper acetate was used **143** formed in a yield of 13% and mostly hydrolyzed product **147** was observed.

Table 2-1 Optimization study: screening of temperature and catalyst loading

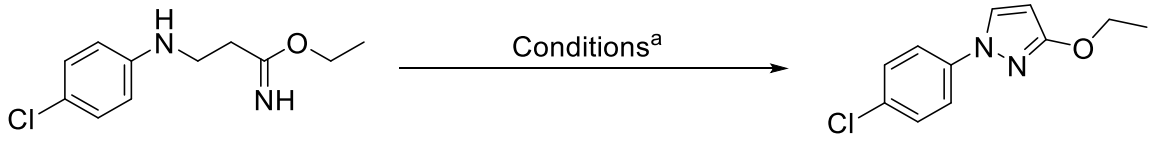

142 **143**

Entry	Additive (mol %)	Temp. (°C)	Solvent	Yield[b] (%)
1	Copper(II) 2-ethylhexanoate (20)	80	DMSO	17
2	$Cu(OAc)_2 \cdot H_2O$ (20)	80	DMSO	27
3	$Cu(OAc)_2$ (20)	80	DMSO	43
4	$Cu(OAc)_2$ (10)	80	DMSO	14
5	$Cu(OAc)_2$ (20)	100	DMSO	33
6	$Cu(OAc)_2$ (20)	70	DMSO	37
7	$Cu(OAc)_2$ (20)	60	DMSO	51

8	$Cu(OAc)_2$ (50)	60	DMSO	35
9	$Cu(OAc)_2$ (100)	60	DMSO	13

[a]all the reactions carried out under oxygen for overnight unless otherwise mentioned. [b]determined by ^1H NMR spectroscopy.

We next examined different solvents using copper acetate as a catalyst at 60 °C. Unfortunately, solvents such as TFE, anisole, dioxane, and propylene carbonate did not improve the results. DMSO was therefore used as the solvent for further optimization studies.

Table 2-2 Optimization study: screening of solvents

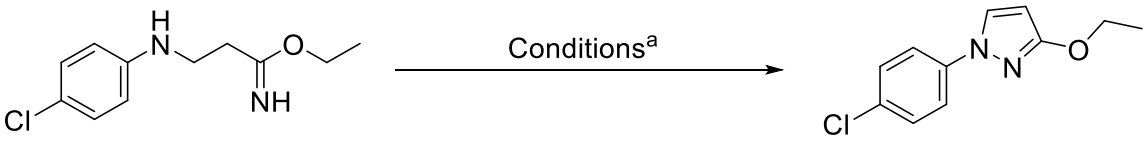

142 **143**

Entry	**Additive (mol %)**	**Temp. (°C)**	**Solvent**	**Yield[b] (%)**
10	$Cu(OAc)_2$ (20)	60	TFE	6
11	$Cu(OAc)_2$ (20)	60	Dioxane	10
12	$Cu(OAc)_2$ (20)	60	Anisole	4
13	$Cu(OAc)_2$ (20)	60	Propylene carbonate	7

[a]all the reactions carried out under oxygen for overnight unless otherwise mentioned. [b]determined by ^1H NMR spectroscopy.

We found that copper(I) salts such as copper(I) chloride, copper(I) bromide, copper(I) iodide gave the desired product in good yield. We found that when one equivalent of copper(I) iodide was used the yield of **143** increases to 52%.

Table 2-3 Optimization study: screening of copper (I) reagents

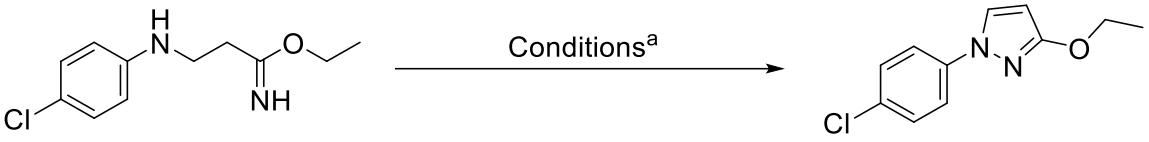

142 **143**

Entry	Additive (mol %)	Temp. (°C)	Solvent	Yield[b] (%)
14	CuCl (100)	60	DMSO	33
15	CuBr (100)	60	DMSO	40
16	CuI (100)	60	DMSO	52

[a]all the reactions carried out under oxygen for overnight unless otherwise mentioned. [b]determined by ^{1}H NMR spectroscopy.

A mixture of Cu(I) and Cu(II) salts in different proportions were tested to probe the effect of catalyst oxidation state. We found that one *total* equivalent of a 1 : 1 mixture of CuI/$Cu(OAc)_2$ gave the best result at 60 °C (entry 20, Table 2-4). Other combinations such as $Cu(OAc)_2$/CuCl and $Cu(OAc)_2$/CuBr also yielded the desired product, but in lower yields. Experiments in the absence of an oxygen sparge results in lower yield (entry 24, Table 2-4). Adding one equivalent of *p*-benzoquinone as an external oxidant gives **143** in 71% yield (entry 28, Table 2-4).

Table 2-4 Optimization study: screening of additives

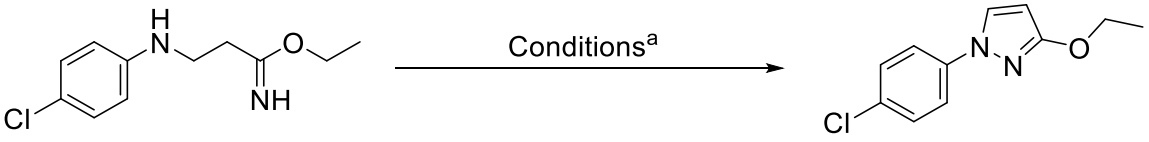

142 **143**

Entry	Additive (mol %)[a]	Yield[b] (%)
17	$Cu(OAc)_2$ (10) + CuI (10)	21
18	$Cu(OAc)_2$ (20) + CuI (20)	40
19	$Cu(OAc)_2$ (40) + CuI (40)	48
20	**$Cu(OAc)_2$ (50) + CuI (50)**	**85(76)[c]**

21[d]	$Cu(OAc)_2$ (50) + CuI (50)	8
22	$Cu(OAc)_2$ (100) + CuI (100)	69
23	$Cu(OAc)_2$ (20) + CuI (80)	49
24[e]	$Cu(OAc)_2$ (20) + CuI (80)	28
25	$Cu(OAc)_2$ (50) + CuCl (50)	43
26	$Cu(OAc)_2$ (50) + CuBr (50)	54
27	$Cu(OAc)_2$ (50) + CuI (50) + *n*-BuNI (50)	30
28	$Cu(OAc)_2$ (50) + CuI (50) + *p*-benziquinone (100)	71

[a]all the reactions carried out under oxygen for overnight unless otherwise mentioned. [b]determined by ^1H NMR spectroscopy. [c]isolated yield. [d]reaction time 4h. [e]without oxygen.

2.3 Mechanistic hypothesis

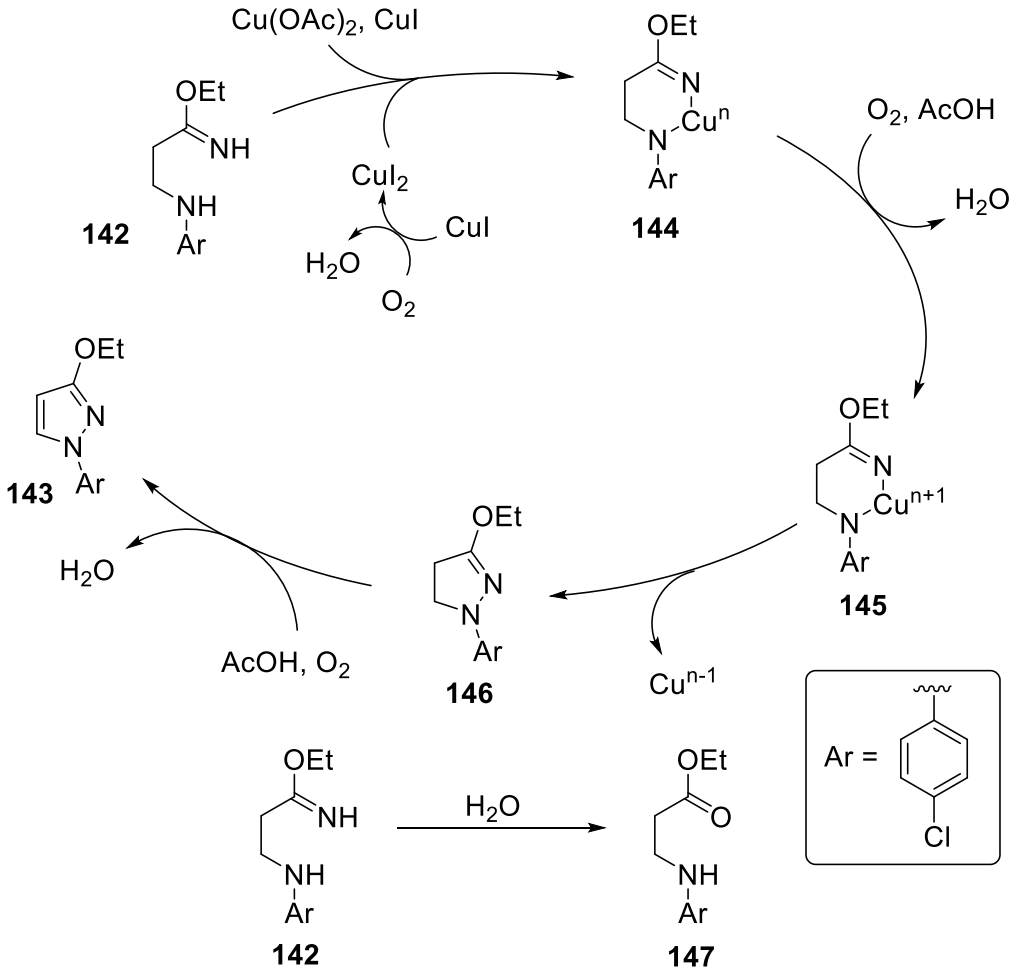

Figure 2-7 Mechanistic hypothesis

A plausible mechanism for the Cu^{I}/Cu^{II} mediated N–N bond formation protocol is proposed in Figure 2-7. We speculate that $Cu(OAc)_2$ coordinates with 3-(4-chloro-anilino)-propionimidic acid ethyl ester **136** to form the intermediate **138**. Whereas CuI can either directly coordinate with **136** or CuI first oxidize to CuI_2 and then coordinate with **136**. Reductive elimination leads to N–N bond formation to afford **140**, which oxidizes to the desired product **137**. However, more controlled experiments and some analytical experiments such as cyclic voltammetry and EPR can be done to understand the mechanism. Rather than pursue further optimization, a more promising alternative was investigated.

2.4 Conclusion

In summary, a new and efficient method to prepare substituted pyrazoles regioselectively was developed. Two side reactions are the major limitations of this method. The hydrolysis side reaction was controlled by using anhydrous DMSO; the ethanol elimination side reaction was controlled by limiting the reaction temperature to 60 °C. At temperatures higher than 60 °C, 3-(4-chlorophenylamino)propanenitrile is formed in a more significant percentage, and at lower temperature the yields of pyrazole were low. Using oxygen as an oxidant is essential for this reaction. Yields decreased significantly in the absence of oxygen. Although the reaction conditions are mild, and the starting materials are inexpensive, using one equivalent of copper reagents limits the industrial applicability. A more promising strategy was thus pursued.

Chapter 3: Electro-chemical Reduction of N-Nitroso and Subsequent Ring-closure to Make Hydrazine and Heterocycles Regioselectively

3.1 Introduction

3.1.1 Towards sustainable organic synthesis

In the past century, molecular synthesis has made enormous progress in the chemistry world. However, even with new methodologies producing complex molecules, and sometimes seemingly simple ones, in a selective and sustainable manner remains challenging.

Most traditional methods do not address the principal criteria of green or sustainable synthesis (Figure 3-1).[104-110] Ideally, an environmental friendly synthesis avoids harsh reaction conditions, undesired waste generation, pre-functionalization of synthetic precursors, toxic solvents and reagents, and precious heavy metals.[108-115]

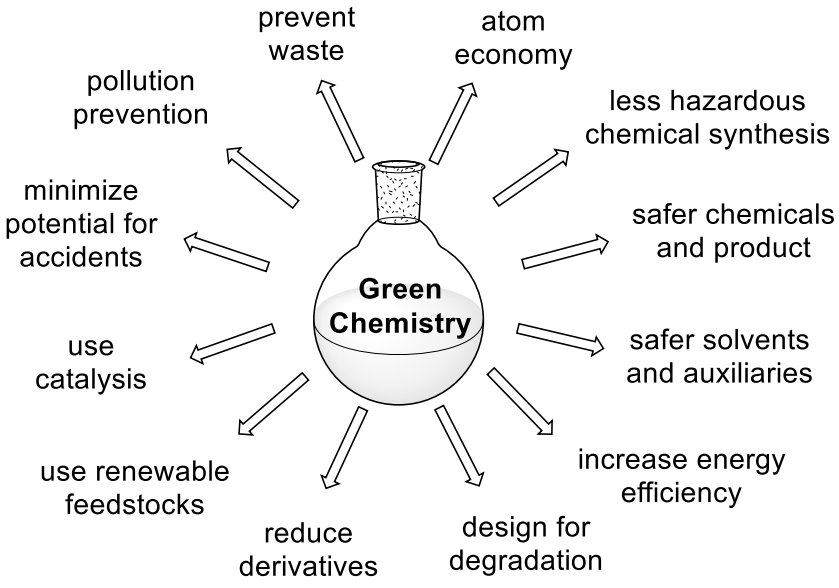

Figure 3-1 Principles of green chemistry

Recently, photoredox catalysis and organic electrochemistry have emerged as more sustainable and atom-economic alternatives to traditional organic synthesis.[115-127] However, photocatalysis typically uses iridium and ruthenium complexes, or organic dyes in the reoxidation step (Figure 3-2).[116,128-129] Complex multi-step transformations often are required to prepare the photoredox catalysts needed for the oxidation/reduction potential. Further, photoredox catalysts only absorb a small portion of visible light to convert the photons into chemical energy (Figure 3-3). Consequently, the quantum yield of the overall reaction is usually low.[130-131] Generally, in a photochemical reaction a monochromatic light source is required. However, most light sources used are polychromatic. Almost all of those light sources generate heat during the radiation; an external cooler (a source of wasted energy) is required.

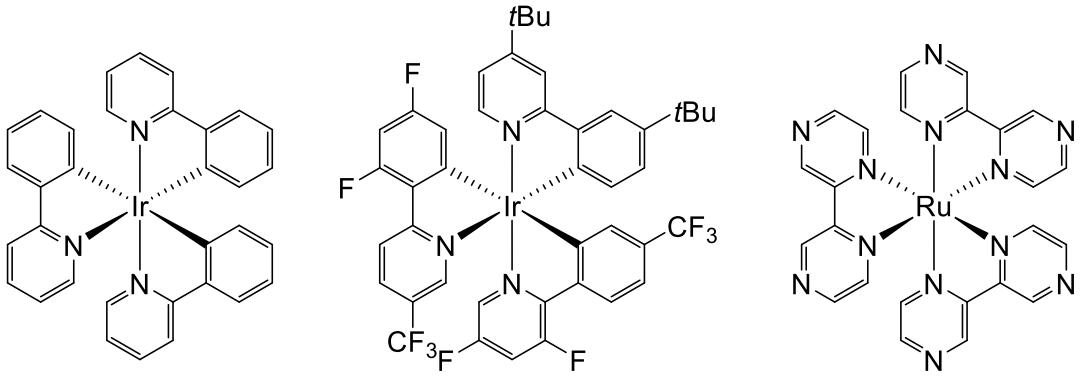

148 **149** **150**

151 **152**

Figure 3-2 Common photocatalysts (PC)

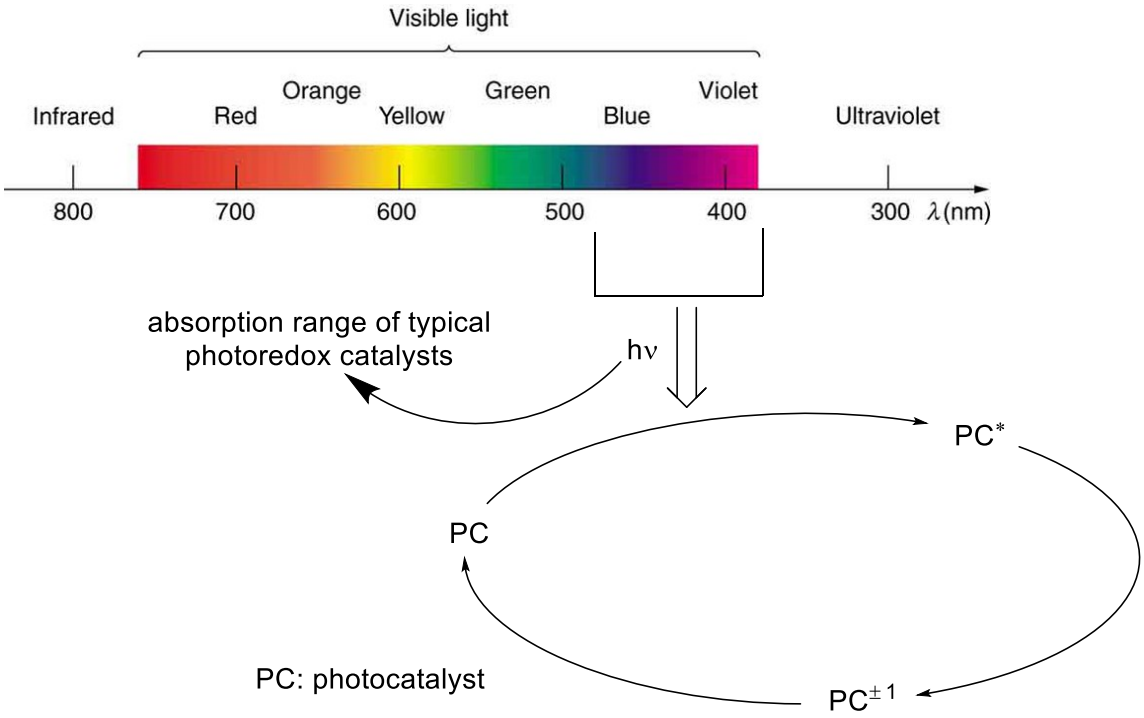

Figure 3-3 Photocatalytic cycle

A redox reaction involves adding or removing electrons to/from a substrate. Depending on the reaction, a stoichiometric amount of reductant or oxidant is required. Excess toxic and hazardous oxidants and reductants are a major source of chemical waste in these processes. Alternatively, electricity can be used for the electron transfer, greatly reducing the amount of chemical reagents needed for a reaction.[132] Electrochemistry is globally accepted as a green and environmental friendly process.[133-135] Further, electrochemistry is experiencing a renaissance in synthetic organic chemistry. In the last two decades there has been an exponential growth in the number of “organic electrochemistry” publications (Figure 3-4).[124]

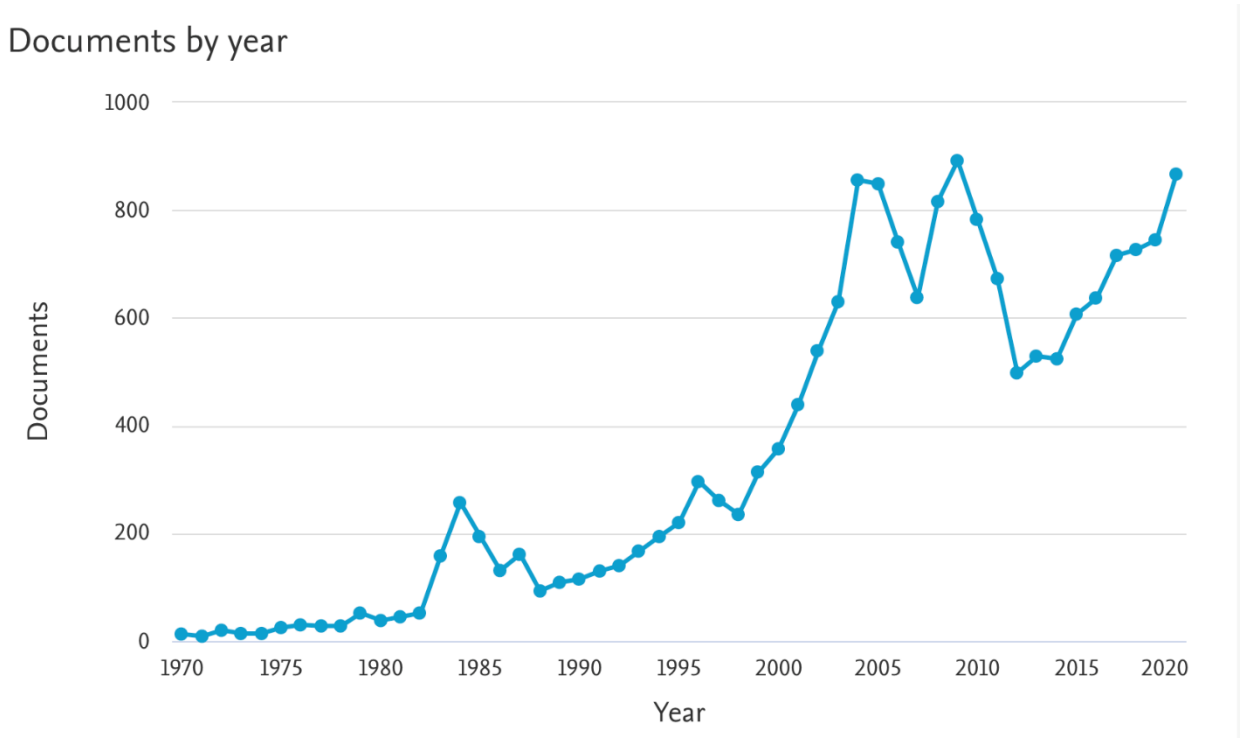

Figure 3-4 Organic electrochemistry documents published per year

Electrochemistry has many other advantages over traditional synthetic organic chemistry. Most electrochemical reactions are run at room temperature, a large energy savings. The reactivity of a reaction can be “tuned” by changing the potential, or by altering the electrode material. Turning off the electricity source stops the electrochemical reaction, whereas quenching is needed to stop a classical synthetic reaction. Electrochemical reactions also typically use mild reaction conditions and have high solvent and functional group tolerance. Despite having several advantages over traditional organic synthesis, organic electrochemistry has not grabbed the attention of the majority of organic chemists until recently.

3.1.2 Basics of electrochemical reactions

An electrochemical cell has an external power source connected to anode, cathode and reference electrode. Cathodes are electron rich and anodes are electron poor since the power source pushes electrons into the cathode from the anode. The electron flow ensures a reductive environment at the cathode and an oxidative environment at the anode. The reactants in solution

donate electrons into the anode and accept electrons from cathode by a heterogeneous interaction. In an electrochemical cell reaction, both oxidative and reductive processes occur simultaneously.

The reaction of interest takes place at one of the electrodes, known as the “working electrode”; the other electrode is called the “counter electrode”. It is important to note that the “working electrode” can be either the cathode or the anode, depending on the reaction of interest. Working electrode potential is measured by reference electrode, and in absence of reference electrode, the external power source controlled the voltage difference between cathode and anode.[136]

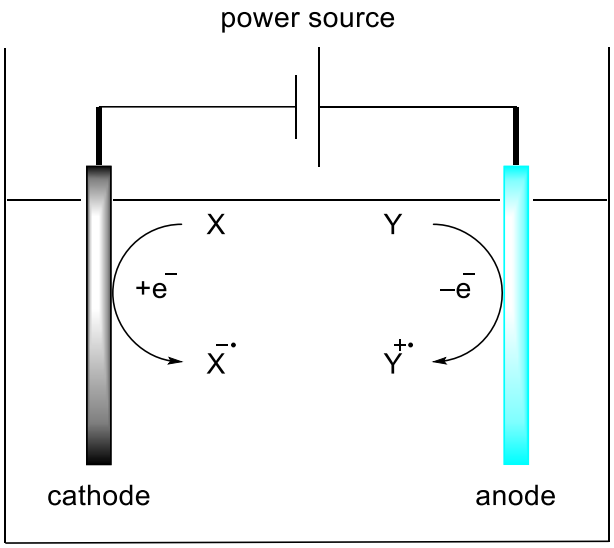

Figure 3-5 Electrochemical cell

Electrolyte additives are often used in an electrochemical reaction to improve conductivity and reduce resistance. The cations and anions of the electrolyte carry charge thorough the circuit. Electrolytes form an electrical double layer near the electrodes, and neutralize the charge imbalance after electrolysis (Figure 3-6a). Tetraalkyl ammonium and lithium cations are common electrolyte cations, whereas halides, borates and phosphates are common electrolyte anions used in organic electrochemistry reactions (Figure 3-6b). Ideally, an electrolyte should be inert

under electrochemical conditions, and soluble in most organic solvents. Similarly, the choice of solvent must dissolve the electrolyte and reagents as well as be indefinitely stable under the reaction condition (Figure 3-6c).

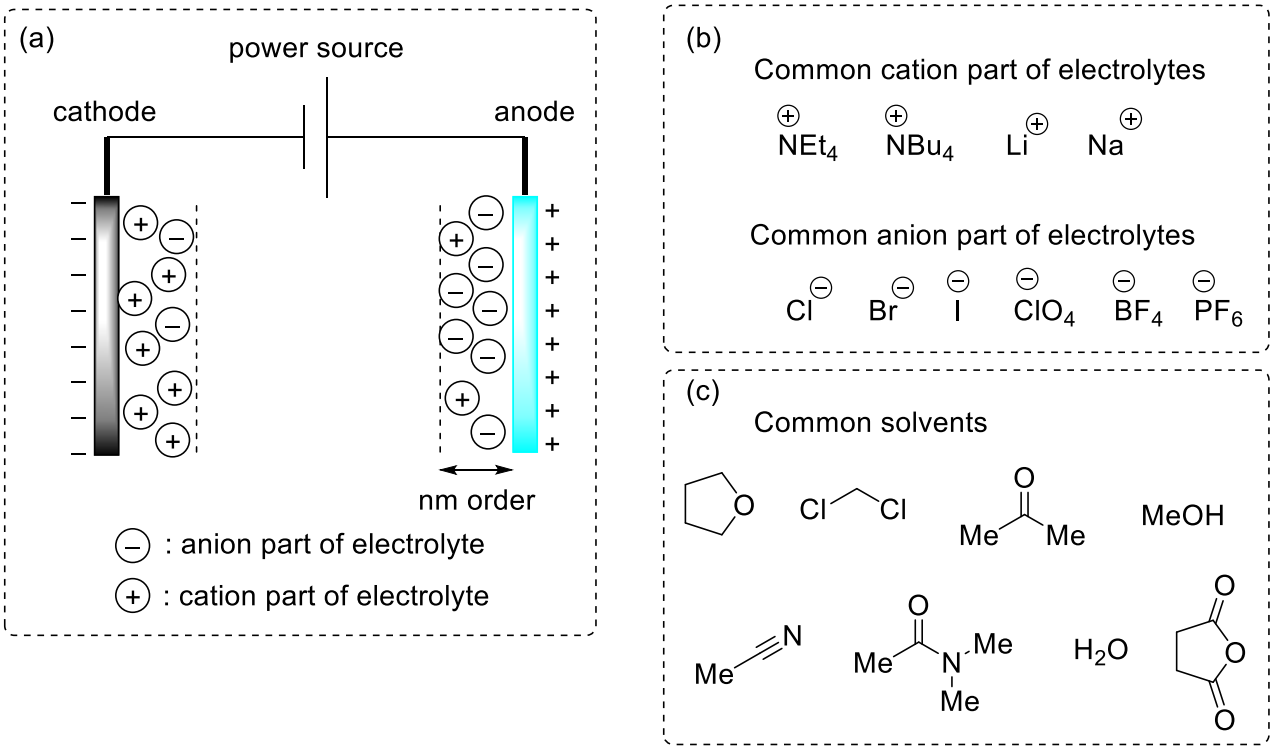

Figure 3-6 (a) Electrical double layer (b) Common electrolytes (c) Common solvents

Electron transfer from electrode to reactant (cathodic reduction) or reactant to electrode (anodic oxidation) depends on the applied potential. Electrode atoms are closely packed and overlap one another. Irrespective of the single atom value, electrodes do not possess well-defined energy levels; instead, a continuum of energy levels is formed. This hypothetical energy level is known as the Fermi level. The Fermi level of electrodes is not fixed and can be moved by varying the applied electrode potential as shown in Figure 3-7.[137] The HOMO energy level of reactant (i.e. reductant) is lower than the Fermi level of electrode, so electron transfer from HOMO of the molecule to the electrode is thermodynamically unfavorable. In contrast, electron transfer from the reactant's HOMO to the electrode is thermodynamically favorable (Figure 3-7a). In an

electrochemical reaction, the reacting species must overcome this activation barrier. In Figure 3-7b, the electron transfer is in equilibrium, so higher potential than optimal is required for a successful experiment. This excess potential above the standard potential is called the overpotential (Figure 3-7c).

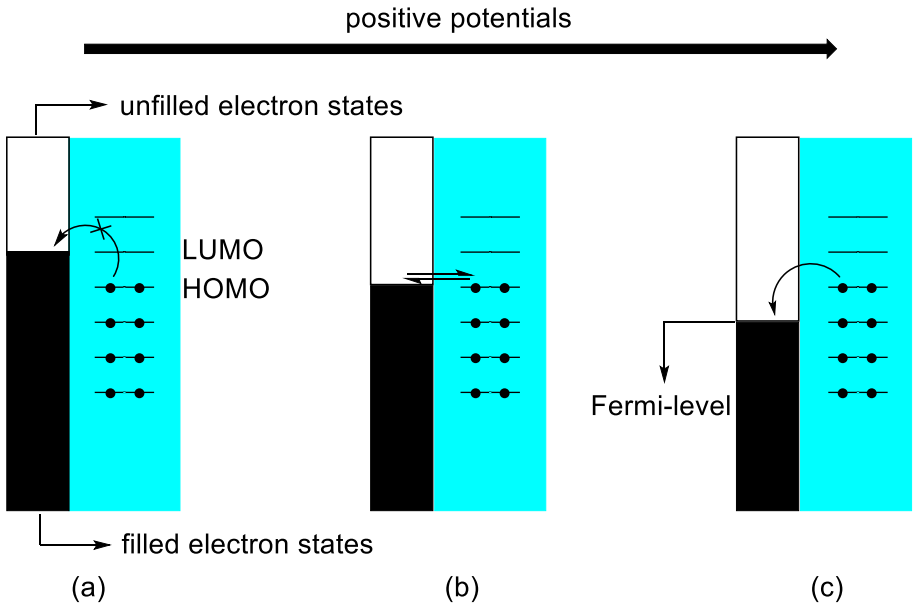

Figure 3-7 Fermi-level in electrode and orbital energies of molecules

Replacing stoichiometric oxidants and reductants in synthesis is very attractive, both economically and environmentally. There are three possible situations for the electron transfer in an electroorganic reaction (Figure 3-8).[138] Using an inert electrode is the most common scenario. In the first case, the oxidation or reduction occurs at the anode or cathode surface, respectively, and selectivity is achieved only by adjusting the electrode potential (Figure 3-8a). In an active electrode system, an electrocatalytically active species on the electrode surface act as restrained redox-active reagents (Figure 3-8b). In redox-mediated electrolysis, a soluble, redox-active additive is added, which is regenerated electrochemically, as shown in Figure 3-8c. Avoiding a large over-potential and reaching optimal reactivity and selectivity are two main advantages of mediated electrolysis.

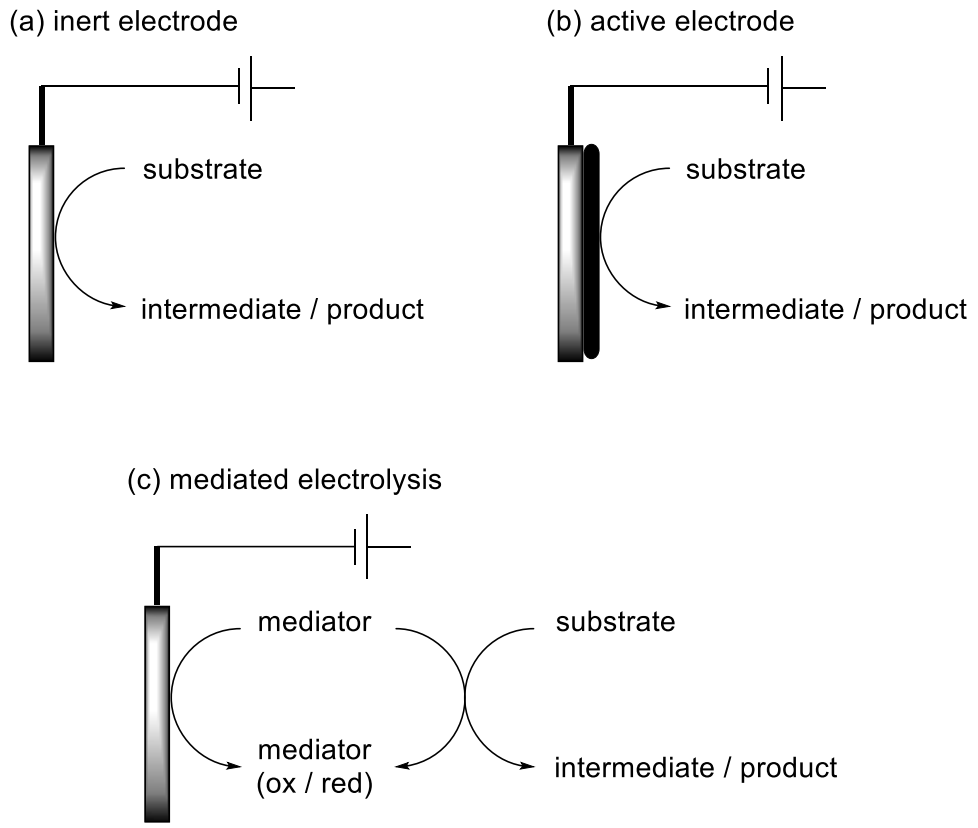

Figure 3-8 Different operation modes of electrodes in an electrochemical reaction

3.1.3 Brief history of organic electrosynthesis

The basis of modern organic electrosynthesis was built in the early 19th century. In 1800, Alessandro Volta invented the “volta pile”, the first model of an electric battery.[139,140] Michael Faraday carried out the first organic electrosynthesis reaction in the1830s, generating gaseous ethane by electrolyzing an acetate solution.[141]

In 1834, Faraday published “Faraday’s laws of electrolysis”.[142] The first law states that the mass (m) of chemical deposition at an electrode due to the flow of electricity is directly proportional to the quantity of charge (Q) in Coulombs passed through the electrolyte. The second law states that the mass (m) of the substances deposited on electrodes is directly proportional to the

respective number of equivalents or the equivalent weight when same amount of electricity passes through different electrolytes.[142,143]

Mathematically, the mass (m) of chemical deposition is straightforward:

$$m \propto Q$$

$$\text{or, } m = Z \times Q$$

In this equation, Q is in Coulombs, which is Amperes $\times$ time (in seconds), and Z is a proportionality constant, called the electrochemical equivalent. The proportionality constant = m when Q = 1, thus an electrochemical equivalent is defined as the mass of the substance deposited per unit charge.

According to 2nd law:

$$m \propto E$$

$$\text{or, } m_1 : m_2 : m_3 : ... = E_1 : E_2 : E_3 : \ldots$$

$$\text{or, } Z_1Q : Z_2Q : Z_3Q : ... = E_1 : E_2 : E_3 : \ldots$$

$$\text{or, } Z_1 : Z_2 : Z_3 : ... = E_1 : E_2 : E_3 : \ldots$$

where the chemical equivalent or equivalent weight E = atomic weight or valency.

Hermann Kolbe reported the first useful organic electrosynthesis. He demonstrated that carboxylate salts **153** lose carbon dioxide via anodic oxidation to give carbon-based radicals, which couple to form hydrocarbons **156** (Scheme 3-1).[144,145]

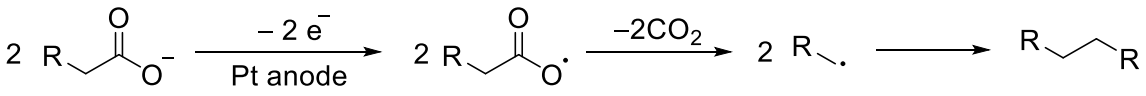

153 **154** **155** **156**

Scheme 3-1 Kolbe Electrolysis

In the late 19th century, several groups (e.g., Haber, Gattermann, Tafel, and Elbs) made progress in organoelectrolysis. Still, only a few organic electrosynthetic processes were used on an industrial scale by the early 20th century.[140] Czech chemist Jaroslav Heyrovský invented polarography, a predecessor to linear sweep voltammetry, in 1922 using a dropping mercury electrode (DME). Early polarography studies were generally used to examine inorganic compounds and simple organic compounds such as nitrobenzene, fructose, cystine, and acetylacetone compounds.[140,146,150] In 1959 Jaroslav Heyrovský won the Nobel Prize for his discovery.

Over the last century, organic electrochemistry applications increased both in the laboratory and in industry. Electrochemical fluorination is an important process to install fluoride into hydrocarbons, organofluorine compounds **158** can be prepared by electrolysis of an organic compound in an anhydrous hydrogen fluoride solution (Equation 3-1).[151]

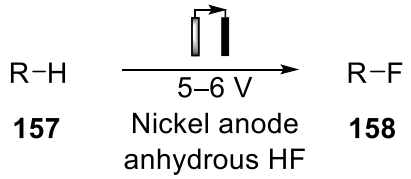

Equation 3-1 Simons process

In 1963, Manual Monsanto Baizer reported that Nylon 66 monomer adiponitrile **160** can be prepared through cathodic hydrocoupling of acrylonitrile **159** (Equation 3-2). The main advantage of this method was the use of water as hydrogen source, with oxygen evolved as the side product. However, use requirement for a cadmium cathode created substantial environmental issues. This process was commercialized in 1965 at a scale of nearly 100000 tons per year during the 1970s.[152]

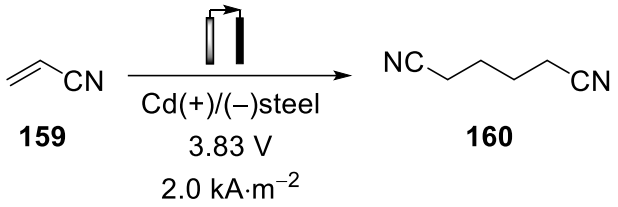

159 **160**

Equation 3-2 Baizer process

In 1984, Tatsuya Shono reported that electroorganic anodic oxidation of unfunctionalized amides **161** generates an *N*-acyliminium intermediate **162**. *N*-acyliminium ions are important intermediates in carbon–carbon bond forming reactions, the result of which can be trapped by an alcohol solvent or (in the absence of alcohol solvents) by nucleophiles at low temperature (Equation 3-3).[153]

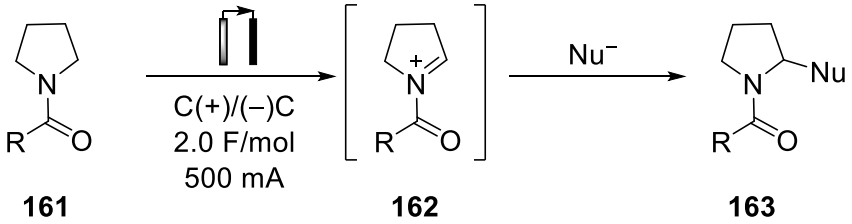

161 **162** **163**

Equation 3-3 Shono oxidation

3.1.4 Reductive electrochemical reaction is less explored

Only a handful of cathodic reduction reactions are known (Figure 3-10, Equations 3-5 and 3-6). The vast majority of electrochemical transformations are oxidative. The difference is primarily because reductive electrochemical reactions most often require divided cells and a mercury pool cathode. These conditions limit the applicability of reductive electrochemical reactions at both laboratory and industrial scale.

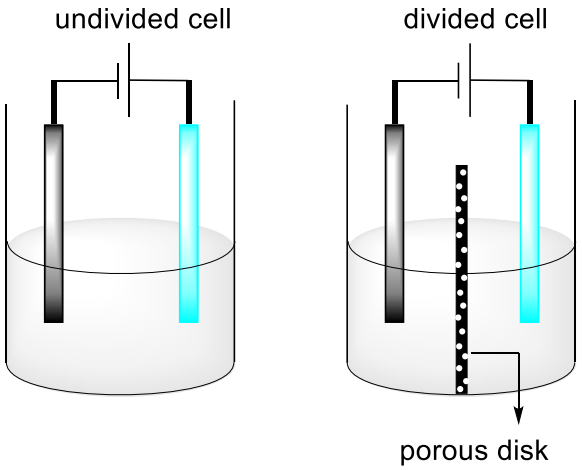

Figure 3-9 Undivided and divided electrochemical cell

The first electrochemical reduction reaction reported in 1845. The authors showed that reductive dehalogenation of trichloromethanesulfonic acid occurs at a zinc electrode to give methanesulfonic acid (Equation 3-4).[124,140]

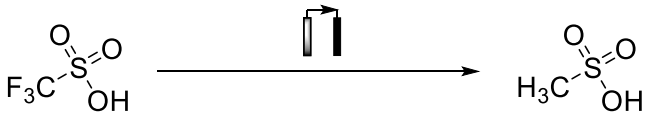

164 **165**

Equation 3-4 First electrochemical reduction

In 1946, Birch reported first electrochemical birch reduction. In this reaction *meta*-tolyl methyl ether was reduced at copper cathode in liquid ammonia solution at –40 °C.[154] Recently, groups have investigated cathodic reduction reactions such as deoxygenation of esters, amides, sulfoxides, and phosphine oxides that use a simple electrochemical setup and mild reaction conditions (Figure 3-10).[155-158]

Markó, *2009*

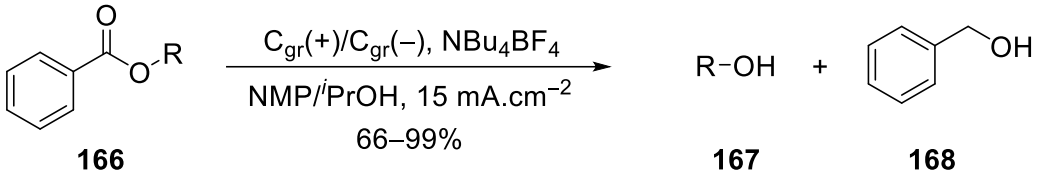

166 **167** **168**

Waldvogel, *2014*

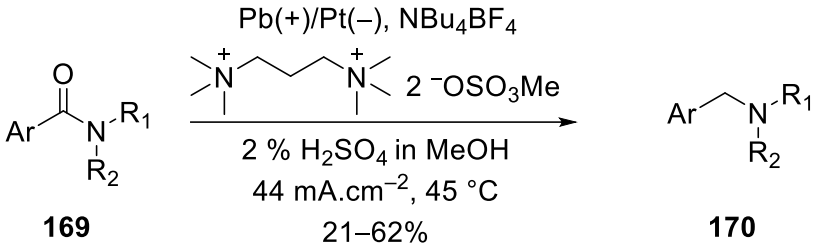

169 **170**

Sevov, *2020*

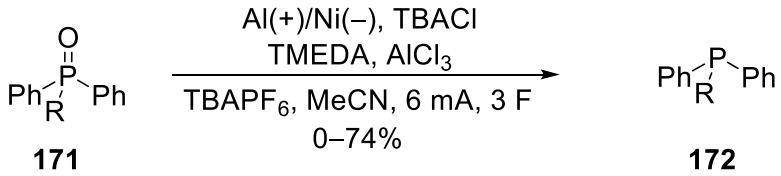

171 **172**

Figure 3-10 Recent development of electrochemical reduction reactions

Reduction of *N*-nitroso compounds is an alternative way to make substituted hydrazines. These processes often uses a metal powder in an acidic medium.

3.1.5 Traditional ways to reduce N-nitro compounds

In 1875, Fischer reported the first *N*-nitroso reduction to a substituted hydrazine using the combination of zinc in acetic acid (Equation 3-4).[159] This methodology is still used extensively for these types of reactions.[160-166] Lithium aluminium hydride ($LiAlH_4$), sodium dithionite ($Na_2S_2O_4$), titanium trichloride ($TiCl_3$), sodium amalgam, and titanium tetrachloride/magnesium ($TiCl_4$/Mg) are other reductant used to reduce *N*-nitroso compounds.[167-182] Some of these reactions require strong acid, elevated temperatures, and/or longer reaction times. In addition, they require inert atmosphere. Scaling to an industrial process is challenging, especially due to the use of excess hazardous reducing agents.

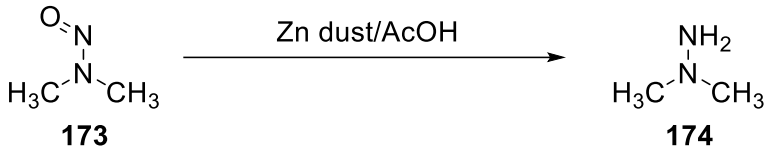

173 **174**

Equation 3-4 Fischer's first *N*-nitroso reduction

3.1.6 History of electrochemical reduction of N-nitro compounds

In 1898, Haber established a stepwise electrochemical reduction of nitrobenzene to aniline (Scheme 3-2).[124] Since this seminal discovery, electrochemical reduction of nitro compounds has been well-studied, whereas selective electrochemical reduction of nitroso compounds is much less common.

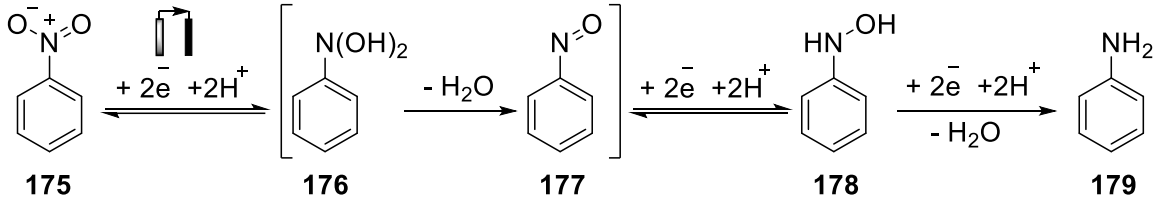

175 **176** **177** **178** **179**

Scheme 3-2 Haber's stepwise reduction of nitrobenzene

Among the few reports on electrochemical reduction of *N*-nitroso compounds to hydrazines, Backer reported the first electrolytic reduction of *N*-nitrosoamine to hydrazine in 1913, but he did not study the reaction in detail.[183] In 1932, Cook and France described the electrolytic reduction of *N*-nitrosoisoindoline **180** to *N*-amidoisoindoline **181** in sulfuric acid using cadmium and lead cathodes at 44 °C (Equation 3-5).[184]

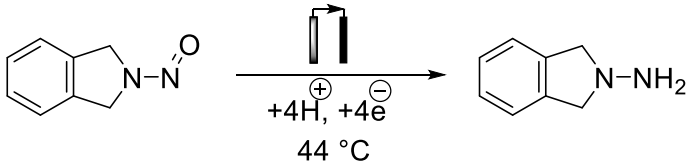

180 **181**
72-92%

Equation 3-5 Cook's electroreduction of N-nitrosoamines

Soon after, in 1936, Wells et al. reported a detailed study on the electrochemical reduction of N-nitrosomethylaniline **182** (Equation 3-6). For this reaction, cadmium (Cd) electrodes were used in 1.0 N hydrochloric acid solution at room temperature.[183]

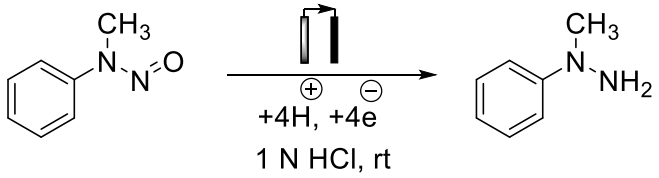

182 **183**
85%

Equation 3-6 Wells's electroreduction of N-nitrosomethylaniline

In 1970, Dorn et al. reported the electrochemical reduction of N-nitroso-1-methylamino-1-deoxysugar alcohols to hydrazine derivatives in the presence of hydrochloric acid.[185] Immediately after, Iversen has reported a similar method of electrolytic reduction of N-nitrosamines in 1 : 1 4 N hydrochloric acid and ethanol (Equation 3-7).[186] Using this method, twenty symmetric, unsymmetric, and cyclic N-nitroso compounds were reduced to their corresponding hydrazines in good yield. However, this method requires a mercury cathode and divided cell in hydrochloric acid, which limits the applicability.

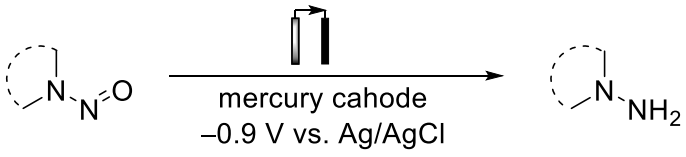

184 **185**
0–82%

Equation 3-7 Iversen's electroreduction of N-nitrosomethylaniline

3.2 Objectives of the project

An alternative, much simpler, and highly efficient method for the reduction of N-nitrosamine compounds is important to both academic and industrial research. We believed that

electrochemical reduction would produce intermediate hydrazines, which would undergo *in situ* intramolecular ring closure, giving the desired substituted pyrazoles (Scheme 3-3).

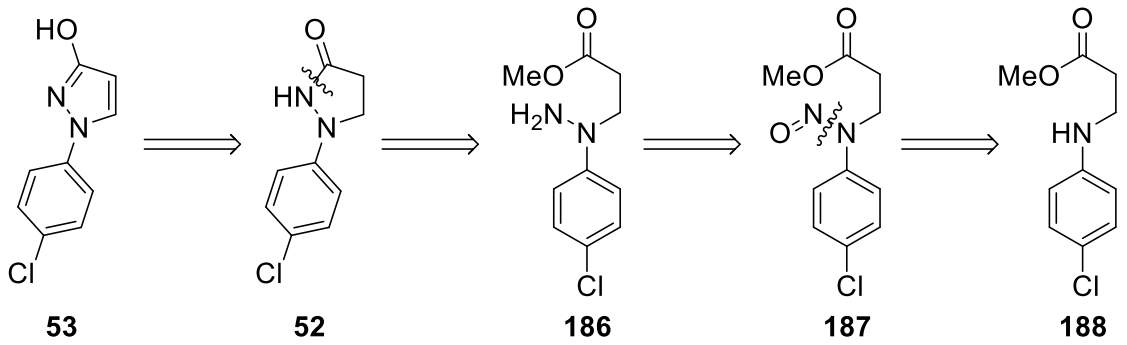

Scheme 3-3 Reaction hypothesis

Our initial thought was to make methyl 3-((4-chlorophenyl)(nitroso)amino)propanoate **187** and reduce it to hydrazine **186** chemically or electrochemically. Subsequent cyclization gives 1-(4-chlorophenyl)pyrazolidin-3-one **52**, and oxidation of 1-(4-chlorophenyl)pyrazolidin-3-one **52** would provide our desire compound 1-(4-chlorophenyl)-1*H*-pyrazol-3-ol **53** (Scheme 3-3). The primary goal of this project was to reduce a broad range of N-nitroso compounds electrochemically in a selective way.

3.3: Result and discussion

3.3.1 Inspiration for starting point

Recently the Baran group reported a modified electrochemical Birch reduction (Figure 3-11).[157] Remarkably, the experimental set-up is simple by design; no special electrodes or electrochemical cells are required. They worked with an undivided cell, at room temperature, using lithium bromide as the electrolyte, magnesium as the sacrificial electrode (to prevent reoxidation of the substrate), and stainless steel (SS) as the working electrode (Figure 3-11).[157] In this reaction, 10 equivalents of tris(pyrrolidino)phosphoramide (TPPA) was used to protect the cathode surface from passivation by lithium oxide. Although simple alcohols could be used as the

proton source, 1,3-dimethylurea (DMU) resulted in improved selectivity. We believed that similar conditions would result in the electrochemical reduction of many previously unexplored substrate classes. Specifically, we envisioned that N-nitroso compounds would reduce and undergo cyclization under the reduction conditions to afford pyrazalones directly (Scheme 3-3).

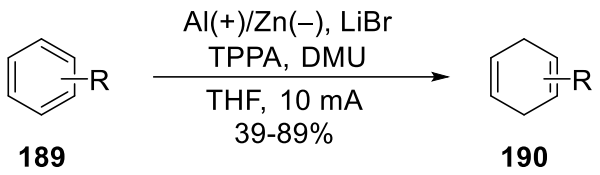

Figure 3-11 Baran's electrochemical Birch reduction

3.3.2 Preparation of N-nitrosoamines

N-nitroso amines can be prepared easily from the corresponding aniline derivatives in high yields. We first prepared ester and ketone **193** via a catalytic Michael addition of the aniline to the acrylate. We found that the ester and ketone analogues required different conditions for the Michael addition reaction (Figure 3-12). Both ester and ketone substrates were prepared without solvent. However, the ester analogues required catalytic lithium tetrafluoroborate at 75 °C, whereas the ketones were prepared without a catalyst at room temperature simply by stirring methyl vinyl ketone with the appropriate amine.

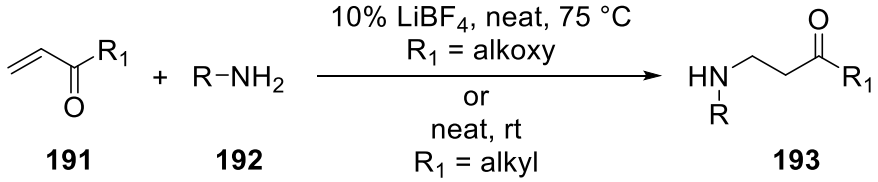

Figure 3-12 General procedure for *N*-nitrosoamines preparation

Although the *N*-nitroso compounds can be prepared via this traditional method (sodium nitrite in aqueous HCl), we found that commercially available *tert*-butyl nitrite in acetonitrile at room temperature affords the desired compounds in similar yields under more controlled reaction

conditions. Nitrosylation of the Michael addition product affords the desired *N*-nitrosoamines (Figures 3-13 and 3-14).

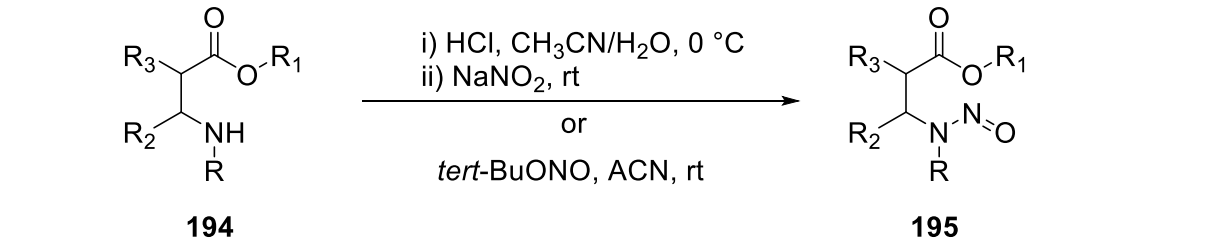

194 **195**

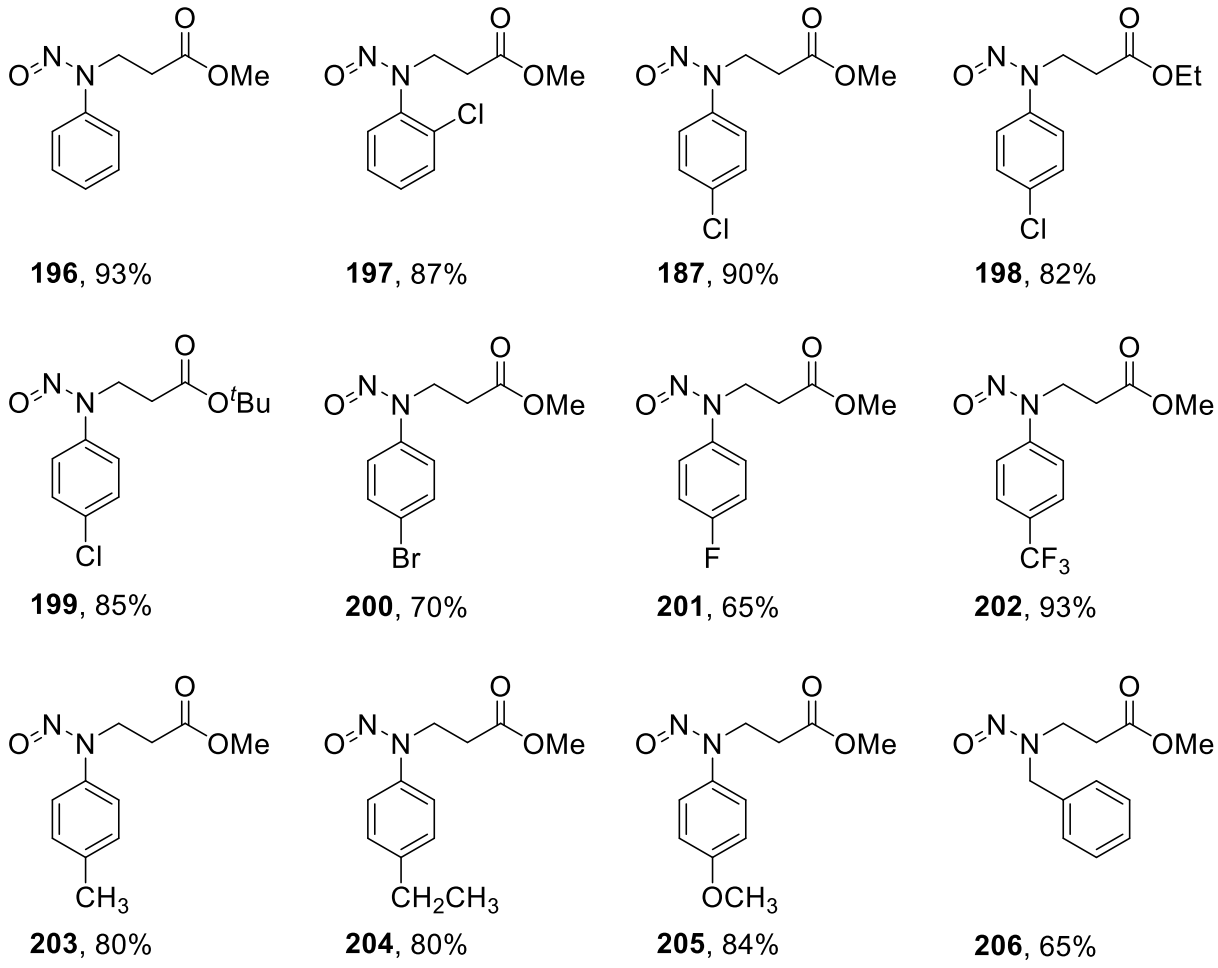

Figure 3-13 Preparation of ester analogues *N*-nitrosoamines

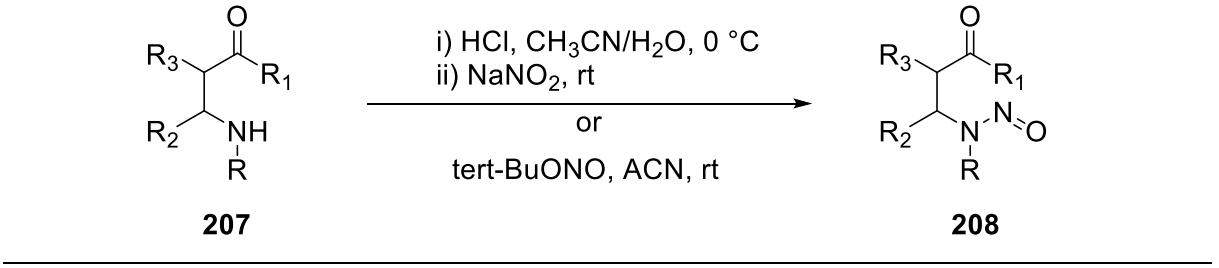

207 **208**

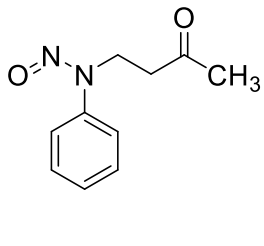

209, 70%

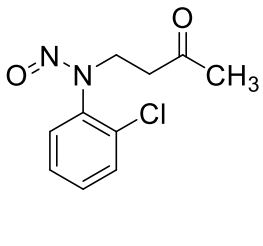

210, 55%

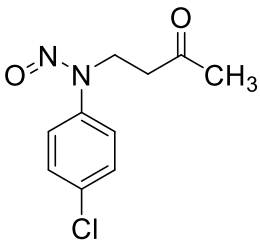

211, 84%

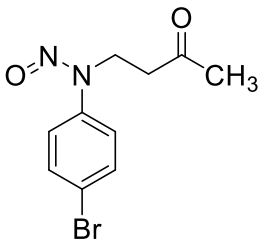

212, 60%

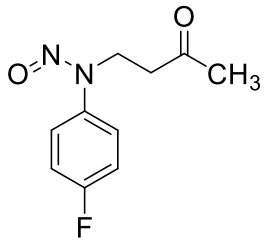

213, 55%

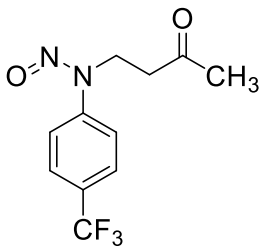

214, 94%

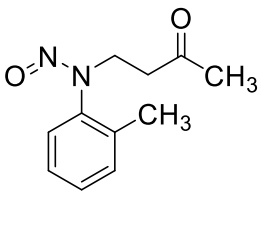

215, 88%

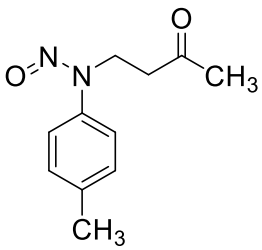

216, 91%

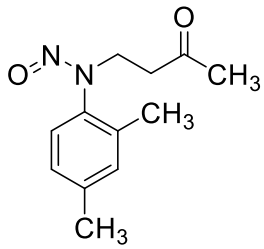

217, 93%

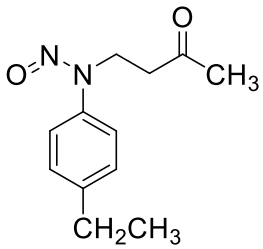

218, 95%

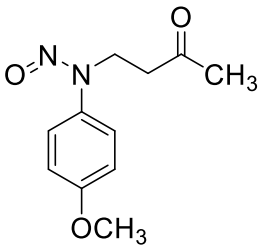

219, 92%

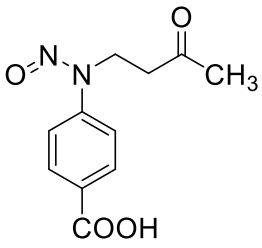

220, 85%

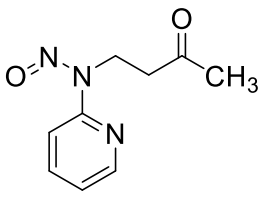

221, 95%

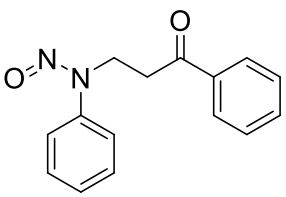

222, 99%

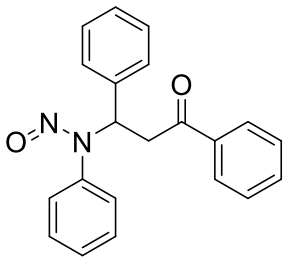

223, 99%

Figure 3-14 Preparation of ketone analogues *N*-nitrosamines

Further, we found that the nitrosylation was general for a broad range of substrates; common carbonyl functionalities and aromatic substitution (**221**, **222**, and **223**) are well-tolerated.

Nitrosoamines **198** and **199** were prepared to investigate the effect of the ester leaving group. 1-Phenyl-3-(phenylamino)propan-1-one **225** was prepared from aniline and 3-chloro-1-phenylpropan-1-one **224** (Equation 3-8). Compound **225** reacts with *tert*-butyl nitrite in acetonitrile to give *N*-(3-oxo-3-phenylpropyl)-*N*-phenylnitrous amide **222** quantitatively.

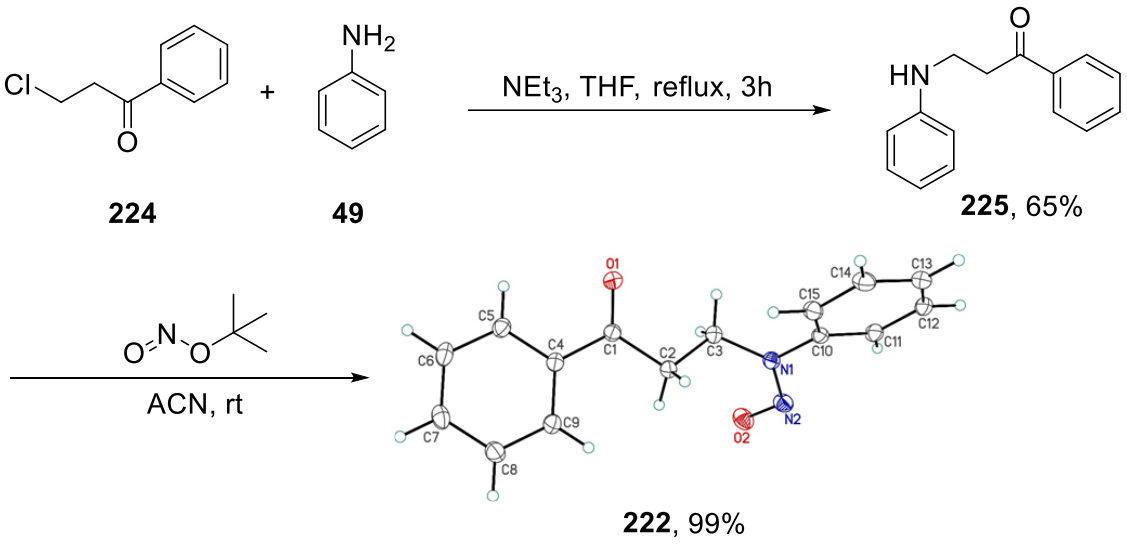

Equation 3-8 Preparation of **222**

To verify that substitution along the chain was also tolerated, N-(3-oxo-1,3-diphenylpropyl)-N-phenylnitrous amide **223** was prepared by a Mannich reaction followed by nitrosylation (Equation 3-9).

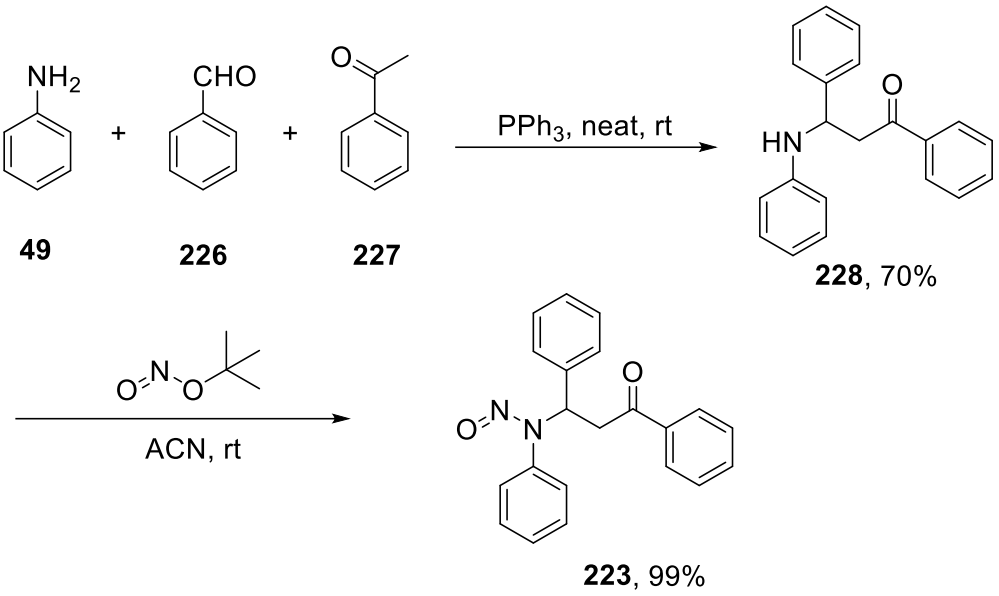

Equation 3-9 Preparation of **223**

3.3.3 Electrochemical reductive cyclization – Optimization

Our initial investigation focused on methyl 3-((4-chlorophenyl)(nitroso)amino)propanoate **187** as a model compound for electrochemical reduction of N-nitroso compounds. We adopted Baran's electrochemical Birch conditions as a reasonable starting point. Baran et al. found that unless a sacrificial anode (Al, Mg, or Zn) is used, the re-oxidation of the Birch products to reform the starting material was competitive with the forward reaction. Surprisingly, some sacrificial electrodes works better than others, although the reasons are not very clear. We tested different sacrificial electrodes as the counter electrode; stainless steel (SS, inexpensive and chemically inert) as the working electrode *in an undivided cell* (Table 3-1). Both aluminum (Al) and magnesium (Mg) anodes yielded no productive reaction. Using SS as both the cathode and anode also did not afford product. Only the product of N–N bond was isolated as a side product. However, when Zn was used as the anode and stainless steel as the cathode ~50% of the desired product **52** was obtained under otherwise identical reaction conditions. Shaohui Yu in the Stryker group has tested different additional variations of electrodes, including Zn(+)/(–)Ni, Zn(+)/(–)Cu,

C(+)/(–)C, Zn(+)/(–)Ti, Zn(+)/(–)Co, Zn(+)/(–)Al, Zn(+)/(–)Pt, and Co(+)/(–)SS with limited success. Zinc and stainless steel were thus selected as the anode and cathode, respectively, for further optimization studies.

Table 3-1 Screening of electrode

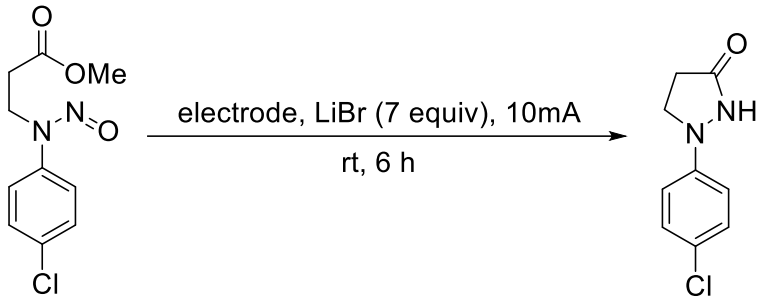

187 **52**

Entry[a]	Cathode	Anode	Solvent	Yield[b] %
1	SS	Mg	THF/MeOH (4 : 1)	0
2	SS	Al	THF/MeOH (4 : 1)	0
3	SS	SS	THF/MeOH (4 : 1)	0
4	Zn	SS	THF/MeOH (4 : 1)	0
5	**SS**	**Zn**	**THF/MeOH (4 : 1)**	**50**

[a]Reaction conditions: methyl 3-((4-chlorophenyl)(nitroso)amino)propanoate **187** (0.2 mmol), LiBr (1.4 mmol), solvent THF/MeOH (4 : 1) (5 mL) were added to a 5 mL IKA flask with constant current 10 mA for 6 h at room temperature. [b]yield was calculated by ^{1}H-NMR spectroscopy.

We found the added base improved the yield of the intramolecular ring-closing step (**186** to **52**, Scheme 3-3), presumably to buffer the solution. The addition of two equivalents of pyridine increases the yield to 43% from 15% under constant current (5 mA, entry 2, Table 3-2). The yield further increases when higher current (10 mA) was applied. These semi-optimized conditions were used to test solvent effects on product formation.

Solvent plays a crucial role in electrochemical reactions. An ideal solvent is inert over the reaction potential range and dissolves both organic compounds and electrolytes. Solvents with higher resistance decrease the overvoltage of the cathode. This is important since the reducing power of a cathode toward an organic substrate is lower with a decrease in overvoltage. Thus an increase in yield was observed in the presence of an increasing the amount of methanol. The yield was highest when methanol alone was used as the solvent (Table 3-2, entry 6). Other protic solvent systems such as EtOH and MeOH/H_2O (9 : 1) do not improve the yield. A more polar solvent, acetonitrile, also failed, presumably because no proton source was present.

Table 3-2 Screening of solvent

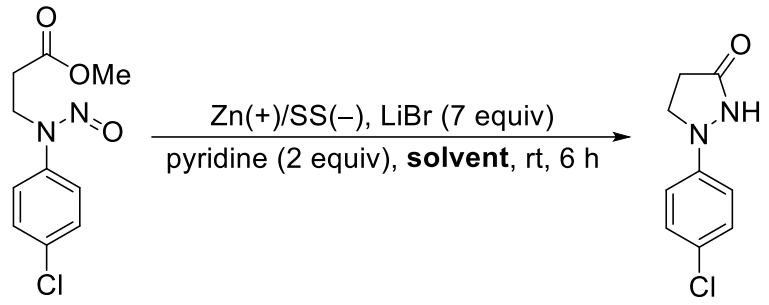

187 **52**

Entry[a]	Current (mA)	Solvent	Base	Yield[b] %
1	5	THF/MeOH (4 : 1)	none	15
2	5	THF/MeOH (4 : 1)	pyridine	43
3	10	THF/MeOH (4 : 1)	pyridine	55
4	10	THF/MeOH (1 : 1)	pyridine	67
5	10	THF/MeOH (1 : 4)	pyridine	75
6	**10**	**MeOH**	**pyridine**	**79**
7	10	MeOH/H_2O (9 : 1)	pyridine	47
8	10	EtOH	pyridine	44
9	10	ACN	pyridine	3 (71)[c]

[a]Reaction conditions: methyl 3-((4-chlorophenyl)(nitroso)amino)propanoate **187** (0.2 mmol), LiBr (1.4 mmol), solvent (5 mL), pyridine (0.4 mmol) were added to a 5 mL IKA flask with constant current 10 mA for 6 h at room temperature. [b]yield was calculated by ^{1}H-NMR spectroscopy. [c]Starting material remains.

Other bases such as 2,4,6-trimethylpyridine, trimethylamine, and 2,5-dibromopyridine were tested to evaluate the effect of base strength on reaction yield. While triethylamine affords reasonable yield, pyridine affords the best result. The yield decreases, however, in the presence of excess pyridine (Table 3-3, entry 4).

Table 3-3 Screening of base

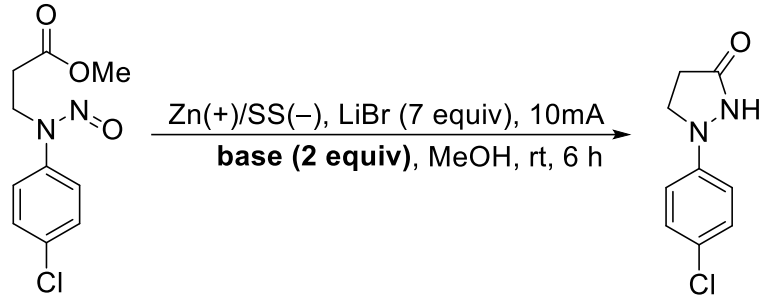

187 **52**

Entry[a]	Base	Yield[b] %
1	2,5 dibromopyridine	23
2	2,4,6 trimethylpyridine	60
3	triethylamine	76
4 [c]	pyridine	71
5	**pyridine**	**79**

[a]Reaction conditions: methyl 3-((4-chlorophenyl)(nitroso)amino)propanoate **187** (0.2 mmol), LiBr (1.4 mmol), base (0.4 mmol), MeOH (5 mL) were added to a 5 mL IKA flask with constant current 10 mA for 6 h at room temperature. [b]yield was calculated by ^{1}H-NMR spectroscopy. [c]5.0 equiv of pyridine was added.

Electrolytes occasionally play a non-innocent role in electrochemical reactions. While the exact role, beyond serving to increase the dielectric of the solvent, is not known, we found that

electrolytes such as lithium chloride, lithium acetate, lithium iodide, and zinc bromide gave a reasonable yield, albeit lower than LiBr. Lithium bromide gave the best results (Table 3-4, entry 3). Reducing the amount of lithium bromide to one equivalent reduces the yield to 61%, while only a slightly lower yield (71%) was obtained using 14 equivs of lithium bromide. Other electrolytes, including Bu_4NCl, Bu_4NBr, Bu_4NPF_6, $LiBF_4$, and KBr were evaluated by Dr. Yu, but using these electrolytes does not improve the yield. The reaction conditions from entry 3, Table 3-4 were selected as "optimal."

Table 3-4 Screening of electrolyte

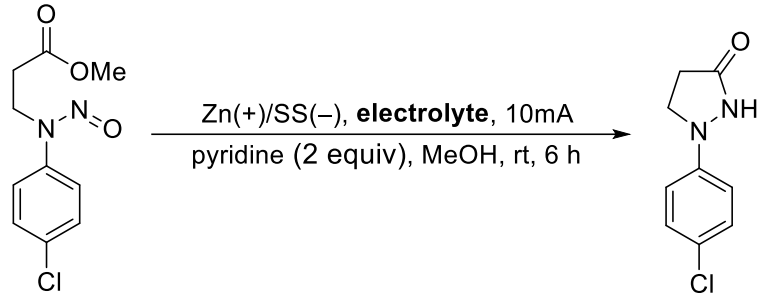

187 **52**

Entry[a]	Electrolyte	Yield[b] %
1[c]	LiBr (1.0 equiv)	61
2[d]	LiBr (14.0 equiv)	71
3	**LiBr (7.0 equiv)**	**79**
4	LiCl (7.0 equiv)	32
5	LiI (7.0 equiv)	17
6	LiOAc (7.0 equiv)	72
7	$ZnBr_2$ (7.0 equiv)	62

[a]Reaction conditions: methyl 3-((4-chlorophenyl)(nitroso)amino)propanoate **187** (0.2 mmol), electrolyte (1.4 mmol), pyridine (0.4 mmol), MeOH (5 mL) were added to a 5 mL IKA flask with constant current 10 mA for 6 h at room temperature.
[b]yield was calculated by ^{1}H-NMR spectroscopy.

The absence of stirring also led to a slight decrease in yield. This result suggests that low rates of ion transportation and diffusion of sacrificial anodic ions adversely affect product formation (Table 3-5, entry 1). No product was observed in the absence of applied current (Table 3-5, entry 2). The result of control experiments show that this reaction is insensitive to ambient light (Table 3-5, entry 3).

Table 3-5 Control experiments

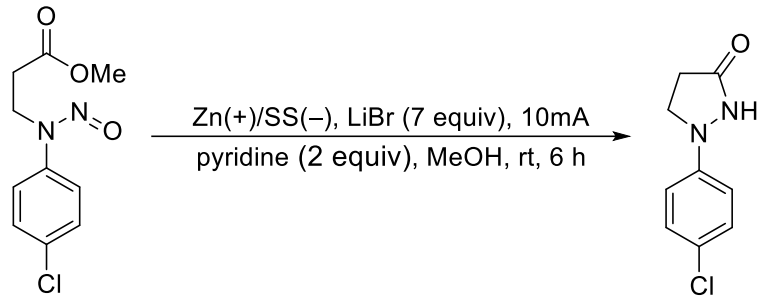

187 **52**

Entry[a]	Changes from above condition	Yield[b] %
1	No stirring	74
2	No current	n.d.
3	No light	78

[a]Reaction conditions: methyl 3-((4-chlorophenyl)(nitroso)amino)propanoate **187** (0.2 mmol), electrolyte (1.4 mmol), pyridine (0.4 mmol), MeOH (5 mL) were added to a 5 mL IKA flask with constant current 10 mA for 6 h at room temperature. [b]yield was calculated by ^{1}H-NMR spectroscopy. n. d. = not detected.

3.3.4 Application to various substrates

Under "optimal" conditions, we examined the scope of the reduction using a listed range of *N*-nitrosoamines. We first examined ester analogues (Figure 3-15), observing substituent electronic effects for both electron-donating and electron-withdrawing groups and giving the corresponding pyrazolidinone products in good to excellent yields. Substituents with electronic

withdrawing groups at the *para*-position suffer from N–N bond cleavage. Lower N–N bond cleavage is observed for *para*-electron donating groups; the intermediate pyrazolidinones aromatize easily under these reaction conditions. Notably, *ortho*-substituted propanoate **196** affords the desired product **217** under optimized conditions. This method is compatible with alkyl nitrasoamine **206**, which gives an excellent yield at 1-benzyl-pyrazolidin-3-one **243**. The ethyl ester **198** also gives 1-(4-chlorophenyl)pyrazolidin-3-one **52**, but at slightly lower yield than the methyl ester. Surprisingly, the yield of **52** was low for *tert*-butyl ester **199**, which has a better leaving group; only the hydrazine was recovered.

A broad range of carbonyl-substituted *N*-nitroso compounds with varying electronic properties were next evaluated. Standard reaction conditions proved compatible not only with esters but also with most other carbonyl substituents (Figure 3-16). Ketones give 3,4-dihydropyrazoles (**246**–**264**) in good to excellent yield. Similar to esters electron-withdrawing substituents lead to increased N–N bond cleavage is a problem. These reduction conditions are also compatible with heteroarene substituents (e.g., **262**). Importantly, *N*-(3-oxo-3-phenylpropyl)-*N*-phenylnitrous amide **223** also gives excellent yield of the bioactive 1,3-diphenyl-4,5-dihydro-1*H*-pyrazole **263**.

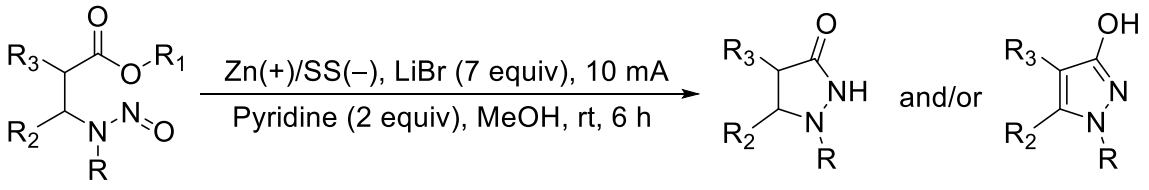

195 **229** **230**

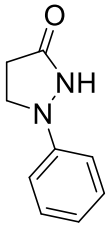

231, 29%

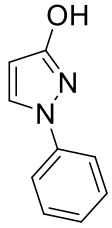

232, 65%

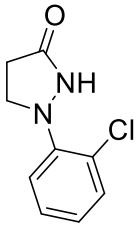

233, 75%

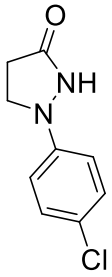

52, 76%

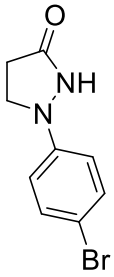

234, 37%

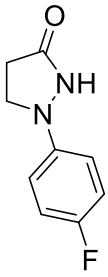

235, 61%

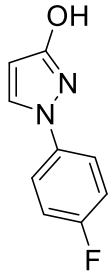

236, 31%

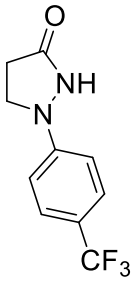

237, 30%

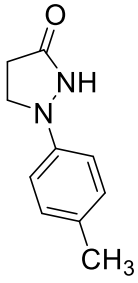

238, 25%

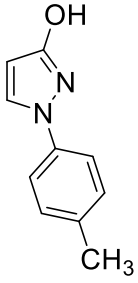

239, 66%

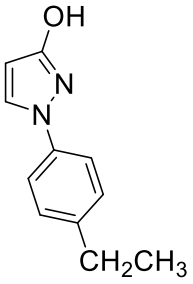

240, 77%

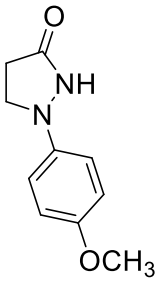

241, 35%

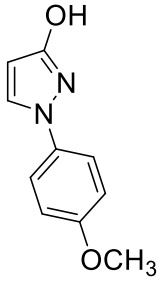

242, 65%

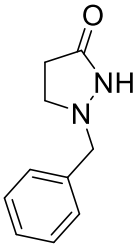

243, 95%

Figure 3-15 Reaction scope

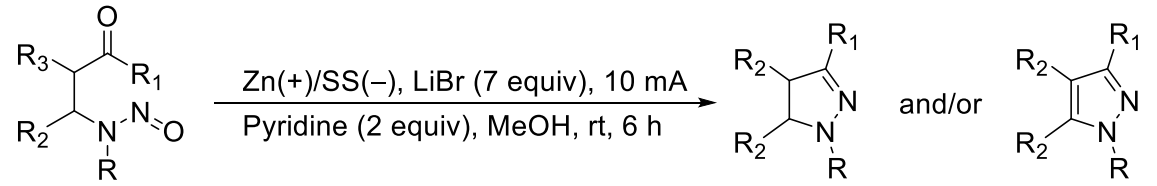

208 **244** **245**

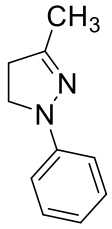

246, 73%

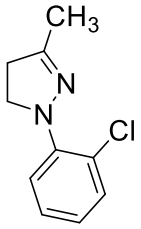

247, 52%

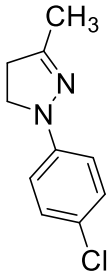

248, 35%

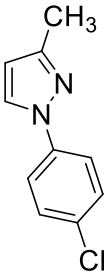

249, 28%

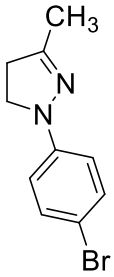

250, 63%

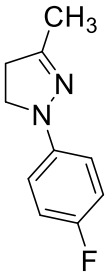

251, 70%

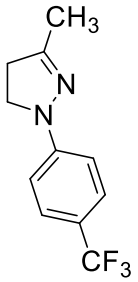

252, 43%

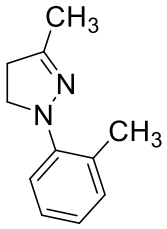

253, 83%

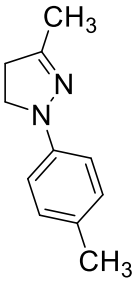

254, 90%
(**255**, 10%)[a]

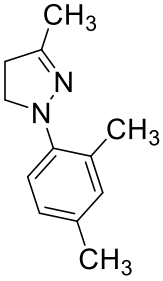

256, 95%

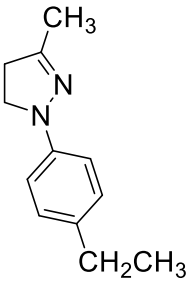

257, 83%
(**258**, 16%)[a]

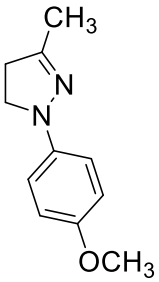

259, 44%
(**260**, 56%)[a]

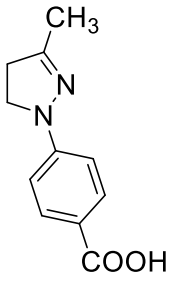

261, 83%

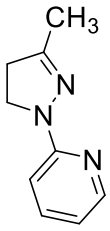

262, 69%

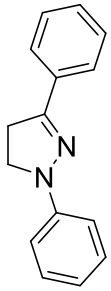

263, 61%
(**264**,12%)[a]

[a]aromatized product and yield in parentheses

Figure 3-16 Reaction scope

Secondary *N*-nitrosoarylamines **182** and **265**–**268** were prepared nearly quantitatively using the standard method to convert them into unsymmetrically-substituted hydrazines (Figure 3-17).

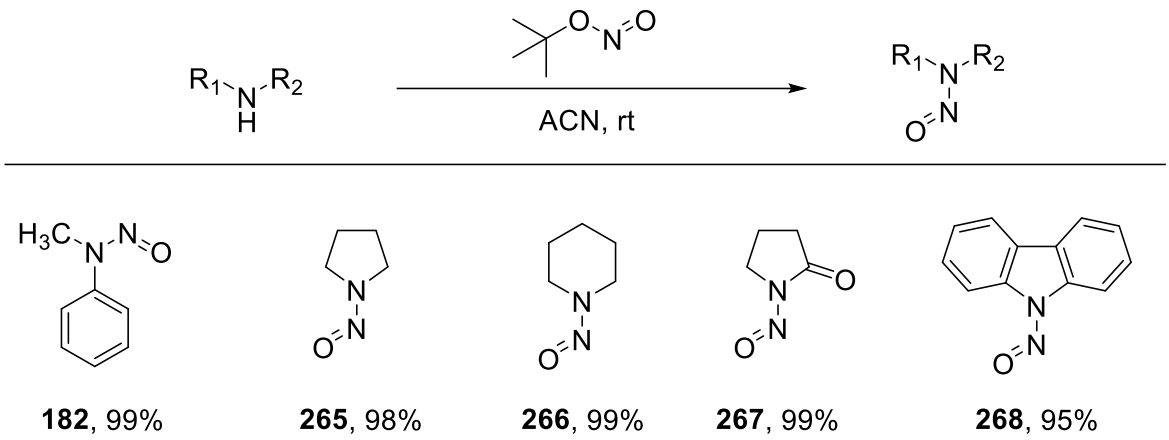

182, 99% **265**, 98% **266**, 99% **267**, 99% **268**, 95%

Figure 3-17 Preparation of secondary *N*-nitrosoamines

Although 1-Methyl-1-phenylhydrazine **183** was obtained in excellent yield from N-nitrosomethylaniline **182**, the yields of hydrazines formed from **265**–**268** were very low, with N–N bond cleavage dominating (Figure 3-18).

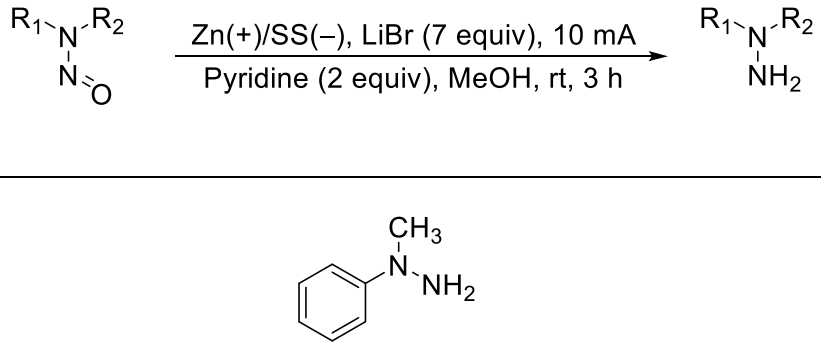

183, 93%

Figure 3-18 Reaction scope

3.3.5 Mechanistic studies

The mechanism of this reductive process remains unclear, but one plausible mechanistic scenario is proposed based on the experiments and observations of the above-mentioned reactions.

3.3.5.1 Plausible mechanism

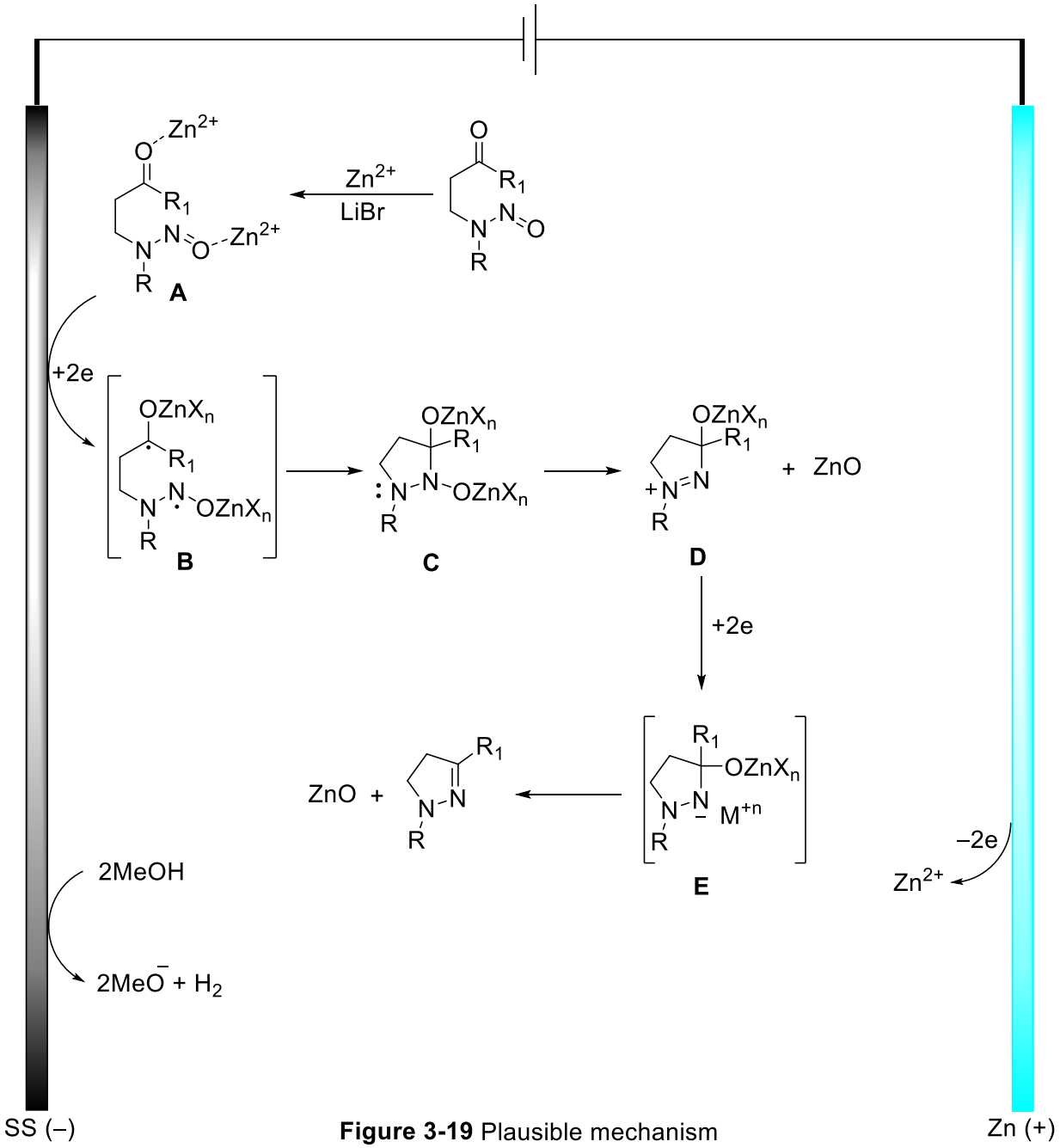

Figure 3-19 Plausible mechanism

One mechanism for the electrolytic reduction of *N*-nitroso compounds is proposed in Figure 3-19. Zinc(II) cations released from the anode coordinate to the weakly basic nitroso oxygen and to the carbonyl oxygen (**A**), facilitating the two-electron reduction that occurs at the cathode (**B**). Radical cyclization forms the five-membered ring (**C**) followed by release of zinc oxide and formation of intermediate **D**. Another two-electron reduction of **D** leads to intermediate **E**, which releases zinc oxide and gives the desired product.

3.3.5.2 Formation and effects of zinc oxide

The sacrificial zinc anode is critical to realize high yields. It is reasonable to assume that Zn^{2+} ions are intimately involved in the reaction mechanism. Zinc oxide is deposited as an off-white solid; no precipitate is formed in the absence of substrate. The identity of the precipitate was confirmed by powder X-ray (Figure 3-20).[187]

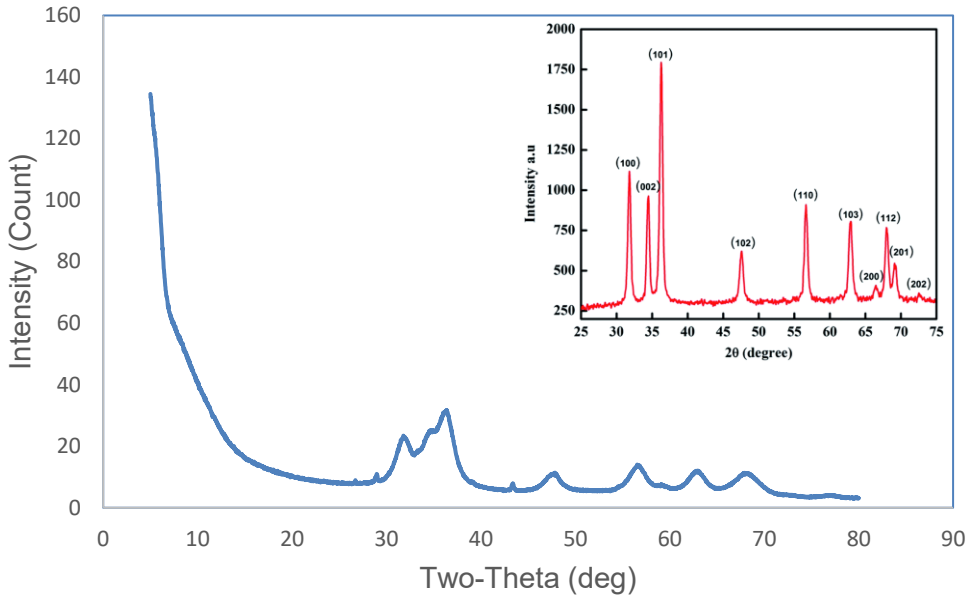

Figure 3-20 Powder X-ray diffraction pattern of the zinc oxide nanoparticles formed during reaction. Inset is an X-ray graph of zinc oxide nanoparticles from literature.[187]

3.3.5.3 Passivation of zinc on cathode; role of electrolyte and pyridine

Electrodeposition of alloy coatings decreases the electrode activity by forming a metallic film on the cathode surface during reaction. The film reacts vigorously with dilute hydrochloric acid solution, concomitant with gas evolution. Powder X-ray diffraction of the film confirmed the formation of zinc metal (Figure 3-21).[188]

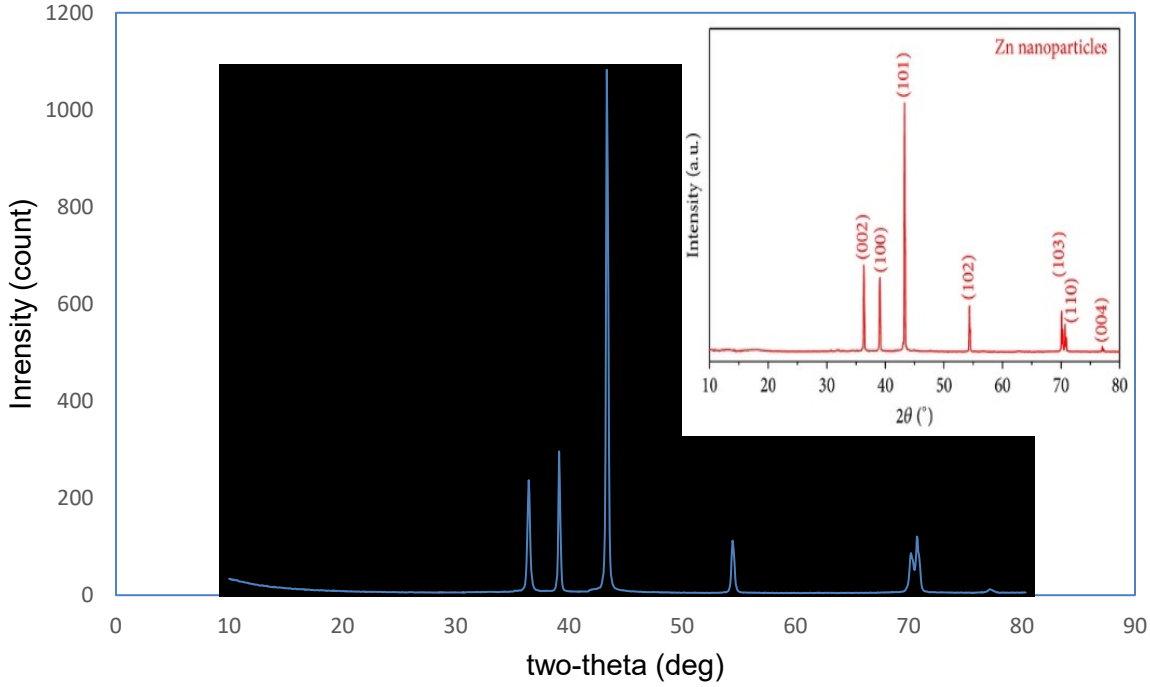

Figure 3-21 X-ray crystallography of the film formed on cathode surface. Inset is X-ray graph of metallic zinc from literature.[188]

During electrolyte optimization, more zinc is passivated on the cathode surface at lower lithium bromide loading. At high loading, a double layer of Li^+ ions protects the cathode inhibiting passivation by zinc (Figure 3-22). Pyridine may coordinate to the electrophilic lithium surface, providing further protection from passivation.[189] The coating of Li^+ also increases the overpotential required for hydrogen evolution, the main energy drain on the process (Figure 3-22).

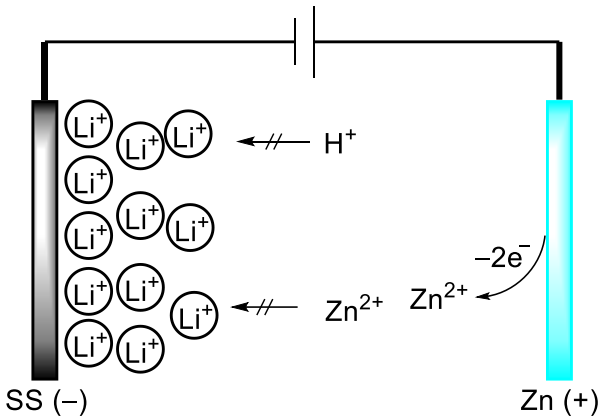

Figure 3-22 Effect of double layer

Pyridine also coordinates to Zn^{2+} in solution, inhibiting diffusion to the surface of electrode. A 15–20 Hz downfield shift of the aromatic C–H signals of pyridine in MeOH-d_4 in the presence of lithium bromide. In the presence of zinc bromide, however, a 755–820 Hz downfield shift was observed, indicating strong coordination of pyridine. XPS analysis confirms the presence of bromide ions on cathode (Appendix A). These experimental results strongly suggest that the soluble zinc complex, $([Zn(py)_2](Br)_2)$, is formed. Equilibrium formation of pyridinium ions provides a more acidic medium promoting proton transfers (Figure 3-23).

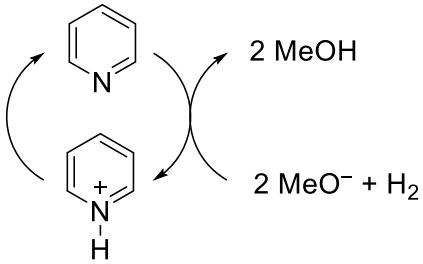

Figure 3-23 Formation of pyridinium ion

3.3.5.4 Role of the solvent

In addition to serving as a proton source, methanol is reduced at the cathode to methoxide anion and a proton, which is reduced to hydrogen (Figure 3-24).

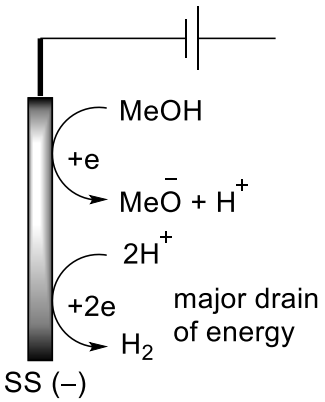

Figure 3-24 Hydrogen evolution reaction

3.3.5.5 Side products formation

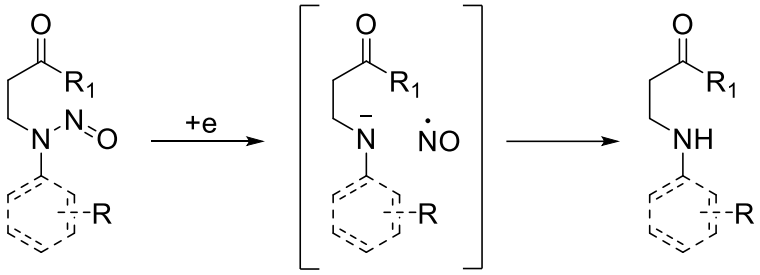

Scheme 3-4 Major side reaction: N–N bond cleavage

One side product was isolated, the result of N–N bond cleavage (Scheme 3-4). Electron donating groups (EDG) on the substituted nitrogen decrease the stability of the N–N bond cleaved anionic intermediate, while electron withdrawing groups increase the stability. Hence, the forward reaction is less favoured for electron withdrawing groups, whereas electron donating groups inhibit the forward reaction. The effect increases with increasing electron-withdrawing character, and the trend is general for both ester and ketone substrates (Figures 3-25 and 3-26).

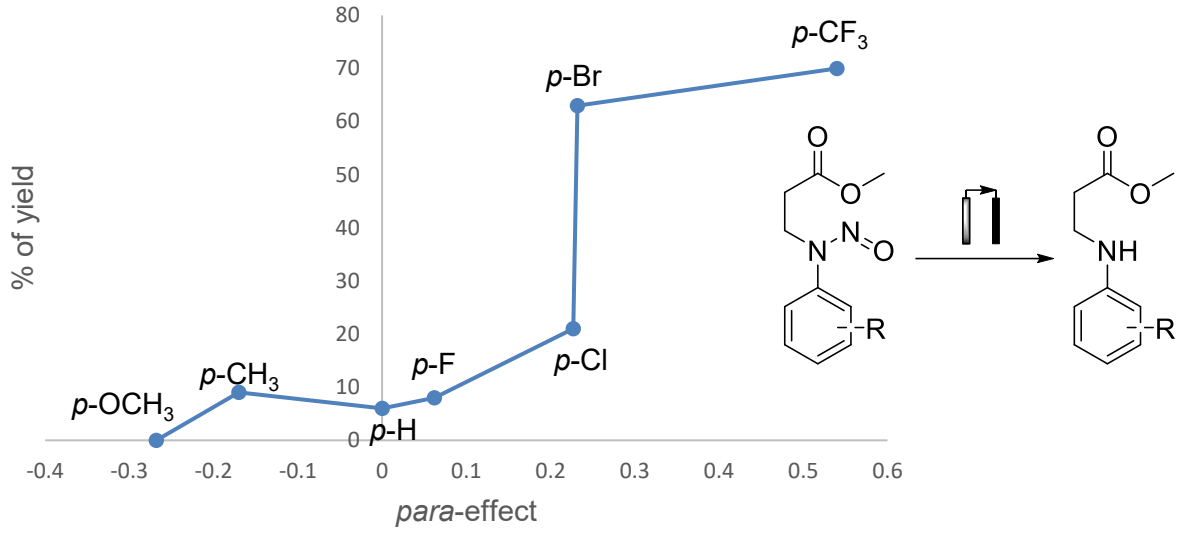

Figure 3-25 Substituent constant vs yield of side product for esters

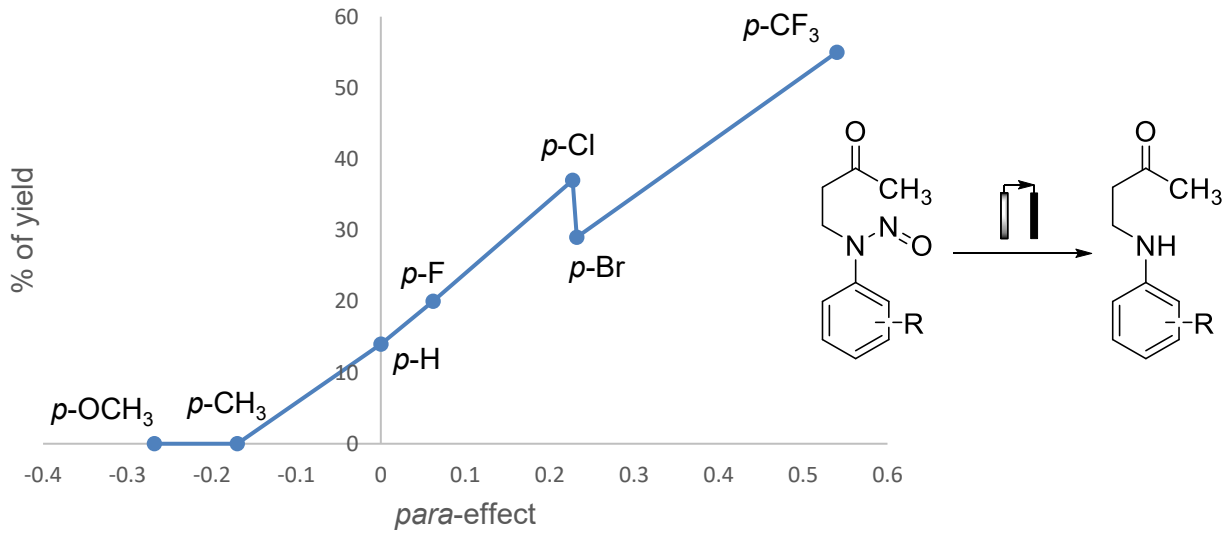

Figure 3-26 Substituent constant vs yield of side product for ketones

3.3.6 Anodic oxidation of pyrazolidin-3-one to pyrazole

Under optimized conditions, stoichiometric chemical oxidants were added to the reaction mixture, with the intention to promote pyrazole aromatization. The addition of cupric ion (1 equiv) to the electroreduction medium produces the pyrazole in 30% yield, although the combined yield

of cyclization product was 80% yield (Table 3.6, entry 2). However, higher copper(II) concentration and/or longer reaction times do not improve the conversion to pyrazole. Ferric ion is more effective; yielding 43% of the pyrazole (Table 3-6, entry 5). Higher iron loading gave no improvement (Table 3-6, entry 6). Direct oxidation of 1-phenylpyrazolidin-3-one itself was equally poor (Equation 3-10).

Table 3-6 Effect of additives

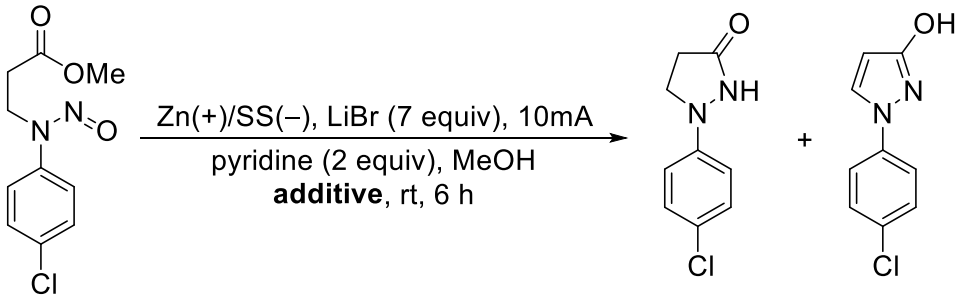

187 **52** **53**

Entry[a]	Additive	Yield[b] %	
		52	**53**
1	none	79	-
2	$Cu(OAc)_2•H_2O$	50	30
3	$Cu(OAc)_2•H_2O$ (2 equiv, 20h)	64	5
4	*p*-benzoquinone	64	8
5	**$FeCl_3•6H_2O$**	**45**	**43**
6	$FeCl_3•6H_2O$ (2 equiv)	49	7

[a]Reaction conditions: methyl 3-((4-chlorophenyl)(nitroso)amino)propanoate **187** (0.2 mmol), electrolyte (1.4 mmol), pyridine (0.4 mmol), MeOH (5 mL) were added to a 5 mL IKA flask with constant current 10 mA for 6 h at room temperature. [b]yield was calculated by ^{1}H-NMR spectrosopy.

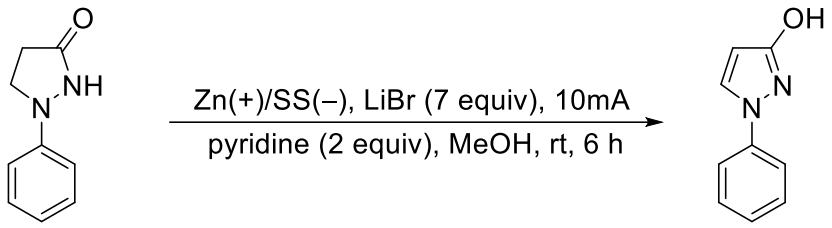

231 **232**, 32%

Equation 3-10 Aromatization of 1-phenylpyrazolidin-3-one **231**

In the presence of lithium bromide and ferric ion (1 equiv each) and at higher substrate concentration (1mM), the use of stainless steel electrodes improves the aromatization process, providing hydroxypyrazole **231** in 96% yield.

Table 3-7 Optimization study aromatization of 231

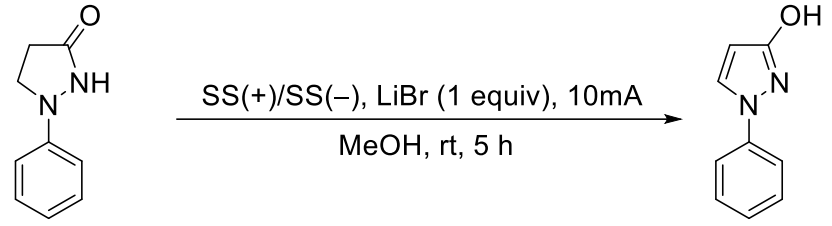

1 mM
231 **232**

Entry[a]	Deviation from above condition	Yield[b] %
1	none	56
2	**1 eq. $FeCl_3$•$6H_2O$**	**96**

[a]Reaction conditions: 1-phenylpyrazolidin-3-one **231** (0.5 mmol), electrolyte (0.5 mmol), MeOH (5 mL) were added to a 5 mL IKA flask with constant current 10 mA for 5 h at room temperature. [b]yield was calculated by ^{1}H-NMR spectroscopy.

3.4 Conclusion

We have developed a new electrochemical method for preparing substituted pyrazoles and pyrazolines by the reduction of *N*-nitrosamines. A broad range of electron withdrawing and electron donating groups are compatible with the electrochemical reaction. Unlike conventional synthetic methods, no transition metal catalysts or air-sensitive reagents are required in the electroreductive process. The reaction procedure is highly selective and leads to efficient construction of many biologically active heterocycles. The most serious limitation, yet to be addressed, is competitive N–N bond cleavage when strong electron-withdrawing groups are present at nitrogen.

This electroreductive process can potentially replace the use of hydrazine and derivatives from fine chemicals synthesis in both academic and industrial setting; continuous electrochemical processes have already been commercialized; flow electrochemical cells are commercially available and readily scaled,[190,191] avoiding toxic and/or explosive reagents and intermediates and generating far less chemical wastes.

Although the *N*-nitrosamine starting materials are stable and air insensitive, some N-nitrosamines are quite toxic. Although intermolecular N–N bond formation by anodic oxidation has been described, coupling of an amine and primary amide remains unknown.[192-196] If possible, oxidative N–N bond formation between an aniline and primary amide (e.g., **101**) is the ultimate objective, avoiding both hydrazine and *N*-nitrosamine entirely (Scheme 3-5). Electrochemical aromatization of pyrazolidinone to pyrazole requires further study. Detailed analytical characterization of the redox cycle (CV, chronopotentiometry, faradic yield calculation and spectroelectrochemisty is planned), along with a more extensive determination of substrate scope.

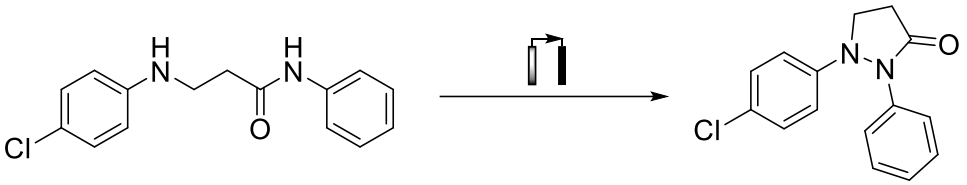

101 **269**

Scheme 3-5 Future work

Experimental Part

General experimental

All manipulations of air sensitive compounds were performed under argon or nitrogen atmosphere using standard Schlenk techniques or in a nitrogen-filled drybox. Dry solvents were used when needed. Anhydrous copper acetate was purchased from Sigma-Aldrich. THF was distilled over sodium/benzophenone under nitrogen. Anhydrous DMSO was purchased from Sigma-Aldrich. Hexane and ethyl acetate were used straight from bottle without distillation for column chromatography. ^{1}HNMR and ^{13}C NMR spectra were recorded on Varian Unity-Inova 400 (^{1}H, 400MHz; ^{13}C, 100 MHz), Varian Mercury 400 (^{1}H, 400MHz; ^{13}C, 100 MHz), Varian Unity-Inova 500 (^{1}H, 500MHz; ^{13}C, 125 MHz) or a Varian Unity-Inova 600 (^{1}H, 600 MHz). Abbreviations were used to explain multiplicities: s = singlet, d = doublet, t = triplet, q = quartet, m = multiplet, br = broad. Coupling constants values are obtained directly from the spectrum and coupling constants are reported in Hertz (Hz). All spectra were recorded at room temperature. High-resolution mass spectra data were recorded by University of Alberta Mass Spectroscopy Facility. University of Alberta Analytical and Instrumentation Laboratory performed IR, elemental analyses, and GC-MS.

Experimental details

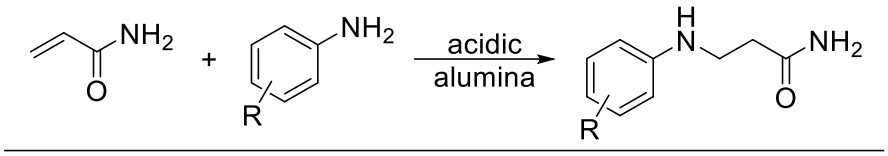

General procedure A:[197] A mixture of the Michael acceptor (1.00 equiv) and amine (1.50 equiv) were heated to reflux in the presence of acidic alumina Al_2O_3 (200 mol%). The reaction was monitored by TLC and cooled to room temperature upon completion. After the addition of ethyl acetate, the reaction mixture was filtered through a filter paper, and the alumina was rinsed with ethyl acetate. The crude reaction mixture was concentrated by rotary evaporation and then purified by silica gel column chromatography using hexane/ethyl acetate as eluents.

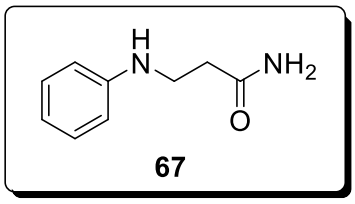

67

3-(Phenylamino)propanamide (67): General procedure **A** was followed for making 3-(phenylamino)propanamide **67**. Flash chromatography of the crude product over silica gel provided **67** as white solid in a yield of 80%:[197] ^{1}H NMR ($CDCl_3$, 500 MHz) δ 2.50 (t, *J* = 6.5 Hz, 2 H), 3.46 (t, *J* = 6.5 Hz, 2 H),, 3.98 (br s, 1 H), 5.63 (br s, 1 H), 5.70 (br s, 1 H), 6.65 (d, *J* = 8.0 Hz, 2 H), 6.73 (t, *J* = 7.5 Hz, 1 H), 7.18 (td, *J* = 7.5, 2.0 Hz, 2 H).

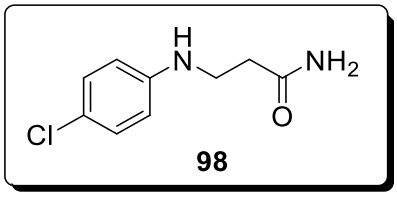

98

3-((4-Chlorophenyl)amino)propanamide (98): General procedure **A** was followed for making **98** The product was obtained as a white solid in a yield of 60%. FTIR ($CDCl_3$, cast) 3449, 3327, 3195, 3100, 2967, 2903, 2855, 2843, 1659, 1606, 1517, 1198 cm^{-1}; ^1H NMR ($CDCl_3$, 500 MHz) δ 2.51 (t, J = 6.0 Hz, 2 H), 3.44 (t, *J* = 6.0 Hz, 2 H), 4.18 (br s, 1 H), 5.44 (br s, 1 H), 5.58 (br s, 1 H), 6.55-6.58 (m, 2 H), 7.11–7.14 (m, 2 H); ^{13}C NMR ($CDCl_3$, 125 MHz) δ 34.6, 39.9, 114.3, 122.5, 129.2, 146.2, 173.6; exact mass (EI) *m/z* calcd for $C_9H_{11}{}^{35}ClN_2O$ $(M + H)^+$ 199.0633, found 199.0632.

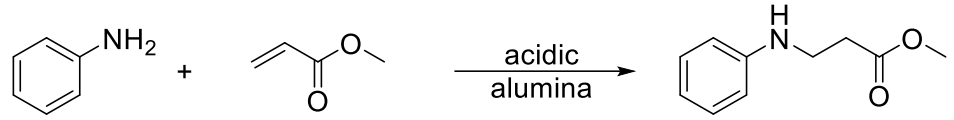

81 **82** **83**, 85%

Methyl 3-phenylaminopropionate (83): General procedure **A** was followed for making methyl 3-phenylaminopropionate **83** using aniline and methyl acrylate. The product was obtained as a white solid in a yield of 85%:[198] ^1H NMR ($CDCl_3$, 500 MHz) δ 2.63 (t, *J* = 8.0 Hz, 2 H), 3.46 (q, *J* = 8.0 Hz, 2 H), 3.70 (s, 3H), 4.01 (br s, 1 H), 6.63 (dd, *J* = 10.5, 1.0 Hz, 2 H), 6.72 (tt, *J* = 9.0, 1.0 Hz, 1 H), 7.16–7.20 (m, 2 H).

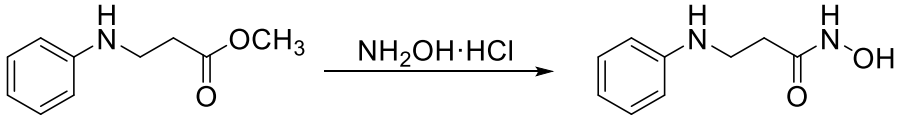

83 **79**, 81%

***N*-Hydroxy-3-(phenylamino)propanamide (79):** A mixture of hydroxylaminehydrochloride (8.00 mmol, 2.00 equiv) and sodium methoxide (12.00 mmol, 3.00 equiv) in anhydrous methanol was stirred for 30 min at 0 °C. To this mixture methyl 3-phenylaminopropionate **79** (4.00 mmol, 1.00 equiv) was added, and the mixture was stirred at room temperature for 4 h. The reaction was

quenched with ice-cold water, neutralized with dilute acetic acid, and extracted with ethyl acetate. The combined organic layers were dried over sodium sulfate, filtered, and evaporated under vacuum. The residue was purified by flash chromatography (methanol-dichloromethane) to afford *N*-hydroxy-3-(phenylamino)propanamide **79** as a white solid in a yield of 81%:[199] ^{1}H NMR ($CDCl_3$, 500 MHz) δ 2.63 (t, *J* = 8.0 Hz, 2 H), 3.46 (q, *J* = 8.0 Hz, 2 H), 3.70 (s, 3H), 4.01 (br s, 1 H), 6.63 (dd, *J* = 10.5, 1.0 Hz, 2 H), 6.72 (tt, *J* = 9.0, 1.0 Hz, 1 H), 7.16–7.20 (m, 2 H).

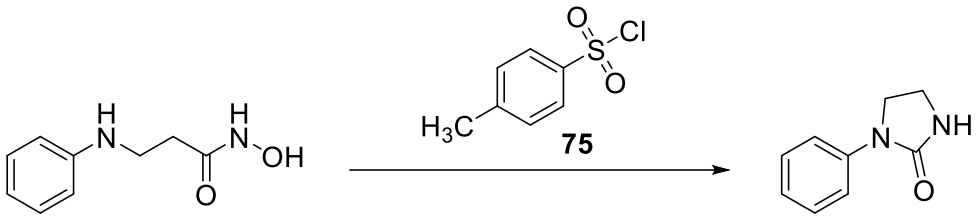

79 **84**, 60%

1-Phenylimidazolidin-2-one (84): To a solution of *N*-hydroxy-3-(phenylamino)propanamide **79** (0.54 mmol, 1.00 equiv) in 3.0 mL DCM was added DMAP (0.50 mmol, 0.10 equiv), TEA (1.08 mmol, 2.00 equiv), and TsCl **75** (0.65 mmol, 1.20 equiv) at room temperature and stirred for 2 hours. The reaction mixture was then heated to reflux overnight, cooled to room temperature, washed with water, brine, dried over $MgSO_4$ and concentrated under vacuum. Flash chromatography of the crude product over silica gel, 25% EtOAc–hexane, gave **84** in 60% of yield as white solid:[200] FTIR ($CDCl_3$, cast film) 3266, 3116, 3061, 2960, 2924, 2855, 1682, 1600, 1506, 1484, 1175 cm^{-1}; ^{1}H NMR ($CDCl_3$, 500 MHz) δ 3.59 (ddd, *J* = 9.0, 7.5, 1.0 Hz, 2 H), 3.95 (dd, *J* = 9.0, 7.5 Hz, 2 H), 4.68 (br s, 1 H), 7.06 (t, *J* = 7.5 Hz, 1 H), 7.33–7.36 (m, 2 H), 7.55 (d, *J* = 8.0 Hz, 2 H); ^{13}C NMR ($CDCl_3$, 125 MHz) δ 37.5, 45.3, 117.9, 122.8, 128.8, 140.0, 159.6; exact mass (EI) *m/z* calcd for $C_9H_{10}N_2O$ $(M + H)^+$ 163.0866, found 163.0865.

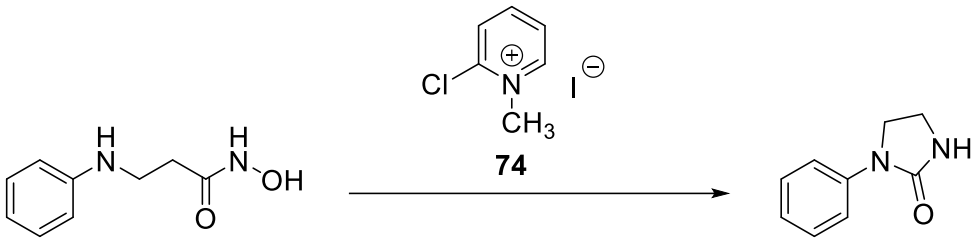

79 **74** **84**, 87%

1-Phenylimidazolidin-2-one (84): To a solution of *N*-hydroxy-3-(phenylamino)propanamide **79** (0.58 mmol, 1.00 equiv) in 3.0 mL DCM was added TEA (1.17 mmol, 2.00 equiv) and **74** (0.58 mmol, 1.00 equiv). The reaction mixture was heated to reflux overnight, cooled to room temperature, washed with 1% aqueous $NaHCO_3$, water, brine, dried over $MgSO_4$ and concentrated under vacuum. Flash chromatography of the crude product over silica gel 25% EtOAc–hexane gave **84** in 87% of yield as white solid.[200]

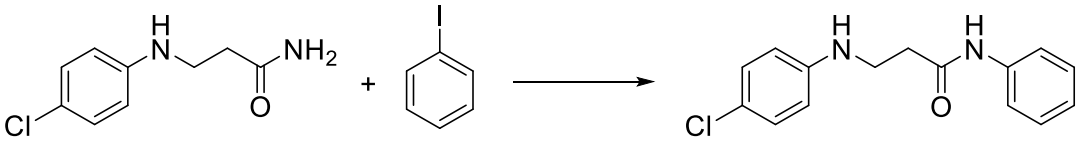

98 **100** **101**, 48%

3-(4-Chlorophenylamino)-*N*-phenylpropanamide (101): The compound was synthesized according to a literature procedure[201] using iodobenzene **100** (0.65 mmol, 1.00 equiv), 3-((4-chlorophenyl)amino)propanamide **98** (0.79 mmol, 1.20 equiv), CuI (0.07 mmol, 0.10 equiv), *N*,*N*′-dimethylethylene diamine (0.07 mmol, 0.10 equiv), and cesium fluoride (1.50 mmol, 2.00 equiv). 3-(4-chlorophenylamino)-*N*-phenylpropanamide **101** obtained in 48% yield as solid.[202]

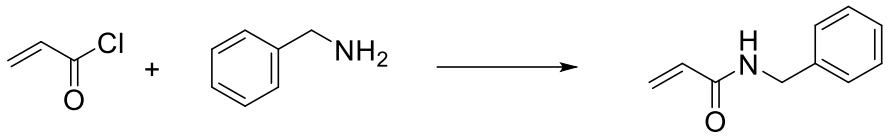

102 **103** **104**, 88%

***N*-Benzylacrylamide (104):** The compound was synthesized according to a literature procedure.[203] *N*-benzylacrylamide **104** was obtained as white solid in 88% yield: ^{1}H NMR ($CDCl_3$, 500 MHz) δ 4.53 (d, *J* = 6.0 Hz, 2H), 5.67 (dd, *J* = 10.5, 1.0 Hz, 1 H), 4.21 (br, 1 H), 6.11 (dd, *J* = 17.0, 10.5 Hz, 1 H), 6.32 (dd, *J* = 17.0, 1.0 Hz, 1 H), 7.27–7.36 (m, 5 H).

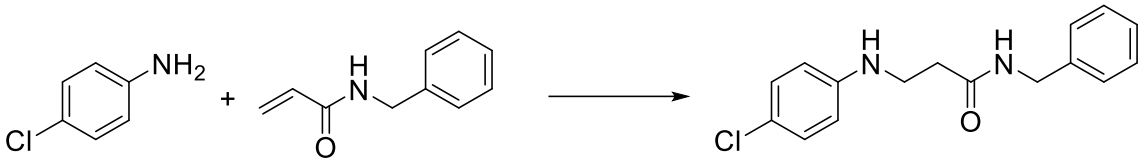

49 **104** **105**, 56%

***N*-Benzyl-3-((4-chlorophenyl)amino)propanamide (105):**[204] To a solution of *N*-benzylacrylamide **104** (18.55 mmol, 1.00 equiv) in water (22.00 mL) and TFE (3.00 mL) 4-chloroaniline (18.55 mmol, 1.00 equiv) was added. Reaction mixture was heated to reflux at 100 °C. Reaction monitored by TLC and stirred until complete conversion of starting materials. The reaction was cooled to room temperature, diluted with ethyl acetate, washed with water and brine solution. Combined organic mixture was dried over $MgSO_4$ and concentrated. The obtained reaction mixture was dissolved in warm DCM and slow addition of Et_2O gave *N*-benzyl-3-((4-chlorophenyl)amino)propanamide **105** in 56 % of yield as a white solid: FTIR ($CDCl_3$, cast) 3411, 3304, 3087, 3065, 3030, 2924, 28778, 1646, 1601, 1549, 1501, cm^{-1}; ^{1}H NMR ($CDCl_3$, 500 MHz) δ 2.49 (t, *J* = 6.0 Hz, 2 H), 3.45 (br, 2 H), 4.43 (d, *J* = 6.0 Hz, 2 H), 6.52 (d, *J* = 8.5 Hz, 2 H), 7.11 (d, *J* = 9.0 Hz, 2 H), 7.24 (d, *J* = 6.5 Hz, 2 H), 7.28–7.34 (m, 3 H); ^{13}C NMR ($CDCl_3$, 125 MHz) δ 35.4, 40.2, 43.7, 114.3, 122.4, 127.7, 127.8, 128.8, 129.1, 138.0, 146.3, 171.2; exact mass (electrospray) *m/z* calcd for $C_{16}H_{17}{}^{35}ClN_2O$ $(M + H)^+$ 289.1102, found 289.1106.

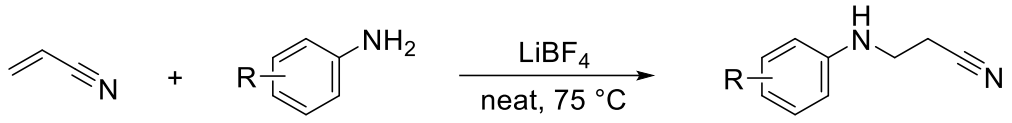

128 **129** **130**

General procedure B: A mixture of acrylonitrile (1.00 equiv) and amine (1.00 equiv) were heated at 75 °C in the presence of lithium tetrafluoroborate (10 mol %) overnight. The reaction was then cooled to room temperature and extracted using ethyl acetate. The combined organic mixture was washed with brine, dried over $MgSO_4$, concentrated by rotary evaporation, and then purified using a silica–filled column chromatography using hexane/ethyl acetate as eluents.

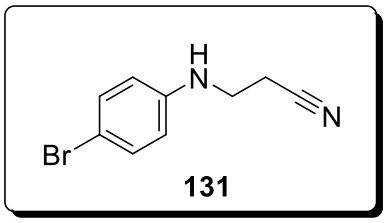

131

3-((4-Bromophenyl)amino)propanenitrile (131):[206] General procedure **B** was followed for making **131**. The product was obtained as a yellow solid in a yield of 84%. ^{1}H NMR ($CDCl_3$, 500 MHz) δ 2.63 (t, *J* = 6.5 Hz, 2 H), 3.49 (t, *J* = 6.5 Hz, 2 H), 4.00 (br s, 1 H), 6.50 (d, *J* = 9.0 Hz, 2 H), 7.29 (d, *J* = 9.0 Hz, 2 H); ^{13}C NMR ($CDCl_3$, 125 MHz) δ 18.1, 39.8, 110.5, 114.7, 117.9, 132.3, 145.2.

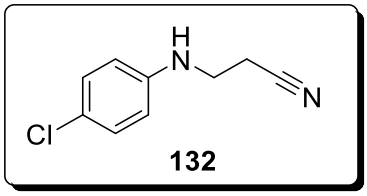

132

3-((4-Chlorophenyl)amino)propanenitrile (132):[205] General procedure **B** was followed for making **132**. The product was obtained as a yellow solid in a yield of 80%. ^{1}H NMR ($CDCl_3$, 500

MHz) δ 2.63 (t, *J* = 6.5 Hz, 2 H), 3.48–3.52 (m, 2 H), 4.00 (br s, 1 H), 6.54–6.57 (m, 2 H), 7.15–7.17 (m, 2 H).

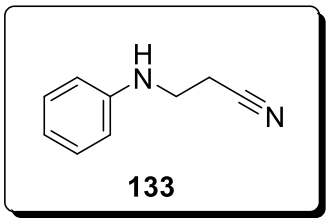

133

3-(Phenylamino)propanenitrile (133):[208] General procedure **B** was followed for making **133**. The product was obtained as a pale yellow solid in a yield of 87%. ^{1}H NMR ($CDCl_3$, 500 MHz) δ 2.63 (t, *J* = 6.5 Hz, 2 H), 3.52 (t, *J* = 6.5 Hz, 2 H), 3.67 (br s, 1 H), 6.63 (d, *J* = 8.5 Hz, 2 H), 6.77–6.81 (m, 1 H), 7.21–7.24 (m, 2H).

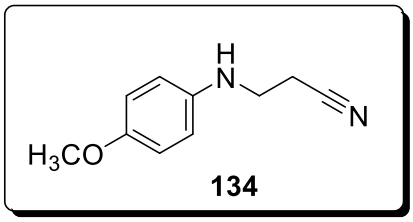

134

3-((4-Methoxyphenyl)amino)propanenitrile (134):[208] General procedure **B** was followed for making **134**. The product was obtained as a yellow solid in a yield of 90%. ^{1}H NMR ($CDCl_3$, 500 MHz) δ 2.62 (t, *J* = 6.5 Hz, 2 H), 3.48 (t, *J* = 6.5 Hz, 2 H), 3.66 (br s, 1 H), 3.76 (s, 3 H), 6.61 (d, *J* = 7.0 Hz, 2 H), 7.81 (d, *J* = 7.0 Hz, 2 H); ^{13}C NMR ($CDCl_3$, 125 MHz) δ 18.2, 40.9, 55.8, 114.8, 115.1, 118.2, 140.1, 153.0.

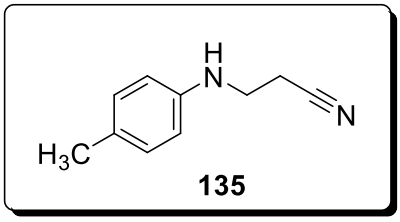

135

3-(4-Methylanilino)propanenitrile (135):[208] General procedure **B** was followed for making **135**. The product was obtained as a white solid in a yield of 95%. ^{1}H NMR ($CDCl_3$, 500 MHz) δ 2.25 (s, 3 H), 2.63 (t, *J* = 6.5 Hz, 2 H), 3.51 (t, *J* = 6.5 Hz, 2 H), 3.79 (br s, 1 H), 6.55 (d, *J* = 7.5 Hz, 2 H), 7.02 (d, *J* = 7.5 Hz, 2 H); ^{13}C NMR ($CDCl_3$, 125 MHz) δ 18.2, 20.4, 40.2, 113.4, 118.3, 128.1, 130.1, 143.8.

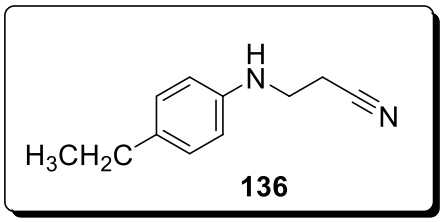

136

3-(4-Ethylanilino)propanenitrile (136): General procedure **B** was followed for making **136**. The product was obtained as a yellow solid in a yield of 93%. ^{1}H NMR ($CDCl_3$, 500 MHz) δ 1.20 (t, *J* = 7.5 Hz, 3 H), 2.56 (q, *J* = 7.5 Hz, 2 H), 2.63 (t, *J* = 6.5 Hz, 2 H), 3.51 (t, *J* = 6.5 Hz, 2 H), 6.58 (d, *J* = 8.5 Hz, 2 H), 7.05 (d, *J* = 8.5 Hz, 2 H); ^{13}C NMR ($CDCl_3$, 125 MHz) δ 15.9, 18.2, 27.9, 40.2, 113.4, 118.3, 128.9, 134.8, 143.9.

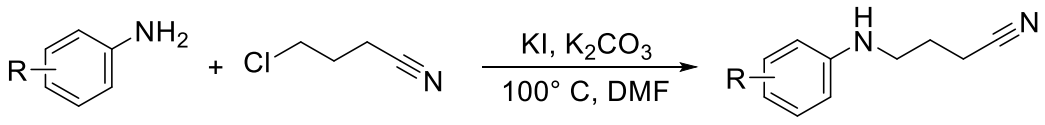

129 **137** **138**

General procedure C:[198] A mixture of 4-chlorobutyronitrile **137** (3.00 mmol, 1.00 equiv) in dimethylformamide (0.80 mL) was added over 1.5 h to a mixture of the arylamine (3.00 mmol, 1.00 equiv), Cs_2CO_3 (3.00 mmol, 1.00 equiv), and KI (6.00 mmol, 2.00 equiv) in a mixture of dimethylformamide (3.50 mL). The mixture was stirred at 100 °C for 8 h. After completion of the reaction, as indicated by TLC, the mixture was cooled to room temperature and was treated with 50 mL ethyl ether and 10 mL water. The aqueous phase was separated and extracted with an

additional 30 mL ethyl ether. The combined organic layer was washed with water, brine, dried over anhydrous sodium sulphate and filtered. The solvent was evaporated in vacuum. The crude product was purified by column chromatography over silica gel using 40% ethylacetate/hexane eluent.

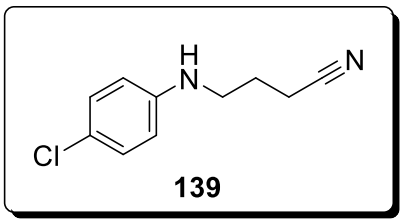

139

4-((4-Chlorophenyl)amino)butanenitrile (139):[210] General procedure **C** was followed for making **139** The product was obtained as a yellow solid in a yield of 80%. ^{1}H NMR ($CDCl_3$, 500 MHz) δ 1.93–1.99 (m, 2 H), 2.47 (t, *J* = 7.0 Hz, 2 H), 3.29 (q, *J* = 6.5 Hz, 2 H), 3.71 (br s, 1 H), 6.52–6.56 (m, 2 H), 7.12–7.15 (m, 2 H); ^{13}C NMR ($CDCl_3$, 175 MHz) δ 14.8, 25.1, 42.5, 113.9, 119.2, 122.6, 129.2, 146.1.

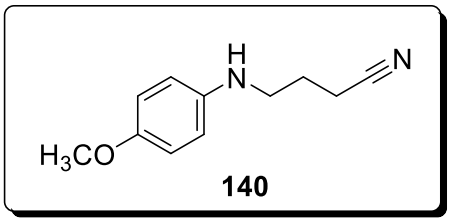

140

4-((4-Methoxy)amino)butanenitrile (140):[210] General procedure **C** was followed for making **140** The product was obtained as a yellow liquid in a yield of 60%. ^{1}H NMR ($CDCl_3$, 500 MHz) δ 1.94–1.96 (m, 2 H), 2.48 (t, *J* = 7.0 Hz, 2 H), 3.24–3.28 (m, 2 H), 3.75 (s, 3 H), 6.59–6.60 (m, 2 H), 6.78–6.80 (m, 2 H); ^{13}C NMR ($CDCl_3$, 125 MHz) δ 14.8, 25.4, 43.4, 55.6, 114.3, 114.9, 119.4, 141.7, 152.4.

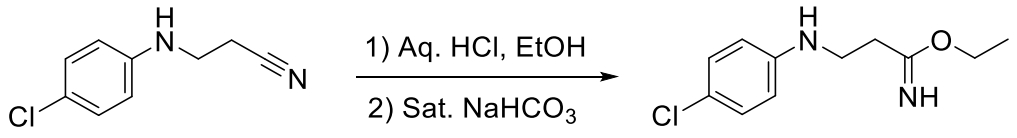

132 **142**

Ethyl 3-((4-chlorophenyl)amino)propanimidate (142):[211] To an ice–cold stirred solution of 3-((4-chlorophenyl)amino)propanenitrile **132** (3.36 mmol, 0.61 g) acetyl chloride AcCl (26.88 mmol, 2.11 g) was added followed by dry ethanol (12.00 mmol, 1.86 g). The stirring was continued at 25 °C under a nitrogen atmosphere. The reaction was monitored by TLC and after the reaction was complete, the volatiles were removed under reduced pressure and ethyl 3-((4-chlorophenyl)amino)propanimidate hydrochloride **141** was isolated as white solid. The imidate hydrochloride was mixed slowly with cold saturated aqueous $NaHCO_3$ solution, and extracted with diethyl ether Et_2O (3 × 6 mL). The combined organic solution was washed with distilled water (1 × 5 mL) and brine (1 × 5 mL), concentrated under reduced pressure to obtain ethyl 3-((4-chlorophenyl)amino)propanimidate **142**. The product was obtained as a yellow liquid in a yield of 87%. ^{1}H NMR ($CDCl_3$, 500 MHz) δ 1.26 (t, *J* = 7.0 Hz, 3 H), 2.59 (t, 6.5 Hz, 2 H), 4.06 (br s, 1 H), 4.16 (q, *J* = 7.0 Hz, 2 H), 6.54 (d, *J* = 7.5, 2 H), 7.12 (q, *J* = 7.5 Hz, 2 H); ^{13}C NMR ($CDCl_3$, 175 MHz) δ 14.2, 33.7, 39.6, 60.7, 114.1, 122.3, 129.1, 146.2, 172.2; exact mass (electrospray) *m/z* calcd for $C_{11}H_{15}{}^{35}ClN_2O$ $(M + H)^+$ 227.0946, found 227.0946.

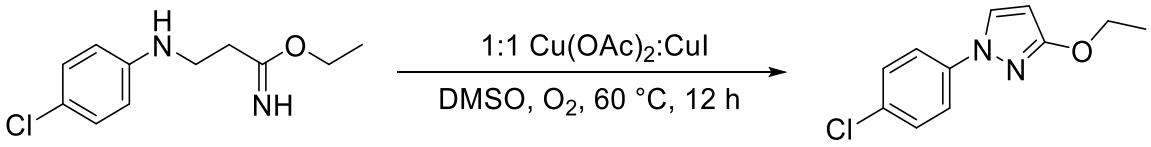

142 **143**

1-(4-Chlorophenyl)-3-ethoxy-1*H*-pyrazole (143): Into a two–neck round-bottomed flask, ethyl 3-((4-chlorophenyl)amino)propanimidate (0.11 mg, 0.48 mmol) was added followed by addition of cupric acetate $Cu(OAc)_2$ (0.04mg, 0.24 mmol) and copper iodide CuI (0.05 mg, 0.24 mmol). The reaction vessel was purged with oxygen, and then 4.0 mL of anhydrous dimethyl sulfoxide was added by syringe. The reaction mixture was stirred at 60 °C for overnight under oxygen atmosphere. The mixture was cooled to room temperature and extracted with ethyl acetate. The combined organic solution was washed with water (3 × 10 mL) and brine, dried over $MgSO_4$ and concentrated under reduced pressure. Flash chromatography of the crude product over silica gel using 5% EtOAc–hexane gave 1-(4-chlorophenyl)-3-ethoxy-1*H*-pyrazole **143** (82 mg, 76%) as a yellow solid. FTIR ($CHCl_3$, cast film) 2980, 2929, 2855, 1598, 1549, 1504, 1488, 1471, 1379, 1354 cm^{-1}; ^1H NMR ($CDCl_3$, 500 MHz) δ 1.43 (t, *J* = 8.0 Hz, 3 H), 4.30 (q, *J* = 8.0 Hz, 2 H), 5.90 (d, *J* = 2.0 Hz, 1 H), 7.37 (d, *J* = 8.5 Hz, 2 H), 7.55 (d, *J* = 8.5 Hz, 2 H), 7.69 (d, *J* = 2.0 Hz, 1 H); ^{13}C NMR ($CDCl_3$, 125 MHz) δ 14.8, 29.7, 65.0, 94.3, 118.9, 127.5, 129.4, 130.5, 138.8, 164.6; exact mass (electrospray) *m/z* calcd for $C_{11}H_{12}{}^{35}ClN_2O$ $(M + H)^+$ 223.0633, found 223.0631.

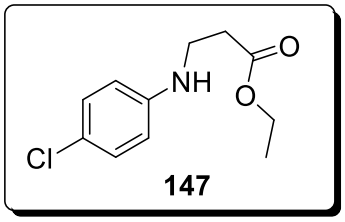

147

1-(4-Chlorophenyl)-3-ethoxy-1*H*-pyrazole (147):[212] ^1H NMR ($CDCl_3$, 500 MHz) δ 1.27 (t, *J* = 7.0 Hz, 3 H), 2.60 (t, *J* = 6.5 Hz, 2 H), 3.42 (t, *J* = 6.5 Hz, 2 H), 4.06 (br s, 1 H), 4.16 (q, *J* = 7 Hz, 2 H), 6.55 (d, *J* = 8.5 Hz, 2 H), 7.12 (d, *J* = 8.5, 2 H); ^{13}C NMR ($CDCl_3$, 125 MHz) δ 14.2, 33.7, 39.5, 60.7, 114.1, 122.3, 129.1, 146.2, 172.2.

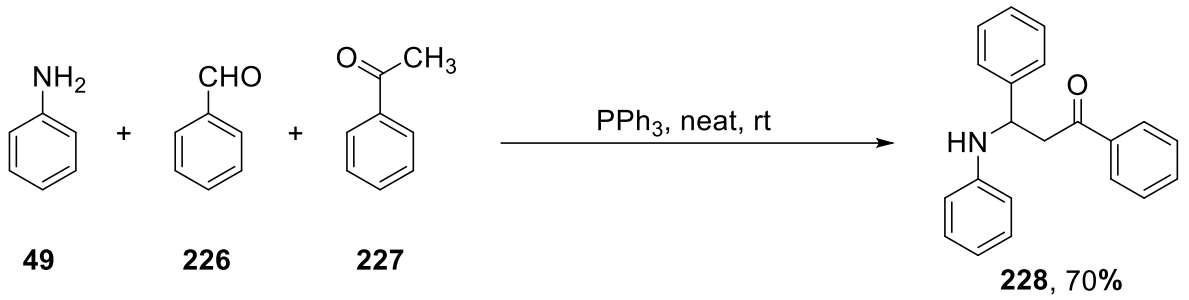

49 **226** **227** **228**, 70%

1,3-Diphenyl-3-(phenylamino)propan-1-one (228):[213] To a mixture of aniline (6.0 mmol, 1.0 equiv), benzaldehyde (6.0 mmol, 1.0 equiv), and acetophenone (7.2 mmol, 1.2 equiv), 5.0 mol% triphenyl phophine was added and the reaction mixture was stirred at room temperature for 4 hr. After that, 12 mL methanol was added followed by addition of water until a precipitate formed. The precipitate was filtered by suction and washed with 3 mL of petroleum ether. White solid product was obtained in a yield of 70% and used for next step without further purification: FTIR ($CHCl_3$, cast film) 3386, 3081, 3061, 3025, 2959, 2918, 2877, 2816, 1962, 1894, 1817, 1766, 1670, 1600 cm^{-1}; ^1H NMR ($CDCl_3$, 500 MHz) δ 3.46 (dd, *J* = 16.0, 7.5 Hz, 1 H), 3.55 (dd, *J* = 16.0, 7.5 Hz, 1 H), 4.59 (br, 1 H), 5.03 (dd, *J* = 7.5, 5.0 Hz), 6.59 (dd, *J* = 8.5, 1.0 Hz, 2 H), 6.69 (t, *J* = 7.5 Hz, 1 H), 7.10–7.13 (m, 2 H), 7.24–7.27 (m, 1 H), 7.33–7.36 (m, 2H), 7.45–7.49 (m, 4H), 7.57–7.60 (m, 1H), 7.92–7.94 (m, 2 H) ; ^{13}C NMR ($CDCl_3$, 125 MHz) δ 46.3, 54.8, 113.8, 117.8, 126.4, 127.4, 128.2, 128.7, 128.8, 129.1, 133.4, 136.7, 143.0, 147.0, 198.3; HRMS (electrospray) *m/z* calcd for $C_{21}H_{19}NO$ $(M + H)^+$ 302.1539, found 302.1537.

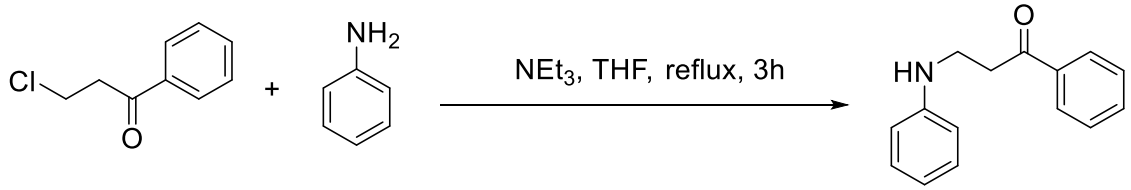

224 **49** **225**, 65%

1-Phenyl-3-(phenylamino)propan-1-one (225): To a mixture of aniline (5.0 mmol, 1.0 equiv) in THF (10 mL) 3-chloropropiophenone **224** (5.0 mmol, 1.0 equiv) and triethylamine (6.0 mmol, 1.2 equiv) were added and the reaction mixture was refluxed for 3 hr. The reaction mixture was cooled to room temperature and extracted with ethyl acetate. Combined organic mixture was washed with brine, dried over sodium sulfate and evaporated to dryness. Recrystallization in diethyl ether afforded 1-phenyl-3-(phenylamino)propan-1-one **225** as white solid in 65% of yield: FTIR (cast film $CHCl_3$) 3409, 3068, 3040, 3018, 2937, 2884, 2850, 1677 cm^{-1}; ^1H NMR (CD_3OD, 500 MHz) δ 3.30 (t, *J* = 6.0 Hz, 2 H), 3.63 (t, *J* = 6.0 Hz, 2 H), 6.65 (br s, 1 H), 6.67 (dd, *J* = 9.0, 0.5 Hz, 2 H), 6.70–6.75 (m, 1 H), 7.17–7.21 (m, 2 H), 7.46–7.49 (m, 2 H), 7.56–7.59 (m, 1 H), 7.95–7.97 (m, 2 H); ^{13}C NMR (CD_3OD, 125 MHz) δ 37.7, 38.7, 113.1, 117.6, 128.1, 128.7, 129.4, 133.4, 136.8, 147.7, 199.3; exact mass (electrospray) *m/z* calcd for $C_{15}H_{15}NO$ $(M + H)^+$ 226.1226, found 226.1221.

General procedure C

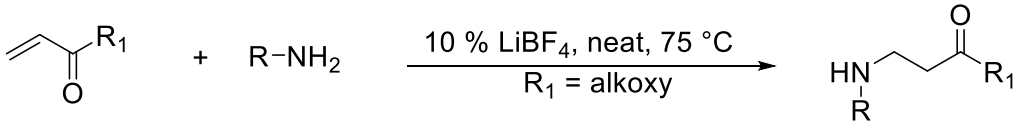

191 **192** **193**

General procedure D for preparation of 193:[214] Lithium tetrafluoroborate (10 mol %) was added to the stirred solution of aniline (10.0 mmol, 1.0 equiv) and Michael acceptor ester (10.0 mmol, 1.0 equiv) and the mixture was stirred at 75 °C until completion (monitored by TLC). The reaction mixture was cooled to room temperature, water (25 mL) was added, and the product was extracted with ethyl acetate (3 X 50 mL). The combined organic layer was washed with brine, dried over anhydride Na_2SO_4 and concentrated under vacuum. The reaction mixture was used for next step without further purification.

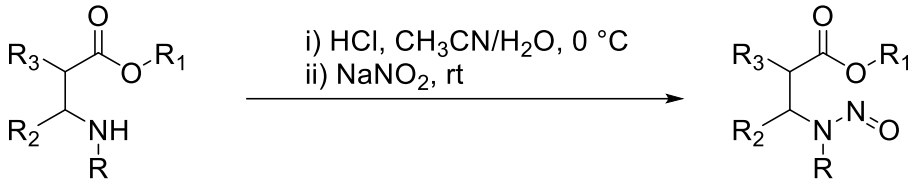

194 **195**

General procedure E for preparation of *N*-nitrosamines 195: *N*-nitrosamines were prepared from their aniline derivatives by following the reported preocedure.[215] To a 1:2 mixture of acetonitrile and water, anilines **193** (1.0 equiv) was dissolved and the reaction mixture was cooled to 0 °C using an ice bath. Then 5.0 equivalent of concentrated hydrochloric acid was added dropwise. For half an hour, the reaction mixture was stirred vigorously. To this stirring mixture, aqueous solution of 1.0 equivalent sodium nitrite ($NaNO_2$) was added slowly. The reaction was monitored by TLC and stopped once complete and extracted with ethyl acetate. The combined organic layer was washed with brine, dried over sodium sulfate, concentrated under reduced pressure. The crude was either purified by flash silica gel column chromatography to give the corresponding *N*-nitrosamines or used directly for the next step without further purification.

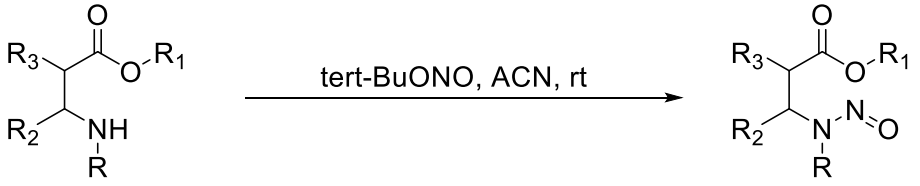

194 **195**

General procedure F for preparation of *N*-nitrosamines 195: *N*-nitrosamines **195** were prepared from their amine derivatives by following the reported procedure.[215] Amine **194** (10.0 mmol, 1.0 equiv) was stirred in 30.0 mL acetonitrile for 5 min at room temperature, and then *tert*-butyl nitrite (TBN) (20.0 mmol, 2.0 equiv) was added to the reaction mixture. The progress of the reaction was monitored by TLC and stirred at room temperature until completion. Next, 50 mL of ethyl acetate added to the reaction mixture and washed with distilled water and then with brine solution. The organic layer was dried over anhydrous sodium sulfate, concentrated under reduced

pressure, and purified by flash silica gel column chromatography to give the corresponding *N*-nitrosamines or used directly for the next step without further purification.

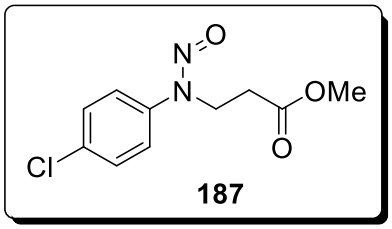

187

Methyl 3-((4-chlorophenyl)(nitroso)amino)propanoate (187): General procedure **D** and **E** were followed for making methyl 3-((4-chlorophenyl)(nitroso)amino)propanoate **187**. The product was obtained as a yellow liquid in a yield of 90%. FTIR ($CDCl_3$, cast) 3102, 3068, 2954, 2852, 1739, 1496, 1466, 1128, 1099 cm^{-1}; ^1H NMR ($CDCl_3$, 500 MHz) δ 2.58 (t, *J* = 7.0 Hz, 2 H), 3.66 (s, 3 H), 4.28 (t, *J* = 7.0 Hz, 2 H), 7.45–7.51 (m, 4 H); ^{13}C NMR ($CDCl_3$, 125 MHz) δ 30.7, 40.1, 52.0, 120.9, 129.7, 133.3, 139.8, 171.0; exact mass (electrospray) *m/z* calcd for $C_{10}H_{11}{}^{35}ClN_2O_3$ $(M + Na)^+$ 265.0350, found 265.0352.

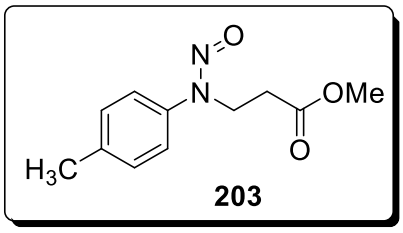

203

Methyl 3-(nitroso(p-tolyl)amino)propanoate (203): General procedure **D** and **E** were followed for making methyl 3-(nitroso(p-tolyl)amino)propanoate **203**. The product was obtained in a yield of 80%: FTIR ($CHCl_3$, cast film) 3038, 3002, 2929, 1903, 1736, 1514, 1462, 1409,1379, 1317, 1200, 1063 cm^{-1}; ^1H NMR ($CDCl_3$, 500 MHz) δ 2.38 (s, 3 H),2.55 (t, *J* = 7.5 Hz, 2 H), 3.62 (s, 3 H), 4.26 (t, *J* = 7.5 Hz, 2 H), 7.27 (d, *J* = 8.5 Hz, 2 H), 7.38 (d, *J* = 8.5 Hz, 2 H); ^{13}C NMR ($CDCl_3$,

125 MHz) δ 21.0, 30.7, 40.5, 52.0, 120.1, 130.1, 137.8, 138.8, 171.1; exact mass (electrospray) *m/z* calcd for $C_{11}H_{14}N_2NaO_3$ $(M + Na)^+$ 245.0897, found 245.0895.

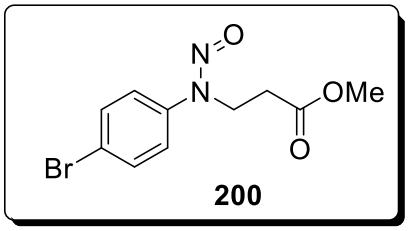

200

Methyl 3-((4-bromophenyl)(nitroso)amino)propanoate (200): General procedure **D** and **E** were followed for making methyl 3-((4-bromophenyl)(nitroso)amino)propanoate **200**. The product was obtained in a yield of 70%: FTIR ($CHCl_3$, cast film) 3098, 3002, 2953, 1897, 1735, 1590, 1490, 1460, 1306, 1198, 1075 cm^{-1}; ^1H NMR ($CDCl_3$, 500 MHz) δ 2.57 (t, *J* = 7.5 Hz, 2 H), 3.65 (s, 3 H), 4.26 (t, *J* = 7.5 Hz, 2 H), 7.43 (d, *J* = 9.0 Hz, 2 H), 7.60 (d, *J* = 9.0 Hz, 2 H); ^{13}C NMR ($CDCl_3$, 125 MHz) δ 30.7, 40.0, 52.1, 121.1, 121.1, 132.7, 140.3, 171.0; exact mass (electrospray) *m/z* calcd for $C_{10}H_{11}{}^{79}BrN_2NaO_3$ $(M + Na)^+$ 308.9845, found 308.9843.

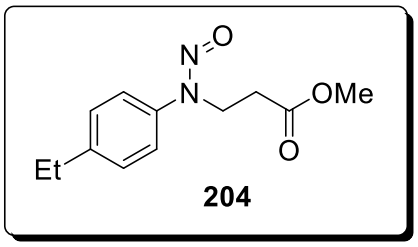

204

Methyl 3-((4-ethylphenyl)(nitroso)amino)propanoate (204): General procedure **D** and **E** were followed for making methyl 3-((4-ethylphenyl)(nitroso)amino)propanoate **204**. The product was obtained in a yield of 80%: FTIR (neat) 3035, 2966, 2935, 2588, 1903, 1740, 1610, 1514, 1459, 1378, 1200, 1064 cm^{-1}; ^1H NMR ($CDCl_3$, 500 MHz) δ 1.24 (t, *J* = 7.5 Hz, 3 H), 2.53 (t, *J* = 7.5 Hz, 2 H), 2.68 (q, *J* = 7.5 Hz, 2 H), 3.61 (s, 3 H), 4.26 (t, *J* = 7.5 Hz, 2 H), 7.28 (d, *J* = 8.5 Hz, 2 H), 7.42 (d, *J* = 8.5 Hz, 2 H); ^{13}C NMR ($CDCl_3$, 125 MHz) δ 15.4. 28.3, 30.7, 40.4, 51.9, 120.1, 128.9,

138.9, 144.0, 171.1; exact mass (electrospray) *m/z* calcd for $C_{12}H_{16}N_2NaO_3$ $(M + Na)^+$ 259.1053, found 259.1048.

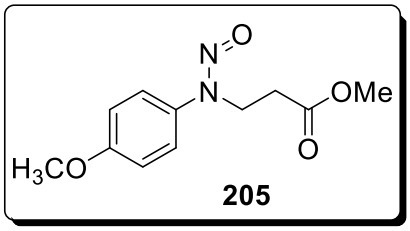

205

Methyl 3-((4-methoxyphenyl)(nitroso)amino)propanoate (205): General procedure **D** and **E** were followed for making methyl 3-((4-ethylphenyl)(nitroso)amino)propanoate **205**. The product was obtained in a yield of 84%: FTIR (neat) 3082, 3004, 2955, 2840, 2051, 1737, 1609, 1589, 1512, 1439, 1379, 1315, 1176, 1066 cm^{-1}; ^1H NMR ($CDCl_3$, 500 MHz) δ 2.58 (t, *J* = 7.5 Hz, 2 H), 3.64 (s, 3 H), 3.86 (s, 3 H), 4.27 (t, *J* = 7.5 Hz, 2 H), 7.99 (d, *J* = 9.0 Hz, 2 H), 7.42 (d, *J* = 9.0 Hz, 2 H); ^{13}C NMR ($CDCl_3$, 125 MHz) δ 30.8, 41.0, 52.0, 55.6, 114.7, 122.2, 134.5, 159.3, 171.2; exact mass (EI) *m/z* calcd for $C_{11}H_{14}N_2O_4$ $(M)^+$ 238.0954, found 238.0954.

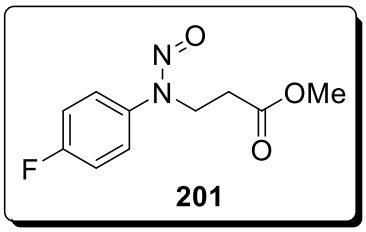

201

Methyl 3-((4-fluorophenyl)(nitroso)amino)propanoate (201): General procedure **D** and **E** were followed for making methyl 3-((4-fluorophenyl)(nitroso)amino)propanoate **201**. The product was obtained in a yield of 65%: FTIR (neat) 3123, 3081, 3005, 2955, 2849, 2588, 2331, 2049, 1889, 1737, 1603, 1511, 1462, 1980, 1201, 1124, 1063 cm^{-1}; ^1H NMR ($CDCl_3$, 500 MHz) δ 2.60 (t, *J* = 7.5 Hz, 2 H), 3.66 (s, 3 H), 4.28 (t, *J* = 7.5 Hz, 2 H), 7.20 (t, *J* = 8.5 Hz, 2 H), 7.51–7.53 (m, 2 H); ^{13}C NMR ($CDCl_3$, 125 MHz) δ 30.7, 41.7, 52.0, 116.5 (d, J_F = 22.9 Hz), 112.2 (d, J_F = 8.4 Hz),

137.5 (d, J_F = 3.1 Hz), 161.9 (d, J_F = 247.9 Hz), 171.1; exact mass (EI) *m/z* calcd for $C_{10}H_{11}FN_2O_3$ $(M)^+$ 226.0754, found 226.0754.

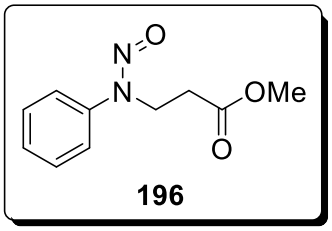

196

Methyl 3-(nitroso(phenyl)amino)propanoate (196): General procedure **D** and **E** were followed for making methyl 3-(nitroso(phenyl)amino)propanoate **196**. The product was obtained in a yield of 93%: FTIR (neat) 3072, 3003, 2954, 2849, 1739, 1596, 1496, 1439, 1379, 1201, 1065 cm^{-1}; ^1H NMR ($CDCl_3$, 500 MHz) δ 2.59 (t, *J* = 7.5 Hz, 2 H), 3.65 (s, 3 H), 4.31 (t, *J* = 7.5 Hz, 2 H), 7.37–7.4 (m, 1 H), 7.47–7.50 (m, 2 H), 7.53–7.54 (m, 2 H); ^{13}C NMR ($CDCl_3$, 125 MHz) δ 30.8, 40.3, 52.0, 119.9, 127.7, 129.6, 141.2, 171.1; exact mass (electrospray) *m/z* calcd for $C_{10}H_{12}N_2NaO_3$ $(M + Na)^+$ 231.0740, found 231.0736.

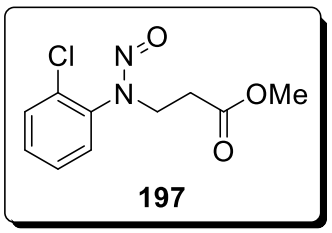

197

Methyl 3-((2-chlorophenyl)(nitroso)amino)propanoate (197): General procedure **D** and **F** were followed for making methyl 3-((2-chlorophenyl)(nitroso)amino)propanoate **197**. The product was obtained in a yield of 87%: FTIR (neat) 3095, 3068, 3001, 2953, 2848, 2600, 2044, 1973, 1936, 1739, 1589, 1485, 1460, 1319, 1204, 1141, 1046 cm^{-1}; ^1H NMR ($CDCl_3$, 500 MHz) δ 2.59 (t, *J* = 7.5 Hz, 2 H), 3.61 (s, 3 H), 4.24 (t, *J* = 7.5 Hz, 2 H), 7.37–7.39 (m, 1 H), 7.43–7.46 (m, 2 H), 7.57–7.59 (m, 1 H); ^{13}C NMR ($CDCl_3$, 125 MHz) δ 30.7, 42.6, 51.9, 127.8, 129.1, 130.7,

1300.8, 131.0, 138.8, 171.0; exact mass (EI) *m/z* calcd for $C_{10}H_{11}{}^{35}ClN_2O_3$ $(M)^+$ 242.0458, found 242.0462.

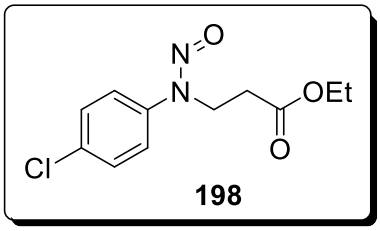

198

Ethyl 3-((4-chlorophenyl)(nitroso)amino)propanoate (198): General procedure **D** and **E** were followed for making ethyl 3-((4-chlorophenyl)(nitroso)amino)propanoate **198**. The product was obtained in a yield of 82%: FTIR (neat) 3101,3077, 2984, 2907, 2876, 2588, 1894, 1734, 1495, 1466, 1193, 1099, 1012 cm^{-1}; ^1H NMR ($CDCl_3$, 500 MHz) δ 1.21 (t, *J* = 7.5 Hz, 3H), 2.58 (t, *J* = 7.5 Hz, 2 H), 4.10 (q, *J* = 7.5 Hz, 2 H), 4.27 (t, *J* = 7.5 Hz, 2 H), 7.44–7.51 (m, 4 H); ^{13}C NMR ($CDCl_3$, 125 MHz) δ 14.06, 30.9, 40.1, 61.0, 121.0, 129.7, 133.2, 139.9, 170.5; exact mass (EI) *m/z* calcd for $C_{11}H_{13}{}^{35}ClN_2O_3Na$ $(M + Na)^+$ 279.0507, found 279.0504.

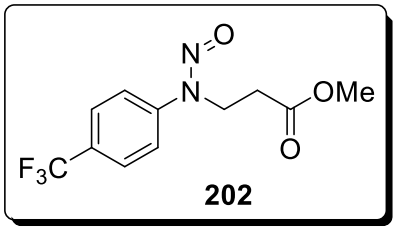

202

Methyl 3-((4-(trifluoromethyl)phenyl)(nitroso)amino)propanoate (202): General procedure **D** and **E** were followed or making methyl 3-((4-(trifluoromethyl)phenyl)(nitroso)amino)propanoate **202**. The product was obtained in a yield of 93%: FTIR (cast film $CHCl_3$) 3121, 3081, 3006, 2957, 2857, 1740, 1618, 1475, 1440, 1328, 1171, 1126 cm^{-1}; ^1H NMR ($CDCl_3$, 500 MHz) δ 2.59 (t, *J* = 7.5 Hz, 2 H), 3.66 (s, 3 H), 4.31 (t, *J* = 7.5 Hz, 2 H), 7.71 (d, *J* = 9.0 Hz, 2 H), 7.75 (d, *J* = 9.0 Hz, 2 H); ^{13}C NMR ($CDCl_3$, 125 MHz) δ 30.7, 39.6, 52.1, 118.9, 126.9, 144.0, 171.0; exact mass (EI) *m/z* calcd for $C_{11}H_{11}F_3N_2O_3$ $(M)^+$ 276.0722, found 276.0723.

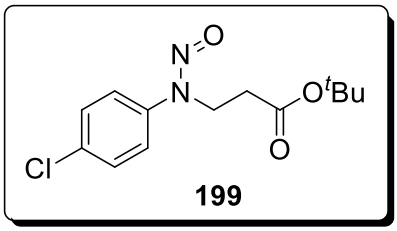

199

***t*Butyl 3-((4-chlorophenyl)(nitroso)amino)propanoate (199):** General procedure **D** and **F** were followed for making *t*butyl 3-((4-chlorophenyl)(nitroso)amino)propanoate **199**. The product was obtained in a yield of 85%: FTIR ($CHCl_3$ cast film) 3103, 2980, 2933, 1728, 1496, 1469, 1190, 1099,1012 cm^{-1}; ^1H NMR ($CDCl_3$, 500 MHz) δ 1.42 (s, 9H), 2.49 (t, *J* = 7.5 Hz, 2 H), 4.25 (t, *J* = 7.5 Hz, 2 H), 7.47 (d, *J* = 9.0 Hz, 2 H), 7.51 (d, *J* = 9.0 Hz, 2 H); ^{13}C NMR ($CDCl_3$, 125 MHz) δ 28.0, 32.1, 40.2, 81.6, 121.1, 129.7, 133.3, 139.9, 169.8; exact mass (electrospray) *m/z* calcd for $C_{31}H_{17}{}^{35}ClN_2O_3Na$ $(M + Na)^+$ 307.0820, found 307.0818.

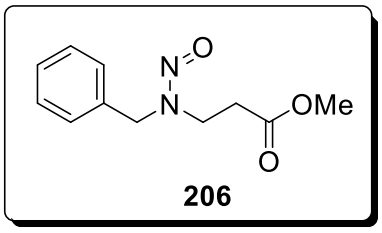

206

Methyl 3-[benzyl(nitroso)amino]propanoate (206): General procedure **D** and **E** were followed for making methyl 3-[benzyl(nitroso)amino]propanoate **206**. The product was obtained in a yield of 65%: FTIR ($CHCl_3$ cast film) 3092, 3065, 3032, 3006, 2953, 1738, 1455, 1438, 1206, 1132 cm^{-1}; ^1H NMR ($CDCl_3$, 500 MHz) δ 2.46 (t, *J* = 7.0 Hz, 2 H), 2.80 (t, *J* = 7.0 Hz, 1 H), 3.65–3.68 (m, 6.5 H), 4.33 (t, *J* = 7.0 Hz, 2 H), 4.83 (s, 3 H), 5.37 (s, 3 H), 7.11 (d, *J* = 7.5 Hz, 1 H), 7.28–7.34 (m, 7.5 H); ^{13}C NMR ($CDCl_3$, 125 MHz) δ 30.5, 33.4, 39.5, 46.9, 47.2, 51.9, 52.1, 56.9, 128.0, 128.2, 128.4, 128.6, 128.9, 129.1, 134.0, 134.7, 171.1, 171.7; exact mass (EI) *m/z* calcd for $C_{11}H_{14}N_2O_3$ $(M)^+$ 222.1004, found 222.1001.

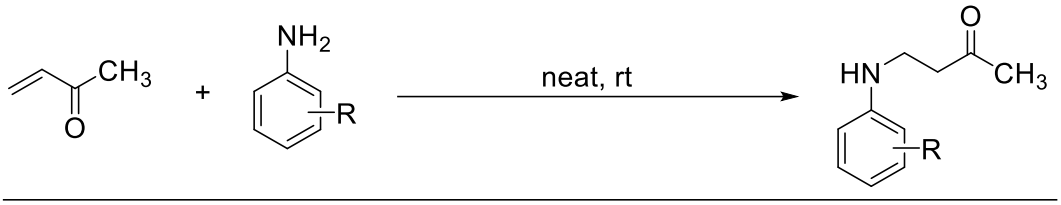

General procedure G: A mixture of methyl vinyl ketone (1.1 equiv) and anilines (1.0 equiv) was stirred at room temperature until completion of the reaction. The reaction was monitored by TLC. Remaining methyl vinyl ketone was evaporated under vacuum. Reaction mixture was used for next step without further purification.

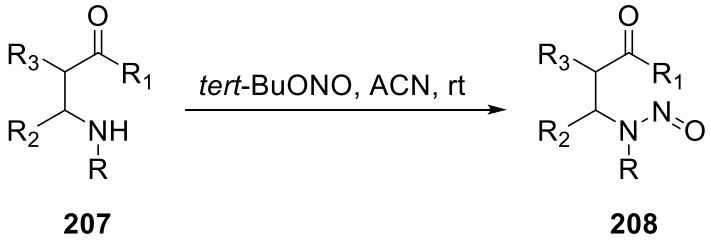

207 **208**

General procedure H for preparation of *N*-nitrosamines 208: *N*-nitrosamines **208** were prepared from their amine derivatives by following the reported procedure.[216] Amines **207** (10.0 mmol, 1.0 equiv) was stir in 30.0 mL acetonitrile for 5 min at room temperature, and then *t*butyl nitrite (TBN) (20.0 mmol, 2.0 equiv) was added to the reaction mixture. The progress of the reaction was monitored by TLC and stirred at room temperature until completion. Next, 50 mL of ethyl acetate added to the reaction mixture and washed with distilled water and then with brine solution. The organic layer was dried over anhydrous sodium sulfate, concentrated under reduced pressure, and purified by flash silica gel column chromatography to give the corresponding *N*-nitrosamines or used directly for the next step without further purification.

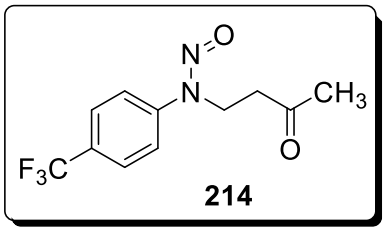

214

***N*-(3-Oxobutyl)-*N*-(4-(trifluoromethyl)phenyl)nitrous amide (214):** General procedure **G** and **H** were followed for making *N*-(3-oxobutyl)-*N*-(4-(trifluoromethyl)phenyl)nitrous amide **214**. The product was obtained in a yield of 94%: FTIR (cast film $CHCl_3$) 3116, 3082, 3006, 2926, 1918, 1718, 1618, 1519, 1474, 1359,1125, 1076 cm^{-1}; ^1H NMR ($CDCl_3$, 500 MHz) δ 2.14 (s, 3 H), 2.73 (t, *J* = 7.5 Hz, 2 H), 4.27 (t, *J* = 7.5 Hz, 2 H), 7.70 (d, *J* = 8.5 Hz, 2 H), 7.75 (d, *J* = 8.5 Hz, 2 H); ^{13}C NMR ($CDCl_3$, 125 MHz) δ 30.2, 38.9, 39.4, 118.9, 123.8 (q, J_F = 272.1 Hz), 126.8 (q, J_F = 3.9 Hz), 129.2 (q, J_F = 33.1 Hz), 144.1, 205.3;); ^{19}F NMR ($CDCl_3$, 469 MHz) δ –62.4; exact mass (EI) *m/z* calcd for $C_{11}H_{11}F_3N_2O_3$ $(M)^+$ 260.0773, found 260.0771.

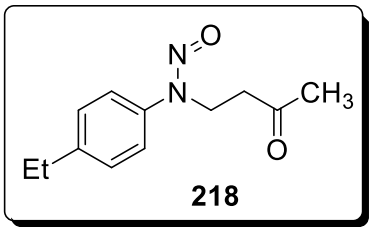

218

***N*-(4-Ethylphenyl)-*N*-(3-oxobutyl)nitrous amide (218):** General procedure **G** and **H** were followed for making *N*-(4-ethylphenyl)-*N*-(3-oxobutyl)nitrous amide **218**. The product was obtained in a yield of 95%: FTIR (cast film $CHCl_3$) 3036, 2967, 2933, 2875, 1903, 1715, 1514, 1459, 1414, 1135, 1077 cm^{-1}; ^1H NMR ($CDCl_3$, 500 MHz) δ 1.27 (t, *J* = 7.5 Hz, 3 H), 2.14 (s, 3 H), 2.69–2.73 (m, 4 H), 4.24 (t, *J* = 7.5 Hz, 2 H), 7.29 (d, *J* = 8.5 Hz, 2 H), 7.41 (d, *J* = 8.5 Hz, 2 H); ^{13}C NMR ($CDCl_3$, 125 MHz) δ 15.4, 28.3, 30.0, 39.4, 39.8, 120.0, 129.0, 139.1, 144.0, 205.5; exact mass (EI) *m/z* calcd for $C_{12}H_{16}N_2NaO_2$ $(M + Na)^+$ 243.1104, found 243.1100.

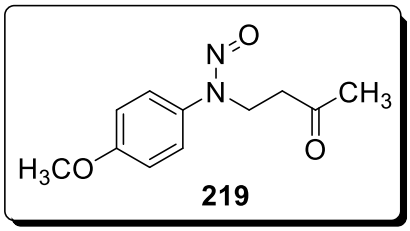

219

***N*-(4-Methoxyphenyl)-*N*-(3-oxobutyl)nitrous amide (219):** General procedure **G** and **H** were followed for making *N*-(4-methoxyphenyl)-*N*-(3-oxobutyl)nitrous amide **219**. The product was obtained in a yield of 92%: FTIR (cast film $CHCl_3$) 3078, 3005, 2962, 2942, 2920, 2839, 2554, 2046, 1880, 1715, 1609, 1589, 1513, 1301, 1252, 1030 cm^{-1}; ^1H NMR ($CDCl_3$, 500 MHz) δ 2.13 (s, 3 H), 2.71 (t, *J* = 7.5 Hz, 2 H), 3.85 (s, 3 H), 4.21 (t, *J* = 7.5 Hz, 2 H), 6.98 (d, *J* = 9.0 Hz, 2 H), 7.40 (d, *J* = 9.0 Hz, 2 H); ^{13}C NMR ($CDCl_3$, 125 MHz) δ 30.0, 39.4, 40.3, 55.6, 114.7, 122.0, 134.6, 159.2, 205.5; exact mass (EI) *m/z* calcd for $C_{12}H_{14}N_2NaO_3$ $(M + Na)^+$ 245.0897, found 245.0893.

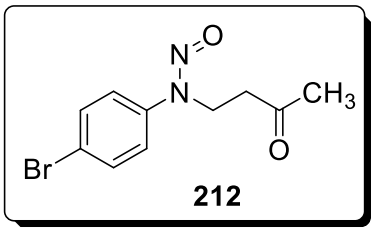

212

***N*-(4-Bromophenyl)-*N*-(3-oxobutyl)nitrous amide (212):** General procedure **G** and **H** were followed for making *N*-(4-bromophenyl)-*N*-(3-oxobutyl)nitrous amide **212**. The product was obtained as solid in a yield of 60%: FTIR (cast film $CHCl_3$) 3097, 3077, 3002, 2956, 2917, 2854,, 2792, 2590, 2310, 1896, 1716, 1590, 1462, 1403, 1306, 1129, 1009 cm^{-1}; ^1H NMR ($CDCl_3$, 500 MHz) δ 2.14 (s, 3 H), 2.70 (t, *J* = 7.5 Hz, 2 H), 4.21 (t, *J* = 7.5 Hz, 2 H), 7.42 (d, *J* = 9.0 Hz, 2 H), 7.59 (d, *J* = 9.0 Hz, 2 H); ^{13}C NMR ($CDCl_3$, 125 MHz) δ 30.0, 39.4, 39.4, 121.0, 121.1, 132.7, 140.5, 205.4; exact mass (EI) *m/z* calcd for $C_{10}H_{11}{}^{79}BrN_2NaO_2$ $(M + Na)^+$ 292.9896, found 292.9894.

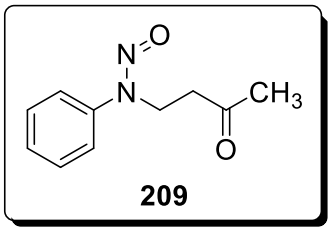

209

***N*-(3-Oxobutyl)-*N*-phenylnitrous amide (209):** General procedure **G** and **H** were followed for making *N*-(3-oxobutyl)-*N*-phenylnitrous amide **209**. The product was obtained as solid in a yield of 70%: FTIR (cast film $CHCl_3$) 3065, 3004, 2957, 2916, 1953, 1885, 1716, 1597, 1496, 1445, 1334, 1131, 1077 cm^{-1}; ^1H NMR ($CDCl_3$, 500 MHz) δ 2.15 (s, 3 H), 2.73 (t, *J* = 7.5 Hz, 2 H), 4.26 (t, *J* = 7.5 Hz, 2 H), 7.37–7.39 (m, 1 H), 7.47–7.54 (m, 4 H); ^{13}C NMR ($CDCl_3$, 125 MHz) δ 30.0, 39.4, 39.6, 119.8, 127.6, 129.6, 141.4, 205.5; exact mass (electrospray) *m/z* calcd for $C_{10}H_{12}N_2NaO_2$ $(M + Na)^+$ 215.0791, found 215.0794.

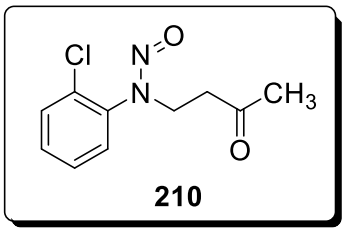

210

***N*-(2-Chlorophenyl)-*N*-(3-oxobutyl)nitrous amide (210):** General procedure **G** and **H** were followed for making *N*-(2-chlorophenyl)-*N*-(3-oxobutyl)nitrous amide **210**. The product was obtained as solid in a yield of 55%: FTIR (cast film $CHCl_3$) 3095, 3068, 3002, 2955, 2920, 2598, 2326, 2120, 1970, 1934, 1814, 1715, 1597, 1522, 1457, 1373, 1140, 1050 cm^{-1}; ^1H NMR ($CDCl_3$, 500 MHz) δ 2.10 (s, 3 H), 2.74 (t, *J* = 7.0 Hz, 2 H), 4.17 (t, *J* = 7.0 Hz, 2 H), 7.34–7.37 (m, 1 H), 7.42–7.45 (m, 2 H), 7.56–7.58 (m, 1 H); ^{13}C NMR ($CDCl_3$, 125 MHz) δ 29.9, 39.3, 42.3, 127.9, 128.9, 130.7, 130.8, 131.0, 139.0, 205.4; exact mass (electrospray) *m/z* calcd for $C_{10}H_{11}ClN_2NaO_2$ $(M + Na)^+$ 249.0401, found 249.0409.

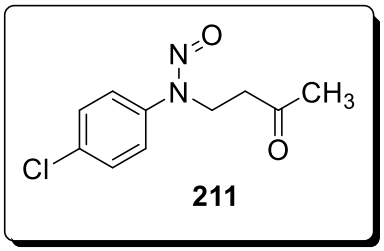

211

***N*-(4-Chlorophenyl)-*N*-(3-oxobutyl)nitrous amide (211):** General procedure **G** and **H** were followed for making *N*-(4-chlorophenyl)-*N*-(3-oxobutyl)nitrous amide **211**. The product was obtained as sticky liquid in a yield of 84%: FTIR (cast film $CHCl_3$) 3351, 3100, 3074, 2937, 1900, 1715, 1495, 1131, 1097 cm^{-1}; ^1H NMR ($CDCl_3$, 500 MHz) δ 2.14 (s, 3 H), 2.71 (t, *J* = 7.0 Hz, 2 H), 4.22 (t, *J* = 7.0 Hz, 2 H), 7.44 (d, *J* = 9.0 Hz, 2 H), 7.49 (d, *J* = 9.0 Hz, 2 H); ^{13}C NMR ($CDCl_3$, 125 MHz) δ 30.0, 39.4, 39.5, 120.8, 129.7, 133.3, 139.9, 205.4; exact mass (electrospray) *m/z* calcd for $C_{10}H_{11}ClN_2O_2$ $(M + H)^+$ 227.0582, found 227.0576.

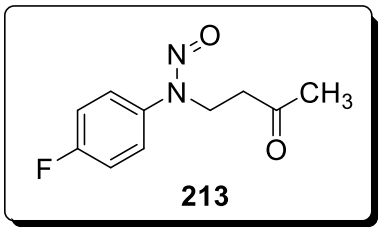

213

***N*-(4-Fluorophenyl)-*N*-(3-oxobutyl)nitrous amide (213):** General procedure **G** and **H** were followed for making *N*-(4-fluorophenyl)-*N*-(3-oxobutyl)nitrous amide **213**. The product was obtained as red liquid in a yield of 55%: FTIR (cast film $CHCl_3$) 3121, 3080, 3006, 2962, 2921, 1716, 1511, 1467, 1412, 1225, 1164, 1134 cm^{-1}; ^1H NMR ($CDCl_3$, 500 MHz) δ 2.14 (s, 3 H), 2.72 (t, *J* = 7.0 Hz, 2 H), 4.22 (t, *J* = 7.0 Hz, 2 H), 7.19 (t, *J* = 9.0 Hz, 2 H), 7.48–7.51 (m, 2 H); ^{13}C NMR ($CDCl_3$, 125 MHz) δ 30.0, 39.4, 40.1, 116.5 (d, J_F = 91 Hz), 122.0 (d, J_F = 34 Hz), 137.7 (d, J_F = 12.0 Hz), 161.9 (d, J_F = 986.5 Hz), 205.4; exact mass (electrospray) *m/z* calcd for $C_{10}H_{11}FN_2NaO_2$ $(M + Na)^+$ 233.0697, found 233.0695.

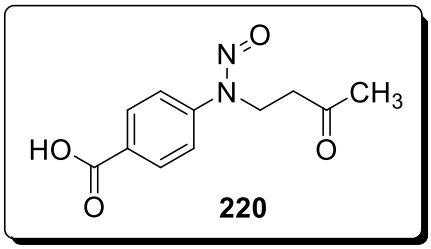

220

4-(Nitroso(3-oxobutyl)amino)benzoic acid (220): General procedure **G** and **H** were followed for making 4-(nitroso(3-oxobutyl)amino)benzoic acid **220**. The product was obtained as yellow solid in a yield of 85%: FTIR (cast film $CHCl_3$) 3111, 3080, 2948, 2977, 2562, 1709, 1682, 1607, 1457, 1292, 1122, 1074 cm^{-1}; ^1H NMR (CD_3OD, 500 MHz) δ 2.11 (s, 3 H), 2.75 (t, *J* = 7.5 Hz, 2 H), 4.28 (t, *J* = 7.5 Hz, 2 H), 7.72 (d, *J* = 8.5 Hz, 2 H), 8.14 (d, *J* = 8.5 Hz, 2 H); ^{13}C NMR (CD_3OD, 125 MHz) δ 29.8, 39.9, 40.2, 120.0, 130.6, 132.2, 146.4, 168.9, 208.0; exact mass (electrospray) *m/z* calcd for $C_{11}H_{11}N_2O_4$ $(M)^+$ 235.0724, found 235.0722.

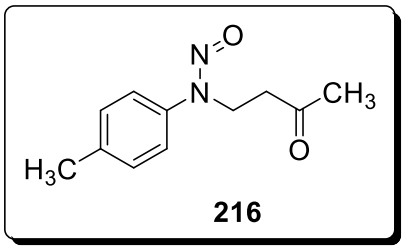

216

***N*-(4-Methylphenyl)-*N*-(3-oxobutyl)nitrous amide (216):** General procedure **G** and **H** were followed for making *N*-(4-methylphenyl)-*N*-(3-oxobutyl)nitrous amide **216**. The product was obtained as solid in a yield of 91%: FTIR (cast film $CHCl_3$) 3037, 2952, 2925, 2857, 1717, 1514, 1458, 1410, 1135 cm^{-1}; ^1H NMR ($CDCl_3$, 500 MHz) δ 2.13 (s, 3 H), 2.40 (s, 3 H), 2.71 (t, *J* = 7.5 Hz, 2 H), 4.23 (t, *J* = 7.5 Hz, 2 H), 7.27 (d, *J* = 8.5 Hz, 2 H), 7.39 (d, *J* = 8.5 Hz, 2 H); ^{13}C NMR ($CDCl_3$, 125 MHz) δ 21.0, 30.0, 39.4, 39.8, 120.0, 130.1, 137.7, 138.9, 205.6; exact mass (electrospray) *m/z* calcd for $C_{11}H_{14}N_2NaO_2$ $(M + Na)^+$ 229.0947, found 229.0947.

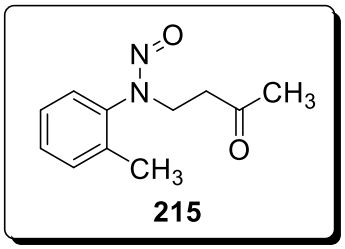

215

***N*-(2-Methylphenyl)-*N*-(3-oxobutyl)nitrous amide (215):** General procedure **G** and **H** were followed for making *N*-(2-methylphenyl)-*N*-(3-oxobutyl)nitrous amide **215**. The product was obtained as solid in a yield of 88%: FTIR (cast film $CHCl_3$) 3065, 2928, 1717, 1495, 1446, 1169, 1148 cm^{-1}; ^1H NMR ($CDCl_3$, 500 MHz) δ 2.09 (s, 3 H), 2.23 (s, 3 H), 2.69 (t, *J* = 7.5 Hz, 2 H), 4.12 (t, *J* = 7.5 Hz, 2 H), 7.17 (d, *J* = 8.0 Hz, 1 H), 7.29–7.33 (m, 2 H), 7.35–7.36 (m, 1 H); ^{13}C NMR ($CDCl_3$, 125 MHz) δ 18.1, 29.9, 39.1, 42.3, 126.6, 127.0, 129.5, 131.7, 134.5, 140.3, 205.4; exact mass (electrospray) *m/z* calcd for $C_{11}H_{14}N_2O_2$ $(M + H)^+$ 207.1128, found 207.1132.

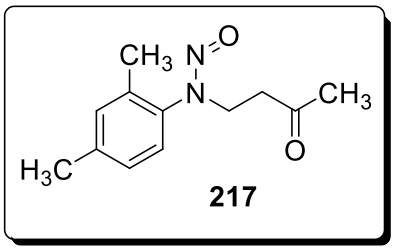

217

***N*-(2,4-Dimethylphenyl)-*N*-(3-oxobutyl)nitrous amide (217):** General procedure **G** and **H** were followed for making *N*-(2,4-dimethylphenyl)-*N*-(3-oxobutyl)nitrous amide **217**. The product was obtained as solid in a yield of 93%: FTIR (cast film $CHCl_3$) 3000, 2960, 2924, 2857, 1717, 1504, 1446, 1422, 1165, 1150, 1129 cm^{-1}; ^1H NMR ($CDCl_3$, 500 MHz) δ 2.10 (s, 3 H), 2.19 (s, 3 H), 2.38 (s, 3H), 2.69 (t, *J* = 7.5 Hz, 2 H), 4.11 (t, *J* = 7.5 Hz, 2 H), 7.07–7.13 (m, 2 H), 7.17 (s, 1 H); ^{13}C NMR ($CDCl_3$, 125 MHz) δ 18.0, 21.1, 29.9, 39.1, 42.4, 126.4, 127.6, 132.3, 134.2, 137.8, 139.5, 205.5; exact mass (electrospray) *m/z* calcd for $C_{12}H_{16}N_2NaO_2$ $(M + Na)^+$ 243.1104, found 243.1103.

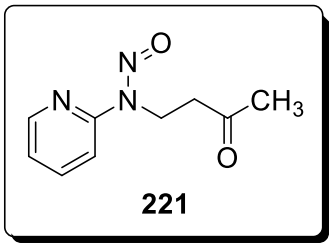

221

***N*-Pyridine-*N*-(3-oxobutyl)nitrous amide (221):** General procedure **G** and **H** were followed for making *N*-pyridine-*N*-(3-oxobutyl)nitrous amide **221**. The product was obtained as off white solid in a yield of 95%: FTIR (cast film $CHCl_3$) 2977, 2923,1710, 1591, 14552, 1437, 1129, 1097 cm^{-1}; ^1H NMR ($CDCl_3$, 500 MHz) δ 2.15 (s, 3 H), 2.71 (t, *J* = 7.5 Hz, 2 H), 4.48 (t, *J* = 7.5 Hz, 2 H), 7.22–7.25 (m, 1 H), 7.78–7.81 (m, 1 H), 7.98 (d, *J* = 8.5 Hz, 1 H), 8.46–8.47 (m, 1 H); ^{13}C NMR ($CDCl_3$, 125 MHz) δ 29.9, 36.2, 39.8, 112.6, 121.7, 138.4, 148.0, 154.1, 206.0; exact mass (electrospray) *m/z* for $C_9H_{11}N_3O_2$ $(M + H)^+$ 194.0924, found 194.0918.

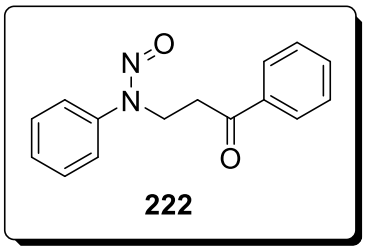

222

3-(*N*-Nitroso-*N*-phenylamino)-1-phenylpropane-1-one (222): General procedure **H** was followed (using the amine **225**) for making 3-(*N*-nitroso-*N*-phenylamino)-1-phenylpropane-1-one **222**. The product was obtained as yellow solid in a yield of 99%: FTIR (cast film $CHCl_3$) 3061, 2916, 1684, 1448, 1125 cm^{-1}; ^1H NMR ($CDCl_3$, 500 MHz) δ 3.26 (t, *J* = 5.5 Hz, 2 H), 4.45 (t, *J* = 5.5 Hz, 2 H), 7.36–7.39 (m, 1 H), 7.44–7.49 (m, 4 H), 7.56–7.58 (m, 3 H), 7.90 (apparent d, *J* = 7.0 Hz, 2 H); ^{13}C NMR ($CDCl_3$, 125 MHz) δ 34.7, 40.3, 119.7, 127.6, 128.1, 128.8, 129.6, 133.6, 136.2, 141.4, 197.1; exact mass (electrospray) *m/z* calcd for $C_{15}H_{14}N_2NaO_2$ $(M + Na)^+$ 277.0947, found 277.0945.

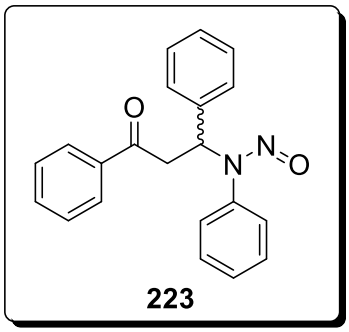

223

***N*-(3-Oxo-1,3-diphenylpropyl)-*N*-phenylnitrous amide (223):** General procedure **H** was followed (using the amine **228**) for making *N*-(3-oxo-1,3-diphenylpropyl)-*N*-phenylnitrous amide **223**. The product was obtained as sticky liquid in a yield of 99%: FTIR (neat) 3062, 3032, 2919, 2598, 2344, 1962, 1888, 1813, 1686, 1597, 1528, 1480, 1132 cm^{-1}; ^{1}H NMR (CD_3OD, 500 MHz) δ 3.66 (dd, *J* = 18.0, 4.5 Hz, 1 H), 3.77 (dd, *J* = 7.0, 2.0 Hz, 1.4 H), 4.76 (dd, *J* = 18.0, 10.0 Hz, 1 H), 6.08 (dd, *J* = 10.0, 4.5 Hz, 1 H), 6.90 (t, *J* = 7.0 Hz, 0.7 H), 6.96 (dd, *J* = 8.0, 2.0 Hz, 2 H), 7.23 (d, *J* = 7.5 Hz, 1.5 H), 7.30–7.63 (m, 19 H), 7.88 (d, *J* = 7.0 Hz, 1.5 H), 8.03 (d, *J* = 7.5 Hz, 2 H); ^{13}C NMR (CD_3OD, 125 MHz) δ 39.8, 44.2, 54.2, 65.2, 124.5, 126.7, 127.1, 127.3, 128.0, 128.0, 128.2, 128.5, 128.6, 128.7, 128.8, 128.8, 129.1, 129.2, 129.3, 133.5, 133.6, 136.3, 136.4, 137.2, 139.0, 139.1, 140.4; exact mass (electrospray) *m/z* calcd for $C_{21}H_{18}N_2NaO_2$ $(M + Na)^+$ 353.1260, found 353.1254.

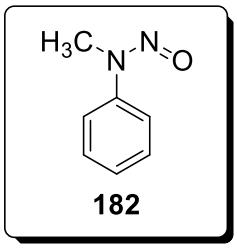

182

***N*-Methyl-*N*-phenylnitrous amide (182):** General procedure **H** was followed for making *N*-methyl-*N*-phenylnitrous amide **182**. The product was obtained as a reddish orange solid in a yield of 99%: FTIR (cast film $CHCl_3$) 3008, 2919, 2851, 1614, 1498, 1225 cm^{-1}; ^{1}H NMR ($CDCl_3$, 500 MHz) δ 3.47 (s, 3 H), 7.37 (t, *J* = 7.5 Hz, 1 H), 7.48 (t, *J* = 8.0 Hz, 2 H), 7.55 (d, *J* = 8.0 Hz, 2 H);

^{13}C NMR ($CDCl_3$, 125 MHz) δ 31.4, 99.3, 119.2, 127.3, 129.5, 142.3; exact mass (EI) *m/z* calcd for $C_7H_8N_2O$ $(M)^+$ 136.0636 found 136.0636.

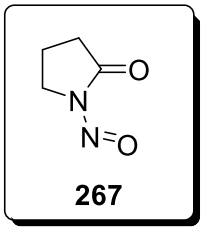

267

1-Nitrosopyrrolidin-2-one (267): General procedure **H** was followed for making 1-nitrosopyrrolidin-2-one **267**. The product was obtained in a yield of 99%: FTIR (neat) 2969, 2900 1767, 1495, 1346, 1148, 1020 cm^{-1}; ^{1}H NMR ($CDCl_3$, 700 MHz) δ 2.12–2.16 (m, 2 H), 2.76–2.79 (m 2 H), 3.65–3.67 (m, 2 H); ^{13}C NMR ($CDCl_3$, 175 MHz) δ 15.8, 30.8, 42.5, 172.9; exact mass (EI) *m/z* calcd for $C_4H_6N_2O_2$ $(M)^+$ 114.0429 found 114.0430.

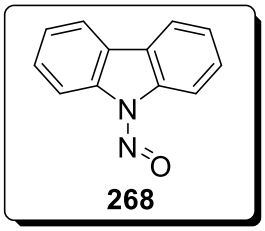

268

9-Nitroso-9*H*-carbazole (268): General procedure **H** was followed for making 9-nitroso-9*H*-carbazole **268.** The product was obtained in a yield of 95%: FTIR (cast film $CHCl_3$) 3119, 3065, 3023, 1944, 1912, 1804, 1492, 1471, 1437, 1247, 1125, 1060 cm^{-1}; ^{1}H NMR ($CDCl_3$, 500 MHz) δ 7.48–7.52 (m, 3 H), 7.57 (t, *J* = 8.0 Hz, 1 H), 7.93–7.96 (m, 2 H), 8.25 (d, *J* = 8.0 Hz, 1H), 8.57–8.59 (m, 1 H); ^{13}C NMR ($CDCl_3$, 125 MHz) δ 112.4, 116.6, 119.9, 120.4, 124.9, 125.4, 126.3, 127.4, 128.2, 128.6, 132.8, 138.7; exact mass (EI) *m/z* calcd for $C_4H_6N_2O$ $(M)^+$ 196.0637 found 196.0635.

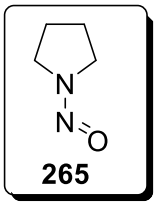

265

1-Nitrosopyrrolidine (265): General procedure **H** was followed for making 1-nitrosopyrrolidine **265**. The product was obtained in a yield of 98%: FTIR (neat) 2980, 2882, 2710, 1545, 1411 1310, 1027 cm^{-1}; ^{1}H NMR ($CDCl_3$, 700 MHz) δ 1.95–2.03 (m, 4 H), 3.51–3.53 (m, 2 H), 4.20–4.22 (m, 2 H); ^{13}C NMR ($CDCl_3$, 175 MHz) δ 22.5, 23.9, 45.1, 49.7; exact mass (EI) *m/z* calcd for $C_4H_8N_2O$ $(M)^+$ 100.0637 found 100.0637.

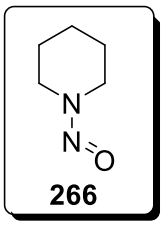

266

1-Nitrosopiperidine (266): General procedure **H** was followed for making 1-nitrosopiperidine **266**. The product was obtained in a yield of 99%: FTIR (neat) 2945, 2862, 1428, 1360, 1181, 1096 cm^{-1}; ^{1}H NMR ($CDCl_3$, 700 MHz) δ 1.51–1.53 (m, 2 H), 1.72–1.74 (m, 2 H), 1.76–1.79 (m, 2 H), 3.74 (dd, *J* = 6.3 Hz, 2 H), 4.15 (dd, *J* = 6.3 Hz, 2 H); ^{13}C NMR ($CDCl_3$, 175 MHz) δ 24.1, 24.7, 26.4, 39.8, 50.8; exact mass (EI) *m/z* calcd for $C_4H_8N_2O$ $(M)^+$ 114.0793 found 114.0794.

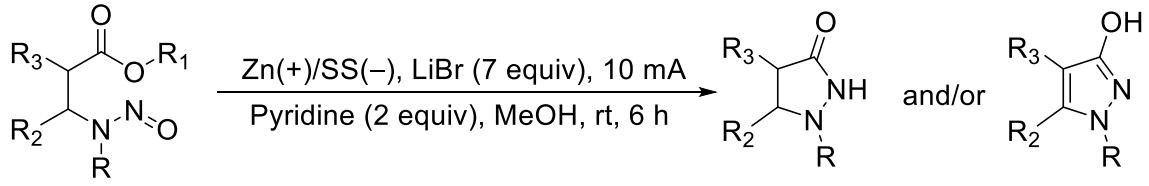

195 **229** **230**

General procedure J for electroreduction of *N*-nitrosamines 195: To an oven-dried 5 mL IKA ElectraSyn 2.0 vial was added *N*-nitrosamines (0.2 mmol, 1.0 equiv), lithium bromide (LiBr, 1.4

mmol, 7.0 equiv) and pyridine (0.4 mmol, 2.0 equiv), followed by 5.0 mL of methanol and a magnetic stir bar. Next, IKA zinc (Zn) and stainless steel (SS) electrodes were attached to the ElectraSyn 2.0 vial head as working and counter electrodes respectively. The vial head with electrodes was attached to vial containing reaction mixture and stirred for 5 mins until the substrate and lithium bromide dissolved completely. Then the reaction set up was attached to the ElectraSyn 2.0 and following steps were followed: New exp. > Constant current > 10 mA > No ref. electrode > Total time > 6 hr > 0.2 mmol > No alternating polarity > start.

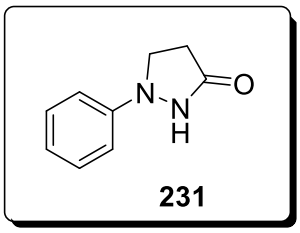

231

1-Phenylpyrazolidin-3-one (231): General procedure **J** was followed for making 1-phenylpyrazolidin-3-one **231.** The product was obtained as pale yellow solid in a yield of 29%.[217]

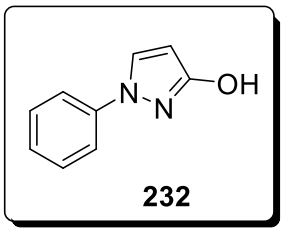

232

1-Phenyl-1*H*-pyrazol-3-ol (232): General procedure **J** was followed for making 1-phenyl-1*H*-pyrazol-3-ol **232**. The product was obtained as brown solid in a yield of 65%:[218] ^{1}H NMR ($CDCl_3$, 500 MHz) δ 5.91 (d, *J* = 2.0 Hz, 2 H), 7.26 (t, *J* = 7.5 Hz, 1 H), 7.44–7.47 (m, 2 H), 7.51–7.52 (m, 2 H), 11.73 (br s, 1 H). ^{13}C NMR ($CDCl_3$, 125 MHz) δ 94.2, 118.7, 126.0, 129.1, 129.7, 139.6, 164.0.

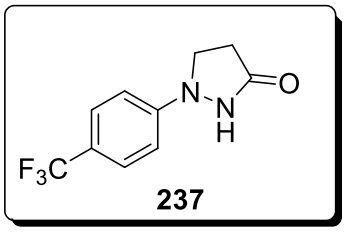

237

1-(4-(Trifluoromethyl)phenyl)pyrazolidin-3-one (237): General procedure **J** was followed for making 1-(4-(trifluoromethyl)phenyl)pyrazolidin-3-one **237**. The product was obtained as pale yellow solid in a yield of 30%: FTIR (cast film $CHCl_3$) 3160, 3071, 2920, 2891,2849, 1902, 1693, 1615, 1327 cm^{-1}; ^1H NMR ($CDCl_3$, 500 MHz) δ 2.62 (t, *J* = 8.0 Hz, 2 H), 4.05 (t, *J* = 8.0 Hz, 2 H), 7.10 (d, *J* = 8.5 Hz, 2 H), 7.58 (d, *J* = 8.5 Hz, 2 H), 7.90 (br s, 1 H); ^{13}C NMR ($CDCl_3$, 125 MHz) δ 29.8, 55.2, 115.7124.3 (q, J_F = 271.7 Hz), 124.4 (q, J_F = 32.8 Hz), 126.6 (q, J_F = 3.7 Hz), 154.0, 175.3; ^{19}F NMR (470 MHz, $CDCl_3$) δ –61.75; exact mass (EI) *m/z* calcd for $C_{10}H_9F_3N_2O$ $(M)^+$ 230.0667, found 230.0668.

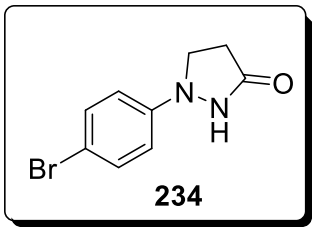

234

1-(4-Bromophenyl)pyrazolidin-3-one (234): General procedure **J** was followed for making 1-(4-bromophenyl)pyrazolidin-3-one **234**. The product was obtained in a yield of 37%:[217] ^1H NMR ($CDCl_3$, 500 MHz) δ 2.57 (t, *J* = 6.0 Hz, 2 H), 3.92 (t, *J* = 6.0 Hz, 2 H), 6.91 (d, *J* = 6.5 Hz, 2 H), 7.41 (d, *J* = 6.5 Hz, 2 H), 8.41 (br, 1 H); ^{13}C NMR ($CDCl_3$, 125 MHz) δ 29.7, 55.6, 115.3, 118.1, 132.2, 150.5, 175.4.

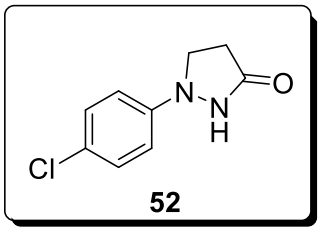

52

1-(4-Chlorophenyl)pyrazolidin-3-one (52): General procedure **J** was followed for making 1-(4-chlorophenyl)pyrazolidin-3-one **52**. The product was obtained in a yield of 77%: FTIR (cast film $CHCl_3$) 3175, 3073, 2959, 2925, 2857, 1881, 1698, 1593, 1491, 1286 cm^{-1}; ^1H NMR ($CDCl_3$, 500 MHz) δ 2.58 (t, *J* = 8.0 Hz, 2 H), 3.93 (t, *J* = 8.0 Hz, 2 H), 6.99 (d, *J* = 8.0 Hz, 2 H), 7.30 (d, *J* = 8.0 Hz, 2 H), 8.36 (br s, 1 H); ^{13}C NMR ($CDCl_3$, 125 MHz) δ 29.7, 55.7, 117.7, 127.9, 129.2, 150.0, 175.4; exact mass (electrospray) *m/z* calcd for $C_9H_9ClN_2O$ $(M - H)^-$ 195.0331, found 195.0330.

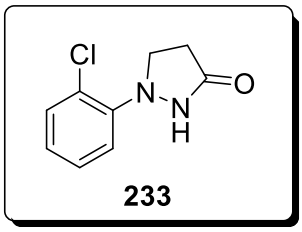

233

1-(2-Chlorophenyl)pyrazolidin-3-one (233): General procedure **J** was followed for making 1-(2-chlorophenyl)pyrazolidin-3-one **233**. The product was obtained as yellow solid in a yield of 75%: FTIR (cast film $CHCl_3$) 3140, 3061, 2969, 2916, 2855, 2741, 1645, 1470 cm^{-1}; ^1H NMR (DMSO–D_6, 500 MHz) δ 2.38 (t, *J* = 8.0 Hz, 2 H), 3.73 (t, *J* = 8.0 Hz, 2 H), 7.09–7.12 (m, 1 H), 7.25 (dd, *J* = 8.0, 1.5 Hz, 1 H), 7.31–7.34 (m, 1 H), 7.26 (dd, *J* = 8.0, 1.0 Hz, 1 H), 9.91 (br s, 1 H); ^{13}C NMR (DMSO–D_6, 125 MHz) δ 28.9, 54.3, 118.8, 124.2, 124.9, 127.6, 130.5, 148.6, 174.6; exact mass (electrospray) *m/z* calcd for $C_9H_9ClN_2O$ $(M + H)^+$ 197.0476, found 197.0473.

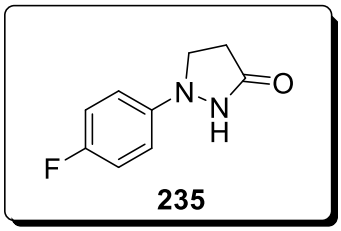

235

1-(4-Fluorophenyl)pyrazolidin-3-one (235): General procedure **J** was followed for making 1-(4-fluorophenyl)pyrazolidin-3-one **235**. The product was obtained in a yield of 61%:[217] ^{1}H NMR ($CDCl_3$, 500 MHz) δ 2.54 (t, *J* = 8.0 Hz, 2 H), 3.91 (t, *J* = 8.0 Hz, 2 H), 7.02–7.04 (m, 4 H), 7.18 (br s, 1 H); ^{13}C NMR ($CDCl_3$, 125 MHz) δ 29.2, 56.9, 116.0 (d, J_F = 22.6 Hz), 118.5 (d, J_F = 7.9 Hz), 147.8, 159.1 (d, J_F = 240.9), 175.5.

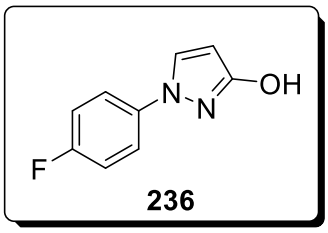

236

1-(4-Fluorophenyl)-1*H*-pyrazol-3-ol (236): General procedure **J** was followed for making 1-(4-fluorophenyl)-1*H*-pyrazol-3-ol **236**. The product was obtained in a yield of 31%:[217] ^{1}H NMR ($CDCl_3$, 500 MHz) δ 5.88 (d, *J* = 2.5 Hz, 1 H), 6.99–7.01 (m, 2 H), 7.39–7.41 (m, 2 H), 7.58 (d, *J* = 2.5 Hz, 1 H).

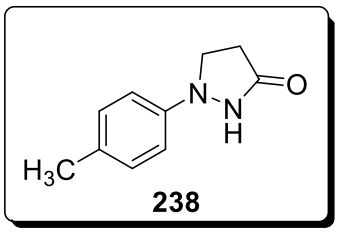

238

1-(4-Methylphenyl)pyrazolidin-3-one (238): General procedure **J** was followed for making 1-(4-methylphenyl)pyrazolidin-3-one **238**. The product was obtained in a yield of 25%:[217] ^{1}H NMR ($CDCl_3$, 500 MHz) δ 2.31 (s, 3 H), 2.53 (t, *J* = 8.0 Hz, 2 H), 3.91 (t, *J* = 8.0 Hz, 2 H), 6.96 (d, *J* =

7.5 Hz, 2 H), 7.13 (d, *J* = 7.5 Hz, 2 H), 7.42 (br, 1 H); ^{13}C NMR ($CDCl_3$, 175 MHz) δ 20.6, 29.4, 56.3, 116.9, 129.8, 132.8, 149.2, 175.5.

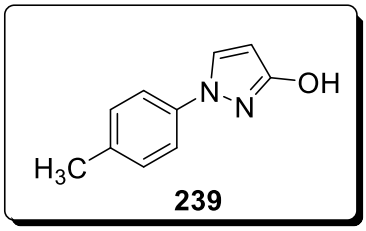

239

1-(4-Methylphenyl)-1*H*-pyrazol-3-ol (239): General procedure **J** was followed for making 1-(4-methylphenyl)-1*H*-pyrazol-3-ol **239**. The product was obtained in a yield of 66%: FTIR (cast film $CHCl_3$) 2952, 2925, 2855, 1457 cm^{-1}; ^{1}H NMR ($CDCl_3$, 500 MHz) δ 2.37 (s, 3 H), 5.87 (d, *J* = 2.5 Hz, 1 H), 7.24–7.26 (m, 2 H), 7.40 (dd, *J* = 7.0, 2.0 Hz, 2 H), 7.61 (d, *J* = 2.5 Hz, 1 H); ^{13}C NMR ($CDCl_3$, 175 MHz) δ 20.9, 93.7, 118.9, 129.0, 130.1, 135.9, 137.4, 163.8; exact mass (electrospray) *m/z* calcd for $C_{10}H_{11}N_2O$ $(M + H)^+$ 175.0866, found 175.0864.

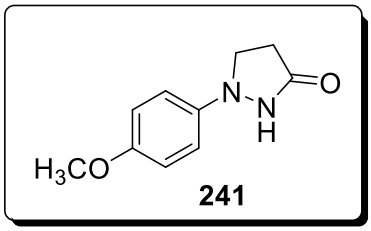

241

1-(4-Methoxyphenyl)pyrazolidin-3-one (241): General procedure **J** was followed for making 1-(4-methoxyphenyl)pyrazolidin-3-one **241**. The product was obtained in a yield of 35%:[219] ^{1}H NMR ($CDCl_3$, 500 MHz) δ 2.57 (t, *J* = 8.0 Hz, 2 H), 3.83 (t, *J* = 8.0 Hz, 2 H), 6.83–6.85 (m, 2 H), 7.00–7.01 (m, 2 H).

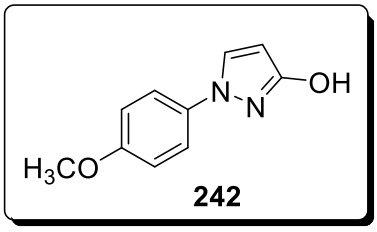

242

1-(4-Methoxyphenyl)-1*H*-pyrazol-3-ol (242): General procedure **J** was followed for making 1-(4-methoxyphenyl)-1*H*-pyrazol-3-ol **242**. The product was obtained in a yield of 65%: FTIR (cast film $CHCl_3$) 3140, 3052, 2960, 2936, 2849, 2728, 2644, 2575, 1545, 1516, 1250 cm^{-1}; ^1H NMR ($CDCl_3$, 500 MHz) δ 3.84 (s, 3 H), 5.85 (d, *J* = 2.5 Hz, 1 H), 6.98 (d, *J* = 9.0 Hz, 2 H), 7.42 (d, *J* = 9.0 Hz, 2 H), 7.54 (d, *J* = 2.5 Hz, 1 H); ^{13}C NMR ($CDCl_3$, 125 MHz) δ 55.6, 93.4, 114.8, 120.7, 129.1, 133.4, 158.0, 163.7; exact mass (electrospray) *m/z* calcd for $C_{10}H_{10}N_2O_2$ $(M + H)^+$ 191.0815, found 191.0813.

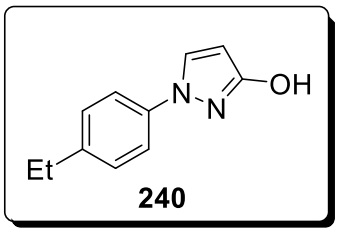

240

1-(4-Ethylphenyl)-1*H*-pyrazol-3-ol (240): General procedure **J** was followed for making 1-(4-ethylphenyl)-1*H*-pyrazol-3-ol **240**. The product was obtained in a yield of 77%: FTIR (cast film $CHCl_3$) 3256, 3020, 2932, 2873, 2724, 2640, 2577, 1521, 1251 cm^{-1}; ^1H NMR ($CDCl_3$, 500 MHz) δ 1.26 (t, *J* = 7.5 Hz, 3 H), 2.67 (q, *J* = 7.5 Hz, 2 H), 5.88 (d, *J* = 2.0 Hz, 1 H), 7.28 (d, *J* = 8.0 Hz, 2 H), 7.42 (d, *J* = 8.0 Hz, 2 H), 7.61 (d, *J* = 2.0 Hz, 1 H); ^{13}C NMR ($CDCl_3$, 125 MHz) δ 15.5, 28.3, 93.8, 129.0, 129.0, 137.5, 142.2, 163.8; exact mass (electrospray) *m/z* calcd for $C_{11}H_{12}N_2O$ $(M + H)^+$ 189.1022, found 189.1023.

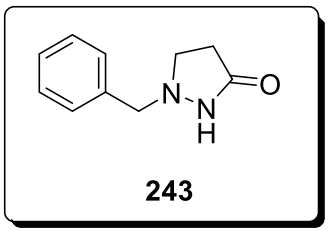

243

1-Benzyl-pyrazolidin-3-one (243): General procedure **J** was followed for making 1-benzyl-pyrazolidin-3-one **243**. The product was obtained in a yield of 95%:[220] FTIR (cast film $CHCl_3$)

3185, 3087, 3062, 2926, 2852, 1688 cm^{-1}; ^1H NMR ($CDCl_3$, 500 MHz) δ 2.51 (br s, 2 H), 3.37 (br s, 2 H), 3.87 (s, 2H), 7.30–7.37 (m, 5 H); ^{13}C NMR ($CDCl_3$, 125 MHz) δ 30.0, 51.9, 63.8, 128.2, 128.8, 129.3, 135.8, 174.8; exact mass (electrospray) *m/z* calcd for $C_{10}H_{12}N_2O$ $(M + H)^+$ 177.1022, found 177.1023.

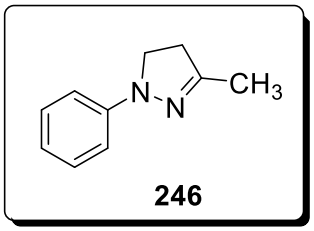

246

3-Methyl-1-phenyl-4,5-dihydro-1*H*-pyrazole (246): General procedure ***J*** was followed for making 3-methyl-1-phenyl-4,5-dihydro-1*H*-pyrazole **246.** The product was obtained in a yield of 73%: FTIR (cast film $CHCl_3$) 3062, 3041, 3028, 2914, 2848, 1598, 1503 cm^{-1}; ^1H NMR ($CDCl_3$, 500 MHz) δ 2.09 (s, 3 H), 2.82–2.86 (m, 2 H), 3.68 (t, *J* = 10 Hz, 2 H), 6.81 (d, *J* = 7.0 Hz, 1 H), 7.02 (d, *J* = 8.5 Hz, 2 H), 7.25–7.28 (m, 2 H); ^{13}C NMR ($CDCl_3$, 125 MHz) δ 16.1, 36.4, 48.5, 112.9, 118.7, 129.0, 147.1, 150.8; exact mass (electrospray) *m/z* calcd for $C_{10}H_{13}N_2$ $(M + H)^+$ 161.1073, found 161.1070.

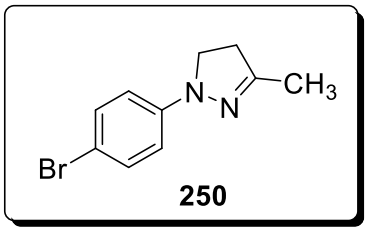

250

1-(4-Bromophenyl)-3-methyl-4,5-dihydro-1*H*-pyrazole (250): General procedure **J** was followed for making 1-(4-bromophenyl)-3-methyl-4,5-dihydro-1*H*-pyrazole **250**. The product was obtained in a yield of 63%:[221] ^1H NMR ($CDCl_3$, 500 MHz) δ 2.07 (s, 3 H), 2.84 (td, *J* = 10, 1.0 Hz, 2 H), 3.66 (t, *J* = 10 Hz, 2 H), 6.86 (dd, *J* = 7.0, 2.0 Hz, 2 H), 7.32 (dd, *J* = 7.0, 2.5 Hz, 2 H); ^{13}C NMR ($CDCl_3$, 175 MHz) δ 16.1, 36.5, 48.3, 110.5, 114.4, 131.8, 146.0, 151.4.

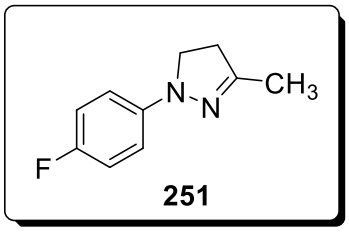

251

1-(4-Fluorophenyl)-3-methyl-4,5-dihydro-1*H*-pyrazole (251): General procedure **J** was followed for making 1-(4-fluorophenyl)-3-methyl-4,5-dihydro-1*H*-pyrazole **251**. The product was obtained in a yield of 70%:[221] FTIR (cast film $CHCl_3$) 3055, 2925, 2854, 1510, 1222 cm^{-1}; ^1H NMR ($CDCl_3$, 500 MHz) δ 2.07 (s, 3 H), 2.83 (t, *J* = 10, Hz, 2 H), 3.62 (t, *J* = 10 Hz, 2 H), 6.94–6.96 (m, 4 H); ^{13}C NMR ($CDCl_3$, 125 MHz) δ 16.1, 36.6, 49.3, 114.0 (d, J_F = 7.5 Hz), 115.5 (d, J_F = 22.3 Hz), 144.0, 151.1, 156.7 (d, J_F = 235.4 Hz); exact mass (electrospray) *m/z* calcd for $C_{10}H_{11}FN_2$ $(M + H)^+$ 179.0979, found 179.0979.

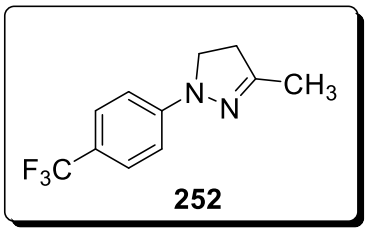

252

1-(4-Trifluoromethyl)-3-methyl-4,5-dihydro-1*H*-pyrazole (252): General procedure **J** was followed for making 1-(4-trifluoromethyl)-3-methyl-4,5-dihydro-1*H*-pyrazole **252**. The product was obtained as yellow solid in a yield of 43%: FTIR (cast film $CHCl_3$) 3013, 2957, 2927, 2856, 1615, 1531, 1328, 1110 cm^{-1}; ^1H NMR ($CDCl_3$, 500 MHz) δ 2.09 (s, 3 H), 2.89 (t, *J* = 10 Hz, 2 H), 3.72 (t, *J* = 10 Hz, 2 H), 6.98 (d, *J* = 8.5 Hz, 2 H), 7.47 (d, *J* = 8.5 Hz, 2 H); ^{13}C NMR ($CDCl_3$, 175 MHz) δ 16.0, 36.4, 47.5, 111.8, 119.7 (q, J_F = 7.6 Hz), 125.0 (q, J_F = 292.8 Hz), 126.3 (q, J_F = 3.8 Hz), 148.6, 152.1; ^{19}F NMR (469 MHz, $CDCl_3$) δ ppm – 60.96 (s, 3F).; exact mass (electrospray) *m/z* calcd for $C_{11}H_{11}F_3N_2$ $(M)^+$ 228.0874, found 228.0873.

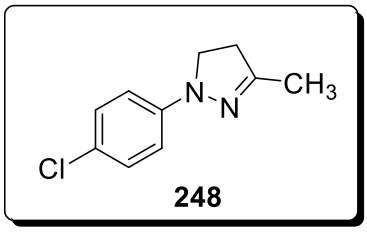

248

1-(4-Chlorophenyl)-3-methyl-4,5-dihydro-1*H*-pyrazole (248): General procedure **J** was followed for making 1-(4-chlorophenyl)-3-methyl-4,5-dihydro-1*H*-pyrazole **248**. The product was obtained in a yield of 35%: FTIR (cast film $CHCl_3$) 2958, 2924, 2853, 1495, 1464 cm^{-1}; ^1H NMR ($CDCl_3$, 500 MHz) δ 2.08 (s, 3 H), 2.85 (t, *J* = 10 Hz, 2 H), 3.64 (t, *J* = 10 Hz, 2 H), 6.93 (d, *J* = 11.0 Hz, 2 H), 7.20 (d, *J* = 11.0 Hz, 2 H); ^{13}C NMR ($CDCl_3$, 175 MHz) δ 16.1, 36.5, 48.5, 113.9, 123.3, 128.9, 145.6, 151.3; exact mass (electrospray) *m/z* calcd for $C_{10}H_9ClN_2$ $(M + H)^+$ 193.0527, found 193.0523.

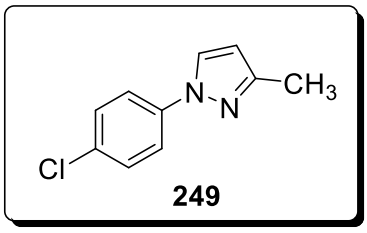

249

1-(4-Chlorophenyl)-3-methyl-1*H*-pyrazole (249): General procedure **J** was followed for making 1-(4-chlorophenyl)-3-methyl-1*H*-pyrazole **249**. The product was obtained in a yield of 28%:[222] ^1H NMR ($CDCl_3$, 500 MHz) δ 2.37 (s, 3 H), 6.25 (s, 1 H), 7.38 (apparent dd, *J* = 7.0, 1.5 Hz, 2 H), 7.59 (apparent dd, *J* = 7.0, 1.5 Hz, 2 H), 7.78 (s, 1 H); ^{13}C NMR ($CDCl_3$, 175 MHz) δ 13.7, 107.9, 119.9, 127.3, 129.4, 131.3, 138.8, 150.9.

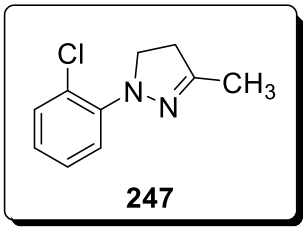

247

1-(2-Chlorophenyl)-3-methyl-4,5-dihydro-1*H*-pyrazole (247): General procedure **J** was followed for making 1-(2-chlorophenyl)-3-methyl-4,5-dihydro-1*H*-pyrazole **247**. The product was obtained in a yield of 52%: FTIR (cast film $CHCl_3$) 3066, 2987, 2948, 2915, 2850, 1589, 1478 cm^{-1}; ^1H NMR ($CDCl_3$, 500 MHz) δ 2.10 (s, 3 H), 2.84 (t, *J* = 10 Hz, 2 H), 3.76 (t, *J* = 10 Hz, 2 H), 6.97–7.00 (m, 1 H), 7.18–7.21 (m, 2 H), 7.33 (dd, *J* = 8.0, 1.5 Hz, 1 H), 7.38 (dd, *J* = 8.0, 1.5 Hz, 1 H); ^{13}C NMR ($CDCl_3$, 175 MHz) δ 16.1, 37.6, 53.4, 121.4, 124.0, 124.9, 127.4, 130.3, 147.3, 153.8; exact mass (electrospray) *m/z* calcd for $C_{10}H_{11}ClN_2$ $(M + H)^+$ 195.0684, found 195.0679.

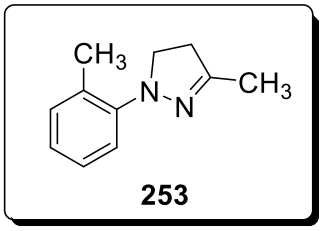

253

3-Methyl-1-(2-methylphenyl)-4,5-dihydro-1*H*-pyrazole (253): General procedure **J** was followed for making 3-methyl-1-(2-methylphenyl)-4,5-dihydro-1*H*-pyrazole **253**. The product was obtained in a yield of 83%:[221] ^1H NMR ($CDCl_3$, 500 MHz) δ 2.09 (s, 3 H), 2.37 (s, 3 H), 2.79 (t, *J* = 9.5 Hz, 2 H), 3.49 (t, *J* = 9.5 Hz, 2 H), 6.98–7.01 (m, 1 H), 7.13–7.15 (m, 3 H); ^{13}C NMR ($CDCl_3$, 175 MHz) δ 16.2, 19.2, 37.2, 53.5, 119.2, 123.4, 126.5, 129.9, 131.0, 148.4, 152.5.

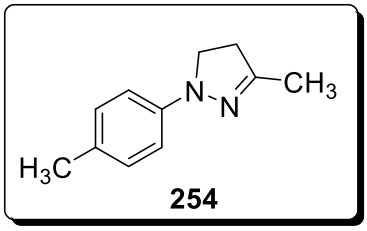

254

3-Methyl-1-(*p*-tolyl)-4,5-dihydro-1*H*-pyrazole (254): General procedure **J** was followed for making 3-methyl-1-(*p*-tolyl)-4,5-dihydro-1*H*-pyrazole **254**. The product was obtained in a yield of 90%:[221] ^1H NMR ($CDCl_3$, 500 MHz) δ 2.08 (s, 3 H), 2.27 (s, 3 H), 2.81 (t, *J* = 10 Hz, 2 H), 3.64 (t,

J = 10 Hz, 2 H), 6.92 (d, *J* = 7.5 Hz, 2 H), 7.06 (d, *J* = 7.5 Hz, 2 H); ^{13}C NMR ($CDCl_3$, 175 MHz) δ 16.1, 20.5, 36.4, 49.1, 113.1, 128.0, 129.5, 145.3, 150.5.

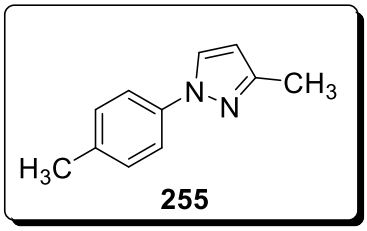

255

3-Methyl-1-(*p*-tolyl)-1*H*-pyrazole (255): General procedure **J** was followed for making 3-methyl-1-(*p*-tolyl)-1*H*-pyrazole **255**. The product was obtained in a yield of 10%: FTIR (cast film $CHCl_3$) 2959, 2924, 2853, 1516 cm^{-1}; ^{1}H NMR ($CDCl_3$, 500 MHz) δ 2.37 (s, 6 H), 6.22 (d, *J* = 2.0 Hz, 1 H), 7.22 (d, *J* = 8.0 Hz, 2 H), 7.52 (d, *J* = 8.0 Hz, 2 H), 7.77 (d, *J* = 2.0 Hz, 1 H); ^{13}C NMR ($CDCl_3$, 175 MHz) δ 13.7, 20.9, 107.2, 118.9, 127.3, 129.9, 135.7, 150.2; exact mass (electrospray) *m/z* calcd for $C_{11}H_{12}N_2$ $(M + H)^+$ 173.1073, found 173.1070.

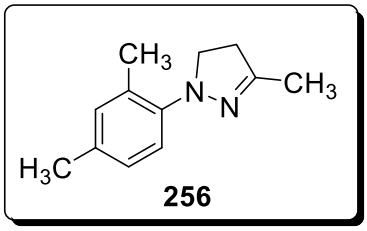

256

3-Methyl-1-(2,4-dimethylphenyl)-4,5-dihydro-1*H*-pyrazole (256): General procedure **J** was followed for making 3-methyl-1-(2,4-dimethylphenol)-4,5-dihydro-1*H*-pyrazole **256**. The product was obtained in a yield of 95%: FTIR (cast film $CHCl_3$) 3052, 2987, 2942, 2912, 2865, 1950, 1872, 1775, 1739, 1597, 1496, 1469, 1439 cm^{-1}; ^{1}H NMR ($CDCl_3$, 500 MHz) δ 2.08 (s, 3 H), 2.28 (s, 3 H), 2.33 (s, 3 H), 2.77 (t, *J* = 9.5 Hz, 2 H), 3.44 (t, *J* = 9.5 Hz, 2 H), 6.95 (d, *J* = 8.0 Hz, 1 H), 6.98 (s, 1 H), 7.06 (d, *J* = 8.0 Hz, 1 H); ^{13}C NMR ($CDCl_3$, 125 MHz) δ 16.2, 18.9, 20.7, 37.3, 54.0, 119.5, 127.1, 130.0, 131.6, 133.0, 146.2, 152.4; exact mass (electrospray) *m/z* calcd for $C_{12}H_{16}N_2$ $(M + H)^+$ 189.1386, found 189.1386.

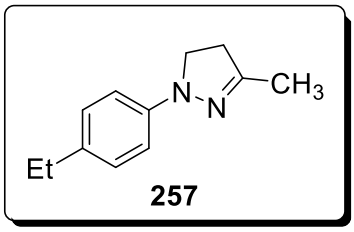

257

1-(4-Ethylphenyl)-3-methyl-4,5-dihydro-1*H*-pyrazole (257): General procedure **J** was followed for making 1-(4-ethylphenyl)-3-methyl-4,5-dihydro-1*H*-pyrazole **257**. The product was obtained in a yield of 83%: ^{1}H NMR ($CDCl_3$, 500 MHz) δ 1.21 (t, *J* = 7.5 Hz, 3H), 2.07 (s, 3 H), 2.57 (q, *J* = 7.5 Hz, 2 H), 2.81 (td, *J* = 10.0, 1 Hz, 2 H), 3.64 (t, *J* = 10.0 Hz, 2 H), 6.95 (d, *J* = 8.5 Hz, 2 H), 7.10 (d, *J* = 8.5 Hz, 2 H); ^{13}C NMR ($CDCl_3$, 175 MHz) δ 15.9, 16.1, 28.0, 36.4, 49.1, 113.1, 128.4, 134.7, 145.5, 150.6.

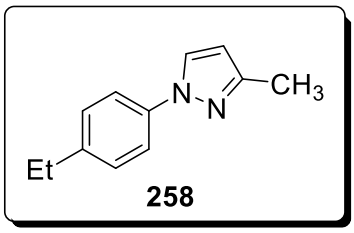

258

3-Methyl-1-(4-ethyl)-1*H*-pyrazole (258): General procedure **J** was followed for making 3-methyl-1-(4-ethyl)-1*H*-pyrazole **258**. The product was obtained in a yield of 16%: FTIR (cast film $CHCl_3$) 3040, 2959, 2927, 2855, 1535 cm^{-1}; ^{1}H NMR ($CDCl_3$, 500 MHz) δ 1.26 (t, *J* = 7.5 Hz, 3H), 2.38 (s, 3 H), 2.68 (q, *J* = 7.5 Hz, 2 H), 6.23 (d, *J* = 2.5 Hz, 1 H), 7.25 (dd, *J* = 7.0, 2.0 Hz, 2 H), 7.56 (dd, *J* = 7.0, 2.0 Hz, 2 H), 7.78 (d, *J* = 2.5 Hz, 1 H); ^{13}C NMR ($CDCl_3$, 125 MHz) δ 13.8, 15.6, 28.3, 107.2, 119.0, 127.3, 128.7, 138.2, 142.1, 150.2; exact mass (electrospray) *m/z* calcd for $C_{12}H_{14}N_2$ $(M + H)^+$ 187.1230, found 187.1227.

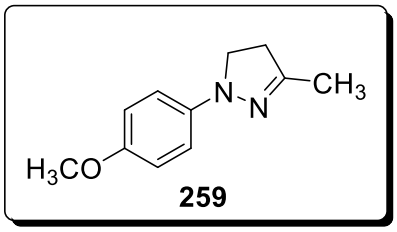

259

1-(4-Methoxyphenyl)-3-methyl-4,5-dihydro-1*H*-pyrazole (259): General procedure **J** was followed for making 1-(4-methoxyphenyl)-3-methyl-4,5-dihydro-1*H*-pyrazole **259**. The product was obtained in a yield of 44%: ^{1}H NMR ($CDCl_3$, 500 MHz) δ 2.07 (s, 3H), 2.80 (t, *J* = 10.0 Hz, 2 H), 3.60 (t, *J* = 10.0 Hz, 2 H), 3.77 (s, 3 H), 6.85 (dd, *J* = 7.0, 2.5 Hz, 2 H), 6.98 (dd, *J* = 7.0, 2.5 Hz, 2 H); ^{13}C NMR ($CDCl_3$, 125 MHz) δ 16.1, 29.7, 36.6, 49.9, 55.7, 114.5, 114.6, 142.2, 150.7, 153.2.

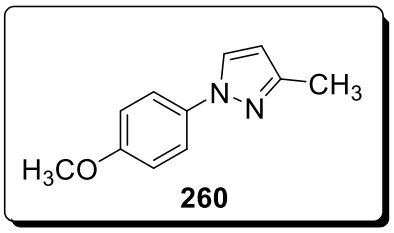

260

1-(4-Methoxyphenyl)-3-methyl-1*H*-pyrazole (260): General procedure **J** was followed for making 1-(4-methoxyphenyl)-3-methyl-1*H*-pyrazole **260**. The product was obtained in a yield of 56%: FTIR (cast film $CHCl_3$) 2957, 2926, 2855, 1532, 1515, 1249 cm^{-1}; ^{1}H NMR ($CDCl_3$, 500 MHz) δ 3.84 (s, 3 H), 6.21 (d, *J* = 2.5 Hz, 1 H), 6.95 (d, *J* = 9.0 Hz, 2 H), 7.54 (d, *J* = 9.0 Hz, 2 H), 7.71 (d, *J* = 2.5 Hz, 1 H); ^{13}C NMR ($CDCl_3$, 175 MHz) δ 13.7, 55.6, 107.0, 114.5, 120.6, 127.4, 134.1, 150.0, 157.9; exact mass (electrospray) *m/z* calcd for $C_{11}H_{13}N_2O$ $(M + H)^+$ 189.1022, found 189.1020.

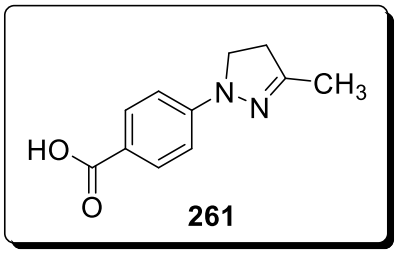

261

4-(3-Methyl-4,5-dihydro-1*H*-pyrazol-1-yl)benzoic acid (261): General procedure **J** was followed for making 4-(3-methyl-4,5-dihydro-1*H*-pyrazol-1-yl)benzoic acid **261**. The product was obtained in a yield of 83%: ^{1}H NMR (DMSO–D_6, 500 MHz) δ 2.00 (s, 3 H), 2.89 (t, *J* = 10 Hz, 2 H), 3.69 (t, *J* = 10 Hz, 2 H), 6.89 (d, *J* = 9.0 Hz, 2 H), 7.60 (d, *J* = 9.0 Hz, 2 H); ^{13}C NMR (DMSO–D_6, 125 MHz) δ 15.6, 35.9, 46.8, 110.9, 118.7, 130.9, 148.9, 153.9, 167.3.

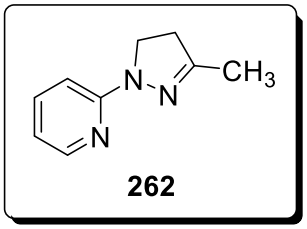

262

2-(5-Methyl-3,4-dihydropyrazol-2-yl)pyridine (262): General procedure **J** was followed for making 2-(5-methyl-3,4-dihydropyrazol-2-yl)pyridine **262**. The product was obtained in a yield of 69%: FTIR (cast film $CHCl_3$) 3100, 3055, 2982, 2953, 2918, 2904, 2833, 1952, 1606, 1558, 1507, 1474, 1457 cm^{-1}; ^{1}H NMR ($CDCl_3$, 500 MHz) δ 2.09 (s, 3 H), 2.84 (t, *J* = 10 Hz, 2 H), 3.95 (t, *J* = 10 Hz, 2 H), 6.63 (t, *J* = 6.0 Hz, 1 H), 7.20 (d, *J* = 8.5 Hz, 1 H), 7.47 (td, *J* = 6.0, 1.5 Hz, 1 H), 8.16 (d, *J* = 4.5 Hz, 1 H); ^{13}C NMR ($CDCl_3$, 125 MHz) δ 16.2, 36.0, 46.3, 108.7, 113.7, 137.0, 147.6, 153.0, 157.0; exact mass (electrospray) *m/z* calcd for $C_9H_{11}N_3$ $(M + H)^+$ 162.1026, found 162.1023.

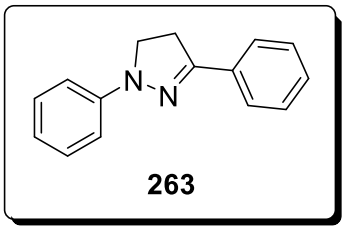

263

1,3-Diphenyl-4,5-dihydro-1*H*-pyrazole (263): General procedure **J** was followed for making 1,3-diphenyl-4,5-dihydro-1*H*-pyrazole **263**. The product was obtained as yellow solid in a yield of 60%;[223] ^{1}H NMR ($CDCl_3$, 500 MHz) δ 3.26 (t, *J* = 10.5 Hz, 2 H), 3.90 (t, *J* = 10.5 Hz, 2 H), 6.86 (t, 7.5 Hz, 1 H), 7.17 (d, 8.0 Hz, 2 H), 7.30–7.36 (m, 3 H), 7.38–7.43 (m, 2 H), 7.77 (d, *J* = 7.0 Hz, 2 H).

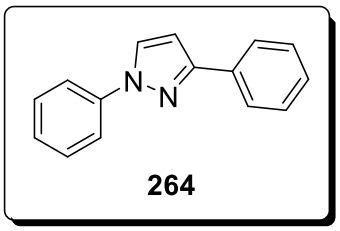

264

1,3-Diphenyl-1*H*-pyrazole (264): General procedure **J** was followed for making 1,3-diphenyl-1*H*-pyrazole **264**. The product was obtained in a yield of 12%: FTIR (cast film $CHCl_3$) 3061, 2926, 2852, 1600, 1506 cm^{-1}; ^{1}H NMR ($CDCl_3$, 500 MHz) δ 6.78 (d, *J* = 2.5 Hz, 1 H), 7.29 (t, *J* = 7.5 Hz, 1 H), 7.34 (t, *J* = 7.5 Hz, 1 H), 7.42–7.49 (m, 4 H), 7.78 (d, 8.0 Hz, 2 H), 7.92 (d, *J* = 7.0 Hz, 2 H), 7.96 (d, *J* = 2.5 Hz, 1 H); ^{13}C NMR ($CDCl_3$, 125 MHz) δ 16.2, 36.5, 46.3, 108.6, 112.8, 137.7, 147.5, 158.3, 208.1; exact mass (electrospray) *m/z* calcd for $C_{15}H_{12}N_2$ $(M + H)^+$ 221.1073, found 221.1070.

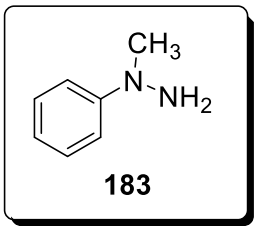

183

1-Methyl-1-phenylhydrazine (183): General procedure **J** was followed for making 1-methyl-1-phenylhydrazine **183**. The product was obtained in a yield of 93%:[224] FTIR (cast film $CHCl_3$) 3140, 3060, 2962, 2923, 2852, 1649, 1506 cm^{-1}; ^1H NMR ($CDCl_3$, 500 MHz) δ 3.12 (s, 3 H), 3.70 (br s, 1 H), 6.82 (apparent t, *J* = 7.5 Hz, 1 H), 7.02 (apparent d, *J* = 8.0 Hz, 2 H), 7.26–7.29 (m, 2 H); ^{13}C NMR ($CDCl_3$, 125 MHz) δ 44.6, 113.5, 118.6, 129.0, 152.7; exact mass (electrospray) *m/z* calcd for $C_7H_{10}N_2$ $(M + H)^+$ 123.0917, found 123.0917.

References

1. Jampilek, J., Heterocycles in medicinal chemistry, *Molecules*, **2019**, *24*, 3839–3842 and references cited therein.

2. Kerru, N.; Gummidi, L.; Maddila, S.; Gangu, K. K.; Jonnalagadda, S. B., A review on recent advances in nitrogen–containing molecules and their biological applications, *Molecules*, **2020**, *25*, 1909–950.

3. Gomtsyan A., Heterocycles in drugs and drug discovery, *Chemistry of Heterocyclic Compounds*, **2012**, *48*, 7–10.

4. Lowe, D., The Most Common Heterocycles in Drugs, *Science Translational Medicine*, **2014**.

5. Zhou, C.; Zhao, J.; Guo, W.; Jiang, J.; Wang, J., *N*-Methoxyamide: an alternative amidation reagent in the Rhodium(III)-catalyzed C–H activation, *Organic Letters*, **2019**, *21*, 9315–9319.

6. März, M.; Chudoba, J.; Kohouta, M.; Cibulka, R., Photocatalytic esterification under Mitsunobu reaction conditions mediated by flavin and visible light, *Organic and Biomolecular Chemistry*, **2017**, *15*, 1970–1975.

7. Reddy, Bijivemula N.; Rani, Chinthaparthi Radha; Reddy; Pathak, Madhvesh, An efficient and green $La(OTf)_3$ catalyzed Petasis borono–Mannich reaction for the synthesis of tertiary amines, *Research on Chemical Intermediates*, **2016**, *42*, 7533–7549.

8. Hałdys, K.; Goldeman, W.; Jewgiński, M.; Wolińska, E.; Anger, N.; Rossowska, J.; Latajkaa, R., Inhibitory properties of aromatic thiosemicarbazones on mushroom tyrosinase: Synthesis, kinetic studies, molecular docking and effectiveness in melanogenesis inhibition, *Bioorganic Chemistry*, **2018**, *81*, 577–586.

9. Chang, M. –Y.; Lu, Y. –J.; Cheng, Y. –C., $In(OTf)_3$-Mediated synthesis of substituted pyridazines, *Tetrahedron*, **2015**, 71, 6840−6845.

10. Li, P.; Shi, L.; Gao, M. –N.; Yang, X.; Xue, W.; Jin, L. –H.; Hu, D. –Y.; Song, B. –A., Antibacterial activities against rice bacterial leaf blight and tomato bacterial wilt of 2-mercapto-5-substituted-1,3,4-oxadiazole/thiadiazole derivatives, *Bioorganic and Medicinal Chemistry Letters*, **2015**, *25*, 481−484.

11. https://enamine.net/index.php?option=com_content&view=article&id=131&Itemid=246 (accessed November 16, 2020).

12. Byrkit, G. D.; Michalek G. A., Hydrazine in organic chemistry, *Industrial & Engineering Chemistry Research*, **1950**, *42*, 1862−1875.

13. Breising, V. M.; Kayser, J. M.; Kehl, A.; Schollmeyer, D.; Liermann, J. C.; Waldvogel, S. R., Electrochemical formation of N,N′-diarylhydrazines by dehydrogenative N–N homocoupling reaction, *Chemical Communication*, **2020**, *56*, 4348−4351 and references cited therein.

14. Boche, G.; Meier, C.; Kleemi, W., Hydrazines and azo compounds from O-diphenylphosphinoyl arylhydroxylamines, *Tetrahedron* Letters, **1988**, *29*, 1777−1779.

15. Samzadeh-Kermani, A., Copper-catalyzed C–N bond formation using dialkyl azodicarboxylate as the amination reagent, *Tetrahedron Letters*, **2016**, *57*, 463−465.

16. Kahn, F. A.; Dash, J.; Sudheer, C.; Gupta, R. K., Chemoselective reduction of aromatic nitro and azo compounds in ionic liquids using zinc and ammonium salts, *Tetrahedron Letters*, **2003**, *44*, 7783−7787.

17. Boche, G.; Reinhard, R. H.; Bosold, F., N-Aryl-O-(diphenylphosphinoyl)hydroxylamines: electrophilic amination of amines to hydrazines; a model reaction for the carcinogenicity of aromatic amines, *Angewandte Chemie International Edition*, **1986**, *25*, 562−563.

18. Loog, O.; Mäeorg, U.; Ragnarsson, U., Synthesis of hydrazines with aromatic substituents using triarylbismuth reagents, *Synthesis*, **2000**, 2000, 1591–1597.

19. Loog, O.; Mäeorg, U., Cu-catalysed N-arylation of hydrazines with bismuthanes: synthesis and pinacol or imino-pinacol coupling of 4-formylphenylhydrazines and their phenylimine derivatives, *Synlett*, **2004**, 2537–2540.

20. Samzadeh-Kermani, A., Copper-catalyzed C–N bond formation using dialkyl azodicarboxylate as the amination reagent, *Tetrahedron* Letters, **2016**, *57*, 463–465.

21. Chen, J.; Zhang, Y.; Hao, W.; Zhang, R.; Yi, F., Efficient synthesis of aryl hydrazines using copper-catalyzed cross-coupling of aryl halides with hydrazine in PEG-400, *Tetrahedron*, **2013**, *69*, 613–617.

22. Wang, Z.; Skerlj, R. T.; Bridger, G. J., Regioselective synthesis of aryl hydrazides by palladium-catalyzed coupling of *t*-butylcarbazate with substituted aryl bromides, *Tetrahedron Letters*, **1999**, *40*, 3543–3546.

23. Blair, L. M.; Sperry, J., Natural products containing a nitrogen−nitrogen bond, *Journal of Natural Products*, **2013**, *76*, 794–812.

24. Faria, J. V.; Vegi, P. F.; Miguita, A. G. C.; Santos, M. S.; Boechat, N.; Bernardino, A. M. R., Recently reported biological activities of pyrazole compounds, *Bioorganic and Medicinal Chemistry*, **2017**, *25*, 5891–5903.

25. Dar, A. M.; Shamsuzzaman, A concise review on the synthesis of pyrazole heterocycles, *Nuclear Medicine & Radiation Therapy*, **2015**, *6*, 1–5.

26. Pizzuti, L.; Barschak, A. G.; Stefanello, F. M.; Farias, M. D.; Lencina, C.; Roesch-Ely, M.; Cunico, W.; Moura, S.; Pereira, C. M. P., Environment-friendly synthesis of bioactive pyrazoles, *Current Organic Chemistry*, **2014**, *18*, 115–126.

27. Faisal, M.; Saeed, A.; Hussain, S.; Dar, P.; Larik, F. A., Recent developments in synthetic chemistry and biological activities of pyrazole derivatives, *Journal of Chemical Sciences*, **2019**, *131*, 1–30.

28. Karrouchi, K.; Radi,S.; Ramli, Y.; Taoufik, J.; Mabkhot, Y. N.; Al-aizari, F. A.; Ansar, M'hammed, Synthesis and pharmacological activities of pyrazole derivatives: A review, *Molecules*, **2018**, *23*, 1–85.

29. Makino, K.; Kim, H. S.; Kurasawa, Y., Synthesis of pyrazoles and condensed pyrazoles, *Journal of Heterocyclic Chemistry*, **1999**, *36*, 321–332.

30. Fustero, S.; Simón-Fuentes, A.; Sanz-Cervera, J. F., Recent advances in the synthesis of pyrazoles. A review, *Organic Preparations and Procedures International*, **2009**, *41*, 253–290 and references cited therein.

31. Kumari, S.; Paliwal, S.; Chauhan, R., Synthesis of pyrazole derivatives possessing anticancer activity: current status, *Synthetic Communications*, **2014**, *44*, 1521–1578.

32. Küçükgüzel, Ş. G.; Şenkardeş, S., Recent advances in bioactive pyrazoles, *European Journal of Medicinal Chemistry*, **2015**, 97, 786–815.

33. Elguero, J.; Goya, P.; Jagerovic, N.; Silva, A. M. S., Pyrazoles as drugs: facts and fantasies, *Targets in Heterocyclic Systems–Chemistry and Properties*, **2002***, 6*, 52–98.

34. Kira, M.; Abdel-Rahman, M.; Gadalla, K., The vilsmeier-haack reaction - III cyclization of hydrazones to pyrazoles, *Tetrahedron Letters*, **1969**, *10*, 109–110.

35. Schmidt, A.; Dreger, A., Recent advances in the chemistry of pyrazoles. properties, biological activities, and syntheses, *Current Organic Chemistry*, **2011**, *15*, 1423–1463.

36. Heller, S. T.; Natarajan, S. R., 1,3-Diketones from acid chlorides and ketones: a rapid and general one-pot synthesis of pyrazoles, *Organic Letters*, **2006**, *8*, 2675–2678.

37. Wang, Z.; Qina, H., Solventless syntheses of pyrazole derivatives, Green Chemistry, **2004**, *6*, 90–92 and references cited therein.

38. Bhat, B. A.; Puri, S. C.; Qurishi, M. A.; Dhar, K. L.; Qazi, G. N., Synthesis of 3,5-diphenyl-1*H*-pyrazoles, Synthetic Communications, **2005**, *35*, 1135–1142.

39. Chang, K. -T.; Choi, Y. H.; Kim, S. -H.; Yoon, Y. -J.; Lee, W.-S., Regioselective synthesis of pyrazolesvia the ring cleavage of 3-substituted N-alkylated 3-hydroxyisoindolin-1-ones, *Journal of the Chemical Society, Perkin Transactions 1*, **2002**, 207–210.

40. Grotjahn, D. B.; Van, S.; Combs, D.; Lev, D. A.; Schneider, C.; Rideout, M.; Meyer, C.; Hernandez, G.; Mejorado, L., New flexible synthesis of pyrazoles with different, functionalized substituents at C3 and C5, *The Journal of Organic Chemistry*, **2002**, *67*, 9200–9209.

41. Liu, H. -L.; Jiang, H. -F.; Zhang, M.; Yao, W. -J.; Zhu, Q. -H.; Tang, Z., One-pot three-component synthesis of pyrazoles through a tandem coupling-cyclocondensation sequence, *Tetrahedron Letters*, **2008**, *49*, 3805–3809.

42. Aggarwal, V. K.; Vicente, J. d.; Bonnert, R. V., A novel one-pot method for the preparation of pyrazoles by 1,3-dipolar cycloadditions of diazo compounds generated in situ, *Journal of Organic Chemistry*, **2003**, *68*, 5381–5383.

43. Lévai, A.; Silva, A. M. S.; Cavaleiro, J. A. S.; Alkorta, I.; Elguero, J.; Jekő, J., Synthesis of pyrazoles by treatment of 3-benzylchromones, 3-benzylflavones and their 4-thio analogues with hydrazine, *European Journal of Organic Chemistry*, **2006**, *2006*, 2825–2832.

44. Martiń, R., Rodríguez, M. R.; Buchwald, S. L., Domino Cu-catalyzed C-N coupling/hydroamidation: a highly efficient synthesis of nitrogen heterocycles, *Angewandte Chemie International Edition*, **2006**, *45*, 7079–7082.

45. Wang, X. -J.; Tan, J.; Grozinger, K., Cross-coupling of 1-aryl-5-bromopyrazoles: regioselective synthesis of 3,5-disubstituted 1-arylpyrazoles, *Tetrahedron Letters*, **2000**, *41*, 4713–4716.

46. Singh, S. K.; Reddy, M. S.; Shivaramakrishna, S.; Kavitha, D.; Vasudev, R.; Babu, J. M.; Sivalakshmidevi, A.; Rao, Y. K., Modified reaction conditions to achieve high regioselectivity in the two component synthesis of 1,5-diarylpyrazoles, *Tetrahedron Letters*, **2004**, *45*, 7679–7682.

47. Gosselin, F.; O´Shea, P. D.; Webster, R. A.; Reamer, R. A.; Tillyer, R. D.; Grabowski, E. J. J., Highly regioselective synthesis of 1-aryl-3,4,5-substituted pyrazoles, *Synlett*, **2006**, 3267–3270.

48. Katritzky, A. R.; Wang, M.; Zhang, S.; Voronkov, M. V., Regioselective synthesis of polysubstituted pyrazoles and isoxazoles, *Journal of Organic Chemistry*, **2001**, *66*, 6787–6791.

49. Deng, X.; Mani, N. S., Reaction of N-monosubstituted hydrazones with nitroolefins: a novel regioselective pyrazole synthesis, *Organic Letters*, **2006***, 8*, 3505–3508.

50. Norris, T.; Colon-Cruz, R.; Ripin, D. H. B., New hydroxy-pyrazoline intermediates, subtle regio-selectivity and relative reaction rate variations observed during acid catalyzed and neutral pyrazole cyclization, *Organic and Biomolecular Chemistry*, **2005,** *3*, 1844–1849.

51. Singh, S. P.; Kumar, Aggarwal, V.; R.; Elguero, J. The reaction of aryl and heteroarylhydrazines with aryl-trifluoromethyl *β*-diketones, *Journal of Heterocyclic Chemistry*, **2006***, 43*, 1003–1014.

52. Knorr, L., Synthesis of pyrrole derivatives, *Berichte der deutschen chemischen Gesellschaft*, **1884**, *17*, 1635–1642.

53. Dang, T. T.; Dang, T. T.; Fischer, C.; Görls, H.; Langer, P., Synthesis of pyrazole-3-carboxylates and pyrazole-1,5-dicarboxylates by one-pot cyclization of hydrazone dianions with diethyl oxalate, *Tetrahedron*, **2008**, *64*, 2207–2215.

54. Lokhande, P.; Hasanzadeh, K.; Konda, S. G., A novel and efficient approach for the synthesis of new halo substituted 2-arylpyrazolo[4,3-c]coumarin derivatives, *Chemistry—A European Journal*, **2011**, *2*, 223–228.

55. Deng, X.; Mani, N. S., Base-mediated reaction of hydrazones and nitroolefins with a reversed regioselectivity: A novel synthesis of 1,3,4-trisubstituted pyrazoles. *Organic Letters*, **2008**, *10*, 1307–13010.

56. Sener, A.; Kasimogullari, R.; Sener, M.; Genç, H., Studies on reactions of cyclic oxalyl compounds with hydrazines or hydrazones. 2. Synthesis and reactions of 4-benzoyl-1-(4-nitrophenyl)-5-phenyl-1Hpyrazole-3-carboxylic acid, *Chemistry of Heterocyclic Compounds*, **2004**, *40*, 1039–1046.

57. Grošelj, U.; Drobnič, A.; Rečnik, S.; Svete, J.; Stanovnik, B.; Golobič, A.; Nina, L.; Ivan, L.; Anton, M.; Simona, G .-G, 1,3-Dipolar Cycloadditions to (5Z)-1-Acyl-5-(cyanomethylidene)-imidazolidine-2,4-diones: Synthesis and Transformations of Spirohydantoin Derivatives, *Helvetica Chimica Acta*, **2001**, *84*, 3403–3417.

58. Panda, N.; Jena, A. K., Fe-catalyzed one-pot synthesis of 1,3-di- and 1,3,5-trisubstituted pyrazoles from hydrazones and vicinal diols, *Journal of Organic Chemistry*, **2012**, *77*, 9401–9406.

59. Tang, M.; Wang, Y.; Wang, H.; Kong, Y., Aluminum chloride mediated reactions of N-alkylated tosylhydrazones and terminal alkynes: a regioselective approach to 1,3,5-trisubstituted pyrazoles, *Synthesis*, **2016**, *48*, 3065–3076.

60. Kong, Y.; Tang, M.; Wang, Y., Regioselective synthesis of 1,3,5-trisubstituted pyrazoles from n-alkylated tosylhydrazones and terminal alkynes, *Organic Letters,* **2014**, *16*, 576–579.

61. Tu, K. N.; Kim, S.; S. Blum, A., Copper-catalyzed aminoboration from hydrazones to generate borylated pyrazoles, *Organic Letters*, **2019**, *21*, 1283−1286.

62. Fan, X. -W.; Lei, T.; Zhou, C.; Meng, Q. -Y.; Chen, B.; Tung, C. -H.; Wu, L. -Z., Radical addition of hydrazones by α-bromo ketones to prepare 1,3,5-trisubstituted pyrazoles via visible light catalysis, *Journal of Organic Chemistry*, **2016**, *81*, 7127−7133.

63. Sha, Q.; Wei, Y., An efficient one-pot synthesis of 3,5-diaryl-4-bromopyrazoles by 1,3-dipolar cycloaddition of in situ generated diazo compounds and 1-bromoalk-1-ynes, Synthesis, **2013**, *45*, 413−420.

64. Hu, J.; Chen, S.; Sun, Y.; Yang, J.; Rao, Y., Synthesis of tri- and tetrasubstituted pyrazoles via Ru(II) catalysis: intramolecular aerobic oxidative C−N coupling, *Organic Letters*, **2012**, *14*, 5030−5033.

65. Ma, C.; Li, Y.; Wen, P.; Yan, R.; Ren, Z.; Huang, G., Copper(I)-catalyzed synthesis of pyrazoles from phenylhydrazones and dialkyl ethylenedicarboxylates in the presence of bases, Synlett, **2011**, 1321−1323.

66. Prieto, A.; Bouyssi, D.; Monteiro, N., Ruthenium-catalyzed tandem C–H fluoromethylation/cyclization of N-alkylhydrazones with CBr_3F: access to 4-fluoropyrazoles, *Journal of Organic Chemistry*, **2017**, *82*, 3311−3316.

67. Wang, Q.; He, L.; Li, K. K.; Tsui, G. C., Copper-mediated domino cyclization/trifluoromethylation/deprotection with $TMSCF_3$: synthesis of 4-(trifluoromethyl)pyrazoles, *Organic Letters*, **2017**, *19*, 658−661.

68. Markovića, V.; Joksović, M. D., “On water” synthesis of N-unsubstituted pyrazoles: semicarbazide hydrochloride as an alternative to hydrazine for preparation of pyrazole-3-carboxylate derivatives and 3,5-disubstituted pyrazoles, *Green Chemistry*, **2015**, *17*, 842−847.

69. Koley, S.; Panja, S. K.; Soni, S.; Singh, M. S., Catalyst-free one-pot access to pyrazoles and disulfide-tethered pyrazoles via deamidative heteroannulation of β-ketodithioesters with semicarbazide hydrochloride in water, *Advanced Synthesis and Catalysis*, **2018**, *360*, 1780−1785.

70. Hari, Y.; Tsuchida, S.; Sone, R.; Aoyama, T., An efficient synthesis of 2-diazo-2-(trimethylsilyl)ethanols and their application to pyrazole synthesis, *Synthesis*, **2007**, 3371−3375.

71. Babinski, D. J.; Aguilar, H. R.; Still, R.; Frantz, D. E., Synthesis of substituted pyrazoles via tandem cross-coupling/electrocyclization of enol triflates and diazoacetates, *Journal of Organic Chemistry*, **2011**, *76*, 5915−5923.

72. Aggarwal, V. K.; Vicente, J. d.; Bonnert, R. V., A novel one-pot method for the preparation of pyrazoles by 1,3-dipolar cycloadditions of diazo compounds generated in situ, *Journal of Organic Chemistry*, **2003***, 68*, 5381−5383.

73. Ueda, S.; Nagasawa, H., Facile synthesis of 1,2,4-triazoles via a copper-catalyzed tandem addition−oxidative cyclization, *Journal of the American Chemical Society*, **2009**, *131*, 15080−15081.

74. Zhang, C.; Jiao, N., Copper-catalyzed aerobic oxidative dehydrogenative coupling of anilines leading to aromatic azo compounds using dioxygen as an oxidant, *Angewandte Chemie International Edition*, **2010**, *49*, 6174−6177.

75. Guru, M. M.; Punniyamurthy, T., Copper(II)-catalyzed aerobic oxidative synthesis of substituted 1,2,3- and 1,2,4-triazoles from bisarylhydrazones via C–H functionalization/C–C/N–N/C–N bonds formation, *Journal of Organic Chemistry*, **2012**, *77*, 5063−5073.

76. Correa, A.; Tellitu, I.; Domínguez, E.; SanMartin, R., Novel alternative for the N−N bond formation through a PIFA-mediated oxidative cyclization and its application to the synthesis of indazol-3-ones, *Journal of Organic Chemistry*, **2006**, *71*, 3501−3505.

77. Hammerl, A.; Klapötke, T. M., Nitrogen: inorganic chemistry, *Encyclopedia of Inorganic and Bioinorganic Chemistry*, **2011**, 1–69.

78. Lewis, R. J. Sr., Sax's Dangerous Properties of Industrial Materials, *11th Edition. Wiley-Interscience, Wiley & Sons, Inc. Hoboken, NJ*. **2004**, 1973.

79. Grakauskas, V.; Baum, K., Direct fluorination of ureas, *Journal of the American Chemical Society*, **1970**, *92*, 2096–2100.

80. Neale, R. S.; Marcus, N. L., Chemistry of nitrogen radicals. IX. Reactions of N-halocyanamides and N-halosulfonamides, *Journal of Organic Chemistry*, **1969**, *34*, 1808–1816.

81. Kuznetsov, V. V.; Syroeshkina, J. S.; Moskvin, D. I.; Struchkova, Marina I.; Makhova, Nina N.; Zharov, Alexey A., High pressure-assisted synthesis of 1,2,3-trialkyldiaziridines from N-chloroalkylamines, *Journal of Heterocyclic Chemistry*, **2008**, *45*, 497–502.

82. Bergman, J., Formation of N–N bonds by thermolysis of 5-(2-dimethylaminoethyl)-5H-indolo[2,3-b]quinoxaline, *Tetrahedron Letters*, **1989**, *30*, 1837–1840.

83. Bolchi, C.; Pallavicini, M.; Binda, M.; Fumagalli, L.; Valoti, E., From carnitinamide to 5-aminomethyl-2-oxazolidinones, *Tetrahedron Asymmetry*, **2012**, *23*, 217–220.

84. Bachand, C.; Driguez, H.; Paton, J. M.; Touchard, D.; Lessard, J., *N*-monochlorination and N-monobromination of carbamates and carboxamides by sodium hypochlorite and hypobromite, *Journal of Organic Chemistry*, **1974**, *39*, 3136–3138.

85. Xie, W.; Yoon, J. H.; Chang, S., (NHC)Cu-Catalyzed mild C–H amidation of (hetero)arenes with deprotectable carbamates: scope and mechanistic studies, *Journal of the American Chemical Society*, **2016**, *138*, 12605–12614.

86. Hiegel, G. A.; Hogenauer, T. J.; Lewis, J. C., Preparation of N-chloroamides using trichloroisocyanuric acid, *Synthetic Communications*, **2005**, *35*, 2099–2105.

87. Mollo, M. C.; Gruber, N.; Diaz, J. E.; Bisceglia, J. A.; Orelli, L. R., An efficient synthesis of *N*-alkyl-*N*-arylputrescines and cadaverines, *Organic Preparations and Procedures International*, **2014**, *46*, 444–452.

88. Counceller, C. M.; Eichman, C. C.; Wray, B. C.; Stambuli, J. P., A practical, metal-free synthesis of 1*H*-indazoles, *Organic Letters*, **2008**, *10*, 1021–1023.

89. Wray, B. C.; Stambuli, J. P., Synthesis of N-arylindazoles and benzimidazoles from a common intermediate, *Organic Letters*, **2010**, *12*, 20 4576–4579.

90. Diccianni, J. B.; Hu, C.; Diao, T., N–N Bond forming reductive elimination via a mixed-valent Nickel(II)–Nickel(III) intermediate, *Angewandte Chemie International Edition*, **2016**, *55*, 7534–7538.

91. Ryan, M.; Martinelli, J. R.; Stahl, S. S., Cu-Catalyzed aerobic oxidative N–N coupling of carbazoles and diarylamines including selective cross-coupling, *Journal of the American Chemical Society*, **2018**, *140*, 9074–9077 and references cited therein.

92. Zheng, Q. –Z.; Feng, P.; Liang, Y. –F.; Jiao, N., Pd-Catalyzed tandem C–H azidation and N–N bond formation of arylpyridines: A direct approach to pyrido[1,2-b]indazoles, *Organic Letters*, **2013**, *15*, 4262–4265.

93. Perkin, W. H.; Tucker, S. H., The oxidation of carbazole, *Journal of the Chemical Society Transactions*, **1921**, *119*, 216–225.

94. Branch, G. E. K.; Smith, J. F., A bivalent nitrogen derivative of carbazole, *Journal of the American Chemical Society*, **1920**, *42*, 2405–2413.

95. McLintock, J.; Tucker, S. H., The dicarbazyls. Part 11. 9 : 9'-dicarbazyl and its halogen derivatives, *Journal of the Chemical Society*, **1927**, 1214–1221.

96. Correa, A.; Tellitu, I.; Domínguez, E.; SanMartin, R., Novel alternative for the N−N bond formation through a PIFA-mediated oxidative cyclization and its application to the synthesis of indazol-3-ones, *Journal of Organic Chemistry*, **2006**, *71*, 3501–3505.

97. Correa, A.; Tellitu, I.; Domínguez, E.; SanMartin, R., An advantageous synthesis of new indazolone and pyrazolone derivatives, *Tetrahedron*, **2006**, *62*, 11100−11105.

98. Dai, G.; Yang, L.; Zhou, W., Copper-catalyzed oxidative dehydrogenative N–N bond formation for the synthesis of N,N′-diarylindazol-3-ones, *Organic Chemistry Frontiers*, **2017,** *4*, 229−231.

99. Ueda, S.; Nagasawa, H., Facile synthesis of 1,2,4-triazoles via a copper-catalyzed tandem addition-oxidative cyclization, *Journal of the American Chemical Society*, **2009**, *131*, 15080–15081.

100. Neumann, J. J.; Suri, M.; Glorius, F., Efficient synthesis of pyrazoles: oxidative C–C/N–N bond-formation cascade, *Angewandte Chemie International Edition*, **2010**, *49*, 7790−7794.

101. Yu, D. –G.; Suri, M.; Glorius, F., Rh^{III}/Cu^{II}-cocatalyzed synthesis of 1*H*-indazoles through C–H amidation and N–N bond formation, *Journal of the American Chemical Society*, **2013**, *135*, 8802−8805.

102. Chen, C.; Tang, G.; He, F.; Wang, Z.; Jing, H.; Faessler, R., A synthesis of 1*H*-indazoles via a $Cu(OAc)_2$-catalyzed N−N bond formation, *Organic Letters*, **2016**, *18*, 1690−1693.

103. Chen, C.; He, F.; Tang, G.; Ding, H.; Wang, Z.; Li, D.; Deng, L.; Faessler, R., A copper-catalyzed tandem C–H *ortho*-hydroxylation and N–N bond-formation transformation: expedited synthesis of 1-(*ortho*-hydroxyaryl)-1*H*-indazoles, *European Journal of Organic Chemistry*, **2017**, 6604−6608.

104. Bryan, M. C.; Dillon, B.; Hamann, L. G.; Hughes, G. J.; Kopach, M. E.; Peterson, E. A.; Pourashraf, M.; Raheem, I.; Richardson, P.; Richter, D.; Sneddon, H. F., *Sustainable practices in medicinal chemistry: Current state and future directions*, *Journal of Medicinal Chemistry*, **2013**, *56*, 6007−6021.

105. Kuttruff, C. A.; Eastgate, M. D.; Baran, P. S., Natural product synthesis in the age of scalability, *Natural Product Reports*, **2014**, *31*, 419–432 and references cited therein.

106. Horn, E. J.; Rosen, B. R.; Baran, P. S., Synthetic organic electrochemistry: An enabling and innately sustainable method, *ACS Central Science*, **2016**, *2*, 302–308.

107. Cernak, T.; Dykstra, K. D.; Tyagarajan, S.; Vachal, P.; Krska, S. W., The medicinal chemist's toolbox for late stage functionalization of drug-like molecules, *Chemical Society Reviews*, **2016**, *45*, 546–576.

108. Li, C. -J.; Trost, B. M., Green chemistry for chemical synthesis, *Proceedings of the National Academy of Sciences USA,* **2008**, *105*, 13197–13202.

109. Anastas, P. T.; Warner, J. C., Green chemistry: Theory and practice, *Oxford University Press,* **1998**, 30–181.

110. Horváth, I. T., Anastas, P. T., Innovations and green chemistry, *Chemical Reviews*, **2007**, *107*, 2169–2173.

111. Kharissova, O. V.; Kharisov, B. I.; González, C. M. O.; Méndez, Y. P.; López, I., Greener synthesis of chemical compounds and materials, *Royal Society Open Science*, **2019**, *6*, 1–41.

112. Sheldon, R. A., Introduction to green chemistry, organic synthesis and pharmaceuticals, *Green Chemistry in the Pharmaceutical Industry*, **2010**, chapter 1, 1–20.

113. Sheldon, R. A., Green solvents for sustainable organic synthesis: state of the art, *Green Chemistry*, **2005**, *7*, 267–278.

114. Tang, S. Y.; Bourne, R. A.; Smith, R. L.; Poliakoff, M., The 24 principles of green engineering and green chemistry: "improvements productively", *Green Chemistry*, **2008**, *10*, 268–269.

115. Trost, B. M., The atom economy – A search for synthetic efficiency, *Science*, **1991**, *254*, 1471–1477.

116. Prier, C. K.; Rankic, D. A.; MacMillan, D. W. C., Visible light photoredox catalysis with transition metal complexes: Applications in organic synthesis, *Chemical Reviews*, **2013**, *113*, 5322–5363.

117. McAtee, R. C.; McClain, E. J.; Stephenson, C. R. J., Illuminating photoredox catalysis. *Trends in Chemistry*, **2019**, *1*, 111–125.

118. Ghosh, I.; Marzo, L.; Das, A.; Shaikh, R.; König, B., Visible light mediated photoredox catalytic arylation reactions. *Accounts of Chemical Research*, **2016**, *49*, 1566–1577.

119. Marzo, L.; Pagire, S. K.; Reiser, O.; König, B., Visible-light photocatalysis: does it make a difference in organic synthesis? *Angewandte Chemie International Edition*, **2018**, *57*, 10034–10072.

120. Devery, J. J.; Stephenson, C. R. J., Dual catalysis at the flick of a switch, *Nature*, **2015**, *519*, 42–43.

121. Moeller, K. D., Synthetic applications of anodic electrochemistry, *Tetrahedron* **2000**, *56*, 9527–9554.

122. Yoshida, J.; Kataoka, K.; Horcajada, R.; Nagaki, A., Modern strategies in electroorganic synthesis, *Chemical Reviews*, **2008**, *108*, 2265–2299.

123. Sperry, J. B.; Wright, D. L., The application of cathodic reductions and anodic oxidations in the synthesis of complex molecules, *Chemical Society Reviews*, **2006**, *35*, 605–621.

124. Yan, M.; Kawamata, Y.; Baran, P. S., Synthetic organic electrochemical methods since 2000: on the verge of a renaissance, *Chemical Reviews*, **2017**, *117*, 13230–13319 and references cited therein.

125. Wiebe, A.; Gieshoff, T.; Möhle, S.; Rodrigo, E.; Zirbes, M.; Waldvogel, S. R., Electrifying organic synthesis, *Angewandte Chemie International Edition*, **2018**, *57*, 5594–5619.

126. Moeller, K. D., Using physical organic chemistry to shape the course of electrochemical reactions, *Chemical Reviews*, **2018**, *118*, 4817–4833.

127. Tang, S.; Liu, Y.; Lei, A., Electrochemical oxidative cross-coupling with hydrogen evolution: a green and sustainable way for bond formation, *Chem*, **2018**, *4*, 27–45.

128. Romero, N. A.; Nicewicz, D. A., Organic photoredox catalysis, *Chemical Reviews*, **2016**, *116*, 10075–10166 and references cited therein.

129. Skubi, K. L.; Blum, T. R.; Yoon, T. P., Dual catalysis strategies in photochemical synthesis, *Chemical Reviews*, **2016**, *116*, 10035–10074 and references cited therein.

130. Schultz, D. M.; Yoon, T. P., Solar synthesis: Prospects in visible light photocatalysis, *Science*, **2014**, *343*, 1239176 1–8 and references cited therein.

131. Blankenship, R. E.; Tiede, D. M.; Barber, J.; Brudvig, G. W.; Fleming, G.; Ghirardi, M.; Gunner, M. R.; Junge, W.; Kramer, D. M.; Melis, A.; Moore, T. A.; Moser, C. C.; Nocera, D. G.; Nozik, A. J.; Ort, D. R.; Parson, W. W.; Prince, R. C.; Sayre, R. T., Comparing photosynthetic and photovoltaic efficiencies and recognizing the potential for improvement, *Science*, **2011**, *332*, 805–809.

132. Francke, R.; Little, R. D., Redox catalysis in organic electrosynthesis: basic principles and recent developments, *Chemical Society Reviews*, **2014**, *43*, 2492–2521.

133. Fuchigami, T.; Tajima, T., Development of new methodologies toward green sustainable organic electrode processes, *ChemInform*, **2006**, *38*, 585–589.

134. Schotten, C.; Nicholls, T. P.; Bourne, R. A.; Kapur, N.; Nguyen, B. N.; Willans, C. E., Making electrochemistry easily accessible to the synthetic chemist, *Green Chemistry*, **2020**, *22*, 3358–3375.

135. Frontana-Uribe, B. A.; Little, R. D.; Ibanez, J. G.; Palma, A.; Vasquez-Medrano, R., Organic electrosynthesis: A promising green methodology in organic chemistry, *Green Chemistry*, **2010**,*12*, 2099–2119.

136. Kingston, C.; Palkowitz, M. D.; Takahira, Y.; Vantourout, J. C.; Peters, B. K.; Kawamata, Y.; Baran, P. S., A survival guide for the “electro-curious”, *Accounts of Chemical Research*, **2020**, *53*, 72–83.

137. Fuchigami, T.; Inagi, S.; Atobe, M., Fundamental principles of organic electrochemistry: Fundamental aspects of electrochemistry dealing with organic molecules, *Wiley Online Books*, **2014**, *Chapter 1*, 1–10.

138. Möhle, S.; Zirbes, M.; Rodrigo, E.; Gieshoff, T.; Wiebe, A.; Waldvogel, S. R., Modern electrochemical aspects for the synthesis of value-added organic products, *Angewandte Chemie International Edition*, ***2018***, *57*, 6018–6041.

139. Volta, A., On the electricity excited by the mere contact of conducting substances of different kinds, *Philosophical Transactions of the Royal Society of London*, **1800**, *90*, 403–431.

140. Lund, H., A century of organic electrochemistry, *Journal of the Electrochemical Society*, **2002**, *149*, S21–S33 and references cited therein.

141. Faraday, M., On new compounds of carbon and hydrogen, and on certain other products obtained during the decomposition of oil by heat, *Philosophical Transactions of the Royal Society London*, **1825**, *115*, 440–466.

142. Faraday, M., Siebente reihe von experimental-untersuchungen u¨ ber elektricita¨t. *Annals of Physics*, **1834**, *109*, 433–451.

143. https://en.wikipedia.org/wiki/Faraday%27s_laws_of_electrolysis (accessed November 16, 2020).

144. Kolbe, H., Beobachtungen über die oxydirende Wirkung des Sauerstoffs, wenn derselbe mit Hülfe einer elektrischen Säule entwickelt wird, *Journal für Praktische Chemie*, **1847**, *41*, 137–139.

145. Kolbe, H., Untersuchungen über die elektrolyse organischer Verbindungen, *Justus Liebigs Annalen der Chemie*, **1849**, *69*, 257–294.

146. Heyrovský, J., Elektrolysa se rtuťovou kapkovou kathodou, Chemické Listy, **1922**, *16*, 256–264.

147. Shikata, M., The electrolysis of nitrobenzene with the mercury dropping cathode, *Transactions of the Faraday Society*, **1925**, *21*, 42–61.

148. Heyrovský, J.; Shikata, M., Researches with the dropping mercury cathode: Part II. The Polarograph, *Recueil des Travaux Chimiques des Pays-Bas*, **1925**, *44*, 496–498.

149. Heyrovský, J.; Smoler, I., Polarographic studies with the dropping mercury kathode. Part XXX. The electro-reduction and estimation of fructose and sorbose, Collection of Czechoslovak Chemical Communications, **1932**, *4*, 521–530.

150. Kolthoff, I. M.; Miller, C. S., Mixed potentials at the dropping mercury electrode, *Journal of the American Chemical Society*, **1940**, *62*, 2171–2174.

151. Simons, J. H., Production of fluorocarbons: the generalized procedure and its use with nitrogen compounds, *Journal of The Electrochemical Society*, **1949**, *95*, 47.

152. Baizer, M. M., Electrolytic reductive coupling, *Journal of the Electrochemical Society*, **1964**, *111*, 215.

153. Shono, T., Electroorganic chemistry in organic synthesis. *Tetrahedron*, **1984**, *40*, 811–850.

154. Birch, A. J., Electrolytic Reduction in Liquid Ammonia, *Nature*, **1946**, *158*, 60.

155. Lam, K.; Markó, I. E., Chemoselective chemical and electrochemical deprotections of aromatic rsters, *Organic Letters*, **2009**, *11*, 2752–2755.

156. Edinger, C.; Waldvogel, S. R., Electrochemical deoxygenation of aromatic amides and sulfoxides, European Journal of Organic Chemistry, **2014**, 5144–5148.

157. Peters, B. K.; Rodriguez, K. X.; Reisberg, S. H.; Beil, S. B.; Hickey, D. P.; Kawamata, Y.; Collins, M.; Starr, J.; Chen, L.; Udyavara, S.; Klunder, K.; Gorey, T. J.; Anderson, S. L.; Neurock, M.; Minteer, S. D.; Baran, P. S., Scalable and safe synthetic organic electroreduction inspired by Li-ion battery chemistry, *Science*, **2019**, *363*, 838–845.

158. Manabe, S.; Wong, C. M.: Sevov, C. S., Direct and scalable electroreduction of triphenylphosphine oxide to triphenylphosphine, *Journal of the American Chemical Society*, **2020**, *142*, 3024–3031.

159. Fischer, E., Ueber die hydrazinverbindungen der fettreihe, *Berichte der deutschen chemischen Gesellschaft*, **1875**, *8*, 1587–1590.

160. Yachuang, W.; Xiudong, D.; Ding, L.; Zhang, Y.; Cui, L.; Sun, L.; Li, W.; Wang, D.; Zhao, Y., Synthesis and antibacterial activity evaluation of novel biaryloxazolidinone analogues containing a hydrazone moiety as promising antibacterial agents, *European Journal of Medicinal Chemistry*, **2018**, *158* , 247–258.

161. Auelbekov, S. A.; Mirzaabdullaev, A. B.; Aslanova, D. K.; Kurchakov, S.; Achilova, G. S., Synthesis and antiviral activity of gossypol derivatives, *Pharmaceutical Chemistry Journal*, **1985**, *19*, 479–481.

162. Yang, W.; Lu, X.; Zhou, T.; Cao, Y.; Zhang, Y.; Ma, M., Selective reduction of N-nitroso aza-aliphatic cyclic compounds to the corresponding N-amino products using zinc dust in CO_2–H_2O medium, *Chemistry of Heterocyclic Compounds*, **2018**, *54*, 780–783.

163. Liu, S.; Liu, Y.; Wang, H.; Ding, Y.; Wu, H.; Dong, J.; Wong, A.; Chen, S. –H.; Li, G.; Chan, M.; Sawyer, N.; Gervais, F. G.; Henault, M.; Kargman, S.; Bedard, L. L.; Han, Y.; Friesen, R.; Lobell, R. B.; Stout, D. M., Design, synthesis, and evaluation of novel 3-amino-4-hydrazine-cyclobut-3-ene-1,2-diones as potent and selective $CXCR_2$ chemokine receptor antagonists, *Bioorganic and Medicinal Chemistry Letters*, **2009**, *19*, 5741–5745.

164. Goel, O. P.; Dembinski, R., Synthesis of dimebon and of its tetrathiomolybdate, *Organic Preparations and Procedures International*, **2015**, *47*, 220–226.

165. Hartman, R., Working with hazardous chemicals, *Organic Syntheses*, **1933**, *13*, 66.

166. Chaudhary, P.; Gupta, S.; Muniyappan, N.; Sabiah, S.; Kandasamy, J., An efficient synthesis of N-nitrosamines under solvent, metal and acid free conditions using tert-butyl nitrite, *Green Chemistry*, **2016**, *18*, 2323–2330.

167. Valenta, V.; Holubek, J.; Svatek, E.; Protiva, M., Synthesis of 4-methoxyphenoxyacetic and 3,4,5-trimethoxyphenoxyacetic acid amides and hydrazides as potential neurotropic and cardiovascular agents, *Collection of Czechoslovak Chemical Communications*, **1987**, *52*, 3013–3023.

168. Hinsberg, W. D.; Schultz, P. G.; Dervan, P. B., Direct studies of 1,1-diazenes syntheses, infrared and electronic spectra, and kinetics of the thermal decomposition of N-(2,2,6,6-tetramethylpiperidyl)nitrene and N-(2,2,5,5-tetramethylpyrrolidyl)nitrene, *Journal of the American Chemical Society*, **1982**, *104*, 766–773.

169. Lucarini, M.; Pedulli, G. F.; Lazzari, D., EPR properties of two new cyclic phosphinylhydrazyl radicals and of their inclusion complexes with cyclodextrins, *Journal of Organic Chemistry*, **2000**, *65*, 2723–2727.

170. Wijngaarden, I. V.; Hamminga, D.; Hes, R. V.; Standaar, P. J.; Tipker, J.; Tulp, M. T. M.; Mol, F.; Olivier, B.; Jonge, A., Development of high-affinity 5-HT3 receptor antagonists. Structure- affinity relationships of novel 1,7-annelated indole derivatives, *Journal of Medicinal Chemistry*, **1993**, *36*, 3693–3699.

171. Li, P.; Zhang, Q.; Robichaud, A. J.; Lee, T.; Tomesch, J.; Yao, W.; Beard, J. D.; Snyder, G. L.; Zhu, H.; Peng, Y.; Hendrick, J. P.; Vanover, K. E.; Davis, R. E.; Mates, S.; Wennogle, L. P., Discovery of a tetracyclic quinoxaline derivative as a potent and orally active

multifunctional drug candidate for the treatment of neuropsychiatric and neurological disorders, *Journal of Medicinal Chemistry*, **2014**, *57*, 2670–2682.

172. Dervan, P. B.; Squillacote, M. E.; Lahti, P. M.; Sylwester, A. P.; Roberts, J. D., Nitrogen-15 NMR spectrum of a 1,1-diazene. N-(2,2,6,6-tetramethylpiperidyl)nitrene, *Journal of the American Chemical Society*, **1981**, *103*, 1120–1122.

173. Kiyoi, T.; York, M.; Francis, S.; Edwards, D.; Walker, G.; Houghton, A. K.; Cottney, J. E.; Baker, J.; Adam, J. M., Design, synthesis, and structure–activity relationship study of conformationally constrained analogs of indole-3-carboxamides as novel CB1 cannabinoid receptor agonists, *Bioorganic and Medicinal Chemistry Letters*, **2010**, *20*, 4918–4921.

174. Dhainaut, A.; Regnier, G.; Atassi, G.; Pierre, A.; Leonce, S.; Kraus-Berthier,L.; Prost, J. F., New triazine derivatives as potent modulators of multidrug resistance, *Journal of Medicinal Chemistry*, **1992**, *35*, 2481–2496.

175. Charrier, J. –D.; Deniaud, D.; Reliqueta, A.; Meslin, J. –C., 1,2-Bis[(2-dimethylamino-2-thioxo-1-phenylethylidene)hydrazino]ethane: a new tetradentate ligand for Ni^{2+}, *Journal of the Chemical Society. Perkin Transactions 1*, **2001**, 1212–1215.

176. Charrier, J. –D.; Reliquet, A.; Meslin, J. –C., Synthesis of a new type of N_2S_2 tetradentate ligand, *Tetrahedron Letters*, **1998**, *39*, 8645–8646.

177. Cecchetti, V.; Calderone, V.; Tabarrini, O.; Sabatini, S.; Filipponi, E.; Testai, L.; Spogli, R.; Martinotti, E.; Fravolini, A., Highly potent 1,4-benzothiazine derivatives as K_{ATP}-channel openers, *Journal of Medicinal Chemistry*, **2003**, *46*, 3670–3679.

178. Denmark, S. E.; Chang, W. –T. T.; Houk, K. N.; Liu, P., Development of chiral bis-hydrazone ligands for the enantioselective cross-coupling reactions of aryldimethylsilanolates, *Journal of Organic Chemistry*, **2015**, *80*, 313–366.

179. Ganesh, V.; Noble, A.; Aggarwal, V. K., Chiral aniline synthesis via stereospecific C(sp^3)–C(sp^2) coupling of boronic esters with aryl hydrazines, *Organic Letters*, **2018**, *20*, 6144–6147.

180. Carpino, L. A.; Santilli, A. A.; Murray, R. W., Oxidative reactions of hydrazines. V. synthesis of monobenzyl 1,1-disubstituted hydrazines and 2-amino-2,3-dihydro-1*H*-benz[de]isoquinoline, *Journal of the American Chemical Society*, **1960**, *82*, 2728–2731.

181. Yakhontov, L. N.; Kutina, N. N.; Shishkin, G. V.; Zhikhareva, G. P.; Vysochin, V. I.; Vorob'eva, V. Y.; Kaminka, M. É.; Shevchenko, I. L.; Mashkovskii,, M. D., Synthesis of a 4-aza analog of phencarol and its pharmacological investigation, *Pharmaceutical Chemistry Journal*, **1989**, *23*, 24–30.

182. Garcia, J.; Vilarrasa, J., From aliphatic amines and amides to azides and/or how to convert RNHCOR′ into RNHCOR″ avoiding drastic hydrolyses, *Tetrahedron Letters*, **1987**, *28*, 341–342.

183. Wells, J. E.; Babcock, D. E.; France, W. G., The nature of electrode reactions. I. factors affecting the electrochemical reduction of *N*-nitrosomethylaniline, *Journal of the American Chemical Society*, **1936**, *58*, 2630–2632.

184. Cook, E. W.; France, W. G., The electrolytic preparation of the isoindolines, *Journal of Physical Chemistry*, **1932**, *36*, 2383–2389.

185. Dorn, H.; Arndt, D.; Wall, H., On the electrochemical and catalytic reduction of N-nitroso-1-methylamino-1-deoxy-sugar alcohols and their O-acetyl derivatives, *Journal for Practical Chemistry*, **1970**, *312*, 519–532.

186. Iversen, P. E., Organic electrosyntheses III. Reduction of N-nitrosamines, *Acta Chemica Scandinavica*, **1971**, *25*, 2337–2340.

187. Muhammad, W.; Ullah, N.; Haroona, M.; Abbasi, B. H., Optical, morphological and biological analysis of zinc oxide nanoparticles (ZnO NPs) using Papaver somniferum L., *RSC Advances*, **2019**, *9*, 29541–29548.

188. Qasim, I.; Mumtaz, M.; Nadeem, K.; Abbas, Q. S., Zinc nanoparticles at intercrystallite sites of $(Cu_{0.5}Tl_{0.5})Ba_2Ca_3Cu_4O_{12-\delta}$ superconductor, *Journal of Nanomaterials*, **2016**, *2016*, 1–6.

189. Jalil, A.; Clymer, R. N.; Hamilton, C. R.; Vaddypally, S.; Gau, M. R.; Zdilla, M. J., Structure of salts of lithium chloride and lithium hexafluorophosphate as solvates with pyridine and vinylpyridine and structural comparisons: $(C_5H_5N)LiPF_6$, $[p\text{-}(CH_2{=}CH)C_5H_4N]LiPF_6$, $[(C_5H_5N)LiCl]n$, and $[p\text{-}(CH_2{=}CH)C_5H_4N]_2Li(\mu\text{-}Cl)_2Li[p\text{-}(CH_2{=}CH)C_5H_4N]_2$, *Acta Crystallographica Section C*, **2017**, *73*, 264–269.

190. Noël, T.; Cao, Y.; Laudadio, G. The fundamentals behind the use of flow reactors in electrochemistry. *Accounts of Chemical Research*, **2019**, *52*, 2858–2869.

191. Pletcher, D.; Green, R. A.; Brown, R. C. D. Flow electrolysis cells for the synthetic organic chemistry laboratory, *Chemical Reviews*, **2018**, *118*, 4573–4591.

192. Breising, V. M.; Kayser, J. M.; Kehl, A.; Schollmeyer, D.; Liermann, J. C.; Waldvogel, S. R., Electrochemical formation of N,N′-diarylhydrazines by dehydrogenative N–N homocoupling reaction, Chemical Communication, **2020**, *56*, 4348–4351.

193. Lv, S.; Han, X.; Wang, J. -Y.; Zhou, M.; Wu, Y.; Ma, L.; Niu, L.; Gao, W.; Zhou, J.; Hu, W.; Cui, Y.; Chen, J., Tunable electrochemical C–N versus N–N bond formation of nitrogen-centered radicals enabled by dehydrogenative dearomatization: Biological applications, *Angewandte Chemie International Edition*, **2020**, *59*, 11583–11590.

194. Rosen, B. R.; Werner, E. W.; O'Brien, A. G.; Baran, P. S., Total synthesis of Dixiamycin B by electrochemical oxidation, *Journal of the American Chemical Society*, **2014**, *136*, 5571–5574.

195. Li, Y.; Ye, Z.; Chen, N.; Chen, Z.; Zhang, F., Intramolecular electrochemical dehydrogenative N–N bond formation for the synthesis of 1,2,4-triazolo[1,5-a]pyridines, Green Chemistry, **2019**, *21*, 4035–4039.

196. Gieshoff, T.; Schollmeyer, D.; Waldvogel, S. R., Access to pyrazolidin-3,5-diones through anodic N–N bond formation, *Angewandte Chemie International Edition*, **2016**, *55*, 9437–9440.

197. Bosica, G.; Abdilla, R., Aza-Michael mono-addition using acidic alumina under solventless conditions, *Molecules*, **2016**, *21*, 815–825.

198. Bosica, G.; Spiteri, J.; Borg, C., Aza-Michael reaction: selective mono- versus bis-addition under environmentally-friendly conditions, *Tetrahedron*, **2014**, *70*, 2449–2454.

199. Liu, Q.; Shi, W. –K.; Ren, S. –Z..; Ni, W. –W.; Li, W. –Y.; Chen, H. –M.; Liu, P.; Yuan, J.; He, X. –S.; Liu, J. –J.; Cao, P.; Yang, P. –Z.; Xiao, Z. –P.; Zhu, H. –L., Arylamino containing hydroxamic acids as potent urease inhibitors for the treatment of Helicobacter pylori infection, *European Journal of Medicinal Chemistry*, **2018**, *156*, 126–136.

200. Doebelin, C.; Schmitt, M.; Antheaume, C.; Bourguignon, J. –J.; Bihel, F., Nucleophilic substitution of azide acting as a pseudo leaving group: One-step synthesis of various aza heterocycles, *Journal of Organic Chemistry*, **2013**, *78*, 11335–11341.

201. Phillips, D. P.; Zhu, X. –F.; Lau, T. L.; He, X.; Yang, K.; Liu, H., Copper-catalyzed C–N coupling of amides and nitrogen–containing heterocycles in the presence of cesium fluoride, *Tetrahedron Letters*, **2009**, *50*, 7293–7296.

202. Orelli, L. R.; Blanco, M. M.; García, M. B.; Hedrera, M. E.; Perillo, I. A., A new synthetic approach to *N*,*N*′- disubstituted 1,*N*-alkanediamines, *Synthetic Communications*, **2001**, *31*, 685–695.

203. Jöst, C.; Nitsche, C.; Scholz, T.; Roux, L.; Klein, C. D., Promiscuity and selectivity in covalent enzyme inhibition: a systematic study of electrophilic fragments, *Journal of Medicinal Chemistry*, **2014**, *57*, 7590−7599.

204. Kuhnert, M.; Köster, H.; Bartholomäus, R.; Park, A. Y.; Shahim, A.; Heine, A.; Steuber, H.; Klebe, G.; Diederich, W. E., Tracing binding modes in hit-to-lead optimization: chameleon-like poses of aspartic protease inhibitors, *Angewandte Chemie International Edition*, **2015**, *54*, 2849−2853.

205. Ai, X.; Wang, X.; Liu, J.; Ge, Z.; Cheng, T.; Li, R., An effective aza-Michael addition of aromatic amines to electron-deficient alkenes in alkaline Al_2O_3, *Tetrahedron*, **2010**, *66*, 5373−5377.

206. Inami, H.; Shishikura, J.; Yasunaga, T.; Hirano, M.; Kimura, T.; Yamashita, H.; Ohno, K.; Sakamoto, S., Synthesis and pharmacological evaluation of 3-[(4-oxo-4*H*-pyrido[3,2-e][1,3]thiazin-2-yl)(phenyl)amino]propanenitrile derivatives as orally active AMPA receptor antagonists, *Chemical and Pharmaceutical Bulletin*, **2019**, *67*, 699−706.

207. Ichitsuka, T.; Kobayashi, S.; Koumura, N.; Sato, K.; Takahashi, I., Continuous synthesis of aryl amines from phenols utilizing integrated packed-bed flow systems, *Angewandte Chemie International Edition*, **2020**, *59*, 15891−15896.

208. Kim, S.; Kang, S.; Kim, G.; Lee, Y., Copper-catalyzed aza-Michael addition of aromatic amines or aromatic aza-heterocycles to α,β-unsaturated olefins, *Journal of Organic Chemistry*, **2016**, *81*, 4048−4057.

209. Mollo, M. C.; Gruber, N.; Diaz, J. E.; Bisceglia, J. A.; Orelli, L. R., An efficient synthesis of *N*-alkyl-*N*-arylputrescines and cadaverines, *Organic Preparations and Procedures International*, **2014**, *46*, 444−452.

210. Yang, L.; Zhang, J. –Y.; Duan, X. –H.; Gao, P.; Jiao, J.; Guo, L. –N., *Journal of Organic Chemistry*, **2019**, *84*, 8615−8629.

211. Yadav, V. K.; Babu, K. G., A remarkably efficient markovnikov hydrochlorination of olefins and transformation of nitriles into imidates by use of AcCl and an alcohol, *European Journal of Organic Chemistry*, **2005**, *2005*, 452–456.

212. Tang, X. –J.; Yan, Z. –L.; Chen, W. –L.; Gao, Y. –R.; Mao, S.; Zhang, Y. –L.; Wang, Y. –Q., Aza-Michael reaction promoted by aqueous sodium carbonate solution, *Tetrahedron Letters*, **2013**, *54*, 2669–2673.

213. Abedini-Torghabeh, J.; Eshghi, H.; Bakavoli, M.; Rahimizadeh, M., PPh_3-catalyzed Mannich reaction: a facile one-pot synthesis of β-amino carbonyl compounds under solvent-free conditions at room temperature, *Research on Chemical Intermediates*, **2015**, *41*, 3649–3658.

214. Lad, U. P.; Kulkarni, M. A.; Desai, U. V.; Wadgaonkar, P. P., Lithium tetrafluoroborate catalyzed highly efficient inter- and intramolecular aza-Michael addition with aromatic amines, *Comptes Rendus Chimie*, **2011**, *14*, 1059–1064.

215. Wang, C.; Huang, Y., Traceless directing strategy: efficient synthesis of N-alkyl indoles *via* redox-neutral C–H activation, *Organic Letters*, **2013**, *15*, 5294–5297.

216. Chaudhary, P.; Gupta, S.; Muniyappan, N.; Sabiah, S.; Kandasamy J., Regioselective nitration of N-alkyl anilines using tert-butyl nitrite under mild condition, *Journal of Organic Chemistry*, **2019**, *84*, 104–119.

217. Liu, J.; Yang, S.; Dong, R.; Jin, Z.; Wang, M., A convenient one-pot synthesis of 1-aryl-substituted 4-iodopyrazol-3-ols via aromatisation and oxidative iodination reactions, *Journal of Chemical Research*, **2018**, *42*, 24–27.

218. Arbačiauskiene, E.; Tolaityte, S. K.; Mitrulevičiene, A.; Bieliauskas, A.; Martynaitis, V.; Bechmann, M.; Roller, A.; Ačkus, A.; Holzer, W., On the tautomerism of *N*-substituted pyrazolones: 1,2-dihydro-3*H*-pyrazol-3-ones versus 1*H*-pyrazol-3-ols, *Molecules*, **2018**, *23*, 129–143.

219. Doebelin, C.; Schmitt, M.; Antheaume, C.; Bourguignon, J. –J.; Bihel, F., Nucleophilic substitution of azide acting as a pseudo leaving group: One-step synthesis of various aza heterocycles, *Journal of Organic Chemistry*, **2013**, *78*, 11335−11341.

220. Sibi, M. P.; Stanley, L. M.; Nie, X.; Venkatraman, L.; Liu, M.; Jasperse, C. P., The role of achiral pyrazolidinone templates in enantioselective Diels-Alder reactions: Scope, limitations, and conformational insights, *Journal of the American Chemical Society*, **2007**, *129*, 395−405.

221. Alex, K.; Tillack, A.; Schwarz, N.; Beller, M., Zinc-catalyzed synthesis of pyrazolines and pyrazoles *via* hydrohydrazination, *Organic Letters*, **2008**, *10*, 2377−2379.

222. Teo, Y. –C. Yong, F. –F.; Poh, C. –Y.; Yana, Y. –K.; Chua, G. –L., Manganese-catalyzed cross-coupling reactions of nitrogen nucleophiles with aryl halides in water, *Chemical communications*, **2009**, 6258−6260.

223. Wang, X.; Pan, Y.; Huang, X.; Maoa, Z.; Wang, H., A novel methodology for synthesis of dihydropyrazole derivatives as potential anticancer agents, *Organic and Biomolecular Chemistry*, **2014**, *12*, 2028−2032.

224. Chaudhary, P.; Gupta, S.; Muniyappan, N.; Sabiah, S.; Kandasamy, J., An efficient synthesis of N-nitrosamines under solvent, metal and acid free conditions using tert-butyl nitrite, *Green Chemistry*, **2016**,*18*, 2323−2330.

Appendix A

Crystallographic Information for 3-[nitroso(phenyl)amino]-1-phenylpropan-1-one. University of Alberta Department of Chemistry Structure Determination Laboratory Report #JMS2002.

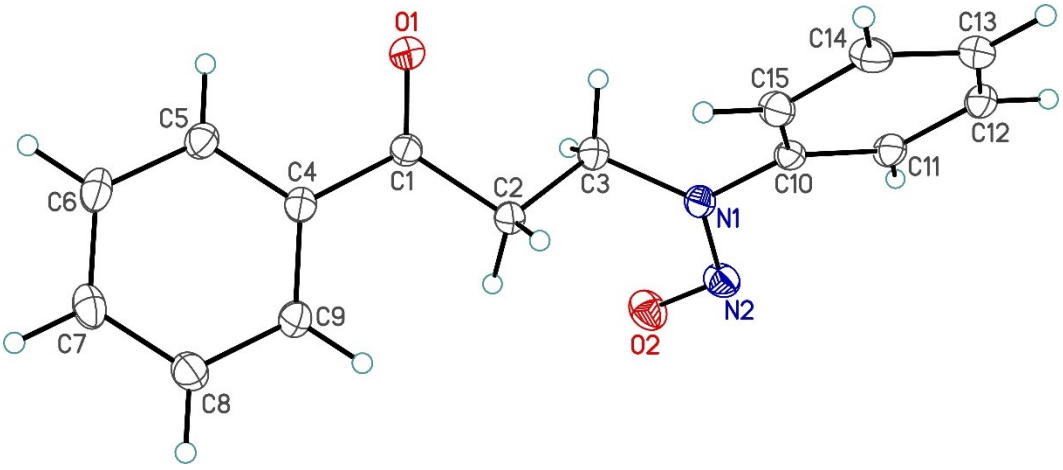

Perspective view of the 3-[nitroso(phenyl)amino]-1-phenylpropan-1-one molecule showing the atom labelling scheme. Non-hydrogen atoms are represented by Gaussian ellipsoids at the 30% probability level. Hydrogen atoms are shown with arbitrarily small thermal parameters.

Crystallographic Experimental Details

A. Crystal Data

formula	$C_{15}H_{14}N_2O_2$
formula weight	254.28
crystal dimensions (mm)	0.34 × 0.20 × 0.12
crystal system	orthorhombic
space group	*Pbca* (No. 61)
unit cell parameters[a]	
a (Å)	7.7758(2)
b (Å)	15.7484(3)

c (Å)	20.3869(4)
V (Å^3)	2496.51(9)
Z	8
ρ_{calcd} (g cm^{-3})	1.353
μ (mm^{-1})	0.741

B. Data Collection and Refinement Conditions

diffractometer	Bruker D8/APEX II CCD[b]
radiation (λ [Å])	Cu Kα (1.54178) (microfocus source)
temperature (°C)	–100
scan type	ω and ϕ scans (1.0°) (5 s exposures)
data collection 2θ limit (deg)	145.21
total data collected	88374 (-9 ≤ h ≤ 9, -19 ≤ k ≤ 19, -25 ≤ l ≤ 25)
independent reflections	2472 (R_{int} = 0.0309)
number of observed reflections (*NO*)	2405 [$F_o^2 \geq 2\sigma(F_o^2)$]
structure solution method	intrinsic phasing (*SHELXT-2014*[c])
refinement method	full-matrix least-squares on F^2 (*SHELXL–2018*[d])
absorption correction method	Gaussian integration (face-indexed)
range of transmission factors	0.9806–0.8344
data/restraints/parameters	2472 / 0 / 172
goodness-of-fit (S)[e] [all data]	1.060
final R indices[f]	
R_1 [$F_o^2 \geq 2\sigma(F_o^2)$]	0.0340

wR_2 [all data]	0.0883
largest difference peak and hole	0.198 and –0.177 e Å^{-3}

[a]Obtained from least-squares refinement of 9817 reflections with $12.04° < 2\theta < 144.74°$.

[b]Programs for diffractometer operation, data collection, data reduction and absorption correction were those supplied by Bruker.

[c]Sheldrick, G. M. *Acta Crystallogr.* **2015**, *A71*, 3–8. (*SHELXT-2014*)

[d]Sheldrick, G. M. *Acta Crystallogr.* **2015**, *C71*, 3–8. (*SHELXL-2018/3*)

[e]$S = [\Sigma w(F_o^2 - F_c^2)^2/(n - p)]^{1/2}$ (n = number of data; p = number of parameters varied; $w = [\sigma^2(F_o^2) + (0.0428P)^2 + 0.7594P]^{-1}$ where $P = [\mathrm{Max}(F_o^2, 0) + 2F_c^2]/3$).

[f]$R_1 = \Sigma||F_o| - |F_c||/\Sigma|F_o|$; $wR_2 = [\Sigma w(F_o^2 - F_c^2)^2/\Sigma w(F_o^4)]^{1/2}$.

Table 2. Atomic Coordinates and Equivalent Isotropic Displacement Parameters

Atom	x	y	z	U_{eq}, Å^2
O1	0.16107(12)	0.09531(5)	0.45366(4)	0.0414(2)*
O2	0.23264(13)	0.13981(5)	0.21418(4)	0.0445(2)*
N1	0.31788(12)	0.22680(5)	0.28916(4)	0.0295(2)*
N2	0.30995(14)	0.20680(6)	0.22594(4)	0.0356(2)*
C1	0.26690(14)	0.05699(6)	0.42109(5)	0.0274(2)*
C2	0.33785(13)	0.09586(6)	0.35859(5)	0.0279(2)*
C3	0.23549(15)	0.17479(7)	0.34009(5)	0.0316(2)*
C4	0.32718(13)	-0.02908(6)	0.44177(5)	0.0265(2)*
C5	0.25375(15)	-0.06572(7)	0.49749(5)	0.0316(2)*
C6	0.30177(16)	-0.14654(7)	0.51706(5)	0.0363(3)*
C7	0.42248(16)	-0.19171(7)	0.48119(6)	0.0363(3)*
C8	0.49663(16)	-0.15569(7)	0.42618(6)	0.0364(3)*
C9	0.44981(15)	-0.07446(7)	0.40656(5)	0.0317(2)*
C10	0.39704(14)	0.30618(6)	0.30481(5)	0.0270(2)*
C11	0.37808(15)	0.37549(7)	0.26302(5)	0.0311(2)*
C12	0.45288(16)	0.45231(7)	0.27987(5)	0.0352(3)*

C13	0.54448(15)	0.46100(7)	0.33769(6)	0.0358(3)*
C14	0.56097(16)	0.39195(7)	0.37943(5)	0.0362(3)*
C15	0.48848(15)	0.31443(7)	0.36284(5)	0.0329(3)*

Anisotropically-refined atoms are marked with an asterisk (*). The form of the anisotropic displacement parameter is: $\exp[-2\pi^2(h^2a^{*2}U_{11} + k^2b^{*2}U_{22} + l^2c^{*2}U_{33} + 2klb^*c^*U_{23} + 2hla^*c^*U_{13} + 2hka^*b^*U_{12})]$.

Table 3. Selected Interatomic Distances (Å)

Atom1	Atom2	Distance	Atom1	Atom2	Distance
O1	C1	1.2174(13)	C5	C6	1.3851(16)
O2	N2	1.2377(13)	C6	C7	1.3863(18)
N1	N2	1.3281(12)	C7	C8	1.3828(17)
N1	C3	1.4694(13)	C8	C9	1.3888(15)
N1	C10	1.4296(14)	C10	C11	1.3925(14)
C1	C2	1.5175(14)	C10	C15	1.3863(15)
C1	C4	1.4950(14)	C11	C12	1.3857(16)
C2	C3	1.5235(14)	C12	C13	1.3841(17)
C4	C5	1.3962(14)	C13	C14	1.3868(16)
C4	C9	1.3911(15)	C14	C15	1.3865(16)

Table 4. Selected Interatomic Angles (deg)

Atom1	Atom2	Atom3	Angle	Atom1	Atom2	Atom3	Angle
N2	N1	C3	122.22(9)	C5	C6	C7	120.14(10)
N2	N1	C10	116.36(9)	C6	C7	C8	119.98(10)
C3	N1	C10	121.16(8)	C7	C8	C9	120.14(11)
O2	N2	N1	114.38(10)	C4	C9	C8	120.29(10)
O1	C1	C2	120.25(9)	N1	C10	C11	120.22(9)
O1	C1	C4	120.50(9)	N1	C10	C15	119.55(9)
C2	C1	C4	119.25(9)	C11	C10	C15	120.20(10)
C1	C2	C3	110.31(8)	C10	C11	C12	119.23(10)
N1	C3	C2	113.70(9)	C11	C12	C13	120.90(10)
C1	C4	C5	118.42(9)	C12	C13	C14	119.51(11)
C1	C4	C9	122.36(9)	C13	C14	C15	120.21(11)
C5	C4	C9	119.20(10)	C10	C15	C14	119.95(10)
C4	C5	C6	120.26(11)				

Table 5. Torsional Angles (deg)

Atom1	Atom2	Atom3	Atom4	Angle	Atom1	Atom2	Atom3	Atom4	Angle
C3	N1	N2	O2	-2.20(15)	C9	C4	C5	C6	-0.48(16)
C10	N1	N2	O2	-176.41(9)	C1	C4	C9	C8	-177.34(10)
N2	N1	C3	C2	79.34(13)	C5	C4	C9	C8	0.90(16)
C10	N1	C3	C2	-106.72(11)	C4	C5	C6	C7	-0.34(17)
N2	N1	C10	C11	34.74(14)	C5	C6	C7	C8	0.74(17)
N2	N1	C10	C15	-147.19(10)	C6	C7	C8	C9	-0.32(18)
C3	N1	C10	C11	-139.54(10)	C7	C8	C9	C4	-0.50(17)
C3	N1	C10	C15	38.52(14)	N1	C10	C11	C12	178.63(9)
O1	C1	C2	C3	-10.17(14)	C15	C10	C11	C12	0.58(16)
C4	C1	C2	C3	169.24(9)	N1	C10	C15	C14	-177.92(10)
O1	C1	C4	C5	2.77(15)	C11	C10	C15	C14	0.15(17)
O1	C1	C4	C9	-178.98(10)	C10	C11	C12	C13	-0.53(16)
C2	C1	C4	C5	-176.64(9)	C11	C12	C13	C14	-0.26(17)
C2	C1	C4	C9	1.61(15)	C12	C13	C14	C15	1.00(17)
C1	C2	C3	N1	167.12(9)	C13	C14	C15	C10	-0.94(17)
C1	C4	C5	C6	177.83(10)					

Table 6. Anisotropic Displacement Parameters (U_{ij}, Å^2)

Atom	U_{11}	U_{22}	U_{33}	U_{23}	U_{13}	U_{12}
O1	0.0532(5)	0.0331(4)	0.0378(4)	0.0028(3)	0.0162(4)	0.0071(4)
O2	0.0560(5)	0.0360(4)	0.0415(5)	-0.0048(4)	-0.0081(4)	-0.0016(4)
N1	0.0380(5)	0.0265(4)	0.0239(4)	0.0029(3)	0.0007(4)	0.0036(4)
N2	0.0452(6)	0.0328(5)	0.0287(5)	-0.0017(4)	-0.0037(4)	0.0055(4)
C1	0.0316(5)	0.0258(5)	0.0248(5)	-0.0017(4)	0.0006(4)	-0.0030(4)
C2	0.0330(5)	0.0247(5)	0.0260(5)	0.0013(4)	0.0016(4)	0.0006(4)
C3	0.0355(5)	0.0286(5)	0.0307(5)	0.0043(4)	0.0047(4)	0.0029(4)
C4	0.0305(5)	0.0259(5)	0.0230(5)	-0.0005(4)	-0.0033(4)	-0.0049(4)
C5	0.0370(5)	0.0319(5)	0.0258(5)	0.0005(4)	0.0008(4)	-0.0038(4)
C6	0.0466(7)	0.0347(6)	0.0274(5)	0.0076(4)	-0.0030(5)	-0.0089(5)
C7	0.0488(6)	0.0274(5)	0.0328(6)	0.0042(4)	-0.0107(5)	-0.0013(5)
C8	0.0433(6)	0.0310(6)	0.0349(6)	0.0006(4)	-0.0012(5)	0.0053(5)
C9	0.0378(6)	0.0299(5)	0.0274(5)	0.0030(4)	0.0015(4)	0.0000(4)
C10	0.0324(5)	0.0252(5)	0.0234(5)	0.0020(4)	0.0036(4)	0.0057(4)
C11	0.0376(6)	0.0318(5)	0.0239(5)	0.0056(4)	0.0022(4)	0.0067(4)
C12	0.0449(6)	0.0285(5)	0.0323(6)	0.0068(4)	0.0114(5)	0.0056(5)
C13	0.0402(6)	0.0293(5)	0.0378(6)	-0.0050(4)	0.0107(5)	0.0008(5)
C14	0.0423(6)	0.0366(6)	0.0296(5)	-0.0055(4)	-0.0010(5)	0.0057(5)
C15	0.0452(6)	0.0289(5)	0.0246(5)	0.0029(4)	-0.0011(5)	0.0077(5)

The form of the anisotropic displacement parameter is:
$\exp[-2\pi^2(h^2a^{*2}U_{11} + k^2b^{*2}U_{22} + l^2c^{*2}U_{33} + 2klb^*c^*U_{23} + 2hla^*c^*U_{13} + 2hka^*b^*U_{12})]$

Table 7. Derived Atomic Coordinates and Displacement Parameters for Hydrogen Atoms

Atom	x	y	z	U_{eq}, Å^2
H2A	0.331447	0.053843	0.322547	0.033
H2B	0.460120	0.111229	0.365089	0.033
H3A	0.120432	0.157117	0.324410	0.038
H3B	0.218901	0.210006	0.379813	0.038
H5	0.170524	-0.035103	0.522075	0.038
H6	0.251875	-0.171071	0.555146	0.044
H7	0.454252	-0.247392	0.494403	0.044
H8	0.579779	-0.186573	0.401753	0.044
H9	0.501756	-0.049786	0.368942	0.038
H11	0.314602	0.370167	0.223418	0.037
H12	0.441136	0.499662	0.251345	0.042
H13	0.595672	0.513888	0.348710	0.043
H14	0.622143	0.397769	0.419516	0.043
H15	0.501449	0.267014	0.391214	0.039

Crystallographic Information for **4-{nitroso[4-(trifluoromethyl)phenyl]amino}butan-2-one**. University of Alberta Department of Chemistry Structure Determination Laboratory Report #JMS2003.

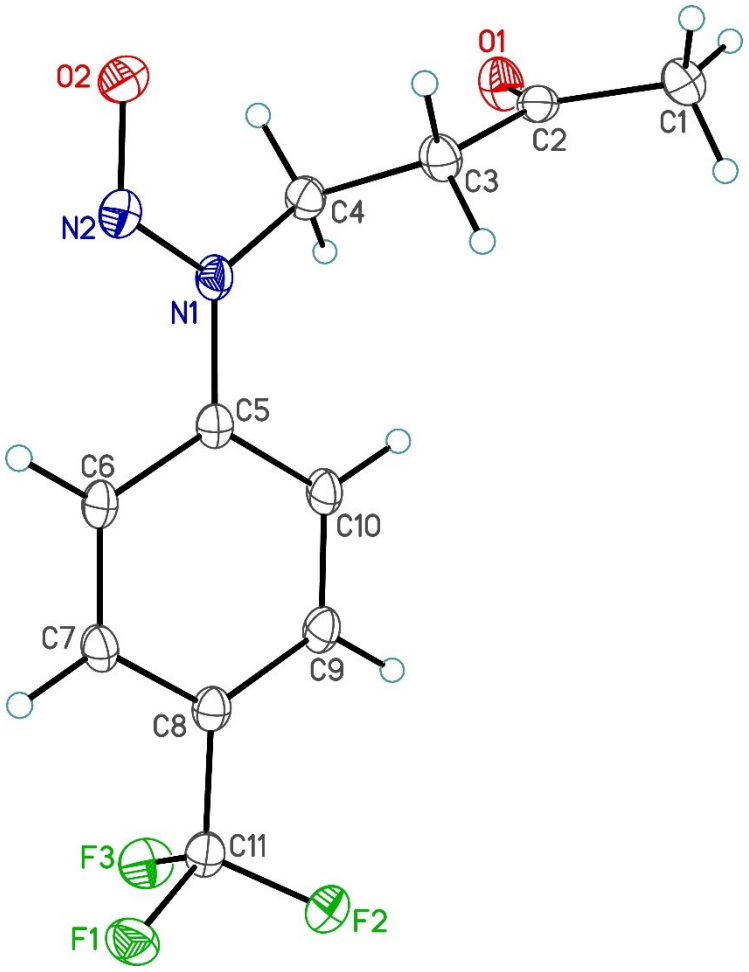

Perspective view of the 4-{nitroso[4-(trifluoromethyl)phenyl]amino}butan-2-one molecule showing the atom labelling scheme. Non-hydrogen atoms are represented by Gaussian ellipsoids at the 30% probability level. Hydrogen atoms are shown with arbitrarily small thermal parameters.

Crystallographic Experimental Details

A. Crystal Data

formula	$C_{11}H_{11}F_3N_2O_2$
formula weight	260.22

crystal dimensions (mm)	0.23 × 0.19 × 0.05
crystal system	triclinic
space group	$P\bar{1}$ (No. 2)
unit cell parameters[a]	
a (Å)	6.12900(10)
b (Å)	8.6035(2)
c (Å)	11.8565(3)
α (deg)	104.8769(7)
β (deg)	104.5203(8)
γ (deg)	98.8563(10)
V (Å^3)	568.80(2)
Z	2
ρ_{calcd} (g cm^{-3})	1.519
μ (mm^{-1})	1.211

B. Data Collection and Refinement Conditions

diffractometer	Bruker D8/APEX II CCD[b]
radiation (λ [Å])	Cu Kα (1.54178) (microfocus source)
temperature (°C)	–100
scan type	ω and ϕ scans (1.0°) (5 s exposures)
data collection 2θ limit (deg)	140.85
total data collected	24747 ($-7 \le h \le 7$, $-10 \le k \le 10$, $-14 \le l \le 14$)
independent reflections	2100 (R_{int} = 0.0259)

number of observed reflections (*NO*)	2018 [$F_o^2 \geq 2\sigma(F_o^2)$]
structure solution method	intrinsic phasing (*SHELXT-2014*[c])
refinement method	full-matrix least-squares on F^2 (*SHELXL–2018*[d])
absorption correction method	Gaussian integration (face-indexed)
range of transmission factors	0.9945–0.7883
data/restraints/parameters	2100 / 0 / 164
goodness-of-fit (*S*)[e] [all data]	1.031
final *R* indices[f]	
R_1 [$F_o^2 \geq 2\sigma(F_o^2)$]	0.0294
wR_2 [all data]	0.0842
largest difference peak and hole	0.238 and –0.228 e Å^{-3}

[a]Obtained from least-squares refinement of 9932 reflections with $8.10° < 2\theta < 140.86°$.

[b]Programs for diffractometer operation, data collection, data reduction and absorption correction were those supplied by Bruker.

[c]Sheldrick, G. M. *Acta Crystallogr.* **2015**, *A71*, 3–8. (*SHELXT-2014*)

[d]Sheldrick, G. M. *Acta Crystallogr.* **2015**, *C71*, 3–8. (*SHELXL-2018/3*)

[e]$S = [\Sigma w(F_o^2 - F_c^2)^2/(n - p)]^{1/2}$ (n = number of data; p = number of parameters varied; $w = [\sigma^2(F_o^2) + (0.0499P)^2 + 0.1221P]^{-1}$ where $P = [\text{Max}(F_o^2, 0) + 2F_c^2]/3$).

[f]$R_1 = \Sigma||F_o| - |F_c||/\Sigma|F_o|$; $wR_2 = [\Sigma w(F_o^2 - F_c^2)^2/\Sigma w(F_o^4)]^{1/2}$.

Table 2. Atomic Coordinates and Equivalent Isotropic Displacement Parameters

Atom	*x*	*y*	*z*	U_{eq}, Å^2
F1	0.55784(13)	0.17086(9)	0.22318(6)	0.0419(2)*
F2	0.90047(12)	0.29588(10)	0.34482(7)	0.0430(2)*
F3	0.63658(14)	0.43101(9)	0.31612(7)	0.0451(2)*
O1	0.86057(16)	0.46821(11)	1.09186(8)	0.0415(2)*
O2	0.13936(15)	0.09961(11)	0.81042(8)	0.0387(2)*
N1	0.39564(15)	0.21047(11)	0.74023(8)	0.0278(2)*
N2	0.19472(16)	0.10579(12)	0.71808(9)	0.0328(2)*
C1	1.0596(2)	0.25299(16)	1.10176(10)	0.0372(3)*
C2	0.87098(19)	0.32769(14)	1.04590(9)	0.0291(2)*
C3	0.6953(2)	0.21777(14)	0.92688(10)	0.0321(3)*
C4	0.53464(19)	0.31089(13)	0.86579(9)	0.0296(2)*
C5	0.46747(18)	0.22063(12)	0.63627(9)	0.0261(2)*
C6	0.30785(18)	0.16088(13)	0.51893(10)	0.0290(2)*
C7	0.37725(19)	0.17726(14)	0.41964(10)	0.0297(2)*
C8	0.60453(18)	0.25366(13)	0.43597(10)	0.0278(2)*
C9	0.76437(19)	0.31014(14)	0.55257(10)	0.0304(2)*
C10	0.69661(18)	0.29252(13)	0.65242(10)	0.0299(2)*
C11	0.67464(19)	0.28675(14)	0.33102(10)	0.0308(2)*

Anisotropically-refined atoms are marked with an asterisk (*). The form of the anisotropic displacement parameter is: $\exp[-2\pi^2(h^2a^{*2}U_{11} + k^2b^{*2}U_{22} + l^2c^{*2}U_{33} + 2klb^*c^*U_{23} + 2hla^*c^*U_{13} + 2hka^*b^*U_{12})]$.

Table 3. Selected Interatomic Distances (Å)

Atom1	Atom2	Distance	Atom1	Atom2	Distance
F1	C11	1.3447(13)	C2	C3	1.5114(14)
F2	C11	1.3398(13)	C3	C4	1.5229(15)
F3	C11	1.3443(13)	C5	C6	1.3973(14)
O1	C2	1.2106(14)	C5	C10	1.3887(16)
O2	N2	1.2358(13)	C6	C7	1.3800(16)
N1	N2	1.3309(14)	C7	C8	1.3883(16)
N1	C4	1.4715(13)	C8	C9	1.3916(15)
N1	C5	1.4270(14)	C8	C11	1.4921(15)
C1	C2	1.5003(16)	C9	C10	1.3843(16)

Table 4. Selected Interatomic Angles (deg)

Atom1	Atom2	Atom3	Angle	Atom1	Atom2	Atom3	Angle
N2	N1	C4	121.32(9)	C6	C7	C8	120.29(10)
N2	N1	C5	116.59(8)	C7	C8	C9	119.81(10)
C4	N1	C5	122.09(9)	C7	C8	C11	120.45(10)
O2	N2	N1	114.66(9)	C9	C8	C11	119.59(10)
O1	C2	C1	122.44(10)	C8	C9	C10	120.22(10)
O1	C2	C3	121.55(10)	C5	C10	C9	119.80(10)
C1	C2	C3	116.00(10)	F1	C11	F2	106.66(9)
C2	C3	C4	112.61(9)	F1	C11	F3	105.66(9)
N1	C4	C3	111.53(8)	F1	C11	C8	113.07(9)
N1	C5	C6	120.33(10)	F2	C11	F3	105.91(9)
N1	C5	C10	119.64(9)	F2	C11	C8	112.80(9)
C6	C5	C10	120.02(10)	F3	C11	C8	112.16(9)
C5	C6	C7	119.81(10)				

Table 5. Torsional Angles (deg)

Atom1	Atom2	Atom3	Atom4	Angle	Atom1	Atom2	Atom3	Atom4	Angle
C4	N1	N2	O2	-0.89(14)	C6	C5	C10	C9	2.31(16)
C5	N1	N2	O2	179.49(9)	C5	C6	C7	C8	-0.37(16)
N2	N1	C4	C3	86.72(12)	C6	C7	C8	C9	1.64(16)
C5	N1	C4	C3	-93.68(12)	C6	C7	C8	C11	-173.87(10)
N2	N1	C5	C6	17.34(14)	C7	C8	C9	C10	-0.94(16)
N2	N1	C5	C10	-163.60(9)	C11	C8	C9	C10	174.62(10)
C4	N1	C5	C6	-162.28(10)	C7	C8	C11	F1	-33.27(14)
C4	N1	C5	C10	16.79(14)	C7	C8	C11	F2	-154.42(10)
O1	C2	C3	C4	8.51(16)	C7	C8	C11	F3	86.09(13)
C1	C2	C3	C4	-170.52(10)	C9	C8	C11	F1	151.20(10)
C2	C3	C4	N1	169.23(9)	C9	C8	C11	F2	30.06(14)
N1	C5	C6	C7	177.44(9)	C9	C8	C11	F3	-89.43(12)
C10	C5	C6	C7	-1.62(16)	C8	C9	C10	C5	-1.04(16)
N1	C5	C10	C9	-176.75(9)					

Table 6. Anisotropic Displacement Parameters (U_{ij}, Å^2)

Atom	U_{11}	U_{22}	U_{33}	U_{23}	U_{13}	U_{12}
F1	0.0441(4)	0.0439(4)	0.0295(4)	0.0034(3)	0.0087(3)	0.0045(3)
F2	0.0296(4)	0.0601(5)	0.0438(4)	0.0188(3)	0.0150(3)	0.0119(3)
F3	0.0570(5)	0.0376(4)	0.0507(4)	0.0213(3)	0.0217(4)	0.0182(3)
O1	0.0410(5)	0.0375(5)	0.0333(4)	0.0004(3)	0.0003(3)	0.0085(4)
O2	0.0333(5)	0.0465(5)	0.0373(4)	0.0130(4)	0.0142(3)	0.0063(4)
N1	0.0208(5)	0.0295(4)	0.0270(4)	0.0046(3)	0.0027(3)	0.0032(4)
N2	0.0251(5)	0.0365(5)	0.0344(5)	0.0100(4)	0.0071(4)	0.0047(4)
C1	0.0353(6)	0.0439(6)	0.0292(5)	0.0119(5)	0.0043(4)	0.0086(5)
C2	0.0267(6)	0.0351(6)	0.0240(5)	0.0086(4)	0.0082(4)	0.0029(5)
C3	0.0310(6)	0.0316(5)	0.0275(5)	0.0048(4)	0.0035(4)	0.0059(5)
C4	0.0274(6)	0.0304(5)	0.0252(5)	0.0022(4)	0.0050(4)	0.0055(4)
C5	0.0231(5)	0.0242(5)	0.0274(5)	0.0049(4)	0.0042(4)	0.0062(4)
C6	0.0190(5)	0.0301(5)	0.0312(5)	0.0064(4)	0.0017(4)	0.0018(4)
C7	0.0239(5)	0.0313(5)	0.0267(5)	0.0051(4)	0.0003(4)	0.0044(4)
C8	0.0252(5)	0.0249(5)	0.0308(5)	0.0060(4)	0.0062(4)	0.0069(4)
C9	0.0201(5)	0.0305(5)	0.0338(6)	0.0049(4)	0.0043(4)	0.0015(4)
C10	0.0213(5)	0.0316(5)	0.0278(5)	0.0035(4)	-0.0001(4)	0.0026(4)
C11	0.0266(6)	0.0301(5)	0.0329(5)	0.0070(4)	0.0066(4)	0.0071(4)

The form of the anisotropic displacement parameter is:

$$\exp[-2\pi^2(h^2a^{*2}U_{11} + k^2b^{*2}U_{22} + l^2c^{*2}U_{33} + 2klb^*c^*U_{23} + 2hla^*c^*U_{13} + 2hka^*b^*U_{12})]$$

Table 7. Derived Atomic Coordinates and Displacement Parameters for Hydrogen Atoms

Atom	x	y	z	U_{eq}, Å^2
H1A	1.154783	0.329905	1.181827	0.045
H1B	1.156710	0.231292	1.047932	0.045
H1C	0.990344	0.148971	1.112015	0.045
H3A	0.601297	0.126370	0.943035	0.039
H3B	0.777969	0.168481	0.870130	0.039
H4A	0.429807	0.341537	0.914764	0.036
H4B	0.628052	0.414127	0.863601	0.036
H6	0.151983	0.109120	0.507526	0.035
H7	0.269042	0.136089	0.339781	0.036
H9	0.920489	0.360958	0.563686	0.036
H10	0.806537	0.329498	0.731756	0.036

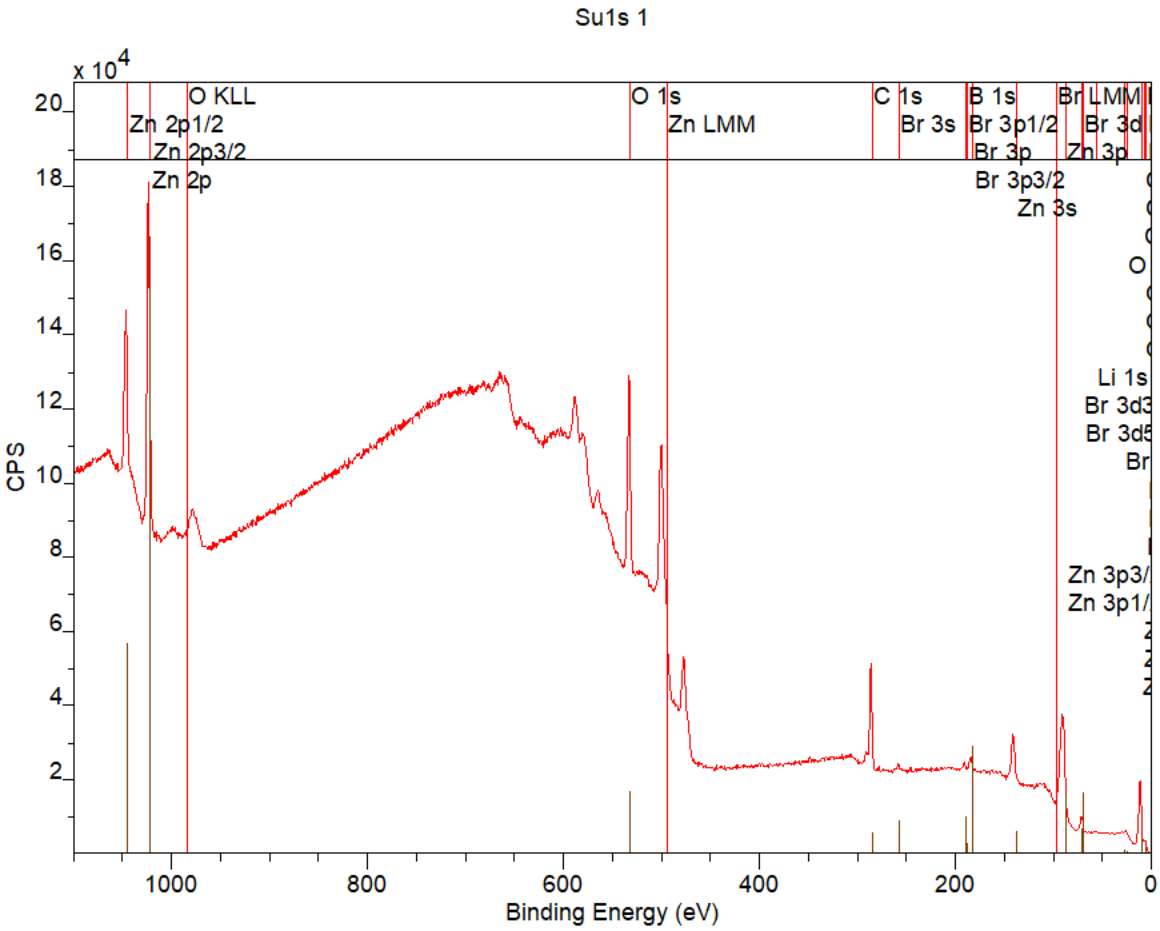

Figure 3-27 XPS data

Appendix B

Tetrahedron 74 (2018) 4343–4350

Contents lists available at ScienceDirect

Tetrahedron

journal homepage: www.elsevier.com/locate/tet

Formation of *meta*-arylsulfanyl- and *meta*-(alkylsulfanyl)phenols from cyclohexane-1,3-diones

Nhan Do Van Thanh, Subrata Patra, Derrick L.J. Clive*

Chemistry Department, University of Alberta, Edmonton, Alberta T6G 2G2, Canada

ARTICLE INFO

Article history:
Received 9 May 2018
Received in revised form
21 June 2018
Accepted 25 June 2018
Available online 30 June 2018

Keywords:
meta-(Arylsulfanyl)phenols
meta-(Alkylsulfanyl)phenols
Aromatization
Bromination
Sulfides

ABSTRACT

Reaction of cyclohexane-1,3-diones with $TsCl/Et_3N$ and treatment of the resulting 3-(tosyloxy)cyclohex-2-en-1-ones with aryl- or alkyl thiols and K_2CO_3 in MeCN gives 3-(arylsulfanyl)cyclohex-2-en-1-ones or 3-(alkylsulfanyl)cyclohex-2-en-1-ones, respectively. These compounds are easily brominated at C-2 by using NBS in MeCN; exposure to DBU in MeCN at room temperature then causes aromatization to afford *meta*-arylsulfanyl- and *meta*-(alkylsulfanyl)phenols.

1. Introduction

Three recent publications from this laboratory have described (Scheme 1) the conversion of 2-bromocyclohex-2-en-1-one systems **2** into phenols [1,2] (**2** → **3**→**4**) as well as the introduction of an alkyl or aryl substituent *meta* to the eventual phenolic hydroxyl (**2** → **5**→**6**) [3]. We have now extended the aromatization of bromocyclohexenones to the preparation of *meta*-(arylsulfanyl)- and *meta*-(alkylsulfanyl)phenols. The process involves preparation of a 2-bromo-3-(arylsulfanyl)cyclohex-2-en-1-one **7** or the corresponding alkylsulfanyl compound, and then aromatization (**7** → **8**) by treatment with DBU (Scheme 2). Some phenols of this type influence intracellular mobilization of Ca^{+2} ions [4a], inhibit the growth of HeLa cells [4b,c] or inhibit 17β-hydroxysteroid dehydrogenase type 1 [5a], and several have been evaluated as potential antidepressants [5b,c,d].

2. Results and discussion

Development of a route to compounds of type **7**, required some exploration in order to identify the best of several alternative approaches. In principle, the bromine can be introduced either before or after the sulfur unit, and both possibilities were investigated.

Cyclohexane-1,3-dione (**9**) was easily brominated in near quantitative yield [6] (**9** → **10**), but conversion to the dibromide **11** [7], with the intention of replacing the C-3 halogen by a sulfur unit, was unsatisfactory as the dibromide seemed to be unstable. Therefore, we treated **10** with TsCl and Et_3N in order to prepare the bromo tosylate **12**. However, the yield was poor (ca 40%) and the product was accompanied by the known tosyloxy phenol [8] **13**.

Several attempts were then made to introduce the sulfur unit directly using the monobromide **10** (see Scheme 3). To that end, treatment of **10** with PhSH, Ph_3P and DEAD gave the desired product (**14**), but only in ca 20% yield. Use of other coupling reagents such as DCC/DMAP [9] or MeOCOCl/HOBT [10] was equally unsatisfactory.

We also treated cyclohexan-1,3-dione (**9**) with PhSSPh and Ph_3P, but again, the yield of the expected 3-(phenylsulfanyl)cyclohexenone was very low (8%). All of these initial experiments were done with CH_2Cl_2 as solvent, except for the experiment with PhSSPh, which was carried out in MeCN. We then examined the use of MeOH and found that in this solvent simple treatment of the bromocyclohexanedione **10** with 1 equiv of PhSH for 24 h afforded **14** in 60% yield; however, attempts to raise the yield by varying the number of equiv of PhSH or the nature of the solvent (MeOH, MeCN, CF_3CH_2OH, EtOH, DMF, DMSO) were unsuccessful. We wondered if the observed formation of **14** was the result of replacement of OH by OMe, followed by displacement of the methoxy group. To test this possibility we added PhSH to a methanol solution of **15** (Scheme 4). However, overnight storage of **15** in MeOH in the

* Corresponding author.
E-mail address: derrick.clive@ualberta.ca (D.L.J. Clive).

https://doi.org/10.1016/j.tet.2018.06.059
0040-4020/

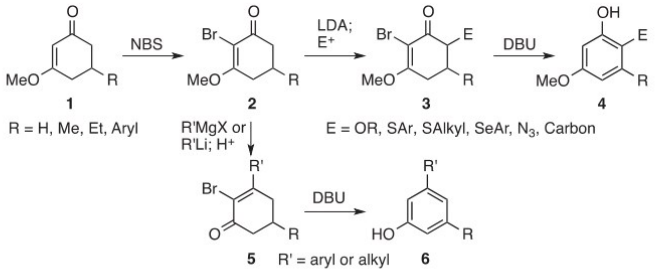

Scheme 1. Our previous routes to phenols from bromocyclohexenones.

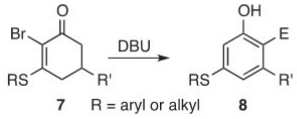

Scheme 2. Extension of the aromatization method to 3-arylsulfanyl and 3-(alkylsulfanyl)phenols.

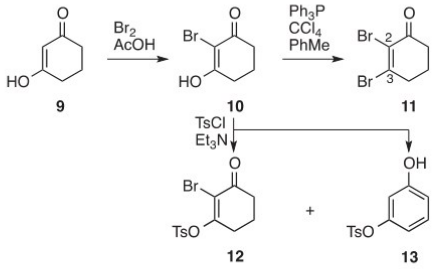

Scheme 3. Formation of 3-bromo- and 3-(tosyloxy)enones.

presence of PhSH did not provide any of the sulfide **14**, as judged by TLC analysis.

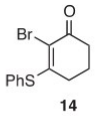

In related experiments (Scheme 5) cyclohexane-1,3-dione (**9**) was stored in MeOH for 1 week but very little ester **16** was formed (ca 10%). However, when PhSH (1 equiv) was added the ester **16** was formed in ca 90% yield after an overnight reaction period. When the keto sulfide **17** was kept overnight in MeOH, vinylogous ester **16** was again produced (ca 90%). This observation cause us to store the brominated compound **14** in MeOH to see if incursion of PhS/MeO

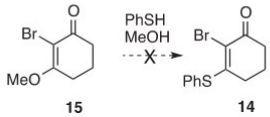

Scheme 4. Attempted displacement of OMe by SPh.

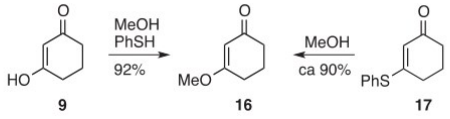

Scheme 5. Studies on MeO/PhS exchange.

exchange was responsible for the modest yield of **14**, but in the event, **14** was found to be stable to MeOH.

The outcome of these exploratory experiments forced us to turn to the alternative approach in which the bromine is introduced *after* the sulfur unit.

The reaction between PhSH and cyclohexane-1,3-dione (**9**) in the presence of $FeCl_3$, but without solvent, afforded **17** in 72% yield [11], but this method is unsuitable for solid thiols as use of a solvent is reported [11] to greatly diminish the yield. At this point we decided to evaluate the tosylate [12] **18**. This compound is easily made in almost 90% yield, but it should be stored in a freezer and used within a week. The best conditions for replacement of the tosyloxy group by PhS involve use of MeCN as solvent with K_2CO_3 (5 equiv) as base and 1 equiv of PhSH (Scheme 6). Under these conditions, which are similar to those reported for the corresponding mesylate [13,14], **17** was isolated in 71% yield. We have applied these conditions to a number of thiols (see Table 1) and prefer it to the use of NaH in DMF, a procedure that also afforded **17** in similar yield.

We next dealt with introduction of the bromine. In the case of the simplest example (**17**) bromination with NBS in CCl_4 had been reported [15,16], but we were uncertain of the generality of the method because of the potential for reaction at the sulfur atom [17] or at the benzene ring [18]. In our hands the action of NBS in MeCN on 3-(arylsulfanyl)cyclohex-2-enones was usually satisfactory irrespective of whether an electron-donating or an electron-withdrawing group is present in the arylsulfanyl unit. In the few examples where we made a comparison, use of CCl_4 for the NBS bromination gave a lower yield than use of MeCN as the solvent. The thiol addition and bromination steps worked equally well in the presence of an *ortho* methyl group (Table 1, entry 6) or an *ortho* ester group (Table 1, entry 7), but in the case of a *t*-butylsulfanyl group the yields were low (entry 10). The bromination was slow

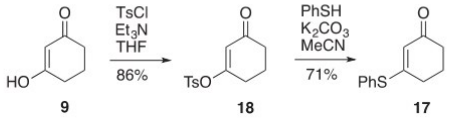

Scheme 6. Displacement of tosyloxy group by PhS.

Table 1
Formation of *meta*-(arylsulfanyl)- and *meta*-(alkylsulfanyl)phenols.

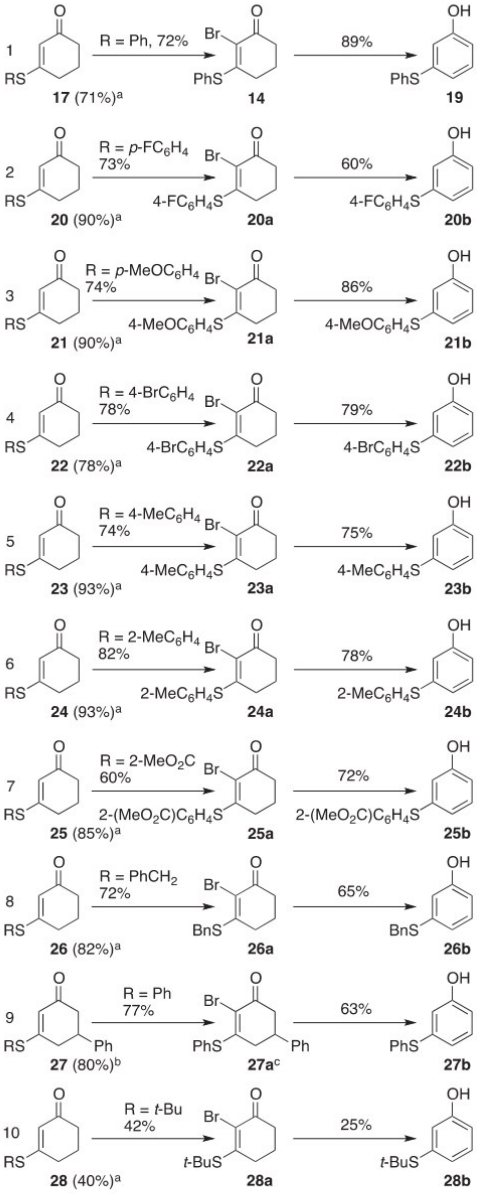

[a]Yield from tosylate **18**. [b]Yield from 3-oxo-5-phenylcyclohex-1-en-1-yl 4-methylbenzene-1-sulfonate. [c]The material contains slight impurities.

and so it was convenient to run the reaction for an arbitrary period of 24 h. Our results are given in Table 1.

Finally, we studied the aromatization with DBU. This step proceeded smoothly but took several hours; however, it was always complete after an overnight reaction period at room temperature. The effect of changing the solvent for the aromatization was also examined; MeCN generally gives a better result than THF, PhMe or CH_2Cl_2, and the reactions are best run at room temperature; raising the temperature (50 °C), with the one example we studied (compound **14**), resulted in a significantly decreased yield (by 20%) in two successive runs. With the exception of entry 10, the yields are in the range 63–90% with an average yield of 74%.

3. Other approaches

Other methods that have been used to prepare *inter alia meta*-(arylsulfanyl)- or *meta*-(alkylsulfanyl)phenols include a number of procedures usually based on transition metals and often run at an elevated temperature: Treatment of 3-(arylsulfanyl)cyclohexanones or the corresponding cyclohex-2-enones with Pd/C in the presence of K_2CO_3 and H_2 at 150 °C in $MeC(O)NMe_2$ effects dehydrogenation to the phenol (Eq. (1)) [19].

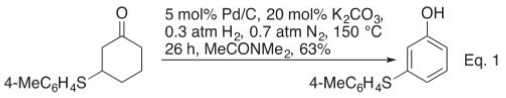

Aryl thiols can be coupled with aryl iodides at modest temperature (80 °C) in a process catalyzed by CuI (Eq. (2)) [20]. Similarly, both alkyl and aryl thiols undergo palladium-mediated coupling with aryl iodides and bromides at 90–110 °C in the presence of a base (Eq. (3)) [21].

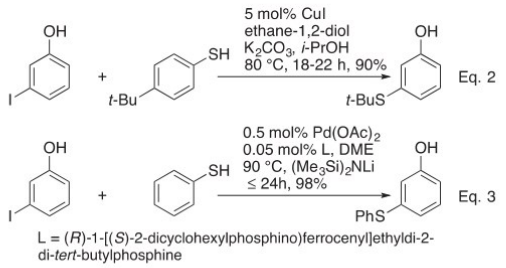

Aryl and alkyl thiols have been coupled with arylboronic acids under the influence of ultrasound in the presence of $Cu(OAc)_2$ (Eq. (4)) [22]. Deprotonation of 3-bromophenol, followed by halogen/metal exchange and reaction with sulfur generates a thiolate that can be alkylated by an alkyl halide (Eq. (5)) [23].

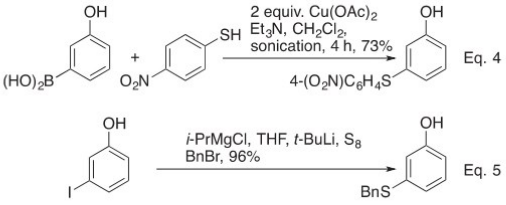

Aryl thiolates made byother methods can, of course, be alkylated with alkyl halides (Eq. (6)) [24]. Aryl halides can also be converted into thiolates by copper(II)-catalyzed reaction at 110 °C with 1,2-ethanedithiol in the presence of KOH and, without isolation, the thiolates can be arylated on sulfur by addition of an aryl iodide in DMF and heating at 120 °C (Eq. (7)) [25].

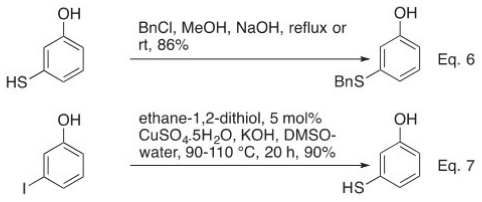

A vinylogous thioester has been aromatized by *dihalogenation* and base treatment to afford a halogenated *meta*-(phenylsulfanyl) phenol (Eq. (8)) [26].

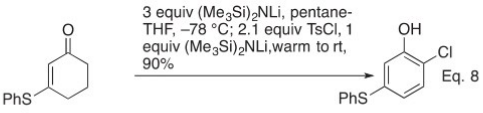

4. Conclusion

3-(Tosyloxy)cyclohex-2-en-1-ones, readily made from cyclohexan-1,3-diones, are convertible into 3-(arylsulfanyl)- or 3-(alkylsulfanyl)cyclohex-2-en-1-ones by reaction at room temperature with thiols in the presence of K_2CO_3. The products can be brominated at C-2 with NBS in MeCN, and treatment with DBU in MeCN affords the corresponding 3-(arylsulfanyl)- or 3-(alkylsulfanyl)phenols. The reaction sequence occurs under mild conditions and avoids the use of heavy metals.

5. Experimental section

5.1. General procedures

Solvents used for chromatography were distilled before use. Commercial thin layer chromatography plates (silica gel, Merck 60F-254) were used. Silica gel for flash chromatography was Merck type 60 (230–400 mesh). Dry solvents were prepared under an inert atmosphere (N_2) and transferred by syringe or cannula. The symbols s, d, t, and q used for ^{13}C NMR spectra indicate zero, one, two, or three attached hydrogens, respectively, the assignments being made from APT spectra. Solutions were evaporated under water pump vacuum, and the residue was then kept under oil pump vacuum. High resolution electrospray mass spectrometric analyses were done with an orthogonal time-of-flight analyzer, and electron ionization mass spectra were measured with a double-focusing sector mass spectrometer. Gradient flash chromatography was done by stepwise small increases in the proportion of the more polar solvent, as described for the individual experiments. NBS was recrystallized from water [27] and K_2CO_3 was stored in an oven at 120 °C.

5.1.1. 3-(Phenylsulfanyl)cyclohex-2-en-1-one (**17**) [11]

PhSH (0.055 mL, 0.50 mmol) was added to a stirred mixture of tosylate **18** (133 mg, 0.50 mmol), K_2CO_3 (413 mg, 2.50 mmol) and dry MeCN (1 mL) and stirring was continued overnight (N_2

atmosphere). Water (10 mL) was added and stirring was continued for 15 min. The mixture was extracted with EtOAc (3 × 15 mL) and the combined organic extracts were washed with brine, dried ($MgSO_4$) and evaporated. Flash chromatography of the residue over silica gel (1 × 25 cm), using 4:1 hexane-EtOAc, gave **17** (72 mg, 71%) as an oil: ^{1}H NMR ($CDCl_3$, 400 MHz) δ 2.01–2.07 (m, 2 H), 2.34–2.38 (m, 2 H), 2.52 (td, J = 6.0, 0.8 Hz, 2 H), 5.47 (t, J = 1.2 Hz, 1 H), 7.40–7.48 (m, 5 H); ^{13}C NMR ($CDCl_3$, 100 MHz) δ 22.9, 30.2, 37.2, 120.9, 128.0, 129.8, 130.1, 135.5, 166.8, 196.0.

5.1.2. 2-Bromo-3-(phenylsulfanyl)cyclohex-2-en-1-one (**14**) [15]

Thio enone **17** (102 mg, 0.50 mmol) and then freshly crystallized NBS (98 mg, 0.55 mmol) were placed in a round-bottomed flask containing a magnetic stirrer. Dry MeCN (1.0 mL) was added and the mixture was stirred for 24 h (N_2 atmosphere) with protection from light (flask wrapped in aluminum foil). EtOAc (15 mL) was added and the mixture was washed successively with aqueous $Na_2S_2O_3$ (1 M), saturated aqueous $NaHCO_3$, and brine. The organic extract was dried ($MgSO_4$) and evaporated. Flash chromatography of the residue over silica gel (3 × 15 cm), using 4:1 hexane-EtOAc, gave **14** (102 mg, 72%) as a solid: mp 112–113 °C; ^{1}H NMR ($CDCl_3$, 400 MHz) δ 1.93–1.97 (m, 2 H), 2.20 (t, J = 6.5 Hz, 2 H), 2.56 (t, J = 6.0 Hz, 2 H), 7.43–7.58 (m, 5 H); ^{13}C NMR ($CDCl_3$, 125 MHz) δ 22.5, 32.2, 37.1, 116.8, 129.1, 129.7, 130.4, 136.0, 164.3, 187.7.

5.1.3. 3-(Phenylsulfanyl)phenol (**19**) [21]

DBU (0.032 mL, 0.212 mmol) was injected into a stirred solution of **14** (30 mg, 0.11 mmol) in dry MeCN (1.0 mL) and stirring was continued overnight (N_2 atmosphere). The mixture was diluted with hydrochloric acid (5%, 10 mL) and stirring was continued for 15 min. The mixture was extracted with EtOAc (3 × 15 mL) and the combined organic extracts were washed with brine, dried ($MgSO_4$) and evaporated. Flash chromatography of the residue over silica gel (1 × 15 cm), using successively hexane (ca 20 mL), 5% EtOAc-hexane (ca 50 mL), 10% EtOAc-hexane (ca 100 mL), gave **19** (19 mg, 89%) as an oil: ^{1}H NMR ($CDCl_3$, 400 MHz) δ 4.98 (br s, 1 H), 6.70–6.80 (m, 1 H), 6.85–6.86 (m, 1 H), 6.98–7.00 (m, 1 H), 7.26 (t, J = 8.0 Hz, 1 H), 7.36–7.39 (m, 1 H), 7.41–7.44 (m, 2 H), 7.48–7.51 (m, 2 H); ^{13}C NMR ($CDCl_3$, 100 MHz) δ 113.9, 116.9, 122.7, 127.5, 129.3, 130.2, 131.9, 134.8, 137.89, 156.0.

5.1.4. 3-[(4-Fluorophenyl)sulfanyl]cyclohex-2-en-1-one (**20**) [28]

The procedure for making **17** was followed exactly, using 4-fluorobenzene-1-thiol (0.042 mL, 0.50 mmol), tosylate **18** (133 mg, 0.50 mmol), K_2CO_3 (413 mg, 2.50 mmol) and dry MeCN (1 mL). Water (10 mL) was added and stirring was continued for 15 min. Flash chromatography of the crude product over silica gel (3 × 15 cm), using 4:1 hexane-EtOAc, gave **20** (100 mg, 90%) as an oil: FTIR ($CDCl_3$, cast) 2949, 1659, 1589, 1491, 1324, 1227, 1187 cm^{-1}; ^{1}H NMR ($CDCl_3$, 500 MHz) δ 2.03–2.06 (m, 2 H), 2.37 (t, J = 6.5 Hz, 2 H), 2.50–2.52 (m, 2 H), 5.41 (s, 1 H), 7.10–7.13 (m, 2 H), 7.44–7.47 (m, 2 H); ^{13}C NMR ($CDCl_3$, 125 MHz) δ 23.0 (t), 30.2 (t), 37.3 (t), 117.2 (d, $^2J_{CF}$ = 22.2 Hz), 120.9 (d, $^4J_{CF}$ = 3.6 Hz), 123.4 (d), 137.7 (d, $^3J_{CF}$ = 8.5 Hz), 164.0 (d, $^1J_{CF}$ = 252.0 Hz), 165.0 (s), 166.7 (s), 196.0 (s); exact mass (EI) m/z calcd for $C_{12}H_{14}FOS$ (M^+) 222.0515, found 222.0515.

5.1.5. 2-Bromo-3-[(4-fluorophenyl)sulfanyl]cyclohex-2-en-1-one (**20a**)

The procedure for making **14** was followed exactly, using thio enone **20** (60 mg, 0.27 mmol), freshly crystallized NBS (53 mg, 0.30 mmol) and dry MeCN (1.0 mL). Flash chromatography of the crude product over silica gel (3 × 15 cm), using 4:1 hexane-EtOAc, gave **20a** (60 mg, 73%) as a solid: mp 135–136 °C; FTIR ($CDCl_3$, cast) 3097, 3070, 2956, 2935, 1665, 1588, 1543, 1491, 1266, 1222, 1185 cm^{-1}; ^{1}H NMR ($CDCl_3$, 500 MHz) δ 1.95 (quintet, J = 6.5 Hz, 2 H), 2.16–2.19 (m, 2 H), 2.55 (t, J = 6.5 Hz, 2 H), 7.12–7.15 (m, 2 H), 7.54–7.56 (m, 2 H); ^{13}C NMR ($CDCl_3$, 125 MHz) δ 22.5 (t), 32.2 (t), 37.1 (t), 117.02 (d, $^2J_{CF}$ = 22.1 Hz), 117.03 (s), 124.6 (d, $^4J_{CF}$ = 3.6 Hz), 138.2 (d, $^3J_{CF}$ = 8.7 Hz), 163.8 (s), 164.1 (d, $^1J_{CF}$ = 252.6 Hz), 187.6 (s); exact mass (EI) m/z calcd for $C_{12}H_{10}^{81}BrFOS$ (M^+) 301.9599, found 301.9597.

5.1.6. 3-[(4-Fluorophenyl)sulfanyl]phenol (**20b**)

The procedure for making **19** was followed exactly, using DBU (0.088 mL, 0.590 mmol) and **20a** (88.4 mg, 0.294 mmol) in dry MeCN (1.0 mL). Flash chromatography of the crude product over silica gel (1 × 15 cm), using 3:7 hexane-CH_2Cl_2, gave **20b** (39 mg, 60%) as an oil: FTIR ($CDCl_3$, cast) 3380, 3092, 1589, 1489, 1474, 1439, 1225, 1156 cm^{-1}; ^{1}H NMR ($CDCl_3$, 500 MHz) δ 4.81 (s, 1 H), 6.65–6.67 (m, 2 H), 6.80–6.82 (m, 1 H), 7.02–7.06 (m, 2 H), 7.14 (td, J = 8.0, 1.0 Hz, 1 H), 7.40–7.43 (m, 2 H); ^{13}C NMR ($CDCl_3$, 125 MHz) δ 113.7 (d), 115.9 (d), 116.5 (d), 116.6 (d, $^2J_{CF}$ = 22.4 Hz), 121.7 (d), 129.3 (d, $^4J_{CF}$ = 3.4 Hz), 130.2 (d), 134.9 (d, $^3J_{CF}$ = 8.5 Hz), 138.7 (d), 156.0 (s), 162.7 (d, $^1J_{CF}$ = 248.5 Hz); exact mass (EI) m/z calcd for $C_{12}H_9OFS$ (M^+) 220.0358, found 220.0355.

5.1.7. 3-[(4-Methoxyphenyl)sulfanyl]cyclohex-2-en-1-one (**21**) [11]

The procedure for making **17** was followed exactly, using 4-methoxybenzene-1-thiol (0.12 mL, 1.00 mmol), tosylate **18** (266 mg, 1.00 mmol), K_2CO_3 (826 mg, 5.00 mmol) and dry MeCN (2 mL) Flash chromatography of the crude product over silica gel (3 × 15 cm), using 4:1 hexane-EtOAc, gave **21** (210 mg, 90%) as an oil: FTIR ($CDCl_3$, cast) 3004, 2962, 1654, 1587, 1578, 1494, 1325, 1290, 1250 cm^{-1}; ^{1}H NMR ($CDCl_3$, 500 MHz) δ 2.04 (quintet, J = 6.5 Hz, 2 H), 2.36 (t, J = 6.5 Hz, 2 H), 2.49–2.51 (m, 2 H), 3.82 (s, 3 H), 5.42 (s, 1 H), 6.90–6.93 (m, 2 H), 7.36–7.38 (m, 2 H); ^{13}C NMR ($CDCl_3$, 125 MHz) δ 22.9 (t), 30.1 (t), 37.3 (t), 55.4 (q), 115.5 (d), 118.5 (s), 120.6 (d), 137.0 (d), 161.2 (s), 168.0 (s), 196.1 (s); exact mass (EI) m/z calcd for $C_{13}H_{14}O_2S$ (M^+) 234.0715, found 234.0718.

5.1.8. 2-Bromo-3-[(4-methoxyphenyl)sulfanyl]cyclohex-2-en-1-one (**21a**)

The procedure for making **14** was followed exactly, using thio enone **20** (86.2 mg, 0.353 mmol), freshly crystallized NBS (69.2 mg, 0.389 mmol) and dry MeCN (1.0 mL). Flash chromatography of the crude product over silica gel (3 × 15 cm), using 4:1 hexane-EtOAc, gave **21a** (81.9 mg, 74%) as a solid: mp 115–117 °C; FTIR ($CDCl_3$, cast) 2971, 2947, 1662, 1590, 1454, 1438, 1253, 1187 cm^{-1}; ^{1}H NMR ($CDCl_3$, 400 MHz) δ 1.93 (quintet, J = 6.4 Hz, 2 H), 2.18 (t, J = 6.4 Hz, 2 H), 2.53 (t, J = 6.4 Hz, 2 H), 3.84 (s, 3 H), 6.94 (d, J = 8.8 Hz, 2 H), 7.46 (d, J = 8.8 Hz, 2 H); ^{13}C NMR ($CDCl_3$, 100 MHz) δ 22.5 (d), 32.1 (d), 37.2 (d), 55.5 (q), 115.2 (d), 116.2 (s), 119.7 (s), 137.6 (d), 161.4 (s), 165.6 (s), 187.7 (s); exact mass (EI) m/z calcd for $C_{13}H_{13}^{81}BrO_2S$ (M^+) 313.9799, found 313.9796.

5.1.9. 3-[(4-Methoxyphenyl)sulfanyl]phenol (**21b**)

The procedure for making **19** was followed exactly, using DBU (0.035 mL, 0.240 mmol) and **21a** (37.5 mg, 0.120 mmol) in dry MeCN (1.0 mL). Flash chromatography of the crude product over silica gel (1 × 15 cm), using successively hexane (ca 20 mL), 5% EtOAc-hexane (ca 50 mL), 10% EtOAc-hexane (ca 100 mL), gave **21b** (24 mg, 86%) as an oil: FTIR ($CDCl_3$, cast) 3396, 1591, 1493, 1439, 1289, 1248, 1173 cm^{-1}; ^{1}H NMR ($CDCl_3$, 500 MHz) δ 3.85 (s, 3 H), 4.92 (br s, 1 H), 6.57–6.60 (m, 2 H), 6.74 (ddd, J = 5.0, 1.5, 1.0 Hz, 1 H), 6.90 (dd, J = 9.0, 3.0 Hz, 2 H); 7.10 (t, J = 8.0 Hz, 1 H), 7.43 (dd, J = 9.0, 3.0 Hz, 2 H); ^{13}C NMR ($CDCl_3$, 125 MHz) δ 55.4 (q), 112.8 (d), 114.4 (d), 115.1 (d), 120.2 (d), 123.6 (s), 130.0 (d), 135.9 (d), 140.6 (s), 156.0 (s), 160.1 (s); exact mass (EI) m/z calcd for $C_{13}H_{12}O_2S$ (M^+) 232.0558, found 232.0561.

*5.1.10. 3-[(4-Bromophenyl)sulfanyl]cyclohex-2-en-1-one (**22**)*

The procedure for making **17** was followed exactly, using 4-bromobenzene-1-thiol (378 mg, 2.00 mmol), tosylate **18** (532 mg, 2.00 mmol), K_2CO_3 (1.652 g, 10 mmol) and dry MeCN (4 mL). Flash chromatography of the crude product over silica gel (2 × 25 cm), using 4:1 hexane-EtOAc, gave **22** (443 mg, 78%) as an oil: FTIR ($CDCl_3$, cast) 3076, 2950, 2889, 1649, 1579 cm^{-1}; ^1H NMR ($CDCl_3$, 500 MHz) δ 2.03–2.08 (m, 2 H), 2.38 (dd, J = 7.5, 1.0 Hz, 2 H), 2.51 (ddd, J = 7.5, 6.0, 1.0 Hz, 2 H), 5.45 (apparent t, J = 1.5 Hz, 1 H), 7.33–7.35 (m, 2 H), 7.54–7.57 (m, 2 H); ^{13}C NMR ($CDCl_3$, 125 MHz) δ 22.9 (t), 30.2 (t), 37.2 (t), 121.1 (d), 125.0 (s), 127.1 (s), 133.1 (d), 137.0 (d), 165.9 (s), 195.9 (s); exact mass (EI) m/z calcd for $C_{12}H_{11}^{81}BrOS$ (M^+) 283.9694, found 283.9691.

*5.1.11. 2-Bromo-3-[(4-bromophenyl)sulfanyl]cyclohex-2-en-1-one (**22a**)*

The procedure for making **14** was followed exactly, using thio enone **22** (200 mg, 0.710 mmol), freshly crystallized NBS (151 mg, 0.840 mmol) and dry MeCN (1.5 mL). Flash chromatography of the crude product over silica gel (1.2 × 25 cm), using 4:1 hexane-EtOAc, gave **22b** (100 mg, 78%) as a solid: mp 118–120 °C; FTIR ($CDCl_3$, cast) 3079, 3060, 2957, 2931, 1666, 1538 cm^{-1}; ^1H NMR ($CDCl_3$, 500 MHz) δ 1.94–1.99 (m, 2 H), 2.20 (dd, J = 6.0, 6.0 Hz, 2 H), 2.55–2.58 (m, 2 H), 7.41–7.44 (m, 2 H), 7.57–7.60 (m, 2 H); ^{13}C NMR ($CDCl_3$, 125 MHz) δ 22.5 (t), 32.3 (t), 37.1 (t), 117.4 (s), 125.4 (s), 128.2 (s), 132.9 (d), 137.4 (d), 163.0 (s), 187.6 (s); exact mass (EI) m/z calcd for $C_{12}H_{10}^{79}BrOS$ $(M + H)^+$ 360.8892, found 360.8894.

*5.1.12. 3-[(4-Bromophenyl)sulfanyl]phenol (**22b**)*

The procedure for making **19** was followed exactly, using DBU (0.08 mL, 0.53 mmol) and **22a** (97 mg, 0.26 mmol) in dry MeCN (1.5 mL). Flash chromatography of the crude product over silica gel (1 × 30 cm), using successively hexane (ca 20 mL), 5% EtOAc-hexane (ca 50 mL), 10% EtOAc-hexane (ca 100 mL), gave **22b** (60 mg, 79%) as an oil: FTIR ($CDCl_3$, cast) 3375, 3059, 2954, 2925, 1583, 1472 cm^{-1}; ^1H NMR ($CDCl_3$, 500 MHz) δ 4.84 (br s, 1 H), 6.72 (ddd, J = 8.0, 2.5, 0.5 Hz, 1 H), 6.77 (m, 1 H), 6.90 (ddd, J = 8.0, 1.5, 0.5 Hz, 1 H), 7.16–7.26 (m, 3 H), 7.43 (dt, J = 9.0, 2.0 Hz, 2 H); ^{13}C NMR ($CDCl_3$, 125 MHz) δ 114.5 (d), 117.4 (d), 121.4 (s), 123.2 (d), 130.4 (d), 132.4 (d), 132.9 (d), 134.5 (s), 136.8 (s), 156.0 (s); exact mass (EI) m/z calcd for $C_{12}H_8^{79}BrOS$ $(M - H)^-$ 278.9485, found 278.9477.

*5.1.13. 3-[(4-Methylphenyl)sulfanyl]cyclohex-2-en-1-one (**23**) [11]*

The procedure for making **17** was followed exactly, using 4-methylbenzene-1-thiol (248 mg, 2.00 mmol), tosylate **18** (532 mg, 2.00 mmol), K_2CO_3 (1.652 g, 10.00 mmol) and dry MeCN (4 mL). Flash chromatography of the crude product over silica gel (2 × 25 cm), using 4:1 hexane-EtOAc, gave **23** (401 mg, 93%) as a solid: mp 45–48 °C; FTIR ($CDCl_3$, cast) 3023, 2948, 2866, 1659, 1578 cm^{-1}; ^1H NMR ($CDCl_3$, 500 MHz) δ 2.02–2.07 (apparent dt, J = 13.0, 6.0 Hz, 2 H), 2.35–2.38 (m, 2 H), 2.38 (s, 3 H), 2.52 (ddd, J = 6.0, 6.0, 1.0 Hz, 2 H), 5.46 (apparent t, J = 1.0 Hz, 1 H), 7.21–7.23 (m, 2 H), 7.35 (dt, J = 8.0, 2.0 Hz, 2 H); ^{13}C NMR ($CDCl_3$, 125 MHz) δ 21.3 (q), 23.0 (t), 30.2 (t), 37.3 (t), 120.7 (d), 124.4 (s), 130.7 (d), 135.4 (d), 140.6 (s), 167.5 (s), 196.1 (s); exact mass (EI) m/z calcd for $C_{13}H_{14}OS$ (M^+) 218.0765, found 218.0766.

*5.1.14. 2-Bromo-3-[(4-methylphenyl)sulfanyl]cyclohex-2-en-1-one (**23a**)*

The procedure for making **14** was followed exactly, using thio enone **23** (209 mg, 1.00 mmol), freshly crystallized NBS (195 mg, 1.10 mmol) and dry MeCN (1.5 mL). Flash chromatography of the crude product over silica gel (1.2 × 25 cm), using 4:1 hexane-EtOAc, gave **23a** (210 mg, 74%) as a solid: mp 128–130 °C; FTIR ($CDCl_3$, cast) 3052, 3033, 2956, 2931, 1662, 1542 cm^{-1}; ^1H NMR ($CDCl_3$, 500 MHz) δ 1.91–2.0 (m, 2 H), 2.20 (dd, J = 6.0, 6.0 Hz, 2 H), 2.41 (s, 3 H), 2.55 (dd, J = 7.0, 7.0 Hz, 2 H), 7.23–7.25 (m, 2 H), 7.42–7.44 (m, 2 H); ^{13}C NMR ($CDCl_3$, 125 MHz) δ 21.4 (q), 22.5 (t), 32.1 (t), 37.2 (t), 116.5 (s), 125.6 (s), 130.4 (d), 135.9 (d), 140.9 (s), 164.9 (s), 187.7 (s); exact mass (EI) m/z calcd for $C_{13}H_{13}^{81}BrOS$ (M^+) 297.9850, found 297.9851.

*5.1.15. 3-[(4-Methylphenyl)sulfanyl]phenol (**23b**) [19]*

The procedure for making **19** was followed exactly, using DBU (0.10 mL, 0.67 mmol) and **23a** (102 mg, 0.33 mmol) in dry MeCN (1.5 mL). Flash chromatography of the crude product over silica gel (1 × 30 cm), using successively hexane (ca 20 mL), 5% EtOAc-hexane (ca 50 mL), 10% EtOAc-hexane (ca 100 mL), gave **23b** (56 mg, 75%) as an oil: FTIR ($CDCl_3$, cast) 3383, 3022, 2920, 2862, 1584, 1474 cm^{-1}; ^1H NMR ($CDCl_3$, 500 MHz) δ 2.37 (s, 3 H), 4.90 (br s, 1 H), 6.63–6.68 (m, 2 H), 6.82–6.85 (m, 1 H), 7.11–7.17 (m, 3 H), 7.35 (dd, J = 6.5, 2.0 Hz, 2 H); ^{13}C NMR ($CDCl_3$, 125 MHz) δ 21.2 (q), 113.4 (d), 115.7 (d), 121.6 (d), 130.1 (d), 130.2 (d), 130.3 (s), 133.1 (d), 138.1 (s), 139.2 (s), 155.9 (s); exact mass (electrospray) m/z calcd for $C_{13}H_{11}OS$ $(M - H)^-$ 215.0536, found 215.0534.

*5.1.16. 3-[(2-Methylphenyl)sulfanyl]cyclohex-2-en-1-one (**24**)*

The procedure for making **17** was followed exactly, using 2-methylbenzene-1-thiol (0.30 mL, 2.46 mmol), tosylate **18** (655 mg, 2.45 mmol), K_2CO_3 (1.70 g, 12.3 mmol) and dry MeCN (4 mL). Flash chromatography of the crude product over silica gel (2 × 25 cm), using 4:1 hexane-EtOAc, gave **24** (500 mg, 93%) as an oil: FTIR ($CDCl_3$, cast) 3059, 2949, 2866, 1656, 1578 cm^{-1}; ^1H NMR ($CDCl_3$, 500 MHz) δ 2.06 (quintet, J = 6.5 Hz, 2 H), 2.37–2.39 (m, 5 H), 2.54 (td, J = 6.0, 1.0 Hz, 2 H), 5.32 (apparent t, J = 1.0 Hz, 1 H), 7.21–7.24 (m, 1 H), 7.30–7.37 (m, 2 H), 7.46 (ddd, J = 7.5, 1.0, 0.5 Hz, 1 H); ^{13}C NMR ($CDCl_3$, 125 MHz) δ 20.4 (q), 23.0 (t), 30.2 (t), 37.3 (t), 120.4 (d), 127.3 (s), 127.3 (d), 130.8 (d), 131.2 (d), 136.6 (d), 142.7 (s), 165.9 (s), 196.1 (s); exact mass (EI) m/z calcd for $C_{13}H_{14}OS$ (M^+) 218.0765, found 218.0765.

*5.1.17. 2-Bromo-3-[(2-methylphenyl)sulfanyl]cyclohex-2-en-1-one (**24a**)*

The procedure for making **14** was followed exactly, using thio enone **24** (224 mg, 1.03 mmol), freshly crystallized NBS (200 mg, 1.13 mmol) and dry MeCN (1.5 mL). Flash chromatography of the crude product over silica gel (1.2 × 25 cm), using 4:1 hexane-EtOAc, gave **24a** (250 mg, 82%) as a solid: mp 111–113 °C; FTIR ($CDCl_3$, cast) 3060, 3011, 2950, 2923, 1671, 1537 cm^{-1}; ^1H NMR ($CDCl_3$, 500 MHz) δ 1.91–1.96 (m, 2 H), 2.1 (t, J = 6.0 Hz, 2 H), 2.45 (s, 3 H), 2.56 (dd, J = 7.5, 6.0 Hz, 2 H), 7.25–7.27 (m, 1 H), 7.33–7.37 (m, 1 H), 7.40 (ddd, J = 7.5, 1.5, 1.5 Hz, 1 H), 7.54 (dd, J = 7.5, 1.5 Hz, 1 H); ^{13}C NMR ($CDCl_3$, 125 MHz) δ 21.2 (q), 22.5 (t), 31.7 (t), 37.2 (t), 117.3 (s), 127.2 (d), 128.7 (s), 130.9 (d), 131.2 (d), 137.0 (d), 143.1 (s), 164.4 (s), 187.7 (s); exact mass (EI) m/z calcd for $C_{13}H_{13}^{79}BrOS$ (M^+) 295.9871, found 295.9872.

*5.1.18. 3-[(2-Methylphenyl)sulfanyl]phenol (**24b**)*

The procedure for making **19** was followed exactly, using DBU (0.10 mL, 0.67 mmol) and **24a** (95 mg, 0.32 mmol) in dry MeCN (1.5 mL). Flash chromatography of the crude product over silica gel (1 × 30 cm), using successively hexane (ca 20 mL), 5% EtOAc-hexane (ca 50 mL), and 10% EtOAc-hexane (ca 100 mL), gave **24b** (54 mg, 78%) as an oil: FTIR ($CDCl_3$, cast) 3376, 3060, 2961, 2923, 1584, 1473 cm^{-1}; ^1H NMR ($CDCl_3$, 500 MHz) δ 2.41 (s, 3 H), 4.76 (br s, 1 H), 6.61–6.62 (m, 1 H), 6.66 (dd, J = 8.0, 1.0 Hz, 1 H), 6.80 (dd, J = 8.0, 1.0 Hz, 1 H), 7.15 (t, J = 8.0 Hz, 1 H), 7.18–7.21 (m, 1 H), 7.26–7.30 (m, 2 H), 7.41 (d, J = 8.0 Hz, 1 H); ^{13}C NMR ($CDCl_3$, 125 MHz) δ 20.7 (q), 113.3 (d), 115.5 (d), 121.4 (d), 126.8 (d), 128.5

*5.1.26. 3-Bromo-5-phenyl-3-(phenylsulfanyl)cyclohex-2-en-1-one (**27a**)*

The procedure for making **14** was followed exactly, using thio enone **27** (200 mg, 0.714 mmol), freshly crystallized NBS (140.6 mg, 0.786 mmol) and dry MeCN (1.0 mL). Flash chromatography of the crude product over silica gel (3 × 15 cm), using 9:1 hexane-EtOAc, gave **27a** (197 mg, 77%) as a solid: mp 128–132 °C; FTIR ($CDCl_3$, cast) 3059, 1671, 1538, 1453, 1440, 1264, 1242 cm^{-1}; ^1H NMR ($CDCl_3$, 500 MHz) δ 2.39–2.48 (m, 2 H), 2.76 (dd, J = 16.0, 13.0 Hz, 1 H), 2.87 (ddd, J = 11.5, 4.0, 1.5 Hz, 1 H), 3.30–3.37 (m, 1 H), 7.06–7.08 (m, 2 H), 7.20–7.30 (m, 3 H), 7.38–7.46 (m, 3 H), 7.52–7.55 (m, 2 H); ^{13}C NMR ($CDCl_3$, 125 MHz) δ 39.2 (t), 40.4 (d), 43.9 (t), 116.9 (d), 126.6 (d), 127.3 (d), 128.8 (d), 128.9 (s), 129.8 (d), 130.6 (d), 135.9 (d), 141.8 (s), 163.0 (s), 187.2 (s); exact mass (EI) m/z calcd for $C_{18}H_{15}^{81}BrOS$ (M^+) 360.0006, found 360.0002.

*5.1.27. 5-Phenyl-3-(phenylsulfanyl)phenol (**27b**)*

The procedure for making **19** was followed exactly, using DBU (0.025 mL, 0.17 mmol) and **27a** (30.6 mg, 0.085 mmol) in dry MeCN (1.0 mL). Flash chromatography of the crude product over silica gel (1 × 15 cm), using 3:7 hexane-CH_2Cl_2, gave **27b** (17 mg, 63%) as an oil: FTIR ($CDCl_3$, cast) 3391, 3059, 2953, 1586, 1570, 1476, 1449, 1196 cm^{-1}; ^1H NMR ($CDCl_3$, 500 MHz) δ 4.83 (s, 1 H), 6.71 (dd, J = 2.0, 1.5 Hz, 1 H), 6.91 (dd, J = 2.0, 1.5 Hz, 1 H), 7.15 (t, J = 1.5 Hz, 1 H), 7.27–7.36 (m, 4 H), 7.40–7.45 (m, 4 H), 7.50–7.52 (m, 2 H); ^{13}C NMR ($CDCl_3$, 125 MHz) δ 112.9 (d), 115.7 (d), 121.6 (d), 127.1 (d), 127.6 (d), 127.8 (d), 128.8 (d), 129.4 (d), 132.0 (d), 134.7 (s), 138.4 (s), 140.1 (s), 143.7 (s), 156.3 (s); exact mass (EI) m/z calcd for $C_{18}H_{14}OS$ (M^+) 278.0765, found 279.0771.

*5.1.28. 3-(tert-Butylsulfanyl)cyclohex-2-en-1-one (**28**)*

The procedure for making **17** was followed exactly, using 2-methylpropane-2-thiol (0.11 mL, 1.00 mmol), tosylate **18** (266 mg, 1.00 mmol), K_2CO_3 (826 mg, 5.00 mmol) and dry MeCN (2 mL). Flash chromatography of the crude product over silica gel (3 × 15 cm), using 4:1 hexane-EtOAc, gave **28** (73.4 mg, 40%) as an oil: FTIR ($CDCl_3$, cast) 2963, 1659, 1570, 1457, 1338 cm^{-1}; ^1H NMR ($CDCl_3$, 500 MHz) δ 1.48 (s, 9 H), 1.99 (quintet J = 6.0 Hz, 2 H), 2.36–2.38 (m, 4 H), 6.11 (s, 1 H); ^{13}C NMR ($CDCl_3$, 125 MHz) δ 22.8 (t), 30.4 (q), 31.7 (t), 37.2 (t), 47.4 (s), 122.6 (d), 164.5 (s), 196.0 (s); exact mass (EI) m/z calcd for $C_{10}H_{16}OS$ (M^+) 184.0922, found 184.0922.

*5.1.29. 2-Bromo-3-(tert-butylsulfanyl)cyclohex-2-en-1-one (**28a**)*

The procedure for making **14** was followed exactly, using thio enone **28** (65 mg, 0.35 mmol), freshly crystallized NBS (63.2 mg, 0.350 mmol) and dry MeCN (0.5 mL). Flash chromatography of the crude product over silica gel (3 × 15 cm), using 4:1 hexane-EtOAc, gave **28a** (40 mg, 42%) as a solid: mp 102–103 °C; FTIR ($CDCl_3$, cast) 2965, 1661, 1517, 1472, 1262, 1248 cm^{-1}; ^1H NMR ($CDCl_3$, 500 MHz) δ 1.56 (s, 9 H), 2.09 (quintet, J = 6.0 Hz, 2 H), 2.60 (t, J = 6.0 Hz, 2 H), 2.93 (t, J = 6.0 Hz, 2 H); ^{13}C NMR ($CDCl_3$, 125 MHz) δ 22.8 (t), 32.3 (q), 32.9 (t), 37.4 (t), 49.6 (s), 119.2 (s), 164.6 (s), 187.8 (s); exact mass (EI) m/z calcd for $C_{10}H_{15}^{81}BrOS$ (M^+) 264.0006, found 264.0004.

*5.1.30. 3-(tert-Butylsulfanyl)phenol (**28b**)*

The procedure for making **19** was followed exactly, using DBU (0.034 mL, 0.226 mmol) and **28a** (29.5 mg, 0.113 mmol) in dry MeCN (1 mL). Flash chromatography of the crude product over silica gel (1 × 15 cm), using 2:8 hexane-CH_2Cl_2, gave **28b** (5 mg, 25%) as an oil: FTIR ($CDCl_3$, cast) 3355, 2961, 1583, 1469, 1456, 1245, 1210, 1159 cm^{-1}; ^1H NMR ($CDCl_3$, 500 MHz) δ 1.29 (s, 9 H), 4.76 (s, 1 H), 6.84 (dd, J = 8.0, 2.5 Hz, 1 H), 7.03 (t, J = 1.5 Hz, 1 H), 7.11 (d, J = 7.5 Hz, 1 H), 7.20 (t, J = 8.0 Hz, 1 H); ^{13}C NMR ($CDCl_3$, 125 MHz) δ 31.0 (q), 46.1 (s), 115.9 (d), 124.0 (d), 129.4 (d), 129.9 (d), 134.1 (s), 155.2 (s); exact mass (EI) m/z calcd for $C_{10}H_{14}OS$ (M^+) 182.0765, found 182.0764.

Acknowledgements

We thank NSERC for financial support.

References

[1] W. Shao, D.L.J. Clive, J. Org. Chem. 80 (2015) 3211–3216.
[2] W. Shao, D.L.J. Clive, J. Org. Chem. 80 (2015) 12280–12287.
[3] G. Yu, D.L.J. Clive, J. Org. Chem. 81 (2016) 8470–8484.
[4] (a) Y. Kohno, K. Tanaka, K. Kuriyama, W. Hori, European Patent 1602660 A1, December 7, 2005.
(b) I.L. Scott, J.M. Ralph, M.E. Voss, WO Patent 2005/055939 A2, June 23, 2005.
(c) I.L. Scott, J.M. Ralph, M.E. Voss, WO Patent 2005/055943 A2, June 23, 2005.
[5] (a) S. Karkola, A. Lilienkampf, K. Wähälä, ChemMedChem 3 (2008) 461–472;
(b) J. Jílek, K. Šindelář, J. Pomykáček, V. Kmoníček, Z. Šedivý, M. Hrubantová, J. Holubek, E. Svátek, M. Ryska, I. Koruna, M. Valchář, A. Dlabač, J. Metyšová, N. Dlohožková, M. Protiva, Collect. Czech Chem. Commun. 54 (1989) 3294–3338;
(c) K. Šindelář, J. Pomykáček, J. Holubek, E. Svátek, M. Valchář, K. Dobrovský, J. Metyšová, Z. Polívka, Collect. Czech Chem. Commun. 56 (1991) 459–477;
(d) K. Šindelář, V. Kmoníček, M. Hrubantová, Z. Polívka, Collect. Czech Chem. Commun. 57 (1992) 194–203.
[6] R. Alexander, A. Balasundaram, M. Batchelor, D. Brookings, K. Crépy, T. Crabbe, M.-F. Deltent, F. Driessens, A. Gill, S. Harris, G. Hutchinson, C. Kulisa, M. Merriman, P. Mistry, T. Parton, J. Turner, I. Whitcombe, S. Wright, Bioorg. Med. Chem. Lett. 18 (2008) 4316–4320.
[7] (a) E. Piers, J.R. Grierson, C.K. Lau, I. Nagakura, Can. J. Chem. 60 (1982) 210–223;
(b) F. Algi, T. Hökelek, M. Balci, J. Chem. Res. (2004) 658–660.
[8] J.T. Joseph, A.M. Sajith, R.C. Ningegowda, A. Nagaraj, K.S. Rangappa, S. Shashikanth, Tetrahedron Lett. 56 (2015) 5106–5111.
[9] B. Neises, W. Steglich, Angew. Chem. Int. Ed. Engl. 17 (1978) 522–524.
[10] B. Dinesh, H.R. Manjunath, S. Naveen, K. Abiraj, A. Ramesh Baba, D. Channe Gowda, M.A. Sridhar, J. Shashidhara Prasad, Mol. Cryst. Liq. Cryst. 517 (2010) 161–166.
[11] K. Kumari, K.N. Singh, Synlett 25 (2014) 213–216.
[12] J.B. Thomas, S.W. Mascarella, R.B. Rothman, J.S. Partilla, H. Xu, K.B. McCullough, C.M. Dersch, B.E. Cantrell, D.M. Zimmerman, F.I. Caroll, J. Med. Chem. 41 (1998) 1980–1990.
[13] B.M. Trost, R.N. Bream, J. Xu, Angew. Chem. Int. Ed. 45 (2006) 3109–3112.
[14] (a) M.S. Shepard, E.M. Carreira, Tetrahedron 53 (1997) 16253–16276;
(b) P.C. Van Dort, P.L. Fuchs, J. Am. Chem. Soc. 116 (1994) 5657–5661.
[15] M. Koreeda, Y. Wang, L. Zhang, Org. Lett. 4 (2002) 3329–3332.
[16] (a) R. Kirchlechner, Chem. Ber. 115 (1982) 2461–2466;
(b) A. Arnoldi, A. Bonsignori, P. Melloni, L. Merlini, M.L. Quadri, A.C. Rossi, M. Valsecchi, J. Med. Chem. 33 (1990) 2865–2869.
[17] (a) M.H. Ali, M. Hartman, K. Lamp, C. Schmitz, T. Wencewicz, Synth. Commun. 36 (2006) 1769–1777;
(b) R. Harville, S.F. Reed Jr., J. Org. Chem. 33 (1968) 3976–3977.
[18] (a) R.H. Mitchell, Y.-H. Lai, R.V. Williams, J. Org. Chem. 44 (1979) 4733–4735;
(b) C.A. Townsend, S.G. Davis, S.B. Christensen, J.C. Link, C.P. Lewis, J. Am. Chem. Soc. 103 (1981) 6885–6888.
[19] J. Zhang, Q. Jiang, D. Yang, X. Zhao, Y. Dong, R. Liu, Chem. Sci. 6 (2015) 4674–4680.
[20] F.Y. Kwong, S.L. Buchwald, Org. Lett. 4 (2002) 3517–3520.
[21] M.A. Fernández-Rodríguez, J.F. Hartwig, J. Org. Chem. 74 (2009) 1663–1672.
[22] B.J. Musolino, G.W. Kabalka, Heterocycles 90 (2015) 271–297.
[23] J. Ko, J. Ham, I. Yang, J. Chin, S.-J. Nam, H. Kang, Tetrahedron Lett. 47 (2006) 7101–7106.
[24] (a) A.M.M. Mahfouz, R.L. Metcalf, T.R. Fukuto, J. Agric. Food Chem. 17 (1969) 917–922;
(b) D.J. Bartkovitz, Y. Chen, X.-J. Chu, K.-C. Luk, P.L. Rossman, S.-S. So, US Patent 2007060607 A1, March 15, 2007.
[25] Y. Liu, J. Kim, H. Seo, S. Park, J. Chae, Adv. Synth. Catal. 357 (2015) 2205–2212.
[26] X. Chen, X. Liu, J.S. Martinez, J.T. Mohr, Tetrahedron 72 (2016) 3653–3665.
[27] W.L.F. Amarego, C.L.L. Chai, Purification of Laboratory Chemicals, seventh ed., Elsevier, Oxford, 2013, p. 121.
[28] S.-R. Guo, Y.-Q. Yuan, Synth. Commun. 38 (2008) 2722–2730.
[29] F. Viani, B. Rossi, W. Panzeri, L. Merlini, A. Martorana, A. Polissi, Y.M. Galante, Tetrahedron 73 (2017) 1745–1761.
[30] C.J. Kowalski, K.W. Fields, J. Org. Chem. 46 (1981) 197–201.
[31] F. Wang, K. Chiba, M. Tada, J. Chem. Soc. Perkin Trans. 1 (1992) 1897–1900.